ACTIVE ROLL CONTROL OF ARTICULATED HEAVY VEHICLES

D. J. M. Sampson

Technical Report CUED/C-Mech/TR 82
January 2002

Summary

This report is concerned with the use of active roll control systems consisting of active anti-roll bars to improve the roll stability of single unit and articulated heavy vehicles.

Chapter 1 reviews previous research into the yaw-roll dynamics of heavy vehicles and into using active roll control systems on trucks, cars and trains.

Chapter 2 details a simplified dynamic model for simulating the handling and roll performance of a torsionally flexible single unit vehicle and a technique for coupling multiple single unit models to enable simulation of any long combination vehicle. A model of the active roll control system hardware is also presented.

Chapter 3 reviews the mechanics of the roll-over process and identifies a mechanism for reducing lateral load transfer by rolling the vehicle body into corners. Functional controllability analysis is used to show that achievable roll stability, even with ideal active anti-roll bars, is ultimately limited by suspension travel. A procedure for identifying critical axles whose lift-off determines the limit of roll stability is presented. The best achievable control objective for maximising roll stability is shown to be balancing the normalised load transfers at all critical axles while taking the largest inward suspension roll angle to the maximum allowable angle.

Chapter 4 proposes an LQR-based method for designing a full-state active roll control system for a single unit vehicle. A more practical partial-state feedback controller, using measurements of suspension roll angles, body roll rate, yaw rate and steering input, is also described. Simulations indicate that a system of active anti-roll bars incorporating moderately priced, low bandwidth hydraulic actuators and servo-valves and relatively simple instrumentation can improve steady-state roll stability of a rigid single unit vehicle by 23% and of a torsionally flexible single unit vehicle by 26%. Improvements in severe transient manoeuvres can be even greater. The effects of actuator bandwidth on system performance are investigated. Active roll control is also shown to increase handling stability, particularly for torsionally flexible vehicles.

Chapter 5 extends the work of chapter 4 to a tractor semi-trailer. Simulations show that active roll control systems can increase the roll-over threshold of a torsionally rigid tractor semi-trailer by 29% and of a torsionally flexible tractor semi-trailer by 29%.

Chapter 6 examines the use of active roll control systems on long combination vehicles, including those with flexible couplings. Simulations show that active roll control can increase the roll-over threshold by 32% for a B-double, by 25% for a truck full-trailer and by 23% for an A-double. The effect of rearward amplification on transient load transfer can be significantly reduced.

Conclusions and recommendations for further work are presented in chapter 7.

Preface

The work described in this report was carried out in the Cambridge University Engineering Department between October 1996 and September 2000.

I would like to thank David Cebon, who suggested and supervised this project, and who contributed his ideas, experience, encouragement and energy.

I am also very grateful to Dan Davison, for enthusiastically and generously sharing his knowledge of control theory.

I would also like to thank: Chris Winkler, Atanas Popov, David Cole and John Aurell, for contributing to discussions on vehicle modelling and simulation; Angie McConnell and Helen Sampson, for proofreading this dissertation; and my family and all my good friends at Churchill College, whose friendship and support throughout this project were invaluable.

This research was funded by the Engineering and Physical Sciences Research Council and the Cambridge Vehicle Dynamics Consortium. I was supported throughout the project by the Cambridge Commonwealth Trust and the Committee of Vice-Chancellors and Principals of the Universities of the United Kingdom. I thank all these organisations, without whose contributions this work would not have been possible.

This report is based on work originally published in my Ph.D. dissertation [76] of the same name. The key difference between the dissertation and this report is that the tyre parameters in this report have been updated to better represent average truck tyres, and in particular, the tyres to be used on the Cambridge Vehicle Dynamics Consortium's experimental vehicle. All controllers have been redesigned and all results recalculated for these amended tyre parameters.

David Sampson, January 2002

Contents

List of Figures

Nomenclature

A, B, C, D	state-space matrices
a	longitudinal distance to axle, measured forwards from centre of sprung mass
a'	longitudinal distance to axle, measured forwards from centre of total mass
$a^\star$	longitudinal distance to axle, measured backwards from front axle (trucks and tractors) or from front articulation point (dollies and semi-trailers)
a_y	lateral acceleration
b	longitudinal distance to articulation point, measured forwards from centre of sprung mass
b'	longitudinal distance to articulation point, measured forwards from centre of total mass
$b^\star$	longitudinal distance to rear articulation point, measured backwards from front axle (tractors) or from front articulation point (dollies and semi-trailers)
c_1, c_2	tyre cornering stiffness coefficients, in $\frac{F_y}{\alpha} = c_1 \times F_z + c_2 \times {F_z}^2$
c_α	tyre cornering stiffness, measured at rated vertical tyre load
F_b	lateral shear force in vehicle frame
F_c	lateral force in vehicle coupling
F_y	lateral tyre force
F_z	vertical tyre force
G	plant tranfer function
g	acceleration due to gravity
h	height centre of sprung mass, measured upwards from roll centre
h_a	height of articulation point, measured upwards from ground
h_b	height of frame twist axis, measured upwards from ground
h_{cm}	height of total centre of mass, measured upwards from ground
h_s	height of centre of sprung mass, measured upwards from ground
h_u	height of centre of unsprung mass, measured upwards from ground

I_{xx}	roll moment of inertia of sprung mass, measured about sprung centre of mass
$I_{x'x'}$	roll moment of inertia of sprung mass, measured about origin of (x', y', z') coordinate system
I_{xz}	yaw-roll product of inertia of sprung mass, measured about sprung centre of mass
$I_{x'z'}$	yaw-roll product of inertia of sprung mass, measured about origin of (x', y', z') coordinate system
I_{yy}	pitch moment of inertia of sprung mass, measured about sprung centre of mass
I_{zz}	yaw moment of inertia of sprung mass, measured about sprung centre of mass
$I_{z'z'}$	yaw moment of inertia of total mass, measured about origin of (x', y', z') coordinate system
J	quadratic performance index
K	controller tranfer function
k	suspension roll stiffness
k_b	vehicle frame torsional stiffness
k_t	tyre roll stiffness
k_ϕ	vehicle coupling roll stiffness
k_ψ	vehicle coupling yaw stiffness
L	wheelbase
l	suspension roll damping rate
l_γ	vehicle frame torsional damping rate
M	axle weight (total mass supported by axle)
m	total mass
m_s	sprung mass
m_l	additional lumped mass
m_u	unsprung mass
N_β	$\frac{\partial M_z}{\partial \beta} = \sum_j a'_j c_{\alpha,j}$ partial derivative of net tyre yaw moment with respect to sideslip angle
N_δ	$\frac{\partial M_z}{\partial \delta} = -a'_1 c_{\alpha,1}$ partial derivative of net tyre yaw moment with respect to steer angle
$N_{\dot\psi}$	$\frac{\partial M_z}{\partial \dot\psi} = \sum_j \frac{{a'_j}^2 c_{\alpha,j}}{U}$ partial derivative of net tyre yaw moment with respect to yaw rate
Q	performance output weighting matrix
R	control input weighting matrix

r	height of roll axis, measured upwards from ground
s	Laplace variable
T	track width
ΔT	tyre spread (for axles with twin tyres)
U	forward speed
u	active roll torque
V	process noise weighting matrix
v	measurement noise
W	measurement noise weighting matrix
w	process noise
x	state vector
x'	longitudinal distance, measured forwards from centre of total mass
x_a	actuator displacement
x_D	disturbance state vector
y	measurement output
y'	lateral distance, measured to the right from vehicle unit centreline
Y_β	$\dfrac{\partial F_y}{\partial \beta} = \sum_j c_{\alpha,j}$ partial derivative of net tyre lateral force with respect to sideslip angle
Y_δ	$\dfrac{\partial F_y}{\partial \delta} = -c_{\alpha,1}$ partial derivative of net tyre lateral force with respect to steer angle
$Y_{\dot\psi}$	$\dfrac{\partial F_y}{\partial \dot\psi} = \sum_j \dfrac{a'_j c_{\alpha,j}}{U}$ partial derivative of net tyre lateral force with respect to yaw rate
z	performance output
z'	vertical distance, measured downwards from roll axis
α	tyre slip angle
β	sideslip angle
γ	frame twist angle
Γ	articulation angle
δ	steer angle
ϕ	absolute roll angle of sprung mass
ϕ_t	absolute roll angle of unsprung mass
ψ	heading angle
$\dot\psi$	yaw rate

Notation

A^T	transpose of A
A^{-1}	inverse of A
$\dot{a}$	first time derivative of a
$\ddot{a}$	second time derivative of a
$\mathrm{diag}\,(a_1, \ldots, a_n)$	an $n \times n$ diagonal matrix with a_i as its ith diagonal element
$\max(a_1, \ldots, a_n)$	maximum value among a set of integers $a_1, \ldots, a_n$
$\min(a_1, \ldots, a_n)$	minimum value among a set of integers $a_1, \ldots, a_n$

Additional subscripts

f	front
i	ith vehicle unit, or ith vehicle coupling, counted from front
j	jth axle, counted from front
r	rear

Chapter 1

Introduction

1.1 Roll-over of heavy vehicles

The roll-over of heavy vehicles is an important road safety problem world-wide. Several studies have reported that a significant proportion of the serious heavy vehicle accidents involve roll-over.

In 1996 and 1997, the US National Highway Traffic Safety Administration documented over 15000 roll-over accidents per year involving commercial heavy vehicles, including 9400 accidents annually involving tractor semi-trailer combinations [6, 7]*.

In 1993, 545 heavy vehicles were involved in roll-over accidents in the UK [3]. Earlier studies in the UK had reported that roll-over accidents accounted for 6% of all accidents to articulated heavy vehicles and 30% of accidents to heavy vehicles at roundabouts [42].

A study by Kusters reported that the majority of roll-over accidents in The Netherlands involve articulated heavy vehicles (typically tractor semi-trailer and tractor full-trailer combinations) and occur on highways [46]. These accidents were attributed to three main causes: sudden course deviation, often in combination with braking, from high initial speed; excessive speed on curves; and load shift.

Ervin conducted a major review of single vehicle accidents involving three axle

*denotes reference (see pages 265–277)

tractors pulling two axle semi-trailers for the US Department of Transport [24]. The review found that, of the 9000 accidents to such vehicles over a four year period in the late 1970s, approximately 2000 were caused by a loss of roll stability.

Winkler et al. reported that, in the US between 1992 and 1996, roll-over was the cause of approximately 12% of fatal truck and bus accidents and 58% of accidents in which truck drivers were killed [107, 108].

Studies by Rakheja et al. in Canada reported that roll-over occurred in around 40% of accidents involving tanker vehicles and 45% of accidents involving the transportation of dangerous goods [72, 73].

Harris estimated the average cost of a roll-over accident to a vehicle operator in the UK as £75 000-100 000, including the costs of recovery and repair of the vehicle, product loss and road resurfacing [30]. There is additional expenditure of approximately £4 million annually on hospitals, emergency services and social security benefits arising directly from these accidents [2]. Therefore a reasonable estimate is that heavy vehicle roll-over accidents cost £40-60 million annually in the UK, excluding costs arising from traffic delays [9].

A review of heavy vehicle safety by von Glasner considered that while some roll-over accidents to articulated vehicles were preventable given a sophisticated warning system and a highly skilled driver, the majority could only be avoided by the intervention of advanced active safety systems [101]. Winkler et al. also noted that it is very difficult for truck drivers to perceive their proximity to roll-over while driving [107, 109]. A driver steers, brakes and accelerates in response almost exclusively to the behaviour of the lead unit of a combination vehicle, and it is very difficult for the driver to sense the behaviour of trailer and semi-trailer units. In particular, the flexible nature of tractor frames tends to isolate the driver from roll motions of trailer and semi-trailer units that might otherwise act as cues to impending roll-over.

Winkler et al. surveyed US accident statistics and reported a strongly negative correlation between steady-state roll stability and the average frequency of roll-over accidents [107, 108, 110]. The study found that an increase in the static roll-over threshold

of 0.1 g in the range 0.4-0.7 g caused a 50% reduction in the frequency of roll-over accidents for tractor semi-trailer combinations. For example, the average frequency of roll-over accidents was 0.16 events per million kilometres travelled among vehicles with a static rollover threshold of 0.5 g but 0.07 events per million kilometres among vehicles with a static roll-over threshold of 0.6 g. The study also established a link between steady-state roll stability and the probability of roll-over in an accident. Roll-over accidents accounted for almost 50% of non-jack-knife accidents to tractor semi-trailers with a static roll-over threshold of 0.4 g but less than 15% to tractor semi-trailers with a roll-over threshold of 0.6 g. Interestingly these statistics indicate that drivers do not drive less stable vehicles more cautiously (and conversely, do not drive more stable vehicles less cautiously). This is because drivers are unable to assess roll-over stability accurately while driving.

It is clear that even a modest increase in roll stability can lead to a significant reduction in the frequency of roll-over accidents. This provides a compelling motivation for research into improving roll stability of heavy vehicles because of the serious safety, cost and environmental implications of roll-over accidents.

1.2 The case for articulated vehicles

The use of long articulated vehicles is economically attractive due to lower fuel and driver costs per tonne of cargo. However it has been shown that poorly designed multiple unit vehicles can suffer from dangerous roll and handling instabilities [57]. For this reason, government regulators have traditionally been hesitant to sanction the use of such vehicles.

McFarlane et al. proposed performance measures to guide regulators assessing the safety of novel long combination vehicles [58]. They suggested that vehicle safety could be assessed with some confidence by considering two key performance indicators: (1) *rearward amplification* (that is, the ratio of the lateral acceleration of a trailing unit of a combination vehicle to the lateral acceleration of the leading unit, in response

to a sinusoidally varying steering input); and (2) *steady-state roll stability*. There are few accident statistics available for long combination vehicles so it is not yet possible to demonstrate a robust statistical correlation between these proposed indicators and the frequency of roll-over accidents. However the authors noted a parallel with the aircraft industry where accidents are rare but the use of performance-based standards is widespread.

McFarlane suggested that governments should consider a flexible, performance-based approach to the regulation of multiple unit vehicles and detailed the potential economic benefits [56, 57]. Woodrooffe documented the history of heavy vehicle regulation in the Canadian province of Saskatchewan through the 1980s and 1990s [112]. Several novel long combination vehicles that had previously been prohibited were permitted to operate on selected routes, and no serious accidents were reported.

Lobbied by fleet operators, regulators are demonstrating an increasing flexibility towards allowing longer combination vehicles to operate on major highways and motorways, providing the vehicles satisfy stringent roll stability and handling performance criteria.

1.3 Review of previous work

1.3.1 Yaw-roll dynamics of heavy vehicles

The safety of road vehicles depends on the the yaw-roll dynamics. A loss of roll stability results in a roll-over accident, and a loss of yaw stability results in spin-out for single unit vehicles and jack-knifing or trailer swing for articulated vehicles. This review focuses on aspects of yaw-roll dynamics that are relevant to heavy vehicles. A familiarity with the yaw-roll dynamics of automobiles is assumed.

Publications from the University of Michigan Transportation Research Institute are among the most comprehensive general reviews of heavy vehicle dynamics [26, 25, 84]. The dynamics of tractor semi-trailer and tractor full-trailer combinations were

summarised by Nalecz [64] and Vlk [99, 100]. Segel and Ervin [85] and Ellis [23] reviewed the dynamics of long combination vehicles.

Handling performance

Handling performance is the yaw response of a vehicle to steering inputs and is determined by the vehicle dimensions and the mechanical properties of the tyres, suspensions and vehicle frames [84]. The distribution of weight among the axles affects handling performance because the cornering stiffness of pneumatic tyres depends on the vertical load. The effects of dual tyres and closely spaced tandem axles are also important, but to a lesser degree [106]. Pacejka reviewed the fundamentals of steady-state cornering for automobiles [65, 66] and more complex vehicles [67].

Handling performance at low levels of lateral acceleration is typically described qualitatively as *understeer* or *oversteer* and quantitatively using the understeer gradient. Understeer is a stable handling regime in which the radius of curvature of a steady turn increases with vehicle speed for a given steer angle. For an oversteering vehicle, the radius of curvature decreases with increasing vehicle speed for a given steer angle. An oversteering vehicle becomes unstable at a critical speed that depends on the vehicle dimensions, weight distribution and the mechanical properties of the tyres.

Handling performance of combination vehicles is influenced by interactions between vehicle units. For example, the handling performance of a tractor changes when it tows a semi-trailer. The tractor may become more or less understeer depending on the location of the vehicle coupling and the resulting changes in axle loads and tyre cornering stiffnesses. It remains possible to characterise the nominal handling of the tractor and trailing units as understeer or oversteer, and analysis by Segel and Ervin [85] shows that handling instability of a tractor semi-trailer combination can be classified into various different regimes: (1) if the tractor is oversteer and the semi-trailer is understeer or mildly oversteer, there exists a critical speed at which tractor *jack-knife* will occur; (2) if the tractor is oversteer and the semi-trailer is strongly oversteer, then the combination will exhibit *trailer swing* instability above a critical

velocity; or (3) the combination is guaranteed stable in handling if the tractor unit is understeer.

The pneumatic tyre exhibits a linear relationship between slip angle and lateral force at small angles of slip and at a given vertical load. However, variations from this linear characteristic at varying vertical loads have an important impact on heavy vehicle handling performance [84].

Automobiles typically exhibit a linear directional response for lateral acceleration levels up to around 0.3 g. Variations from this linear response at higher levels of lateral acceleration are due primarily to the nonlinear relationship between slip angle and lateral force at large slip angles. The sensitivity of the slip angle-to-lateral force relationship to changes in vertical tyre force has little effect since changes in vertical force due to cornering are relatively small for automobiles [28].

Nonlinearities in the directional behaviour of heavy vehicles, conversely, are dominated by the sensitivity of the slip angle-to-lateral force relationship to changes in vertical load. Heavy vehicles typically feature elevated payloads and comparatively narrow track widths, so lateral load transfer is significant even at modest levels of lateral acceleration.

Because of the curvature of the cornering stiffness versus vertical load characteristic, the lateral force produced by the outside tyre increases less than the lateral force produced by the inside tyre decreases for a given lateral load transfer. Therefore the combined cornering stiffness of an axle reduces as lateral load transfer increases. Some heavy vehicles exhibit nonlinear directional behaviour at lateral acceleration levels as low as 0.1 g [84].

The distribution of the total lateral load transfer among the axles, which controls the way handling changes as lateral acceleration increases, is strongly dependent on both the effective roll stiffness of the suspension units (including anti-roll bars) and the torsional stiffness of the vehicle frames. Heavy vehicles tend to have significantly stiffer suspensions at the more heavily loaded axles to ensure that static spring deflections are reasonable. Thus the tractor drive axle and semi-trailer axles of a typical

tractor semi-trailer combination are much stiffer in roll than the tractor steer axle [25]. Consequently these axles carry a disproportionate amount of load transfer in cornering. As lateral acceleration increases, the relative cornering stiffness of the tractor drive axle and the semi-trailer axles compared to the tractor steer axle decreases and the vehicle becomes more oversteer. Handling stability is reduced. Torsional compliance of the tractor frame, which is a practical necessity to limit stress when traversing uneven ground, contributes further to this effect by reducing the relative amount of lateral load transfer borne by the lightly loaded tractor steer axle in cornering.

Roll stability

Roll stability refers to the ability of a vehicle to resist overturning moments generated during cornering, that is, to avoid roll-over. Roll stability is determined by the height of the centre of mass, the track width and the kinematic and compliance properties of the suspensions. The mechanics of roll-over are discussed in detail in section 3.3, but a brief discussion of some important effects is included here.

The roll and yaw dynamics of road vehicles are coupled. The layout of typical road vehicle suspensions is such that the roll centre is below the centre of mass, so a passively suspended road vehicle rolls outwards under the influence of lateral acceleration in steady-state cornering. In transient manoeuvres, the coupling between yaw and roll through the yaw-roll cross product of inertia means that roll motions influence yaw motions and vice versa.

The roll dynamics of heavy vehicles when cornering are much more relevant to vehicle safety than those of automobiles [25]. Heavy vehicles feature relatively high centres of mass and narrow track widths and can lose roll stability at moderate levels of lateral acceleration. Whereas the performance limit of an automobile is characterised by a loss of yaw stability, the performance limit of a heavy vehicle is typically characterised by a loss of roll stability. That is, in typical operating conditions, the maximum lateral acceleration beyond which a heavy vehicle loses stability is limited by roll-over rather than by jack-knifing or trailer swing [24, 26, 42], whereas an automobile can

never generate sufficient lateral tyre force to roll over unless a tyre strikes an obstacle.

Under lateral acceleration, the vehicle body rolls out of the corner and the centre of mass is shifted outboard of the vehicle centreline. This effect creates an additional destabilising moment that diminishes the roll stability. Thus roll compliance of the suspensions and torsional compliance of the vehicle frames reduce the roll-over threshold. Load shift caused by slosh in liquid tankers also adversely affects roll stability [25, 84].

Influence of vehicle parameters

Several authors have conducted comprehensive studies of the sensitivity of yaw-roll dynamics to vehicle design parameters.

Fancher and Mathew simulated the yaw-roll dynamics of a wide range of heavy vehicles including single unit trucks, tractor semi-trailers, truck full-trailers and double and triple combinations [26]. Combinations were compared on the bases of rearward amplification (as defined on page 3), steady-state roll stability, handling performance and low speed and high speed offtracking. The study found that the roll stiffness, yaw stiffness and location of vehicle couplings strongly affect the interaction between adjacent units of a combination vehicle. Pintle hitch couplings (for example, between a truck and trailer) decouple the roll motions of adjacent units and the roll stability of each unit could be evaluated separately, whereas the roll motions of units linked by a fifth wheel (for example, between a tractor and semi-trailer) are strongly coupled. Long articulated vehicles are prone to dangerous levels of rearward amplification, particularly when pintle hitch couplings are used to join vehicle units.

Blow et al. reported on an exhaustive simulation study of more than 5000 heavy vehicle combinations conducted for the US Department of Transport [5]. The authors again focused on rearward amplification and steady-state roll stability and found that these two performance indices were most sensitive to vehicle weights, tyre properties and vehicle coupling designs.

1.3.2 Vehicle dynamics simulation

Computer models for simulating vehicle dynamics and control systems have been in use for many years [44]. The advantages of simulation are: (1) an ability to evaluate alternative designs prior to building prototypes; (2) the possibility of studying the behaviour of existing systems; and (3) studying the behaviour of humans and hardware components through real time *man-in-the-loop* or *hardware-in-the-loop* simulation [81].

Complex nonlinear vehicle models with many degrees of freedom can be generated reliably using current mechanical multibody simulation programs such as AutoSim, ADAMS and DADS [44, 81, 80]. However the use of such complex models for designing vehicle control systems is impractical. Modern control system design techniques emphasise the use of state-space methods that usually require measurement or estimation of *all* system states. Financial constraints typically limit the number of sensors used in a control application, and the estimation of many states based on just a few measurements is computationally expensive and may lack robustness to measurement noise and modelling uncertainties [35, 98].

A preferable approach is to design vehicle control systems using relatively simple vehicle models. For example, a model used for the design of an active roll control system for a long combination vehicle should capture the important roll and yaw dynamics but need not include the pitch and bounce motions. By judiciously reducing the complexity of the vehicle model, it is possible to simplify the task of control system design and the cost and complexity of implementation considerably. The performance of the control system can subsequently be verified on a prototype vehicle or using alternative simulation software. Many studies have demonstrated that the performance of well designed control systems based on simplified vehicle models is often very good [43, 82, 97].

1.3.3 Advanced suspension systems

The design of vehicle suspension systems involves trade-offs between handling performance, roll stability, driver comfort, payload ride and road friendliness. Sharp and Crolla conducted a comprehensive review of the relevant issues for automobile suspension design [88], while Claar and Vogel published a similar review for both on and off-highway vehicles [12]. Several authors have investigated the design trade-offs through formal studies of the performance limitations and constraints inherent in suspension design [18, 31, 39, 95, 103, 104].

Conventional passive suspension systems typically consist of springs, dampers and anti-roll bars, and can only dissipate energy. Recently there has been significant research activity in a new class of so called *advanced suspension* systems. Advanced suspensions can be divided into three categories: *fully active*, *slow active* and *semi-active*.

Fully active suspensions use powered actuators to replace conventional spring and damper arrangements. These systems operate over a wide frequency range and attempt to control the motion of both the vehicle body and the wheels [89]. The bandwidth and power consumption requirements are severe and the hardware costs are significant, so fully active systems are only feasible for special high performance applications.

Slow active suspensions represent a more practical compromise in suspension control. These systems typically consist of a low bandwidth actuator in series with a passive spring and operate up to a maximum frequency of around 5 Hz. They control only the low frequency body modes (notably roll and pitch) of a vehicle. Control of high frequency wheel hop modes is achieved by the passive springs and dampers. The bandwidth and power consumption requirements are moderate and the hardware costs are lower than for fully active systems [90].

Semi-active suspensions consist of controllable dampers and conventional springs. Such systems can only dissipate energy, by contrast with fully active and slow active systems, which can supply energy. Hardware costs are lower than for slow active systems and power consumption is limited to that required to operate the damper

valves [91].

Fully active and slow active suspension systems are attractive because they allow more design flexibility than passive suspension systems for specifying the transfer functions that govern the handling, ride and roll performance of a vehicle [103, 104]. The costs of this improved design freedom include additional power consumption, hardware costs and system complexity.

Karnopp evaluated the feasibility of using advanced suspension systems on automobiles [38]. He concluded that the improvements to handling and ride performance over a passive system could be large enough to justify the additional costs and complexity.

Von Glasner et al. considered the feasibility of using advanced suspension systems on heavy vehicles [102]. They concluded that fully active systems are generally unsuitable due to prohibitively high hardware and operating costs but slow active and semi-active systems are feasible and can significantly improve heavy vehicle dynamics. The use of adaptive slow active and semi-active suspensions where spring and damping rates are tuned to varying load and road conditions also promises major improvements over conventional passive suspensions.

Studies into the use of slow active and semi-active roll control systems to increase vehicle roll stability and to control other aspects of vehicle performance are detailed in the following sections.

1.3.4 Active roll control for reducing perceived lateral acceleration

Until the 1980s, most of the work on active roll control was conducted in the railway industry. The limiting factor in train speed is the cornering lateral acceleration at which passenger comfort can be maintained. Passenger comfort requires that the perceived lateral acceleration is less than 0.1 g [34]. While it is possible to reduce lateral acceleration at a given speed by reducing track curvature, this requires major investments in modifications to railway infrastructure. A more cost effective alternative is to modify

train carriages to tilt into corners, since an inward roll angle of ϕ produces an apparent reduction of the level of lateral acceleration by a factor of secϕ.

By 1983, when Goodall and Kortüm reviewed the state of the art in active control of ground vehicles [29], prototype active tilting trains had been tested in Sweden, Britain, Italy, Germany and Japan. The Italian and Japanese versions are now in widespread commercial service. The bogies of these trains run parallel to the tracks and the body rolls inwards as an inverted pendulum under an active roll moment. The tilting mechanisms are mounted on the vehicle body, separated from the bogies by air springs to isolate passengers from vibration. The trains roll up to 10° and can maintain perceived lateral acceleration levels below 0.1 g at speeds of up to 250 km/h.

An alternative approach used in Spanish and American prototypes in the 1970s was to suspend the body from a high roll centre [29]. Under lateral acceleration, the body naturally rolls towards the outside of the corner like a pendulum, thereby banking the passengers towards the inside. It is possible to implement a passive or semi-active system using this arrangement.

There are a number of important differences between the design requirements for active roll control systems for trains and road vehicles. Trains operate along a known path so the worst case turning radius is known in advance, whereas road vehicles are involved in emergency cornering manoeuvres from time to time. Furthermore, since tilting of trains is solely for the purpose of passenger comfort, it is possible to use a non-tilting lead engine car to provide a preview signal to the following cars to start tilting before a curve or in the transition section of a curve.

One of the earliest road vehicles with active roll control was a three wheeled motorcycle-based machine designed and built at MIT in 1968 [48]. The initial prototype used a simple feedback control scheme based on a tuned pendulum to measure body roll angle and a hydraulic servo-valve actuator to apply a roll moment between the body and the rear axle. Since a pendulum aligns itself with the apparent vertical in steady-state cornering, the system acted to reduce perceived lateral acceleration. The steady-state performance of the vehicle was satisfactory but the transient perfor-

mance was hampered by the unavailability of sensors with sufficiently fast response. The large and heavy mechanical roll angle sensor introduced unwanted lag into the closed-loop system dynamics. Transient performance was later improved somewhat by adding feedforward action from the driver steering input for a second generation prototype. (The use of such mechanical sensors also hampered the development of tilting trains throughout the 1970s [34].)

General Motors also developed a prototype tilting vehicle, the *Lean Machine*, in the 1970s, although tilting was controlled by the driver through a pedal rather than by an automatic control system [34]. The aim again was to allow the driver to execute a coordinated turn, controlling both yaw and roll like an aircraft pilot to reduce the perceived lateral acceleration.

1.3.5 Active roll control for controlling body roll

As detailed in section 1.3.1, a passively suspended road vehicle rolls outwards under the influence of lateral acceleration when cornering. For many types of automobile suspension systems, excessive body roll causes the camber angles between the tyres and the road to increase significantly, reducing tyre traction and adversely affecting vehicle handling. Body roll is also unpleasant for the driver and increases stress and fatigue [45]. Through the 1980s and 1990s, the majority of research into active vehicle roll control focused on reducing body roll.

Karnopp investigated the potential for using active control of load levellers to regulate low frequency automobile body motions. He found that proportional-derivative control on load leveller deflection could be used to reduce roll and pitch under the influence of cornering and braking respectively [40]. However the stability of closed-loop system was reduced to a marginal level as feedback gains were increased.

Pham et al. researched the possibilities for controlling the roll angle of an automobile in steady-state cornering [70]. They used a three degree of freedom (yaw, sideslip and sprung mass roll angle) model and a lateral acceleration-based roll controller. The

authors concluded that it was possible to select feedback gains such that the vehicle would operate in one of three performance regimes: rolling outward, like a passive suspension; maintaining zero roll angle; or rolling inward.

Cech investigated using a system consisting of high and low bandwidth hydraulic actuators mounted in series to control the roll angle and vertical motion of a bounce-roll half-car model [10]. He concluded that even slow active suspension systems could be used to eliminate body roll and static deflection in a steady turn.

Sharp and Hassan reported that a system consisting of low bandwidth hydraulic actuators and semi-active dampers could be used to reduce roll and pitch motions of an automobile in cornering and braking [90]. The system was based on rotary hydraulic actuators incorporated into an existing anti-roll bar, controlled in response to the lateral acceleration of the vehicle. By rotating the actuators, it was possible to twist the anti-roll bars and generate a roll moment between the sprung and unsprung masses. Inclusion of feedforward action from steering inputs and vehicle speed was found to improve system performance.

Lang and Walz studied a system based on similar hardware using a complex multi-body model consisting of 35 bodies and 80 degrees of freedom [47]. The actuator moments were set by a proportional-derivative controller on lateral acceleration. The authors reported that such a system could reduce body roll in cornering and recommended a servo-valve bandwidth of 20 Hz.

Sharp and Pan studied the effect of control hardware limitations on active roll control of automobiles [92, 93]. The authors concluded that increasing servo-valve bandwidth above 10 Hz had little effect on system performance, providing the servo-valve was appropriately sized and the control system was well designed. Peak power delivered to the actuators was approximately 2.5 kW and was strongly dependent on the steering input. This power consumption result differed considerably from those of Lang and Walz [47], even considering differences in vehicle parameters.

Mizuno et al. designed an active roll control system where the inputs to the feedback controller were the relative roll angle and roll rate between the sprung and un-

sprung masses [61]. Although it was possible to regulate the relative roll angle using this strategy, it was not possible to regulate the roll angle of the sprung mass with respect to the ground because of tyre compliance.

Darling et al. used time domain simulations of a five degree of freedom (yaw, sideslip, roll, pitch and bounce) nonlinear model to investigate the performance potential of an automobile active roll control system [16]. The hardware considered again consisted of rotary hydraulic actuators incorporated into standard anti-roll bars [14, 15]. The aim was to reduce body roll and the controller used lateral acceleration measurements. A servo-valve bandwidth of 3 Hz was found to give satisfactory performance in normal manoeuvres but optimal performance in severe manoeuvres required a servo-valve bandwidth of 10 Hz. System performance lacked robustness to changes in forward speed unless a speed-based gain scheduling control scheme was introduced. The authors noted that the roll control system caused some degradation in ride performance at low speeds.

Several authors have investigated the use of active roll control to reduce the body roll of heavy vehicles.

Mercedes-Benz developed an active roll control system consisting of switchable air springs (incorporating additional air volume) and switchable dampers for a single unit two axle medium duty truck [69]. The system, which used measurements from driver inputs and other on-board sensors, reduced body roll in lane change manoeuvres by 30-50%.

Kusahara et al. also investigated the use of an active roll control system to reduce the body roll of a single unit truck [45]. The active roll control system consisted of anti-roll bars front and rear linked to the vehicle frame by single rod double-acting hydraulic actuators. By extending or contracting the hydraulic actuators, the vehicle body roll angle could be controlled. Wheel speed and steering angle sensors were used to estimate the lateral acceleration of the vehicle, which was input to a proportional feedforward controller to produce actuator force demand signals. The controller could switch between several modes for different loading conditions by measuring the

static suspension deflections when the vehicle was at rest. The system reduced body roll by 67% in steady-state cornering and in high speed lane changes. The authors attributed some differences between predicted and measured responses to excessive torsional flexibility of the vehicle frame. The active roll control system could be deactivated during straight running to improve ride performance. Used in conjunction with an active rear wheel steering system, the active roll control system provided a small improvement in directional controllability. Subjective tests showed that the system improved overall driver comfort.

Dorling studied the problem of simultaneously controlling the roll, bounce, pitch and yaw motions of a single unit vehicle using an active suspension system [17, 18]. He concluded that, under certain basic assumptions, it is possible to control body roll independent of the other three modes.

1.3.6 Active roll control for enhancing roll stability

Recently the use of active roll control systems to improve vehicle roll stability and reduce the likelihood of roll-over accidents has been proposed by several authors. Vehicles with conventional passive suspensions tilt out of corners under the influence of lateral acceleration. The centre of sprung mass shifts outboard of the vehicle centreline and this contributes a destabilising moment that reduces roll stability. (See section 3.3 for a complete analysis.) The aim of a stabilising active roll control system is to lean the vehicle *into* corners such that the centre of sprung mass shifts inboard of the vehicle centreline and contributes a stabilising roll moment.

Dunwoody and Froese used simulations to investigate the potential benefits of using an active roll control system to increase the steady-state roll stability of a tractor semi-trailer [22]. The roll control system hardware was contained entirely within the trailer unit and consisted of a tiltable fifth wheel coupling and hydraulic actuators at the trailer axles. The sole input to the roll controller was a lateral acceleration signal from an accelerometer mounted on the trailer. Controller gains were selected using a

simple steady-state roll-plane model[†]. The authors concluded that the system could increase the roll-over threshold by 20-30% for a wide range of trailer loading conditions. To ensure good transient performance, the authors suggested filtering the lateral acceleration signal with a first order 1 Hz low-pass filter, although no simulation results were given.

Lin et al. investigated the use of an active roll control system to reduce the total lateral load response of a single unit truck to steering inputs [51, 52, 55]. A linear model with four degrees of freedom (yaw, sideslip, sprung mass roll angle and unsprung mass roll angle) was used. A steering input spectrum was derived by considering the low frequency steering inputs required to follow the road (based on road alignment data) as well as the higher frequency inputs needed to perform frequent lane change manoeuvres. This spectrum was used to design an optimal full state linear quadratic controller to regulate load transfer. This control scheme caused the vehicle to lean into corners. The lateral acceleration level at which wheel lift-off is first achieved was increased by 66% and the total RMS load transfers in response to a random steering input were reduced by 34%. A proportional-derivative lateral acceleration feedback controller was also designed using pole placement. Although the reductions in total load transfer were smaller, the lateral acceleration controller was attractive because of its simpler instrumentation requirements. The effects of actuation system bandwidth were also considered. A bandwidth of 3 Hz was found to give satisfactory performance, and increasing bandwidth above 6 Hz gave no improvement in performance. The average power requirement was 17 kW for a "worst case" steering input.

Lin et al. also investigated the use of active roll control to enhance the roll stability of a tractor semi-trailer [51, 54]. The design of the roll control system was performed using an eight degree of freedom linear model. The controller used lateral acceleration signals from the tractor and trailer to control active anti-roll bars fitted to the tractor and trailer axles. The proportional controller gains were selected for good steady-state roll stability and the derivative gains were chosen to equate the normalised RMS

[†]The assumption that lateral tyre force is proportional to the static axle load is debatable.

load transfers of the two units. The system reduced steady-state and transient load transfers by up to 30%. Results were confirmed by time domain simulations using a validated nonlinear yaw-roll model [53]. The total power required by the system was 9 kW, which was considerably less than for the single unit case [51, 55]. The required actuation system bandwidth was 1 Hz, also less than required by the single unit vehicle. The authors reasoned that the transfer of roll moment across the fifth wheel coupling allowed the tractor roll control system to contribute to the trailer roll stability. They suggested that torsional compliance of vehicle frames may have a significant effect on the effectiveness of active roll control systems.

Hibbard and Karnopp proposed a new class of small, relatively tall and narrow commuter vehicles [32, 33, 34, 41]. These vehicles had a track width of less than 1.0 m, a height of around 1.6 m and a weight of 250-350 kg. Such vehicles would be much more susceptible to overturning than conventional automobiles and would be unstable at moderate levels of lateral acceleration unless fitted with an active roll control system to tilt the body into corners. The authors calculated the optimum steady-state roll angle such that the destabilising moment of lateral acceleration about the roll centre was exactly balanced by the stabilising moment due to shift of the centre of mass inboard of the vehicle centreline (as for a motorcycle) [33, 41]. This minimised actuator torque requirements and alleviated the need for a self-locking mechanism as used on train roll control systems, but the resulting inward roll angles were extreme. A roll control system based on lateral acceleration and roll angle feedback was designed and simulated using a three degree of freedom linear model. The authors proposed a range of control strategies to increase driver comfort in transient manoeuvres [34]. They did not, however, consider the space requirements of the long stroke actuators that would be required for this application.

1.3.7 Active roll moment distribution

As detailed in section 1.3.1, directional stability and handling performance are strongly influenced by the distribution of roll stiffness among the axles of a vehicle because of the nonlinear relationship between normal tyre load and cornering stiffness. In the absence of torsional frame flexibility, axles with greater roll stiffness will carry a greater proportion of the total lateral load transfer generated during cornering. This leads to an effective reduction of cornering stiffness at those axles, affecting the handling balance [28, 87]. Several authors have investigated the possibility of influencing automobile handling through using advanced suspensions to vary roll moment distribution.

Abe proposed an active roll control law for automobiles where the combined roll moment of the front and rear suspensions was designed to reduce body roll and the distribution of roll moment distribution between the front and rear suspensions was tuned to prevent handling instability [1].

Williams and Haddad investigated the potential for using full active suspension to influence handling dynamics of an automobile through active roll moment distribution [105]. They used a two degree of freedom (yaw and sideslip) vehicle model with nonlinear tyres where cornering stiffness varied as a quadratic function of normal load. The problem was cast as a yaw rate tracking controller design and a nonlinear controller was synthesised using feedback linearisation. Simulations demonstrated the possibility of reducing understeer and improving yaw rate tracking by actively reducing the front-to-rear roll stiffness distribution. An alternative, heavily simplified control law was also derived and implemented on a test vehicle. Results from field tests showed that the handling characteristics could be varied from understeer to oversteer by altering the roll controller gains.

Hwang and Park noted that the performance of automobile feedforward roll control algorithms based on lateral acceleration signals was sensitive to actuator dynamics [36]. They developed a predictive roll control algorithm to account for the lag inherent in the response of active roll control system actuators. The aim was to control both body roll and the front-to-rear distribution of the roll control moments. Simula-

tions on a nonlinear multiple degree of freedom model showed that this control strategy could reduce body roll and simultaneously improve handling stability.

1.3.8 Other systems for enhancing roll stability

Palkovics et al. suggested an alternative system for increasing the roll-over stability of a single unit truck by reprogramming the existing electronic braking system [27, 68]. Their proposed electronic braking system regularly applies a small braking force to each of the wheels and monitors the slip response. Excessive slip response to a pulse indicates that a given wheel is lightly loaded and that lift-off is imminent. The brakes are activated to momentarily lock the outside wheel of that axle and reduce the lateral tyre force so that the axle suddenly slips laterally. A prototype system was constructed and tested and was shown to prevent roll-over in a severe lane change manoeuvre. The key advantages of the system are zero additional hardware cost and low power consumption. However, since the system works by effectively changing the vehicle path, the directional controllability of the vehicle in emergency situations is reduced. A further drawback is the inability of the system to improve roll stability significantly in steady-state cornering.

1.4 Research needs

It is clear from the literature that there are a number of fundamental questions concerning active roll control of heavy vehicles where further research is required:

1. There is a need to develop a vehicle modelling framework that allows a wide range of heavy vehicles, from trucks to long combinations, to be represented.

2. The nature of fundamental limitations in achievable roll stability for vehicles with active roll control systems is not well understood. An understanding of these limitations is necessary to enable the formulation of achievable control system design objectives that maximise vehicle roll stability.

3. It is necessary to investigate which control system design techniques are well suited to the task of designing active roll control systems.

4. There is a need to quantify the achievable improvements in roll stability for a range of heavy vehicles, from single unit vehicles to long combinations, and for a range of manoeuvres, from steady-state cornering to severe transient manoeuvres, that are possible using active roll control.

5. It is not known to what extent torsional flexibility of vehicle frames and couplings is favourable or detrimental to the achievable roll stability of vehicles with active roll control systems.

6. It is necessary to investigate some of the hardware requirements (for example, sensor selection, servo-valve flow rates, actuator forces and controller bandwidth requirements) for a practical active roll control system.

The research described in this report aims to address these issues.

Chapter 2

Vehicle modelling

2.1 Introduction

Linear system models of the handling and roll dynamics of heavy vehicles are required for control system design. A systematic modelling procedure that can describe single and multiple unit vehicles is desirable. In reality, vehicle components such as tyres, springs and actuators exhibit nonlinear characteristics, and models of these components suitable for analysing the effects of nonlinearities on system stability and transient performance are also required.

2.2 Linear single unit vehicle model

The linear model used to describe the roll and handling response of a single unit vehicle to steering inputs builds on models formulated by Segel [83] and Lin [51]. Pitching and bouncing motions have only a small effect on the roll and handling behaviour of the vehicle and so can be neglected in formulating a model to investigate roll and handling performance. The effects of aerodynamic inputs (wind disturbances) and road inputs (cross-gradients, dips and bumps) are also neglected.

2.2.1 Rigid frame model

The single unit vehicle is modelled using three rigid bodies – one to represent the sprung mass, and one each for the front and rear axles – as shown in figure 2.1. For vehicles with multiple axles at the rear, these axles are combined to form a single rigid body.

The vehicle as a whole can translate longitudinally and laterally, and can yaw. The sprung mass can rotate about a horizontal axis (the *roll axis*) fixed in the unsprung masses. The location of the roll axis is dependent on the kinematic properties of the front and rear suspensions. The unsprung masses can also rotate in roll, enabling the effect of the vertical compliance of the tyres on the roll performance to be included in the model.

The equations of motion of the vehicle are formulated by equating the rates of change of momentum (or, in the rotational case, moment of momentum) with the sum of external forces (or moments) acting on the system. The motion is described using a coordinate system (x', y', z') fixed in the vehicle, as shown in figure 2.1. The roll axis is replaced by an x' axis parallel to the ground, and the z' axis passes downward through the centre of mass of the vehicle.

The suspension springs, dampers and anti-roll bars generate moments between the sprung and unsprung masses in response to roll motions. The active roll control systems at each axle consist of a pair of actuators and a series of mechanical linkages in parallel with the existing passive springs and dampers, and these roll control systems generate additional (controlled) roll moments between the sprung and unsprung masses.

The tyres produce lateral forces that vary linearly with slip angle. This assumption of linearity is reasonable for lateral motions of moderate amplitude and is discussed in further detail in section 2.4.1. The effects of aligning moment, camber thrust, roll steer and rolling resistance generated by the tyres are of secondary importance and are neglected.

The linear model assumes that the forward speed of the vehicle is constant during

any lateral manoeuvre. (Although forward speed is an important stability parameter, it is not considered to be a variable of motion.) The driving thrust remains constant and is evenly distributed between the driving wheels, so does not contribute a yaw moment about the centre of mass. Neither driving thrust nor lateral load transfer affects the lateral mechanical properties of the tyres.

The roll stiffness and damping of the vehicle suspension systems are assumed to be constant for the range of roll motions considered.

The nonlinear effects of varying speed and tyre and suspension properties on the stability and performance of the system may be considered separately.

The five equations of vehicle motion are

$$m_s h\ddot{\phi} = -mU\left(\dot{\beta}+\dot{\psi}\right) + Y_\beta\beta + Y_{\dot{\psi}}\dot{\psi} + Y_\delta\delta, \quad (2.1)$$

$$-I_{x'z'}\ddot{\phi} + I_{z'z'}\ddot{\psi} = N_\beta\beta + N_{\dot{\psi}}\dot{\psi} + N_\delta\delta, \quad (2.2)$$

$$\begin{aligned} I_{x'x'}\ddot{\phi} - I_{x'z'}\ddot{\psi} &= m_s g h\phi - m_s U h\left(\dot{\beta}+\dot{\psi}\right) \\ &\quad - k_f\left(\phi-\phi_{t,f}\right) - l_f\left(\dot{\phi}-\dot{\phi}_{t,f}\right) + u_f \\ &\quad - k_r\left(\phi-\phi_{t,r}\right) - l_r\left(\dot{\phi}-\dot{\phi}_{t,r}\right) + u_r, \end{aligned} \quad (2.3)$$

$$\begin{aligned} -r\left(Y_{\beta,f}\beta + Y_{\dot{\psi},f}\dot{\psi} + Y_{\delta,f}\delta\right) &= m_{u,f}U\left(h_{u,f}-r\right)\left(\dot{\beta}+\dot{\psi}\right) + k_{t,f}\phi_{t,f} \\ &\quad - m_{u,f}gh_{u,f}\phi_{t,f} - k_f\left(\phi-\phi_{t,f}\right) \\ &\quad - l_f\left(\dot{\phi}-\dot{\phi}_{t,f}\right) + u_f, \end{aligned} \quad (2.4)$$

$$\begin{aligned} -r\left(Y_{\beta,r}\beta + Y_{\dot{\psi},r}\dot{\psi}\right) &= m_{u,r}U\left(h_{u,r}-r\right)\left(\dot{\beta}+\dot{\psi}\right) + k_{t,r}\phi_{t,r} \\ &\quad - m_{u,r}gh_{u,r}\phi_{t,r} - k_r\left(\phi-\phi_{t,r}\right) \\ &\quad - l_r\left(\dot{\phi}-\dot{\phi}_{t,r}\right) + u_r. \end{aligned} \quad (2.5)$$

Nomenclature is detailed on pages xv–xviii. Equation (2.1) is a lateral force balance for the entire vehicle. Equation (2.2) is a yaw moment balance for the entire vehicle. Equation (2.3) describes the balance of roll moments on the sprung mass. Detailed derivations of equations (2.1)–(2.3) are given in [83] and [51]. Equations (2.4) and (2.5) describe the roll motions of the front and rear unsprung masses respectively.

These equations can more conveniently be expressed using a state space representation, which is suitable for linear systems analysis and for numerical integration:

$$\dot{x} = Ax + B_0 u + B_1 \delta \tag{2.6}$$

where

$$x = \begin{bmatrix} \beta & \dot{\psi} & \phi & \dot{\phi} & \phi_{t,f} & \phi_{t,r} \end{bmatrix}^T, \tag{2.7}$$

$$u = \begin{bmatrix} u_f & u_r \end{bmatrix}^T, \tag{2.8}$$

$$E = \begin{bmatrix} mU & 0 & 0 & m_s h & 0 & 0 \\ 0 & I_{z'z'} & 0 & -I_{x'z'} & 0 & 0 \\ m_s U h & -I_{x'z'} & 0 & I_{x'x'} & -l_f & -l_r \\ -m_{u,f} U \left(h_{u,f} - r\right) & 0 & 0 & 0 & -l_f & 0 \\ -m_{u,r} U \left(h_{u,r} - r\right) & 0 & 0 & 0 & 0 & -l_r \\ 0 & 0 & 1 & 0 & 0 & 0 \end{bmatrix}, \tag{2.9}$$

$$A = E^{-1} \begin{bmatrix} Y_\beta & Y_{\dot{\psi}} - mU & 0 \\ N_\beta & N_{\dot{\psi}} & 0 \\ 0 & -m_s h U & m_s g h - k_f - k_r \\ rY_{\beta,f} & rY_{\dot{\psi},f} + m_{u,f} U \left(h_{u,f} - r\right) & -k_f \\ rY_{\beta,r} & rY_{\dot{\psi},r} + m_{u,r} U \left(h_{u,r} - r\right) & -k_r \\ 0 & 0 & 0 \end{bmatrix}$$

$$\begin{bmatrix} 0 & 0 & 0 \\ 0 & 0 & 0 \\ -l_f - l_r & k_f & k_r \\ -l_f & k_f + k_{t,f} - m_{u,f} g h_{u,f} & 0 \\ -l_r & 0 & k_r + k_{t,r} - m_{u,r} g h_{u,r} \\ 1 & 0 & 0 \end{bmatrix}, \tag{2.10}$$

$$B_0 = E^{-1} \begin{bmatrix} 0 & 0 & 1 & 0 & 1 & 0 \\ 0 & 0 & 1 & 1 & 0 & 0 \end{bmatrix}^T, \tag{2.11}$$

$$B_1 = E^{-1} \begin{bmatrix} Y_\delta & N_\delta & 0 & rY_{\delta,f} & 0 & 0 \end{bmatrix}^T . \quad (2.12)$$

2.2.2 Flexible frame model

The model presented in section 2.2.1 assumes that the vehicle frame is a rigid body. Previous investigations into the use of active roll control systems on heavy vehicles have all used this assumption. However, torsional compliance of the vehicle frame influences the distribution of roll moments between axle groups, and significant frame compliance might be expected to affect roll and handling performance noticeably. Winkler et al. noted that "the torsional compliance of the vehicle frame stands out as a uniquely important element in establishing the roll stability of some vehicles, particularly those with flat-bed trailers" [107]. This point is illustrated clearly in figure 2.2, which shows the rear end of a torsionally compliant flat-bed trailer rolling over independently of the front end. It is essential to include the torsional flexibility of the frame in the vehicle model to predict the roll-over threshold of such vehicles accurately.

In order to represent the torsional flexibility of a vehicle frame, it is necessary either to model the frame as a series of two or more rigid bodies (interconnected by joints of appropriate torsional stiffness), or to embed a complex (finite element-based) model of the frame within the existing rigid body formulation.

Since the motivation for including the frame flexibility is only to capture the influence of compliance on the distribution of roll moments between axles, a simple model of the frame using two rigid bodies is sufficient. The sprung mass is split into front and rear sections, each with appropriate inertial properties, as shown in figure 2.3. These two sections of the sprung mass are connected with a torsional spring whose stiffness matches the torsional stiffness of the vehicle frame. The torsional spring must be sited at the centroid height of the frame, so that the line of action of the lateral shear force in the vehicle frame is properly represented. A small amount of torsional damping (5% damping ratio), representing the energy dissipation inherent in the structure of the vehicle frame, is also included. The incorporation of frame torsional flexibility

introduces an additional degree of freedom and an additional equation of motion compared to the model described in section 2.2.1. The equations of motion for the linear torsionally flexible single unit vehicle model are

$$m_{s,f}h_f\ddot{\phi}_f + m_{s,r}h_r\ddot{\phi}_r = -mU\left(\dot{\beta}+\dot{\psi}\right) + Y_\beta\beta + Y_{\dot{\psi}}\dot{\psi} + Y_\delta\delta, \quad (2.13)$$

$$-I_{x'z',f}\ddot{\phi}_f - I_{x'z',r}\ddot{\phi}_r + I_{z'z'}\ddot{\psi} = N_\beta\beta + N_{\dot{\psi}}\dot{\psi} + N_\delta\delta, \quad (2.14)$$

$$\begin{aligned} I_{x'x',f}\ddot{\phi}_f - I_{x'z',f}\ddot{\psi} &= m_{s,f}gh_f\phi_f - m_{s,f}Uh_f\left(\dot{\beta}+\dot{\psi}\right) \\ &\quad - k_f\left(\phi_f-\phi_{t,f}\right) - l_f\left(\dot{\phi}_f-\dot{\phi}_{t,f}\right) \\ &\quad - k_b\left(\phi_f-\phi_r\right) - l_b\left(\dot{\phi}_f-\dot{\phi}_r\right) \\ &\quad - F_bh_b + u_f, \end{aligned} \quad (2.15)$$

$$\begin{aligned} I_{x'x',r}\ddot{\phi}_r - I_{x'z',r}\ddot{\psi} &= m_{s,r}gh_r\phi_r - m_{s,r}Uh_r\left(\dot{\beta}+\dot{\psi}\right) \\ &\quad - k_r\left(\phi_r-\phi_{t,r}\right) - l_r\left(\dot{\phi}_r-\dot{\phi}_{t,r}\right) \\ &\quad + k_b\left(\phi_f-\phi_r\right) + l_b\left(\dot{\phi}_f-\dot{\phi}_r\right) \\ &\quad + F_bh_b + u_r, \end{aligned} \quad (2.16)$$

$$\begin{aligned} -r\left(Y_{\beta,f}\beta + Y_{\dot{\psi},f}\dot{\psi} + Y_{\delta,f}\delta\right) &= m_{u,f}U\left(h_{u,f}-r\right)\left(\dot{\beta}+\dot{\psi}\right) + k_{t,f}\phi_{t,f} \\ &\quad - m_{u,f}gh_{u,f}\phi_{t,f} - k_f\left(\phi_f-\phi_{t,f}\right) \\ &\quad - l_f\left(\dot{\phi}_f-\dot{\phi}_{t,f}\right) + u_f, \end{aligned} \quad (2.17)$$

$$\begin{aligned} -r\left(Y_{\beta,r}\beta + Y_{\dot{\psi},r}\dot{\psi}\right) &= m_{u,r}U\left(h_{u,r}-r\right)\left(\dot{\beta}+\dot{\psi}\right) + k_{t,r}\phi_{t,r} \\ &\quad - m_{u,r}gh_{u,r}\phi_{t,r} - k_r\left(\phi_r-\phi_{t,r}\right) \\ &\quad - l_r\left(\dot{\phi}_r-\dot{\phi}_{t,r}\right) + u_r. \end{aligned} \quad (2.18)$$

The lateral shear force in the vehicle frame F_b is given by

$$F_b = \left(Y_{\beta,f}\beta + Y_{\dot{\psi},f}\dot{\psi} + Y_{\delta,f}\delta\right) - m_fU\left(\dot{\beta}+\dot{\psi}\right) - m_{s,f}h_f\ddot{\phi}_f. \quad (2.19)$$

These equations can also be expressed in a state space representation similar to equations (2.6)–(2.12).

2.3 Linear multiple unit vehicle model

Linear models of multiple unit articulated heavy vehicles can be assembled using modified versions of the single unit equations of motion presented in section 2.2. The modifications are necessary to account for the forces and moments applied between adjacent vehicle units through the couplings. An additional equation to describe the kinematic constraint between adjacent vehicle units is required at each coupling.

The velocity vector $\mathbf{U}_{\mathbf{O_i}}$ of the articulation point can be expressed in the frames of reference of both the leading unit i and the trailing unit $i+1$:

$$\mathbf{U}_{\mathbf{O_i,i}} = U\mathbf{i_i} + \left(U\beta_i - (r_i - h_{a,r,i})\dot{\phi}_{r,i} + b'_{r,i}\dot{\psi}_i\right)\mathbf{j_i}, \tag{2.20}$$

$$\mathbf{U}_{\mathbf{O_i,i+1}} = U\mathbf{i_{i+1}} + \left(U\beta_{i+1} - (r_{i+1} - h_{a,f,i+1})\dot{\phi}_{f,i+1} + b'_{f,i+1}\dot{\psi}_{i+1}\right)\mathbf{j_{i+1}}. \tag{2.21}$$

A detailed derivation may be found in [51]. Figure 2.4 shows the dimensions needed to describe the kinematic constraint between a tractor unit ($i = 1$) and a semi-trailer ($i = 2$). After applying the coordinate transformation $(\mathbf{i_i}, \mathbf{j_i}, \mathbf{k_i}) \rightarrow (\mathbf{i_{i+1}}, \mathbf{j_{i+1}}, \mathbf{k_{i+1}})$, the kinematic constraint equation is

$$\beta_i - \beta_{i+1} - \frac{(r_i - h_{a,r,i})}{U}\dot{\phi}_{f,i} + \frac{(r_{i+1} - h_{a,f,i+1})}{U}\dot{\phi}_{r,i+1} + \frac{b'_{r,i}}{U}\dot{\psi}_i - \frac{b'_{f,i+1}}{U}\dot{\psi}_{i+1} + \psi_i - \psi_{i+1} = 0. \tag{2.22}$$

Several additional forces and moments, transmitted through couplings between adjacent vehicle units, affect the handling and roll responses of interconnected vehicle units:

- lateral forces $F_{c,i-1}$ and $F_{c,i}$ at the couplings,
- roll torques $(r_i - h_{a,f,i})F_{c,i-1}$ and $(r_i - h_{a,r,i})F_{c,i}$ on the sprung mass due to the moments of the lateral coupling forces about the roll axis,
- roll torques $k_{\phi,i-1}(\phi_{r,i-1} - \phi_{f,i})$ and $k_{\phi,i}(\phi_{r,i} - \phi_{f,i+1})$ on the sprung mass due to the roll stiffness of the couplings and the relative roll angles between adjacent vehicle units,

- yaw torques $b'_{f,i}F_{c,i-1}$ and $b'_{r,i}F_{c,i}$ due to the moments of the lateral coupling forces about the centre of mass,

- yaw torques $k_{\psi,i-1}(\psi_{i-1}-\psi_i)$ and $k_{\psi,i}(\psi_i-\psi_{i+1})$ due to the yaw stiffness of the couplings and the articulation angles between adjacent vehicle units.

These additional forces and moments are included in the modified equations of motion for a vehicle unit i, joined at couplings $i-1$ and i to vehicle units $i-1$ and $i+1$ respectively:

$$\begin{aligned}
m_{s,f,i}h_{f,i}\ddot{\phi}_{f,i}+m_{s,r,i}h_{r,i}\ddot{\phi}_{r,i} &= -m_iU\left(\dot{\beta}_i+\dot{\psi}_i\right)+Y_{\beta,i}\beta_i+Y_{\dot{\psi},i}\dot{\psi}_i \\
&\quad +Y_{\delta,i}\delta_i+F_{y,i-1}-F_{y,i}, \qquad (2.23)\\
-I_{x'z',f,i}\ddot{\phi}_{f,i}-I_{x'z',r,i}\ddot{\phi}_{r,i}+I_{z'z',i}\ddot{\psi}_i &= N_{\beta,i}\beta_i+N_{\dot{\psi},i}\dot{\psi}_i+N_{\delta,i}\delta_i \\
&\quad +b'_{f,i}F_{y,i-1}+k_{\psi,i-1}\left(\psi_{i-1}-\psi_i\right) \\
&\quad -b'_{r,i}F_{y,i}-k_{\psi,i}\left(\psi_i-\psi_{i+1}\right), \qquad (2.24)\\
I_{x'x',f,i}\ddot{\phi}_{f,i}-I_{x'z',f,i}\ddot{\psi}_{f,i} &= m_{s,f,i}gh_{f,i}\phi_{f,i}-m_{s,f,i}Uh_{f,i}\left(\dot{\beta}_i+\dot{\psi}_i\right) \\
&\quad -k_{f,i}\left(\phi_{f,i}-\phi_{t,f,i}\right)-l_{f,i}\left(\dot{\phi}_{f,i}-\dot{\phi}_{t,f,i}\right) \\
&\quad -k_{b,i}\left(\phi_{f,i}-\phi_{r,i}\right)-l_{b,i}\left(\dot{\phi}_{f,i}-\dot{\phi}_{r,i}\right) \\
&\quad +k_{\phi,i-1}\left(\phi_{r,i-1}-\phi_{f,i}\right)-\left(r_i-h_{a,f,i}\right)F_{y,i-1} \\
&\quad -F_{b,i}h_{b,i}+u_{f,i}, \qquad (2.25)\\
I_{x'x',r,i}\ddot{\phi}_{r,i}-I_{x'z',r,i}\ddot{\psi}_i &= m_{s,r,i}gh_{r,i}\phi_{r,i}-m_{s,r,i}Uh_{r,i}\left(\dot{\beta}_i+\dot{\psi}_i\right) \\
&\quad -k_{r,i}\left(\phi_{r,i}-\phi_{t,r,i}\right)-l_{r,i}\left(\dot{\phi}_{r,i}-\dot{\phi}_{t,r,i}\right) \\
&\quad +k_{b,i}\left(\phi_{f,i}-\phi_{r,i}\right)+l_{b,i}\left(\dot{\phi}_{f,i}-\dot{\phi}_{r,i}\right) \\
&\quad -k_{\phi,i}\left(\phi_{r,i}-\phi_{f,i+1}\right)+\left(r_i-h_{a,r,i}\right)F_{y,i} \\
&\quad +F_{b,i}h_{b,i}+u_{r,i}, \qquad (2.26)\\
-r_i\left(Y_{\beta,f,i}\beta_i+Y_{\dot{\psi},f,i}\dot{\psi}_i+Y_{\delta,f,i}\delta_i\right) &= m_{u,f,i}U\left(h_{u,f,i}-r_i\right)\left(\dot{\beta}_i+\dot{\psi}_i\right)+k_{t,f,i}\phi_{t,f,i} \\
&\quad -m_{u,f,i}gh_{u,f,i}\phi_{t,f,i}-k_{f,i}\left(\phi_{f,i}-\phi_{t,f,i}\right) \\
&\quad -l_{f,i}\left(\dot{\phi}_{f,i}-\dot{\phi}_{t,f,i}\right)+u_{f,i}, \qquad (2.27)
\end{aligned}$$

$$
\begin{aligned}
-r_i\left(Y_{\beta,r,i}\beta_i + Y_{\dot{\psi},r,i}\dot{\psi}_i\right) &= m_{u,r,i}U\left(h_{u,r,i} - r_i\right)\left(\dot{\beta}_i + \dot{\psi}_i\right) + k_{t,r,i}\phi_{t,r,i} \\
&\quad - m_{u,r,i}gh_{u,r,i}\phi_{t,r,i} - k_{r,i}\left(\phi_{r,i} - \phi_{t,r,i}\right) \\
&\quad - l_{r,i}\left(\dot{\phi}_{r,i} - \dot{\phi}_{t,r,i}\right) + u_{r,i}. \qquad (2.28)
\end{aligned}
$$

The lateral shear force in the vehicle frame $F_{b,i}$ is given by

$$
\begin{aligned}
F_{b,i} &= F_{y,i-1} + \left(Y_{\beta,f,i}\beta + Y_{\dot{\psi},f,i}\dot{\psi}_i + Y_{\delta,f,i}\delta_i\right) \\
&\quad - m_{f,i}U\left(\dot{\beta}_i + \dot{\psi}_i\right) - m_{s,f,i}h_{f,i}\ddot{\phi}_{f,i}. \qquad (2.29)
\end{aligned}
$$

2.3.1 Assembly of equations of motion

The assembly of the equations of motion for a long combination vehicle uses a procedure that is valid for an arbitrarily large number of vehicle units. The equations of motion for an n unit vehicle are formed by writing the equations of motion (2.23)–(2.28) for each vehicle unit $i = 1, \ldots, n$ and the constraint equation (2.22) for each vehicle coupling $i = 1, \ldots, n-1$. Note that, for vehicle units $i = 1, \ldots, n-1$, the lateral force equation (2.23) is used only indirectly to obtain an expression for the (dependent) lateral coupling force F_c in terms of the independent variables of motion. This assembly procedure lends itself particularly well to implementation in software.

The equations of motion for a two axle tractor two axle semi-trailer combination can be assembled to illustrate the procedure outlined above.

The five independent equations of motion for the tractor unit are

$$
\begin{aligned}
-I_{x'z',f,1}\ddot{\phi}_{f,1} - I_{x'z',r,1}\ddot{\phi}_{r,1} + I_{z'z',1}\ddot{\psi}_1 &= N_{\beta,1}\beta_1 + N_{\dot{\psi},1}\dot{\psi}_1 + N_{\delta,1}\delta \\
&\quad - b'_{r,1}F_{y,1} - k_{\psi,1}\left(\psi_1 - \psi_2\right), \qquad (2.30) \\
I_{x'x',f,1}\ddot{\phi}_{f,1} - I_{x'z',f,1}\ddot{\psi}_1 &= m_{s,f,1}gh_{f,1}\phi_{f,1} - m_{s,f,1}Uh_{f,1}\left(\dot{\beta}_1 + \dot{\psi}_1\right) \\
&\quad - k_{f,1}\left(\phi_{f,1} - \phi_{t,f,1}\right) - l_{f,1}\left(\dot{\phi}_{f,1} - \dot{\phi}_{t,f,1}\right) \\
&\quad - k_{b,1}\left(\phi_{f,1} - \phi_{r,1}\right) - l_{b,1}\left(\dot{\phi}_{f,1} - \dot{\phi}_{r,1}\right) \\
&\quad - F_{b,1}h_{b,1} + u_{f,1}, \qquad (2.31)
\end{aligned}
$$

$$
\begin{aligned}
I_{x'x',r,1}\ddot{\phi}_{r,1} - I_{x'z',r,1}\ddot{\psi}_1 &= m_{s,r,1}gh_{r,1}\phi_{r,1} - m_{s,r,1}Uh_{r,1}\left(\dot{\beta}_1 + \dot{\psi}_1\right) \\
&\quad - k_{r,1}\left(\phi_{r,1} - \phi_{t,r,1}\right) - l_{r,1}\left(\dot{\phi}_{r,1} - \dot{\phi}_{t,r,1}\right) \\
&\quad + k_{b,1}\left(\phi_{f,1} - \phi_{r,1}\right) + l_{b,1}\left(\dot{\phi}_{f,1} - \dot{\phi}_{r,1}\right) \\
&\quad - k_{\phi,1}\left(\phi_{r,1} - \phi_{f,2}\right) + (r_1 - h_{a,r,1})F_{y,1} \\
&\quad + F_{b,1}h_{b,1} + u_{r,1}, \qquad (2.32) \\
-r_1\left(Y_{\beta,f,1}\beta_1 + Y_{\dot{\psi},f,1}\dot{\psi}_1 + Y_{\delta,f,1}\delta_1\right) &= m_{u,f,1}U\left(h_{u,f,1} - r_1\right)\left(\dot{\beta}_1 + \dot{\psi}_1\right) + k_{t,f,1}\phi_{t,f,1} \\
&\quad - m_{u,f,1}gh_{u,f,1}\phi_{t,f,1} - k_{f,1}\left(\phi_{f,1} - \phi_{t,f,1}\right) \\
&\quad - l_{f,1}\left(\dot{\phi}_{f,1} - \dot{\phi}_{t,f,1}\right) + u_{f,1}, \qquad (2.33) \\
-r_1\left(Y_{\beta,r,1}\beta + Y_{\dot{\psi},r,1}\dot{\psi}_1\right) &= m_{u,r,1}U\left(h_{u,r,1} - r_1\right)\left(\dot{\beta}_1 + \dot{\psi}_1\right) + k_{t,r,1}\phi_{t,r,1} \\
&\quad - m_{u,r,1}gh_{u,r,1}\phi_{t,r,1} - k_{r,1}\left(\phi_{r,1} - \phi_{t,r,1}\right) \\
&\quad - l_r\left(\dot{\phi}_{r,1} - \dot{\phi}_{t,r,1}\right) + u_{r,1}. \qquad (2.34)
\end{aligned}
$$

The internal, dependent, lateral forces $F_{y,1}$ and $F_{b,1}$ can be expressed in terms of the independent variables of motion:

$$
\begin{aligned}
F_{y,1} &= -m_{s,f,1}h_{f,1}\ddot{\phi}_{f,1} - m_{s,r,1}h_{r,1}\ddot{\phi}_{r,1} - m_1U\left(\dot{\beta}_1 + \dot{\psi}_1\right) \\
&\quad + Y_{\beta,1}\beta_1 + Y_{\dot{\psi},1}\dot{\psi}_1 + Y_{\delta,1}\delta_1, \qquad (2.35) \\
F_{b,1} &= \left(Y_{\beta,f,1}\beta + Y_{\dot{\psi},f,1}\dot{\psi}_1 + Y_{\delta,f,1}\delta_1\right) - m_{f,1}U\left(\dot{\beta}_1 + \dot{\psi}_1\right) \\
&\quad - m_{s,f,1}h_{f,1}\ddot{\phi}_{f,1}. \qquad (2.36)
\end{aligned}
$$

The kinematic constraint at the vehicle coupling is described by

$$
\beta_1 - \beta_2 - \frac{(r_1 - h_{a,r,1})}{U}\dot{\phi}_{r,1} + \frac{(r_2 - h_{a,f,2})}{U}\dot{\phi}_2 + \frac{b'_{r,1}}{U}\dot{\psi}_1 - \frac{b'_{f,2}}{U}\dot{\psi}_2 + \psi_1 - \psi_2 = 0. \quad (2.37)
$$

The system of equations is completed by four independent equations of motion for the semi-trailer unit:

$$
-I_{x'z',2}\ddot{\phi}_2 + I_{z'z',2}\ddot{\psi}_2 = N_{\beta,2}\beta_2 + N_{\dot{\psi},2}\dot{\psi}_2 + b'_{f,2}F_{y,1} + k_{\psi,1}\left(\psi_1 - \psi_2\right), \quad (2.38)
$$

$$
\begin{aligned}
I_{x'x',2}\ddot{\phi}_2 - I_{x'z',2}\ddot{\psi}_2 &= m_{s,2}gh_2\phi_2 - m_{s,2}Uh_2\left(\dot{\beta}_2 + \dot{\psi}_2\right) \\
&\quad - k_{r,2}\left(\phi_2 - \phi_{t,r,2}\right) - l_{r,2}\left(\dot{\phi}_2 - \dot{\phi}_{t,r,2}\right) \\
&\quad + k_{\phi,1}\left(\phi_{r,1} - \phi_2\right) - (r_2 - h_{a,f,2})F_{y,1} + u_{r,2}, \quad (2.39) \\
-r_2\left(Y_{\beta,2}\beta_2 + Y_{\dot{\psi},2}\dot{\psi}_2\right) &= m_{u,r,2}U\left(h_{u,r,2} - r_2\right)\left(\dot{\beta}_2 + \dot{\psi}_2\right) + k_{t,r,2}\phi_{t,r,2} \\
&\quad - m_{u,r,2}gh_{u,r,2}\phi_{t,r,2} - k_{r,2}\left(\phi_2 - \phi_{t,r,2}\right) \\
&\quad - l_r\left(\dot{\phi}_2 - \dot{\phi}_{t,r,2}\right) + u_{r,2}, \quad (2.40) \\
m_{s,2}h_2\ddot{\phi}_2 &= -m_2U\left(\dot{\beta}_2 + \dot{\psi}_2\right) + Y_{\beta,2}\beta_2 + Y_{\dot{\psi},2}\dot{\psi}_2 + F_{y,1}. \quad (2.41)
\end{aligned}
$$

Note that, in the above equations of motion, the sprung mass of the semi-trailer has a single degree of freedom. The motivation for including the torsional flexibility of the vehicle frame is to account for its influence on roll moment distribution among axles. Since the semi-trailer features axles only at the rear of the vehicle, the sprung mass of the semi-trailer is modelled as a single rigid body, and the coupling stiffness k_ϕ represents the combined torsional compliance of the coupling and the semi-trailer frame between the hitch point and the semi-trailer axles. There is just a single equation to describe the roll motion of the unsprung mass of a semi-trailer, since all axles are located at the rear of the vehicle unit.

2.3.2 Parametrisation of vehicle couplings

The parametrisation of the vehicle couplings using the distances b'_f, b'_r, $h_{a,f}$ and $h_{a,r}$ and the stiffnesses k_ϕ and k_ψ enables the representation of a range of coupling configurations. Specifically, it is possible to represent the three common heavy vehicle coupling types – A-type (pintle hitch), B-type (fifth wheel) and C-type (draw bar) – within this modelling framework by making appropriate choices of these distances and stiffnesses.

2.4 Nonlinear extensions to linear models

Simplified models of the nonlinear characteristics of tyres and suspensions, sufficient for analysing the effect of nonlinearities on roll stability and vehicle handling, are presented below.

2.4.1 Nonlinear tyre behaviour

The nonlinear variation of tyre cornering stiffness F_y/α with vertical load F_z was discussed in detail in section 1.3.1 and is typically described using the quadratic equation

$$\frac{F_y}{\alpha} = c_1 \times F_z + c_2 \times {F_z}^2 \tag{2.42}$$

where c_1 and c_2 are constants. This equation is generally suitable for lateral accelerations up to the roll-over point and is widely used in heavy vehicle simulation studies [25]. A plot of tyre cornering stiffness against vertical load for a typical truck tyre is shown in figure 2.5.

2.4.2 Nonlinear suspension behaviour

The dominant nonlinear feature of the suspension behaviour occurs when the suspension roll angle reaches the maximum allowable angle. At this point the axles come into contact with the solid rubber bump stops, causing the roll stiffness to increase dramatically. This nonlinearity is captured with a piece-wise linear model, using the nominal value of suspension stiffness for roll angles below the maximum allowable value and a much greater stiffness (several orders of magnitude greater) for roll angles exceeding the maximum allowable value.

The springs and dampers also exhibit certain nonlinear force-deflection and force-velocity behaviours respectively. These behaviours are highly component-specific and are modelled using fitted data provided by the manufacturers. The geometric nonlinearity between wheel deflection and spring or damper deflection is a function of the

kinematics of the suspension linkages.

For stability analysis it is necessary to verify the dynamic stability of the vehicle for the maximum and minimum values of roll stiffness and roll damping. For simulation of transient performance, a simplified representation of roll stiffness and roll damping as a function of roll angle can be used. It is important to note, however, that the effects of component and geometric nonlinearities on roll stiffness and roll damping in percentage terms are typically small, particularly for air suspensions.

2.5 Active roll control system model

The active roll control system at an axle group generates a roll moment between the sprung and unsprung masses in response to a demand signal from the controller. Figure 2.6 shows how the dynamics of the roll control system (as described by the transfer function G_{arcs} from the moment demanded to the moment generated) affect the closed-loop stability and performance of the controlled vehicle.

2.5.1 Components and arrangement

A general arrangement of an active roll control system suitable for non-driven axles of heavy vehicles is shown in figure 2.7. This system was designed by Pratt, McKevitt et al. for a semi-trailer [59, 71]. The system is based on a conventional trailing arm suspension. Air springs between the trailing arms and the vehicle frame provide ride suspension and passive roll stiffness. A stiff U-shaped anti-roll bar is connected to the trailing arms directly and to the vehicle frame by a pair of double-acting hydraulic actuators. The position of the anti-roll bar is therefore determined by both the wheel positions and the actuator positions. Figure 2.7(b) illustrates how, by extending one actuator and retracting the other, it is possible to apply a roll moment to the sprung mass and tilt the vehicle body. A triaxle semi-trailer suspension has been built using this concept and is currently being commissioned [78].

The hydraulic actuators and servo-valves were sized according to two criteria:

- *Steady-state response:* The actuators can provide sufficient force to hold the sprung mass at maximum roll angle during steady cornering at 0.5 g.

- *Dynamic response:* The actuators can provide sufficient force and the servo-valves can supply fluid at a sufficient rate to oscillate the sprung mass sinusoidally to the limits of maximum roll angle at 1 Hz.

2.5.2 Controller architecture

For practical reasons of distributing computational load and ensuring fail-safety, the active roll control system uses a hierarchical control architecture [79, 94]. A top-level *global* controller uses signals from on-board instrumentation and an internal model of the vehicle dynamics to calculate the active roll torque required at each axle group, and a *local* controller at each axle group regulates the displacement of the servo-valve spools to provide the torque demanded. The global and local controllers communicate via a CAN (control area network) bus.

A detailed model of all mechanical and hydraulic components of the active roll control system is necessary for designing this local controller. However a reduced order model of the transfer function G_{arcs} is appropriate for designing the global contoller (see figure 2.6).

Section 2.5.3 reviews the modelling strategies used by McKevitt [59] for performing a detailed design of the local controller for a tractor semi-trailer roll control system. The purpose is to identify an appropriate characteristic form of the reduced order model (see section 2.5.4) for use in the design of the global controller.

2.5.3 Detailed system model

The active roll control system regulates the forces in the hydraulic actuators to track the roll moment u_{ref} demanded by the global controller. Force regulation is achieved by controlling the servo-valves that govern the flow of hydraulic fluid into and out of each actuator. The active roll control system must also regulate the position of the

floating anti-roll bar such that the bar remains in the centre of the actuator travel, clear of the road below and the vehicle frame above. The bar remains central on average if the actuator displacements are equal and opposite; however, a feedback mechanism is required to eliminate the effects of drift.

McKevitt developed a comprehensive model of the roll moment controller, as shown in figure 2.8. The actuator controller, which is located inside the roll moment control feedback loop, is shown in more detail in figure 2.9.

Actuator displacement control

The transfer function G_a from the actuator displacement demanded $x_{a,ref}$ to the displacement generated x_a depends on the dynamics of the actuator and anti-roll bar G_{act} and the frequency response of the servo-valve G_{valve}, as shown in figure 2.9. McKevitt used displacement feedback, a feedback controller K_{act} and a pre-filter K_{xpf} to shape the dynamics of G_a.

The actuator-load model used was a valve-controlled piston driving an inertial load through a spring and damper, derived by Merritt [60] (see figure 2.10(a)). The inertial load was set proportional to the moment of inertia of the anti-roll bar and the spring stiffness was proportional to the effective torsional stiffness of the anti-roll bar (see figure 2.10(b)). Damping in the rubber bushes at the bar ends was neglected.

Using a result from Merritt, McKevitt described the dynamics G_{act} from the displacement of the servo-valve spool to the actuator displacement x_a using a third order transfer function. The locations of the poles of this transfer function depend on the linearised servo-valve coefficients, the piston area, the volume and bulk modulus of compressed oil, the inertial load and the spring stiffness. For appropriate parameter values, the transfer function has one low frequency real pole and two lightly damped poles near the (very high) hydraulic natural frequency. The frequency response of the servo-valve G_{valve} was modelled using a second order low-pass filter with a cut-off frequency of 15 Hz. The constant gain K_4 maps the demand actuator displacement $x_{a,ref}$ to servo-valve spool displacement.

McKevitt used a proportional-integral controller K_{act} and a lead-lag pre-filter K_{xpf} to shape the response of G_a. He tuned the controller gains so that the system performed well for a step input, providing acceptable displacement tracking performance with zero overshoot and without exceeding the maximum allowable flow rate through the servo-valves. Overshoot is highly undesirable as it increases actuator stroke requirements; the requirement for zero overshoot is the design criterion that most limits the achievable bandwidth of G_a.

Roll moment control

The transfer function G_{arcs} from the roll moment demanded u_{ref} to the moment generated u depends on the vehicle roll dynamics G_{roll} and the actuator dynamics G_a, as shown in figure 2.8. McKevitt used roll moment feedback, a feedback controller K_u and a pre-filter K_{upf} to shape the dynamics of G_{arcs}.

He used a simplified model of the roll-plane dynamics with two degrees of freedom: the roll angles of the body and the anti-roll bar. The constant gain K_1, which depends on the suspension geometry and the anti-roll bar stiffness, maps the demand roll moment u_{ref} to a required actuator displacement. K_2 maps actuator displacement to anti-roll bar roll angle, and K_3 is the roll stiffness of the anti-roll bar. The actuator dynamics G_a were described previously.

He used a proportional-integral-derivative controller K_u and a lag pre-filter K_{upf} to shape the response of G_{arcs} to a step input. The controller gains were selected to provide acceptable roll moment tracking performance without excessive actuator displacement overshoot or servo-valve flow rates. He showed that actuator overshoot and high instantaneous flow rates were effectively avoided by using a relatively slow (1 Hz) first order lag pre-filter

$$K_{upf} = \frac{2\pi}{s + 2\pi} \tag{2.43}$$

on the roll moment demand signal. The low bandwidth of this pre-filter smooths the roll moment and actuator displacement responses and reduces peak servo-valve flow

rate requirements, all at the expense of a reduction in rise time.

2.5.4 Reduced order system model

The frequency response of McKevitt's local controller is dominated by the dynamics of the pre-filter K_{upf}, which are significantly slower than the dynamics of the actuators and servo-valves and the roll dynamics of the vehicle. Such a slow pre-filter is required to prevent overshoot in the actuator displacement response and excessive peak flow rates through the servo-valves.

Therefore a reasonable low order description of the frequency response of the active roll control system (G_{arcs} in figure 2.6) is

$$G_{arcs} = \frac{u}{u_{ref}} = \frac{\omega}{s+\omega}, \tag{2.44}$$

where ω is the cut-off frequency of the roll moment pre-filter in rad/s. This simplification is used extensively throughout this report.

The higher the value of ω, the faster the response of the active roll control system. However the dynamics of the actuators, the maximum flow rate through the servo-valves and the roll-plane dynamics of the vehicle all influence the achievable system bandwidth.

2.6 Conclusions

1. A linearised model for the handling and roll performance of a torsionally flexible single unit vehicle has been developed.

2. A technique for coupling multiple single unit models to form a model of an arbitrarily long combination vehicle has been presented. A range of vehicle couplings can be modelled within this framework.

3. The linear models can be described in state space form, which is particularly

suitable for control system design and numerical integration.

4. The cornering stiffness of pneumatic tyres varies with vertical load. A simplified tyre model can be used to investigate the influence of this effect on vehicle handling stability and performance.

5. Limits on hydraulic actuator response and flow rate through the servo-valves strongly influence the performance characteristics of the active roll control system. A simplified system model to investigate the effects of actuator performance limitations has been presented.

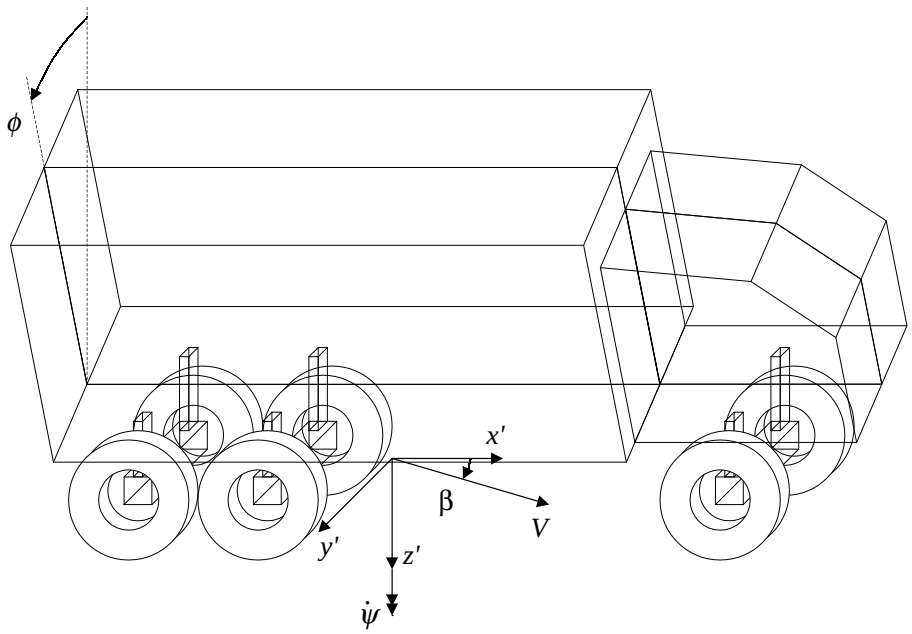

Figure 2.1: Single unit vehicle with rigid frame (ϕ measured from vertical).

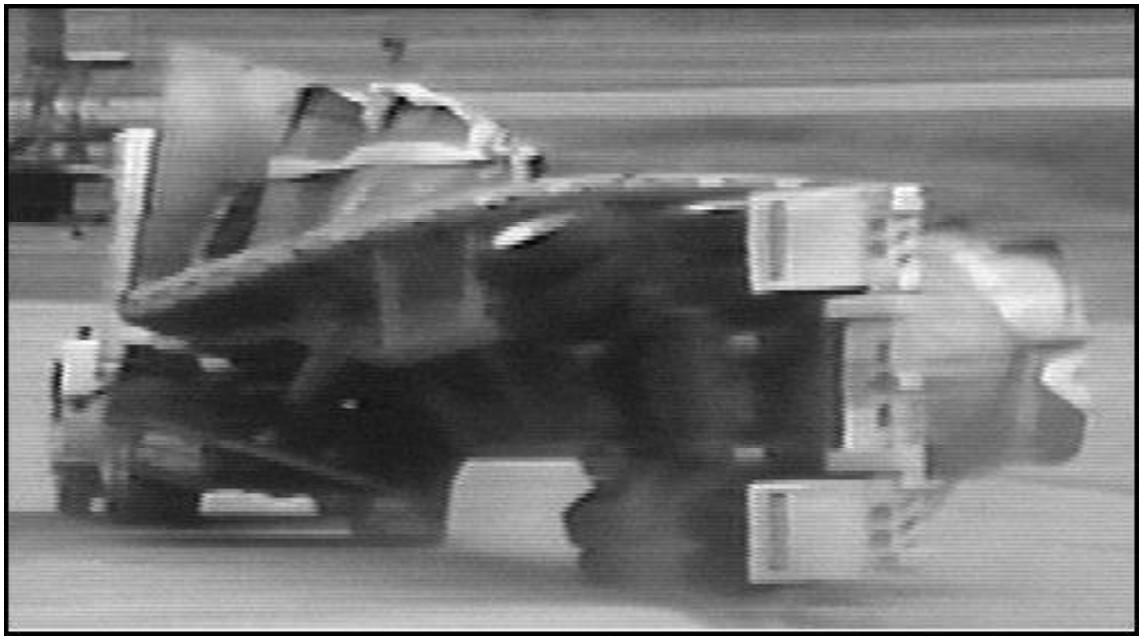

Figure 2.2: The rear end of a torsionally compliant flat-bed trailer rolls over independently of the front end [107].

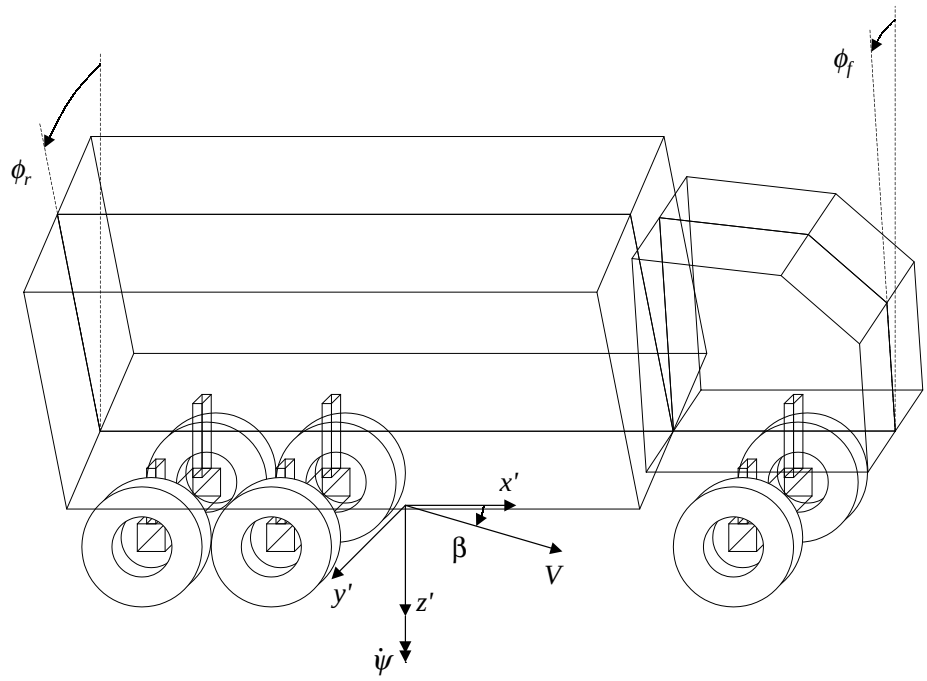

Figure 2.3: Single unit vehicle with flexible frame (ϕ_f, ϕ_r measured from vertical).

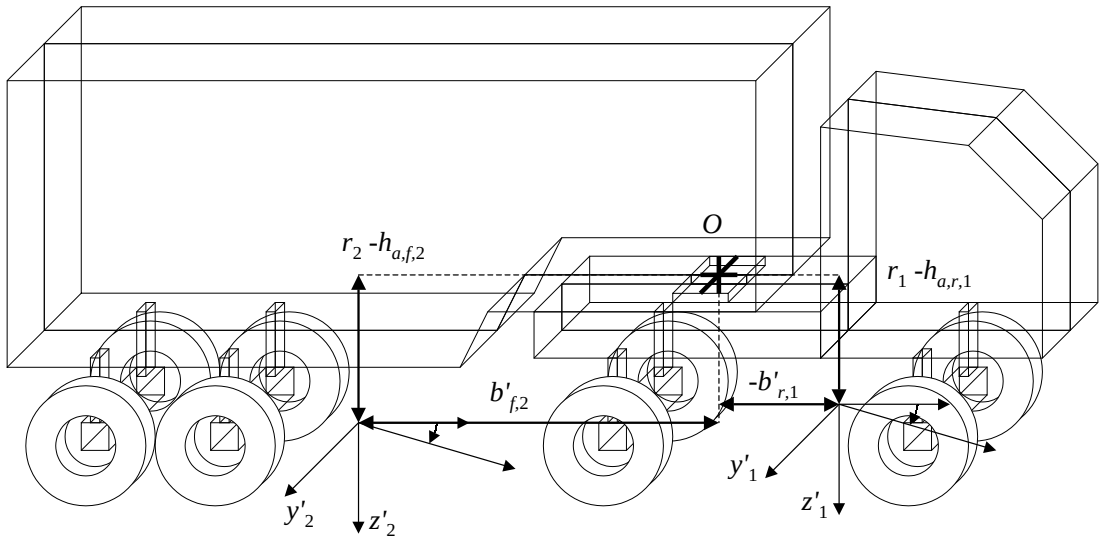

Figure 2.4: Coordinate systems used to describe the kinematic constraint at vehicle couplings.

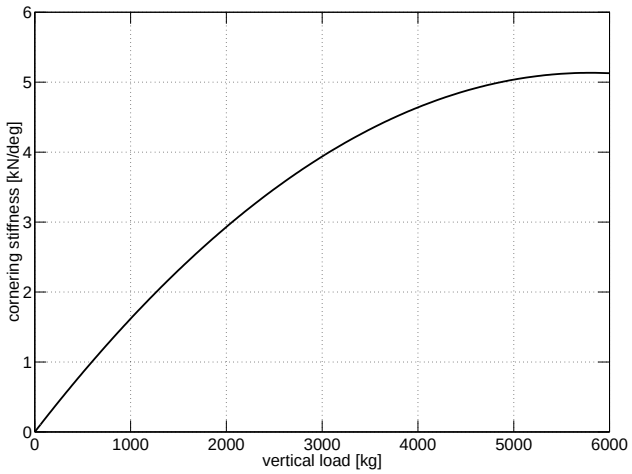

Figure 2.5: Truck tyre cornering stiffness as a function of vertical load. Parameter values in equation 2.42: $c_1 = 0.181\ \mathrm{deg}^{-1}$, $c_2 = -1.59 \times 10^{-6}\ \mathrm{N}^{-1}.\mathrm{deg}^{-1}$.

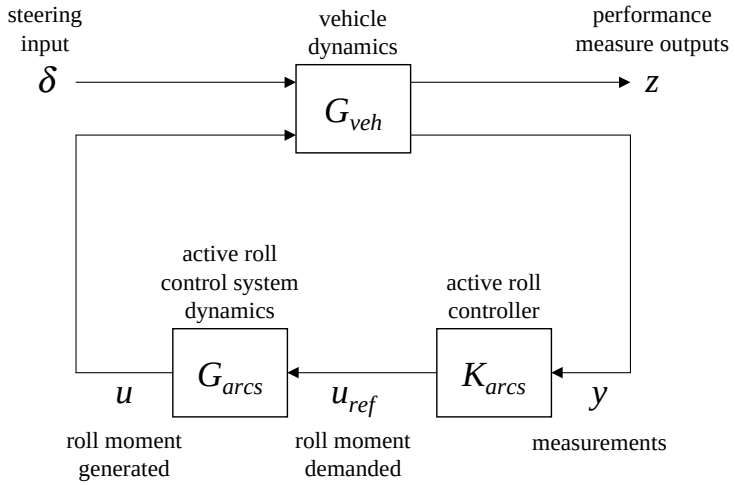

Figure 2.6: Active roll control system architecture.

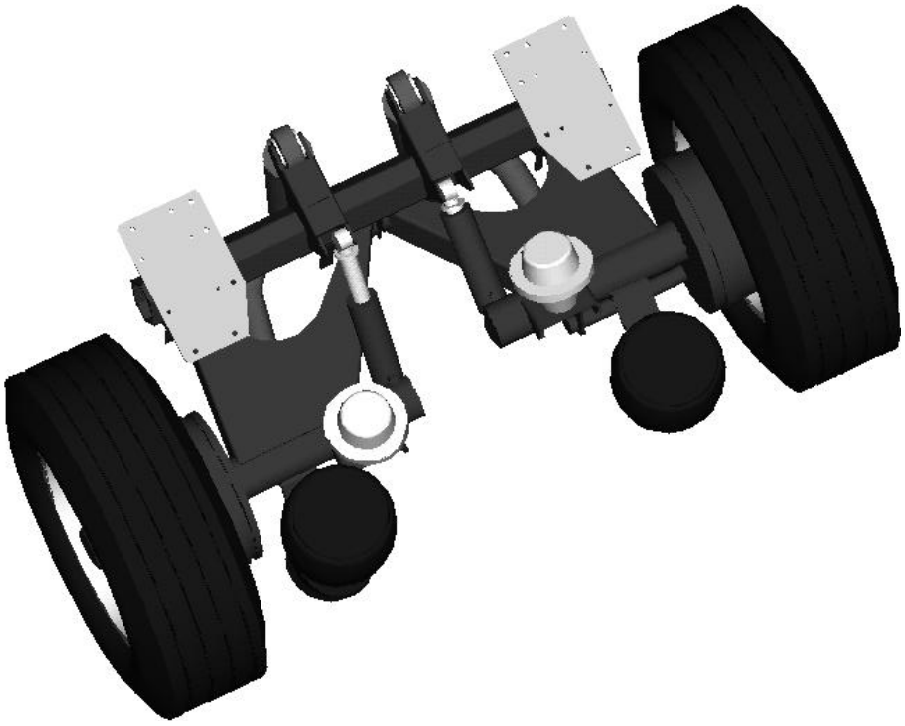

(a) Plan view.

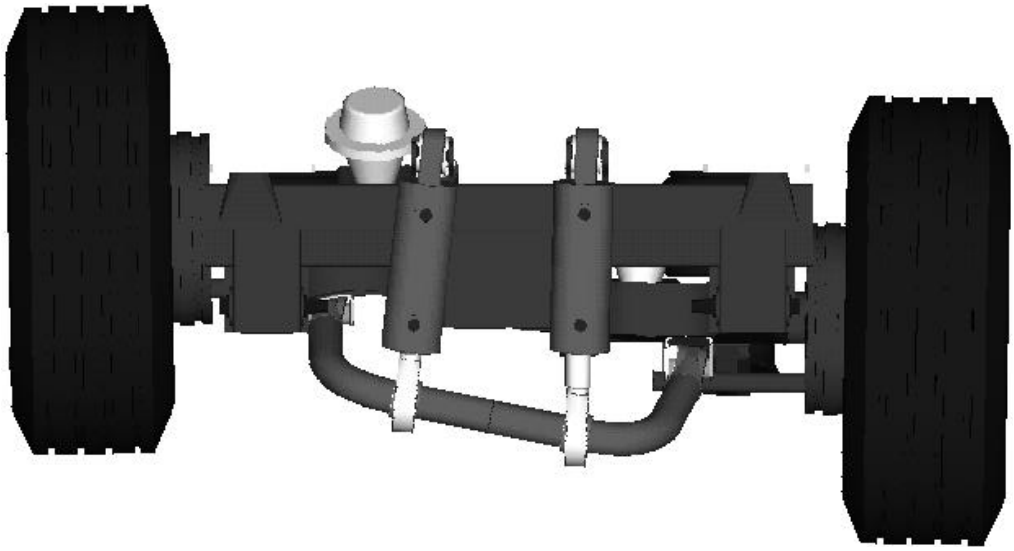

(b) Front elevation.

Figure 2.7: Active anti-roll bar general arrangement [59].

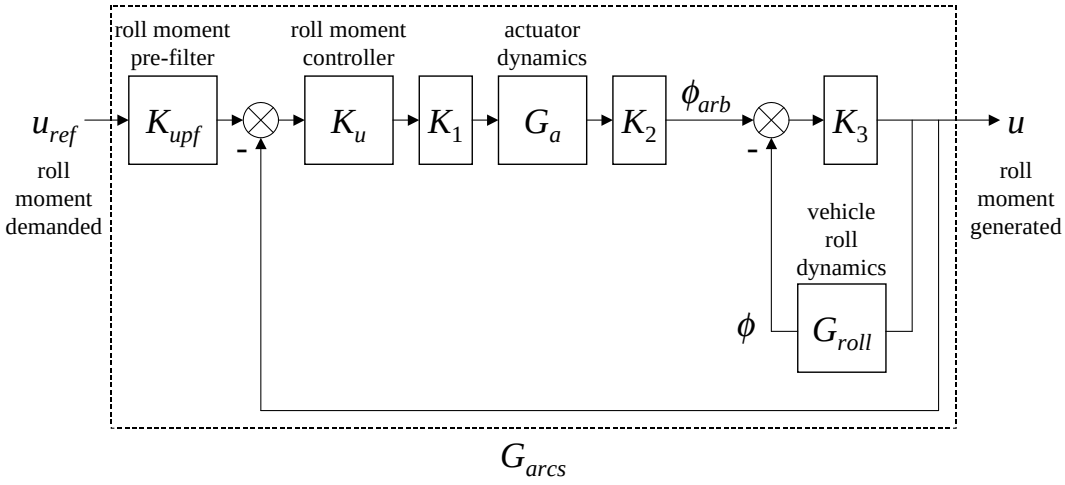

Figure 2.8: Roll moment control block diagram [59].

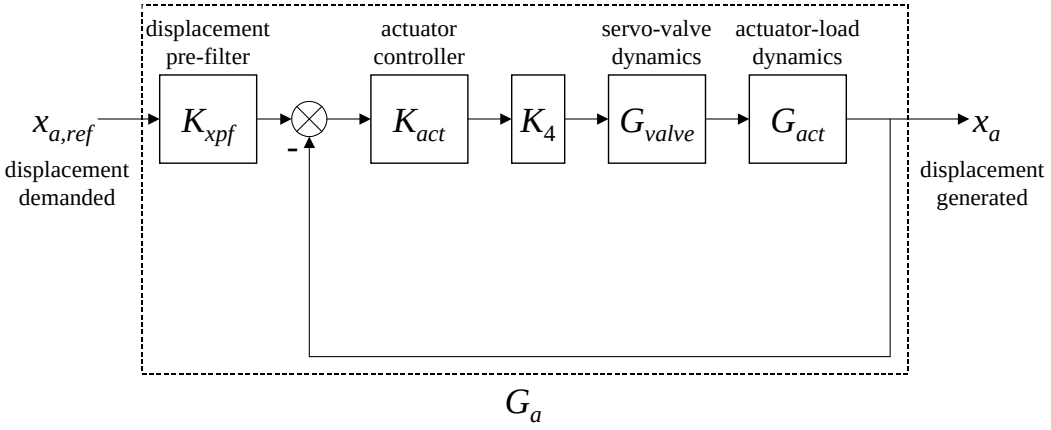

Figure 2.9: Actuator control block diagram [59].

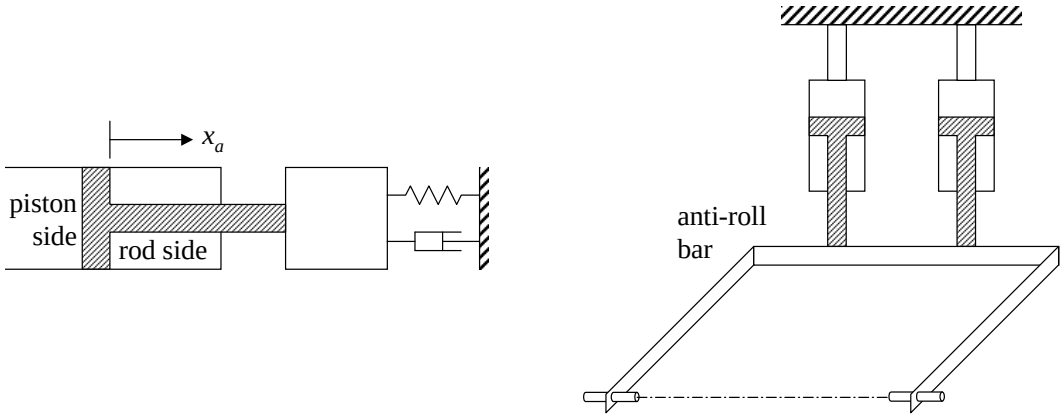

(a) Valve-controlled piston [60].

(b) Actuator load [59].

Figure 2.10: Actuator dynamics model.

Chapter 3

Achievable roll stability

3.1 Introduction

In order to design systems that improve the roll stability of heavy vehicles, it is first necessary to study the mechanics of the roll-over process. It is then possible to identify mechanisms by which active anti-roll bars can be used to improve roll stability. There are limits to achievable roll stability that are inherent in any vehicle (as opposed to being inherent in some particular controller structure, for example). By understanding these limits, it is possible to formulate a set of achievable objectives for the control system design and to measure the performance of a candidate controller against the best achievable performance.

3.2 The roll-over threshold

For a vehicle travelling on a level, paved highway, the main inputs that can cause roll-over are the lateral forces on the tyres during cornering. The effects of cross winds, excessive road camber and irregularities in the road surface are of secondary importance and are neglected here.

The accepted method for quantifying roll stability is to use the *roll-over threshold*.

Definition 3.1 (Roll-over threshold) *The roll-over threshold is the limit of steady-state lateral acceleration that a vehicle can sustain without losing roll stability.*

Accident statistics for heavy vehicles show a strong correlation between low static roll stability (that is, low roll-over threshold) and the likelihood of being involved in a roll-over accident [84]. Although it is clear that both static and dynamic effects influence roll stability, a steady-state analysis of the roll stability is sufficient to give an insight into the major elements governing the roll response of the vehicle. Once the steady-state roll-over problem is well understood, it is possible to extend the analysis to a more general treatment of the dynamic roll-over problem.

3.3 Mechanics of roll-over

The fundamental mechanics of the roll-over process can be investigated using a number of simplified vehicle models.

3.3.1 Rigidly suspended vehicle

To begin the discussion of roll-over, consider a rigidly suspended vehicle, as shown in figure 3.1 [84]. This simple model can represent any vehicle with a single roll degree of freedom, for example, a single unit truck with a stiff frame and rigid suspensions and tyres.

The lateral tyre forces generated at the ground during cornering produce a steady-state lateral acceleration of the vehicle. A sum of moments about the point on the ground plane at the mid-track position reveals that three moments act on the vehicle:

- the *primary overturning moment*, $ma_y h_{cm}$, arising from the lateral acceleration,
- the *restoring moment*, $\Delta F_z\, T$, arising from the lateral load transfer from the inside tyres to the outside tyres,

- the *lateral displacement moment*, $mgh_{cm}\phi$, arising from the roll motion which displaces the centre of mass laterally from the nominal centre line of the vehicle.

A steady state moment balance yields

$$ma_y h_{cm} = \Delta F_z \, T + mgh_{cm}\phi. \tag{3.1}$$

This balance can be represented on a *roll response graph*, as shown in figure 3.2. This graph is a useful tool for understanding the roll stability of heavy vehicles [84]. The primary overturning moment is plotted against lateral acceleration on the left side of the graph. The *net restoring moment*, which is the sum of the restoring moment and the lateral displacement moment, is plotted against roll angle on the right side of the graph.

The primary overturning moment is a destabilising moment, and the vehicle will be unstable in roll whenever this moment exceeds the net stabilising moment that can be provided by the vehicle. For this reason, *the analysis of the roll stability of heavy vehicles focuses on the ability of the vehicle to provide a stabilising moment*.

From the roll response graph, the roll-over threshold is the lateral acceleration corresponding to the maximum value of the net stabilising moment (point A in figure 3.2). In the case of the rigidly suspended vehicle, the roll-over threshold is simply

$$a_y = \frac{Tg}{2h_{cm}}. \tag{3.2}$$

3.3.2 Simplified suspended vehicle

Now consider a vehicle suspended on compliant suspensions and tyres, as shown in figure 3.3. Initially it is convenient to assume that the total mass of the vehicle is in the sprung mass, that the compliance of the suspensions and tyres is lumped into a single equivalent compliance, and that the roll of the sprung mass on the tyres and suspension springs takes place about the point on the ground plane at the mid-track position [84].

Again the moment balance on the vehicle is described using equation (3.1) and

can be represented on a roll response graph, as shown in figure 3.4. In this case, the suspension can only generate a moment by some rolling of the sprung mass. The suspension moment increases linearly with roll angle up to a maximum value of $\frac{1}{2}mgT$ at point A. The peak value of the net restoring moment curve (B) is reduced when compared to the rigidly suspended vehicle. The roll-over threshold is

$$a_y = \frac{Tg}{2h_{cm}} + \phi^\star g \tag{3.3}$$

where $\phi^\star$ is the critical roll angle at wheel lift-off. (Note that $\phi^\star < 0$ for a passive suspension.) The figure shows that the roll-over threshold is reduced by increasing the roll compliance of the tyres and suspension because softer suspensions and tyres cause the lateral displacement moment at wheel lift-off to increase.

In reality, the sprung mass rolls about a suspension roll centre that is not at ground level, as shown in figure 3.3. The position of the roll centre is determined by the suspension geometry and is generally some distance above the level of the road surface. The unsprung mass rotates about a separate roll centre in the ground place. In general, a higher roll centre will promote less body roll. Since body roll towards the outside of the corner reduces the roll-over threshold, increasing the suspension roll centre height will typically increase the overall roll stability of the vehicle.

3.3.3 Suspended vehicle with multiple axles

To extend the discussion of the mechanics of roll-over further, consider a vehicle suspended on multiple compliant suspensions and tyres [84].

The analysis in section 3.3.2 used a single lumped roll compliance to represent the combined roll compliance of all the suspensions and tyres on the vehicle. This representation is valid for multiple axle vehicles if the effective roll stiffnesses of the axles (taking into account the suspension stiffness, the tyre stiffness and the roll centre locations) are in proportion with the vertical loads carried by the axles. However this is generally not the case, and a model featuring representations of each individual axle

is required.

The roll response diagram for a typical tractor semi-trailer is shown in figure 3.5. The trailer axle has the highest stiffness-to-load ratio, followed by the tractor drive axle and the tractor steer axle. The trailer axle group is also the most heavily laden, again followed by the tractor drive axle and the tractor steer axle.

For a given track width, the more heavily laden the axle, the greater the maximum restoring moment it can provide. Thus the maximum suspension moment that can be supplied is higher for the trailer axle group (point A) than for the tractor drive axle (B) or the tractor steer axle (C).

The roll angle at wheel lift-off for a given axle is dictated by the ratio of effective roll stiffness to vertical load, such that axles with a higher stiffness-to-load ratio lift off at smaller roll angles. Thus the roll angle at which the trailer axle group lifts off (A) is lower than the corresponding angles for the tractor drive axle (B) or the tractor steer axle (C).

The net restoring moment is the sum of the suspension moments and the lateral acceleration moment. Up to point D, all suspensions contribute a moment proportional to the body roll angle and the multiple axle vehicle model behaves identically to the simplified model in section 3.3.2. At point D, the trailer axle group lifts off. The slope of the net restoring moment is reduced beyond D because the trailer axles can not provide any additional moment. At point E, the tractor drive axle lifts off. The slope of the net restoring moment curve decreases again beyond E. In fact since the tractor steer axle is not sufficiently stiff to provide a restoring moment to balance the lateral displacement moment, the roll-over threshold of the vehicle is defined by the lift off of the inside wheel of the tractor drive axle (E) rather than of the steer axle (F).

Figure 3.5 shows that the non-uniformity of the stiffness-to-load ratios and the resulting non-simultaneous wheel lift-offs reduce the roll-over threshold from that which would be computed using the lumped suspension model presented in section 3.3.2.

It is clear that the distribution of roll stiffness among the suspensions has an important influence on the roll-over threshold.

An increase in the roll stiffness of the trailer suspension will shift the trailer lift-off point (D) to the left on the roll response graph but will not affect the vehicle roll-over threshold. A decrease in the roll stiffness of the trailer axle will decrease the roll-over threshold only if the stiffness-to-load ratio of the trailer axle is reduced below that of the tractor drive axle, such that the inside wheel of the tractor drive axle lifts off before the inside wheel of the trailer axle.

A change in the roll stiffness of the tractor drive axle will directly affect the roll-over threshold, since the lift-off of the inside wheel of the tractor drive axle defines the roll-over condition for this vehicle. Increasing the roll-over stiffness of the tractor drive axle will increase the roll-over threshold (moving B to the left and E up and to the left), while decreasing the roll-over stiffness of the tractor drive axle will reduce the roll-over threshold (moving B to the right and E down and to the right).

The roll-over threshold can also be increased by increasing the stiffness of the tractor steer axle. If the steer axle is stiffened to the point where the positive slope of the steer axle roll moment curve is steeper than the negative slope of the lateral displacement moment curve, then the roll-over threshold of the vehicle will be determined by the lift-off of the inside wheel of the tractor steer axle (F) not the tractor drive axle (E).

Other factors influencing roll stability

Suspension lash, present in the leaf spring suspension systems commonly used on heavy vehicles, degrades the roll-over threshold by reducing the effective roll stiffness of the suspensions.

Torsional compliance of the vehicle frames also reduces the roll-over threshold. For example, a flexible trailer frame rolls to a greater angle under the influence of lateral acceleration, thus increasing the magnitude of the destabilising lateral displacement moment. Furthermore torsional compliance of the tractor frame reduces the ability of the tractor steer axle to provide a stabilising moment to resist the roll motion of the payload.

Torsional compliance of the vehicle couplings reduces roll stability in a similar way. Note that the roll stiffness of a conventional fifth wheel coupling decreases with articulation angle.

Winkler et al. noted that most real world roll-over accidents feature some dynamic component that is needed to raise the vehicle's centre of mass a small distance through its apex height after all axles have left the ground [107]. Cooperrider et al. investigated the energy required for dynamic roll-over and concluded that the lateral acceleration required to achieve roll-over in the dynamic case is slightly higher than the static roll-over threshold [13].

3.4 Control objectives

The objective of the roll control system is to use roll moments from active anti-roll bars to maximise the roll stability of the vehicle. The general notion of roll stability must be translated into a specific set of plant outputs to be regulated. Roll stability is achieved by limiting the lateral load transfers

$$\Delta F_z = \frac{k_t \phi_t}{T} \tag{3.4}$$

to below the levels required for wheel lift-off. While attempting to minimise load transfers, it is also necessary to constrain the roll angles between the sprung and unsprung masses $(\phi - \phi_t)$ to be within the limits of travel of the suspensions. A maximum suspension roll angle of 6-7° is typical.

These objectives may be considered to form a preliminary design specification for an active roll control system. The following section considers the fundamental limitations to how well this preliminary specification can be met.

3.5 Controllability analysis

Before performing a detailed controller design, it is important to consider three questions about the vehicle to be controlled:

1. *How well can the vehicle be controlled?* Are the control objectives easy, difficult or even impossible to meet arbitrarily well?

2. *What controller structure should be used?* What sensors and actuators should be fitted? Which measurements should affect which controls?

3. *How might the vehicle be changed to improve control?*

These questions can be answered using a technique called *controllability analysis*. The motivation for performing such an analysis is to produce an achievable controller design specification and to gain an insight into the reasons behind any limits to achievable response.

3.5.1 System model

The vehicle is cast as a multiple input multiple output (MIMO) plant with a series of inputs, internal states and outputs. The open-loop system is shown in figure 3.6.

The *inputs* are external disturbances (steering inputs δ from the driver) and control inputs. The control inputs are roll moments u between the sprung and unsprung mass generated by active anti-roll bars sited at some or all of the axles.

The *internal states* x could be, for example, the state variables used in the models in chapter 2, although other combinations are also possible.

The *performance outputs* z are combinations of the vehicle states that are to be controlled in some way.

Measurements $y = y_0 + v$, where v is the measurement noise, are available for feedback. (An important case is the *state feedback* case, where all plant states are available for feedback.)

The dynamics of the nominal plant model (without the steering disturbance δ and the output disturbance v) are described by

$$y_0 = C_0(sI - A)^{-1}B_0u. \tag{3.5}$$

This is often abbreviated using the shorthand notation (A, B_0, C_0). (A more general model of the nominal plant dynamics includes a direct transmission term D such that $y_0 = C_0(sI - A)^{-1}B_0u + D$. However any practical engineering system is *strictly proper*, that is it has zero gain at sufficiently high frequencies and $D = 0$ [94].)

In terms of the state vector x, and with the steering disturbance and the output disturbance included, the input-output dynamics are given by

$$\dot{x} = Ax + B_0u + B_1\delta, \quad y = C_0x + v, \quad z = C_1x. \tag{3.6}$$

3.5.2 Input-output controllability

The question of how well it is possible to control the roll motion of a heavy vehicle using active anti-roll bars is essentially a question of *input-output controllability analysis* (also known in the literature as *performance targeting* or *dynamic resilience* [63]). Such an analysis is used to investigate and quantify what control performance can be expected.

Definition 3.2 (Input-output controllability) *Input-output controllability is the ability to achieve acceptable control performance, that is, to regulate outputs within specified bounds from their references, in spite of unknown but bounded variations, such as disturbances and plant changes, using the available inputs and measurements* [94].

As applied to the roll control of heavy vehicles, input-output controllability refers to the ability to use torques generated by active anti-roll bars to regulate lateral load transfers and roll motions, thereby increasing roll stability. Roll stability should be maintained despite steering inputs from the driver, variations in vehicle response char-

acteristics from the nominal vehicle model and noise in measurements from sensors.

The notion of input-output controllability is a broader and more practical notion of controllability than state controllability (see section 3.5.3) or functional controllability (see section 3.5.4).

Controllability is independent of the controller and is a property of the plant (in this case the vehicle) only. Controllability can only be affected by plant design changes. These may include changing the properties of vehicle components, relocating sensors and actuators, adding sensors and actuators or even changing or relaxing the control objectives.

Techniques for input-output controllability analysis

Given the wide range of mathematical methods available for control system analysis and design, it is perhaps surprising that the methods commonly used for input-output controllability analysis are largely qualitative [94].

The most common method is to evaluate performance by exhaustive simulations. However this requires a specific controller design and specific values of disturbances and set points. The key disadvantage of this approach is that it is not possible to know if the apparent controllability limits are a fundamental property of the plant or if they are dependent on the controller designs, disturbances and set points used in the simulations.

A more rigorous approach to input-output controllability analysis is to describe mathematically the control objectives, the class of disturbances and the model uncertainty, and then to synthesize controllers to see whether the objectives can be met. However this approach is difficult and time consuming, particularly when there are a large number of candidate actuators and measurements.

A two part input-output controllability analysis is presented in the following section. First, the notion of functional controllability is used to determine the maximum number of control objectives that may be satisfied using a given arrangement of active anti-roll bars. If it proves impossible to satisfy all the objectives in section 3.4

then some judicious relaxation of the specification is required. Second, the mechanisms for roll stabilisation at high levels of lateral acceleration are examined in detail to understand the trade-offs between the different control objectives of limiting lateral load transfers and roll angles. This allows decisions about actuator placement, sensor placement and the key control objectives to be made a priori, without having to perform a detailed controller design. It also allows the limits to achievable roll stability to be quantified.

3.5.3 State controllability

Definition 3.3 (State controllability) *State controllability is the ability to bring a system from a given initial state to any final state within a finite time [37].*

This rather theoretical notion of controllability is typically verified by evaluating the rank of the controllability matrix or by several other equivalent algebraic or geometric criteria [113].

However, state controllability gives no regard to either the quality of response between or after these two states or the size of the control inputs required. While the concept of state controllability is important for some numerical calculations, it is of no practical importance as long as all unstable modes are both controllable and observable. In fact, Rosenbrock notes that "most industrial plants are controlled quite satisfactorily though they are not [state] controllable" [74], and Skogestad and Postlethwaite give examples of plants that are state controllable but not input-output controllable [94].

3.5.4 Functional controllability

The notion of *functional controllability*, which was first introduced by Rosenbrock [74], is frequently used in the study of performance limitations on MIMO systems. Functional controllability is a necessary condition for input-output controllability. Functional controllability analysis quantifies the number of plant outputs that can be con-

trolled independently and thus the number of control objectives that can be satisfied simultaneously.

Definition 3.4 (Functional controllability) *An m input l output system $G(s)$ is functionally controllable if the normal rank of $G(s)$, r, is equal to the number of outputs, that is, if $G(s)$ has full row rank. The system is functionally uncontrollable if $r < l$ [94].*

The strictly proper m input l output system (A, B_0, C_0) described by equations (3.6) in section 3.4 is functionally uncontrollable if any of the following three conditions is true [94]:

1. The system is input deficient, rank$(B_0) < l$.
2. The system is output deficient, rank$(C_0) < l$.
3. There are fewer states than outputs, rank$(sI - A) < l$.

(This follows from the fact the that rank of a product of matrices is less than or equal to the minimum rank of the individual matrices.)

Functional controllability is generally a structural property of a system, that is it does not depend on specific parameter values. A typical example of a system that is functionally uncontrollable is one with fewer inputs than outputs. Another example is a system where none of the inputs affects a particular output.

Inputs and outputs for active roll control systems

The roll moment generated by each active anti-roll bar (or group of active anti-roll bars on a multi-axle suspension group) represents a single control input to the active roll control system.

Each axle group also contributes a single output in the form of an unsprung mass roll angle (or equivalently a lateral load transfer, by equation (3.4)) to the vehicle roll control system. In addition, each vehicle unit contributes either one or two outputs in

the form of one or two sprung mass roll angles to the roll control system. Torsionally rigid units contribute one output each, while torsionally flexible units contribute two outputs.

For example a tractor semi-trailer combination with a flexible tractor frame will have six roll outputs (the tractor front roll angle, tractor rear roll angle, trailer roll angle, and the load transfers at the tractor steer axle, tractor drive axle and trailer axle group) and three roll control inputs (the active anti-roll bar roll moments at the tractor steer axle, the tractor drive axle and the trailer axle group).

Such systems are clearly input deficient, that is, there are not sufficient inputs to independently control all outputs (roll angles and load transfers). Therefore a specification that requires independent controllability of all roll angles and load transfers is not achievable using active anti-roll bars alone.

Output selection

A plant that is functionally uncontrollable has $(l - r)$ frequency dependent uncontrollable output directions. For plants that are functionally uncontrollable, it is necessary to decide whether it is acceptable to keep certain output combinations uncontrolled (that is, to relax the control objectives), or if additional actuators are needed to increase the rank of $G(s)$.

Additional hardware to control the torque transmitted between the sprung masses of adjacent vehicle units (by tilting the coupling) or between the front and rear sprung sections of flexible vehicle units (by twisting the vehicle frame) could be fitted to increase the rank of $G(s)$ and reduce the plant input deficiency. However the practicality of such systems is questionable. Furthermore it would not be possible to completely eliminate the plant input deficiency using this method, so clearly some judicious relaxation of the control objectives is necessary.

To demonstrate how the requirement for functional controllability compromises the ability to meet the preliminary control objectives, consider the simple case of a single unit vehicle with a torsionally rigid frame. Such a vehicle has two roll control

inputs (one each at the steer and drive axles) and three roll-plane degrees of freedom (the sprung mass roll angle and the lateral load transfers at the steer and drive axles). The following are possible selections for the two controllable roll outputs:

- Control the sprung mass roll angle and the load transfer at the drive axle. The load transfer at the steer axle could not then be specified independently.
- Control the load transfers at the steer and drive axles. The sprung mass roll angle could not then be independently specified.
- Control the sprung mass roll angle and the balance of load transfers between the steer and drive axles. For example, set the normalized load transfers at the steer and drive axles to be the same, so that both axles lift off simultaneously at the roll-over threshold. The total load transfer could not then be independently specified.

Computing inputs and self-regulating outputs

For a functionally controllable plant, it is possible to compute the control inputs required to meet certain control objectives. Consider a vehicle in a steady-state cornering manoeuvre ($\dot{x} = 0$) under a constant steering input δ. The vehicle is fitted with m active anti-roll bars and is required to track m roll control objectives. The required anti-roll bar torques u can be computed if the system is functionally controllable. A modified version of the full state-space model described by equation (2.6), with the steering input δ and the active anti-roll bar torques u stacked to form a single input vector, is used. The state vector x is partitioned into three parts: the handling states x_h, the controllable roll states $x_{r,c}$ and the uncontrollable roll states $x_{r,u}$. The matrices A and $B = \left[\begin{array}{c|c} B_1 & B_0 \end{array}\right]$ are partitioned correspondingly. The aim is to find active roll

moments u to meet the control objectives $x_{r,c}$ such that

$$\begin{bmatrix} A_{11} & A_{12} & A_{13} \\ A_{21} & A_{22} & A_{23} \\ A_{31} & A_{32} & A_{33} \end{bmatrix} \begin{bmatrix} x_h \\ x_{r,c} \\ x_{r,u} \end{bmatrix} + \left[\begin{array}{c|c} B_{11} & B_{12} \\ B_{21} & B_{22} \\ B_{31} & B_{32} \end{array}\right] \begin{bmatrix} \delta \\ u \end{bmatrix} = \begin{bmatrix} 0 \\ 0 \\ 0 \end{bmatrix}. \tag{3.7}$$

The active anti-roll bar torques u have no effect on the steady state handling performance of the linearised system, that is, $A_{12} = A_{13} = B_{12} = 0$. Equation (3.7) can therefore be rewritten as

$$0 = A_{11}x_h + B_{11}\delta, \tag{3.8}$$

$$0 = A_{21}x_h + A_{22}x_{r,c} + A_{23}x_{r,u} + B_{21}\delta + B_{22}u, \tag{3.9}$$

$$0 = A_{31}x_h + A_{32}x_{r,c} + A_{33}x_{r,u} + B_{31}\delta + B_{32}u. \tag{3.10}$$

Rearranging equation (3.8) gives an expression for the handling states x_h in terms of the steering input δ:

$$x_h = -{A_{11}}^{-1}B_{11}\delta. \tag{3.11}$$

Combining equations (3.9) and (3.10) to eliminate the terms in the uncontrollable roll states $x_{r,u}$ and then replacing terms in x_h with terms in δ using equation (3.11) gives a one-to-one mapping between the controllable roll states $x_{r,c}$ and the control inputs u, of the form

$$u = K_c x_{r,c} + K_\delta \delta \tag{3.12}$$

where K_c and K_δ are constant matrices depending on the vehicle parameters:

$$K_c = \left(B_{22} - A_{23}{A_{33}}^{-1}B_{32}\right)^{-1}\left(A_{23}{A_{33}}^{-1}A_{32} - A_{22}\right), \tag{3.13}$$

$$K_\delta = \left(B_{22} - A_{23}{A_{33}}^{-1}B_{32}\right)^{-1} \left[A_{23}{A_{33}}^{-1}\left(B_{31} - A_{31}{A_{11}}^{-1}B_{11}\right) - B_{21} + A_{21}{A_{11}}^{-1}B_{11}\right]. \tag{3.14}$$

The values of the uncontrollable roll states $x_{r,u}$ can then be solved by back substitution

into equation (3.10).

Implications for control objectives

The functional controllability analysis above indicates that it is not possible to control all axle load transfers and body roll angles independently using active anti-roll bars alone. What is possible is to control a *subset* of roll-plane states, $x_{r,c}$; the remaining roll-plane states, $x_{r,u}$, are uncontrollable. This implies that it is possible to satisfy only a subset of the control objectives from section 3.4.

Since the roll-over threshold depends on both axle lateral load transfers and body roll angles (from section 3.3), the existence of uncontrollable output directions implies that there is a limit to achievable roll stability.

Functional controllability is a necessary but not sufficient condition for input-output controllability. That a system is functionally controllable implies that a set of control of inputs can influence a set of performance outputs *to some extent*. However input-output controllability may still be limited by other factors, including control input saturation, such as occurs at wheel lift-off.

3.5.5 Roll stability and wheel lift-off

The roll response graphs from section 3.3.3 show that the lateral acceleration at which wheel lift-off first occurs is not necessarily a reliable indicator of the roll-over threshold of the vehicle. It is important to establish the conditions under which the vehicle can retain roll stability even when some axles are off the ground and to understand the stabilising mechanisms. The motivation is to identify whether or not the roll stability of the vehicle is dependent only on the lateral load transfers at particular axles.

To investigate the implications of wheel lift-off on vehicle roll stability, consider a linear vehicle model of the type presented in chapter 2 but with two modifications:

1. The lateral load transfer at each axle is limited to a maximum value determined by the wheel lift-off condition.

2. The roll angle between the sprung and unsprung masses is limited to a maximum value determined by the available suspension travel.

Roll stability without active roll control

First consider the case of a vehicle fitted with a conventional passive suspension system. When all load transfers are sub-critical, for example at low levels of lateral acceleration, the linearised response of the vehicle is governed by

$$\dot{x} = Ax + B_1\delta \tag{3.15}$$

where the matrices A and B_1 are formed as in chapter 2. The stability of the system (both in roll and in handling) can be checked by verifying that the eigenvalues of A all lie in the open left half plane.

If the steering inputs excite a response that causes the wheels at one or more axles to lift off, then equation (3.15) does not hold since the restoring moment at one or more axles reaches a limit. Beyond lift-off the vehicle response is governed by an equation of the form

$$\dot{x} = \tilde{A}x + \left(A - \tilde{A}\right)\tilde{x} + B_1\delta. \tag{3.16}$$

The matrix $\tilde{A}$ is a modified version of A with the tyre roll stiffness terms k_t set to 0 at the lifted axles. This accounts for the fact that, after lift-off, an axle can no longer provide any additional restoring moment. The constant vector $\tilde{x}$ is a modified version of x with the unsprung mass roll angles ϕ_t at the lifted axles set to the lift-off value $\phi_t^\star$ and all other entries set to zero.

The concept is best explained using the simple example of a single unit rigid vehicle (from section 2.2.1) with maximum lateral load transfer on the rear axle. The

matrix A is given by

$$A = E^{-1}\begin{bmatrix} * & * & 0 & 0 & 0 & 0 \\ * & * & 0 & 0 & 0 & 0 \\ 0 & * & m_s g h - k_f - k_r & * & k_f & k_r \\ * & * & -k_f & * & k_f + k_{t,f} - m_{u,f} g h_{u,f} & 0 \\ * & * & -k_r & * & 0 & k_r + k_{t,r} - m_{u,r} g h_{u,r} \\ 0 & 0 & 0 & 1 & 0 & 0 \end{bmatrix} \tag{3.17}$$

where $*$ denotes a non-zero element. The matrix E is from equation (2.9). The state vector x is given by

$$x = \begin{bmatrix} \beta & \dot{\psi} & \phi & \dot{\phi} & \phi_{t,f} & \phi_{t,r} \end{bmatrix}^T. \tag{3.18}$$

The matrix $\tilde{A}$ is given by

$$\tilde{A} = E^{-1}\begin{bmatrix} * & * & 0 & 0 & 0 & 0 \\ * & * & 0 & 0 & 0 & 0 \\ 0 & * & m_s g h - k_f - k_r & * & k_f & k_r \\ * & * & -k_f & * & k_f + k_{t,f} - m_{u,f} g h_{u,f} & 0 \\ * & * & -k_r & * & 0 & k_r - m_{u,r} g h_{u,r} \\ 0 & 0 & 0 & 1 & 0 & 0 \end{bmatrix} \tag{3.19}$$

and the constant vector $\tilde{x}$ is given by

$$\tilde{x} = \begin{bmatrix} 0 & 0 & 0 & 0 & 0 & \phi^{\star}_{t,r} \end{bmatrix}^T. \tag{3.20}$$

Since $\left(A - \tilde{A}\right)\tilde{x}$ is constant, the stability of the system (both in roll and handling) can be checked by verifying that the eigenvalues of $\tilde{A}$ all lie in the open left half plane. Recall that roll stability is determined by the ability of the vehicle to generate an increase in net restoring moment to balance the increase in primary overturning moment caused by an increase in the steering input. For a vehicle with no active roll control sys-

tem, the change in net restoring moment is the increase in the stabilising roll moment generated by load transfers at the axles minus the destabilising lateral displacement moment generated by the outboard shift of the sprung masses. Thus, for the vehicle to retain roll stability after wheel lift-off, the compliance of the couplings, frames, and tyres and suspensions of the axles remaining on the ground must be sufficiently small that the destabilising effect of the lateral displacement moment does not exceed the stabilising effect of the lateral load transfer.

This analysis can be used to check the stability of the vehicle with any combination of axle groups on or off the ground and provides a technique for identifying which axles must be on the ground for the vehicle to retain roll stability. The roll stability of the vehicle is dependent only on the lateral load transfers at these axles.

Roll stability with active roll control

Next consider the case of a vehicle with an active roll control system. When all load transfers are sub-critical, the linearised response of the vehicle is governed by

$$\dot{x} = Ax + B_0 u + B_1 \delta \tag{3.21}$$

where $B_0 u$ represents the effect of the roll moments from the active anti-roll bars (see chapter 2).

Again the roll stability of the vehicle is determined by the ability of the vehicle to generate a net restoring moment to balance the increase in primary overturning moment generated by an increase in steering input. By varying the control torques between the sprung and unsprung masses, the active roll control system can manipulate the axle load transfers and the body roll angles, thus controlling the net stabilising moment. Specifically it is possible to increase the inward lean of the vehicle units, thus using the lateral displacement moment to provide a stabilising effect. (This assumes that the vehicle units whose wheels have lifted off are torsionally coupled to the vehicle units whose wheels remain on the ground, or equivalently, that control torques from

vehicle units whose axles remain on the ground can influence the roll angles of the vehicle units whose wheels have lifted off.) Clearly, given a sufficient stabilising effect from the lateral displacement moment, it is possible to nullify the destabilising effect of the primary overturning moment and to stabilise the vehicle in roll.

Achievable roll stability is therefore limited by the ability of the active roll control system to provide a sufficient stabilising lateral displacement moment such that the net restoring moment can balance the primary overturning moment. This ability is in turn limited by the maximum allowable suspension deflection. Once the maximum allowable deflection is reached, the stabilising effect is limited to that which would be provided by infinitely stiff suspension springs holding the sprung masses at the maximum inward roll angle. By analogy with the passive case, the stability of the system can be checked by verifying that the eigenvalues of $\tilde{A}$ all lie in the open left half plane. In the active case, $\tilde{A}$ is formed from A by: (1) setting the tyre roll stiffness terms k_t at the lifted axles to 0 (as before); and (2) setting the suspension roll stiffness terms k at the other axles towards ∞. For the single unit rigid truck,

$$\tilde{A} = \lim_{k_f \to \infty} \left(E^{-1} \begin{bmatrix} * & * & 0 & 0 & 0 & 0 \\ * & * & 0 & 0 & 0 & 0 \\ 0 & * & m_s g h - k_f - k_r & * & k_f & k_r \\ * & * & -k_f & * & k_f + k_{t,f} - m_{u,f} g h_{u,f} & 0 \\ * & * & -k_r & * & 0 & k_r - m_{u,r} g h_{u,r} \\ 0 & 0 & 0 & 1 & 0 & 0 \end{bmatrix} \right). \tag{3.22}$$

Even if the axles on the ground provide sufficient moment to tilt the vehicle units into the turn at the maximum allowable angle, the vehicle will still be unstable after wheel lift-off if the compliance of the couplings, frames and tyres of the axles remaining on the ground is sufficiently large that the destabilising effect of the lateral displacement moment exceeds the stabilising effect of the lateral load transfer.

Implications for control objectives

The roll stability of a vehicle may not depend on the lateral load transfers at *all* axles. If there is excessive torsional compliance in vehicle frames, couplings or tyres, then it is possible for one section of a combination vehicle to lose roll stability while the lateral load transfers at other axles remain sub-critical. (This was demonstrated clearly in figure 2.2)

All control effort should be directed toward controlling the lateral load transfers at these axles, since the control system cannot stabilise the vehicle once the lateral load transfers at these axles reach the critical value required for wheel lift-off.

3.5.6 Roll moment distribution to maximise the roll-over threshold

The functional controllability analysis in section 3.5.4 demonstrates that it is not possible to simultaneously and independently control all axle load transfers and body roll angles. This motivates the question: Which subset of load transfers and roll angles should be controlled, and which should be left uncontrolled? To answer this question, it is necessary to identify the vehicle state that maximises the net restoring moment and thus maximises the roll stability of the vehicle.

The net restoring moment is equal to the sum of the restoring moments at the axles due to lateral load transfer plus the sum of the stabilising moments due to the lateral displacements of the sprung masses. Since in general it is not possible to simultaneously maximise these two quantities, some compromise is required. Two alternative options for maximising the roll-over threshold of a tractor semi-trailer are now presented. These options are extreme and impractical but are useful because together they provide great insight into the physics behind the limitations to achievable roll stability.

Case I: Maximising restoring moment from the axles

The first option is to maximise the restoring moment from the axles at roll-over, that is, to implement a scheme that sets the lateral load transfer at each axle to the maximum

possible load transfer. The steady-state roll angle and normalised lateral load transfer* responses of a tractor semi-trailer employing such a control scheme are shown in figure 3.7.

The load transfer specification forms a full set of functionally controllable states $x_{r,c}$ in equation (3.7). It is not possible to specify any of the sprung mass roll angles independently, but instead the sprung mass roll angles required to achieve this specification are dependent states $x_{r,u}$ that are a function of the steering input.

At low levels of lateral acceleration, it is not possible to lean the vehicle out of the turn enough to generate full load transfer at the axles. However at 0.45 g it is possible to generate maximum load transfer at the tractor and semi-trailer axles by tilting the tractor out of the turn by around 2° and the semi-trailer out of the turn by around 6° (see figure 3.7(a)). As lateral acceleration increases, it is possible to maintain normalised load transfers of 1 by leaning the tractor and semi-trailer into the turn. The maximum allowable lateral acceleration corresponds to the vehicle state where the maximum inward sprung mass roll angle is equal to the maximum allowable roll angle. In this case, the tractor roll angle is 6° into the turn (point A), the semi-trailer roll angle is 3.2° into the turn (point B) and the lateral acceleration at roll-over is 0.54 g (points A and B). The relative roll angle between the tractor and semi-trailer reduces the load transfer on the semi-trailer and increases the load transfer on the tractor. Although the restoring moment from the axles is maximised, the stabilising lateral displacement moment is not.

It is possible that all sprung mass roll angles will reach the maximum allowable roll angle simultaneously, in which case the restoring moment and the stabilising lateral displacement moment would be maximised simultaneously. However, in general this will not be the case and the roll angles between the sprung masses at roll-over will be non-zero. These relative roll angles are necessary to allow the total overturning moment to be shared among the axles to meet the control specification.

*The lateral load transfer is normalised such that a value of ± 1 corresponds to the maximum load transfer possible.

Case II: Maximising stabilising lateral displacement moment

The second option is to maximise the stabilising effect of the lateral displacement moment at roll-over, that is, to implement a scheme that sets the inward roll angle of the sprung mass at each axle to the maximum allowable roll angle. The steady-state roll angle and normalised lateral load transfer responses of a tractor semi-trailer employing such a control scheme are shown in figure 3.8.

The roll angle specification forms a full set of functionally controllable states $x_{r,c}$ in equation (3.7). It is not possible to specify any of the lateral load transfers independently, but instead the lateral load transfers required to achieve this specification are dependent states $x_{r,u}$ that are functions of the steering input.

At very low levels of lateral acceleration, the inward lean of the tractor and semi-trailer causes a small inward lateral load transfer. However at modest levels of lateral acceleration (more than approximately 0.05 g) the load transfer is towards the outside of the turn. When the lateral acceleration increases to 0.45 g, load transfer reaches the critical level at the semi-trailer axles (point D) while the tractor axles still have significant additional load transfer capacity (point F). However the lateral acceleration at which wheel lift-off first occurs is not a reliable indicator of the roll-over threshold (by sections 3.3.3 and 3.5.5). That is, the vehicle can remain stable with a limited number of axles on the ground, subject to the stability conditions detailed in section 3.5.5, at levels of lateral acceleration higher than that required to cause the first wheel lift-off. As the steering input continues to increase, the semi-trailer roll angle can not be maintained at the maximum value, and the roll angle decreases towards point C. This is because the wheel lift-off point sets a maximum value of control torque that can be generated at an axle, so any additional overturning moment must cause a reduction in the inward sprung mass roll angle; or equivalently, since the restoring torque at the lifted axle reaches a maximum at wheel lift-off, then some roll angle outward relative to the adjacent sprung masses is required to provide an additional stabilising torque to balance any additional destabilising overturning moment. Once the semi-trailer axles lift off, the load transfer at the tractor axles increases rapidly until roll stability is lost

at 0.54 g (point E). By this point the semi-trailer roll angle has been reduced to 3.2° (point C).

It is possible that the lateral load transfer at each axle will reach the maximum allowable load transfer simultaneously, in which case the restoring moment and the stabilising lateral displacement moment would be maximised simultaneously. However, in general this will not be the case, and one of the axles will reach its maximum lateral load transfer and lift off before the others.

Implications for control objectives

Significantly, the vehicle states (load transfers and roll angles) at roll-over for the two control schemes described above in case I and case II are identical, and both schemes yield the same roll-over threshold. *The techniques of maximising the restoring moment and maximising the stabilising lateral displacement moment are therefore two different but equivalent ways of thinking about maximising the roll-over threshold.* The following equivalent control strategies can therefore be used to maximise the roll stability of the vehicle:

1. Balance the normalised load transfers at all critical axles while taking the maximum inward roll angle among the sprung masses to the maximum allowable angle.

2. Maximise the inward roll angle of the sprung masses.

Figures 3.9 and 3.10 illustrate these two alternative strategies. The normalised load transfers of the tractor and semi-trailer are balanced in figure 3.9, so that as lateral acceleration increases, the normalised load transfers and suspension roll angles build up smoothly until both the tractor and semi-trailer axles lift off simultaneously at 0.54 g. The inward roll angles of the tractor and semi-trailer are maximised in figure 3.10, as described in case II and figure 3.8. The semi-trailer axles lift off at 0.45 g, and as lateral acceleration continues to increase, the inward roll angle of the semi-

trailer decreases from 6°. The vehicle loses roll stability at 0.54 g, by which point the semi-trailer roll angle has decreased to 3.2°.

The first control strategy is preferable for several reasons: (1) actuator force and power requirements are reduced; (2) actuator bandwidth requirements are reduced; (3) the more progressive transition towards roll-over minimises the variation in handling characteristics; and (4) an undesirable sign change in the roll rate response of the semi-trailer is avoided.

3.6 Achievable control objectives

The number of controllable roll-plane states is limited to the number of active anti-roll bars fitted to the vehicle (by section 3.5.4). Therefore the preliminary control specification detailed in section 3.4 can not be met arbitrarily well since the system is *input deficient*. The specification must be relaxed.

From section 3.5.6, the best achievable control strategy is to form a set of control outputs to balance the normalised load transfers at all critical axles, while simultaneously holding the maximum inward roll angle among the sprung masses at the maximum allowable angle.

The control inputs required to regulate these outputs may or may not include active anti-roll bars at all axle groups. To maximise roll stability, active anti-roll bars need only be fitted at axles from where they can exert some influence on the control outputs[†]. This can be verified by a functional controllability analysis from a reduced set of candidate control inputs to the new set of control outputs.

[†]It may be desirable to modify the control strategy for the steer axle so as to produce acceptable handling performance, possibly at the expense of some degradation of roll-over threshold.

3.7 Conclusions

1. Roll stability is best quantified by the roll-over threshold, which is the limit of steady-state lateral acceleration that a vehicle can sustain without losing roll stability.

2. Roll-over occurs when the vehicle is unable to provide a stabilising net restoring moment in response to an overturning moment. Since the roll motions of the vehicle units are typically coupled, wheel lift-off at a particular axle does not necessarily imply a loss of roll stability of the entire vehicle. A stability analysis can be used to identify the critical axle lift-off that defines the roll-over threshold.

3. Functional controllability analysis can be used to verify that a candidate set of active anti-roll bars can exert some degree of control over a given set of roll-plane states (load transfers and roll angles).

4. It is not possible to control all axle load transfers and body roll angles independently using active anti-roll bars alone. Thus it is generally not possible to simultaneously maximise both the restoring moment at each axle (by using the full lateral load transfer capacity) and the stabilising lateral displacement moment (by tilting all vehicle units into a turn at the maximum angle).

5. Roll stability of a vehicle with an ideal active roll control system is ultimately limited by the available suspension travel.

6. There is an apparent compromise between the aims of maximising the restoring moment provided by the axles and maximising the stabilising lateral displacement provided by the inward tilt of the vehicle units. However these control objectives yield identical roll-over thresholds. The best control strategy is to balance the normalised load transfers at all critical axles while taking the maximum inward roll angle among the sprung masses to the maximum allowable angle.

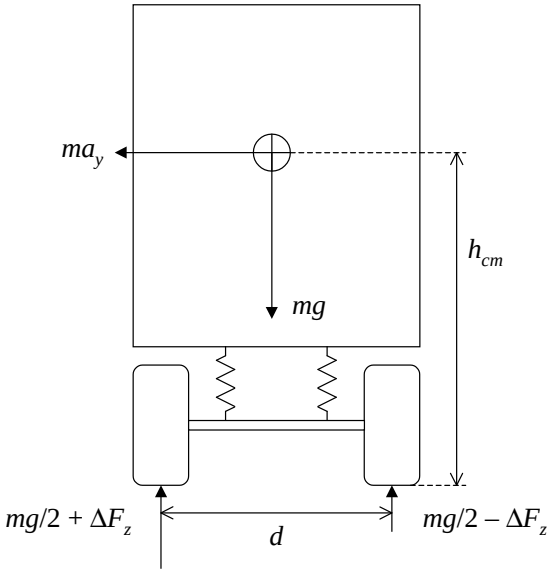

Figure 3.1: Rigid vehicle model.

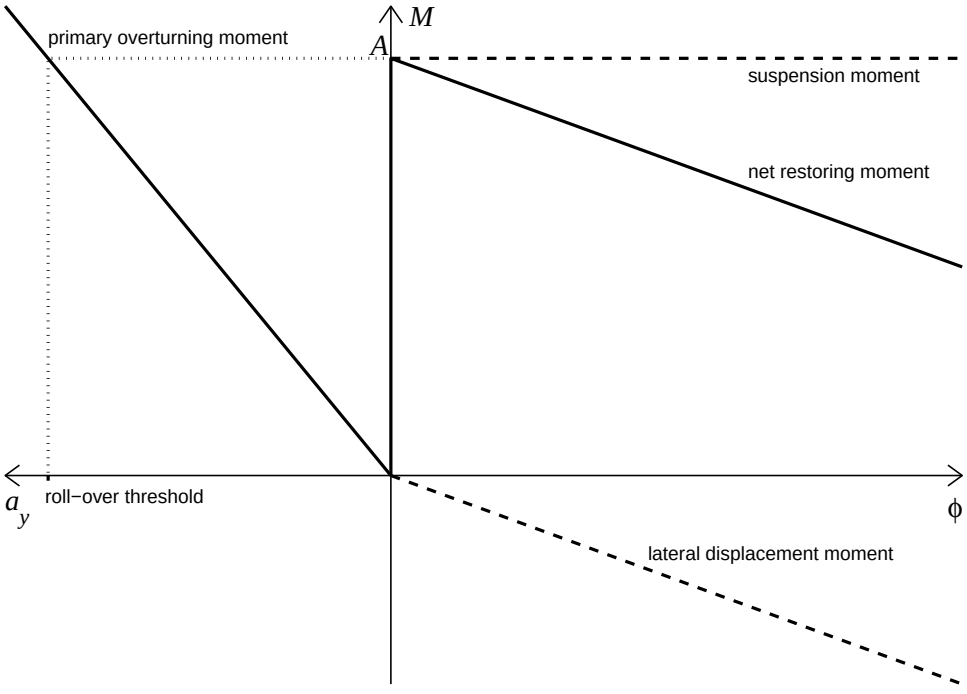

Figure 3.2: Generic roll response graph for the rigid vehicle model [84].

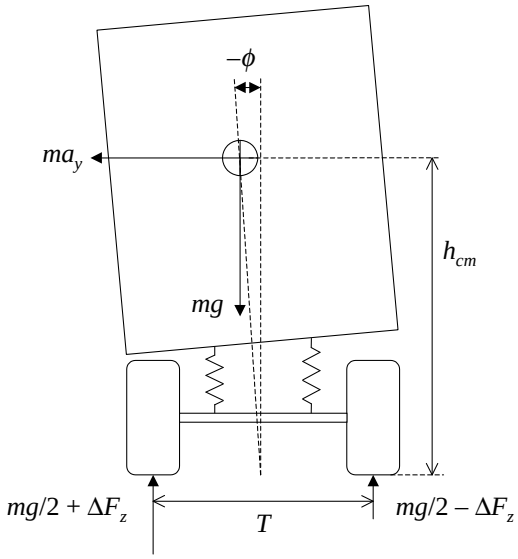

Figure 3.3: Simplified suspended vehicle model.

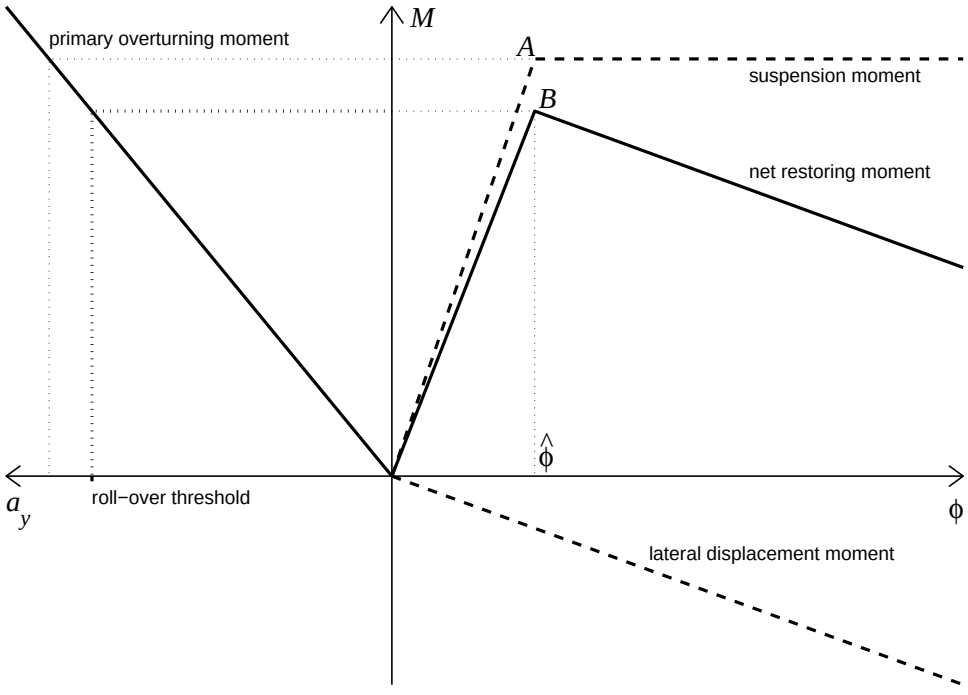

Figure 3.4: Generic roll response graph for the simplified suspended vehicle model.

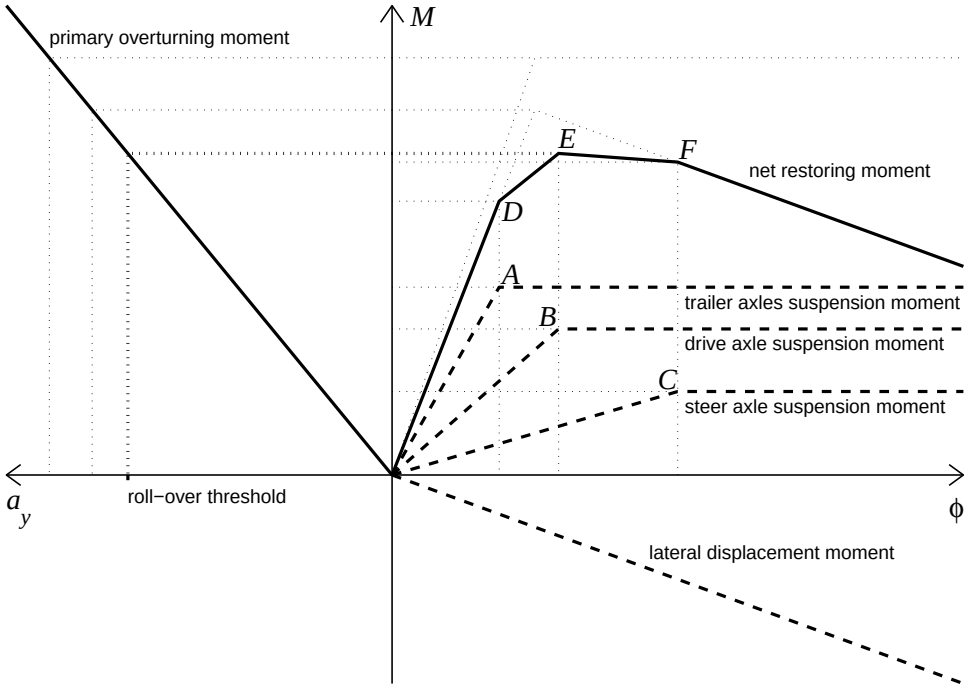

Figure 3.5: Generic roll response graph for suspended vehicle with multiple axles [84].

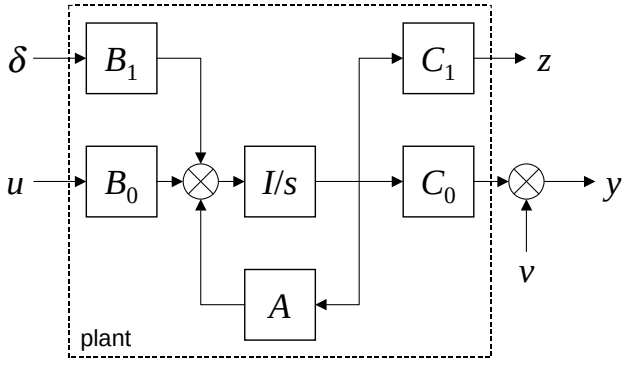

Figure 3.6: Open-loop system.

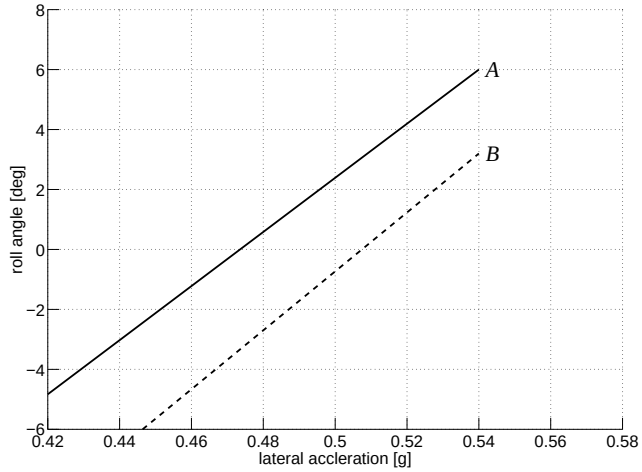

(a) Suspension roll angles. Active roll control: *tractor (——), semi-trailer (– – –).*

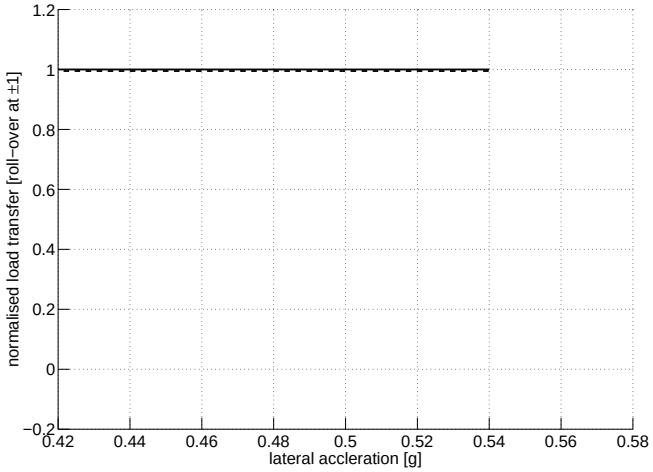

(b) Normalised load transfers. Active roll control: *tractor (——), semi-trailer (– – –).*

Figure 3.7: Increasing the roll-over threshold of the tractor semi-trailer by maximising the stabilising axle moment.

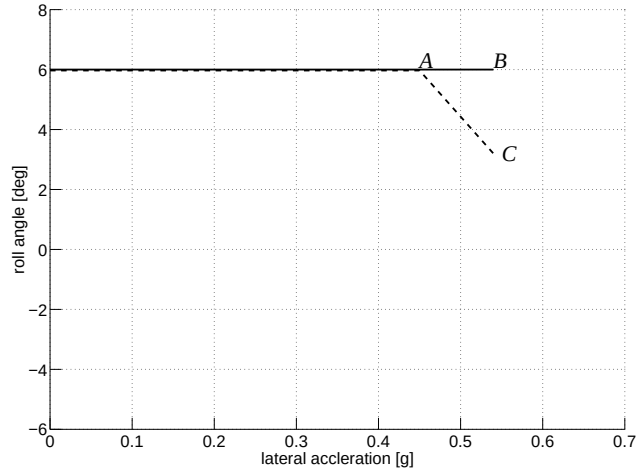

(a) Suspension roll angles. Active roll control: *tractor (——), semi-trailer (– – –).*

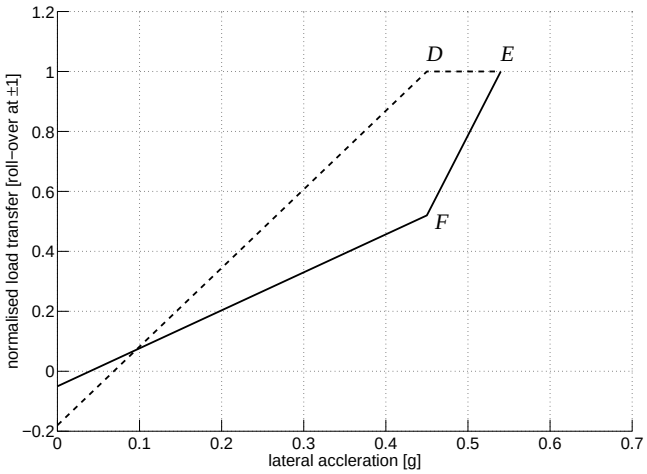

(b) Normalised load transfers. Active roll control: *tractor (——), semi-trailer (– – –).*

Figure 3.8: Increasing the roll-over threshold of the tractor semi-trailer by maximising the stabilising lateral displacement moment.

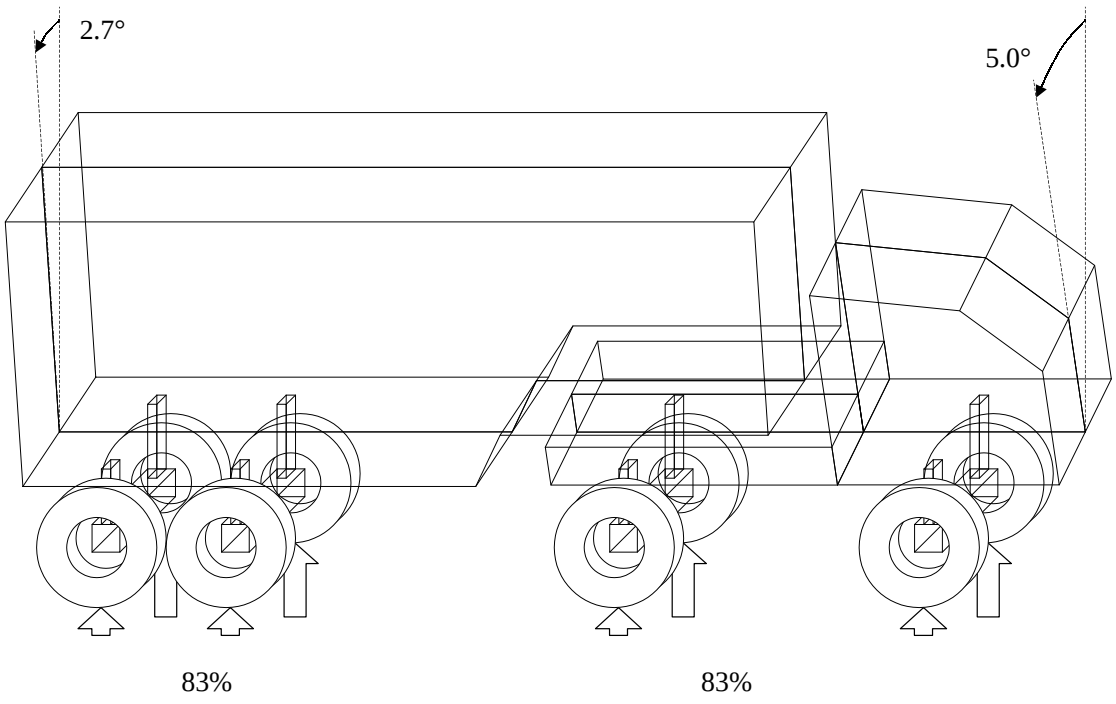

(a) Roll angles and normalised load transfers at 0.45 g.

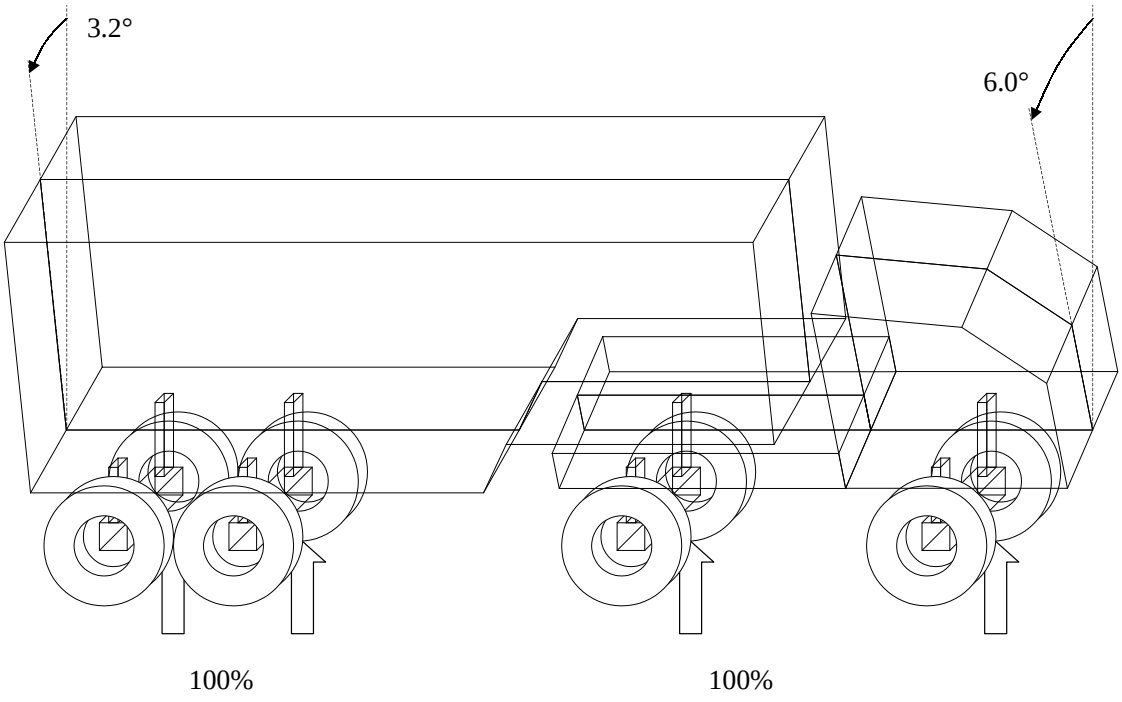

(b) Roll angles and normalised load transfers at 0.54 g.

Figure 3.9: Balancing the normalised load transfers to increase the roll-over threshold.

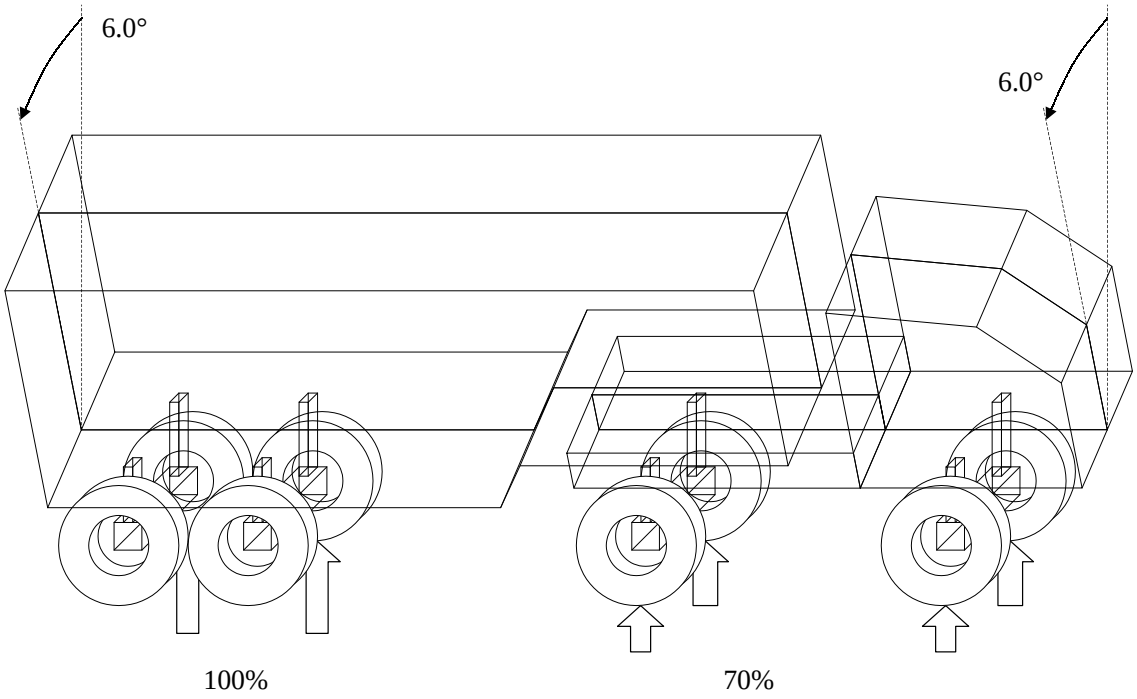

(a) Roll angles and normalised load transfers at 0.45 g.

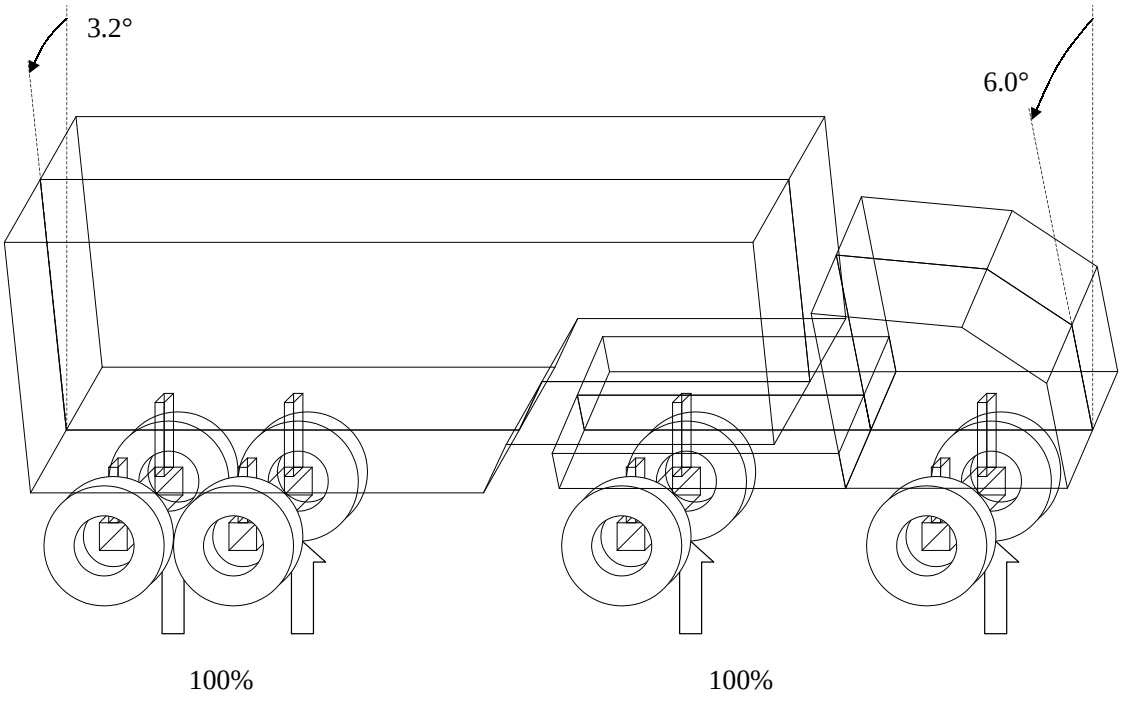

(b) Roll angles and normalised load transfers at 0.54 g.

Figure 3.10: Maximising the inward lean of vehicle bodies to increase the roll-over threshold.

Chapter 4

Active roll control of a single unit vehicle

4.1 Introduction

This chapter considers the problem of designing an active roll control system for a single unit vehicle. Since the dynamics of single unit vehicles are simpler than those of multiple unit articulated vehicles, this is an ideal starting point for an investigation of the design of active roll control systems.

4.2 Vehicle description

The single unit vehicle is a two axle tractor unit, as would typically be used to tow a tanker semi-trailer. The vehicle parameters are from an experimental tractor unit, fitted with an active roll control system, that is currently being designed and built by members of the Transportation Research Group at the University of Cambridge, UK. The unit has a wheelbase of 3.7 m, with a pair of single tyres on the steer axle and a pair of twin tyres on the drive axle. The unladen axle weights are 4559 kg on the steer axle and 1966 kg on the drive axle. The torsional stiffness of the vehicle frame is 629 kN.m/rad. The complete set of vehicle parameters is given in appendix A.

A lumped mass of 8828 kg is attached above the fifth wheel, with the centre of this mass at a height of 2.475 m above ground. This mass was chosen to represent the portion of a fully laden tanker semi-trailer that is supported by the tractor unit at the fifth wheel coupling. The height was selected to give the same body roll angle as the tractor semi-trailer for a given level of lateral acceleration. This approach has been used in previous studies [51, 55] and serves as a starting point from which to build up to a study of tractor semi-trailers and longer combination vehicles. While the single unit vehicle model is less complex than the tractor semi-trailer that it approximates, the response characteristics (for example, the actuator forces and servo-valve flow rates) are comparable.

4.3 Control system design objectives

First consider the case of the torsionally rigid single unit vehicle. The vehicle is modelled using the techniques described in chapter 2. There are three roll outputs (the body roll angle and the load transfers at the steer and drive axles) and two roll control inputs (the roll moments from the active anti-roll bars at the steer and drive axles). Without active roll control, the system is stable (with poles at $-1.76 \pm j3.59$, $-12.2 \pm j6.20$, -582 and -602 rad/s) and minimum phase (that is, there are no zeros in the right half plane). The system is input deficient — that is, by the controllability analysis presented in section 3.5.4, there are not sufficient inputs to independently control all three outputs — so some compromise is required. By an eigenvalue analysis outlined in section 3.5.5, it is possible for the vehicle (both with and without active roll control) to maintain roll stability after either the steer or drive axle lifts off, so it is important to control the load transfers at both axles. From section 3.6, the achievable design objective that maximises the vehicle's roll stability is to balance the normalised load transfers at the steer and drive axles while taking the larger suspension roll angle to the maximum allowable inward angle.

Next consider the case of the torsionally flexible single unit vehicle. There are

four roll outputs (the body roll angles at the front and rear of the vehicle and the load transfers at the steer and drive axles) and two roll control inputs, and the system is again input deficient. Without active roll control, the system is stable (with poles at $-1.58 \pm j3.39$, $-14.1 \pm j5.50$, $-3.78 \pm j20.8$, -583 and -602 rad/s) and minimum phase. The eigenvalue analysis shows that, for a frame stiffness of 629 kN.m/rad, it is still possible for the vehicle (both with and without active roll control) to maintain roll stability after either the steer or drive axle lifts off, so again it is important to control the load transfers at both axles. By the results presented in section 3.6, the achievable design objective that maximises the roll stability of the vehicle is to balance the normalised load transfers at the steer and drive axles while taking the larger suspension roll angle to the maximum allowable inward angle.

Sections 4.4 and 4.5 consider techniques for designing control systems to meet these objectives.

4.4 Classical control techniques

4.4.1 Control of SISO systems

In classical control system design techniques such as the root locus method, the objective is to adjust the gains of a feedback controller such that the closed loop system has a desirable eigenvalue pattern. The fact that the closed loop eigenvalues of a single input single output (SISO) system characterise the response to a large extent has allowed the successful application of classical control system design techniques to a wide range of practical SISO control problems [86]. The stability of an SISO system depends on the eigenvalues being located in the left half plane. The damping ratios of the fundamental modes strongly influence transient properties such as the overshoot and settling time in response to a step input. The magnitudes of the eigenvalues are related to the speed of response and the bandwidth of the system.

4.4.2 Control of MIMO systems

The roll control of articulated vehicles and even of single unit vehicles is an MIMO control problem. The problem is to regulate multiple load transfers (outputs) using multiple active anti-roll bar moments (inputs).

The fundamental difference between SISO and MIMO systems is the existence of directions, as described by the eigenvectors. In general, a change to a single input of a multivariable system will affect all the outputs.

The suitability of the root locus method for multivariable control system design depends on the extent to which the performance of a multivariable system is characterised by the eigenvalues of the matrix transfer function. In fact, the eigenvalues of an MIMO system do carry stability properties but do not sufficiently characterise the performance of the system, which depends on both the eigenvalues *and* the eigenvectors [50]. Furthermore the eigenvalues of the transfer function matrix of a multivariable system are a poor measure of the gain from a single input to a single output [94]. This is because the eigenvalues measure gain for the special case where the inputs and outputs are in the same direction, and this is not the case in general. Thus the use of eigenvalue assignment (that is, the root locus method) should not be expected to yield satisfactory performance for multivariable control system designs.

An exception is the case where the transfer function matrix is strongly diagonal and the system is comprised essentially of a number of independent SISO sub-systems. The multivariable control system design problem then reduces to a number of SISO problems, allowing feedback controllers for each sub-system to be designed independently. This is not the case for the dynamics of heavy vehicles, where the different roll-plane and yaw-plane motions are strongly coupled.

4.4.3 Eigenstructure assignment

The fact that MIMO system stability and performance are strongly influenced by *both* the closed loop eigenvalues and eigenvectors is the motivation for the method of eigen-

structure assignment. (An eigenstructure is a set of eigenvalues and corresponding eigenvectors.) The objective of this method is to find a feedback controller such that the closed loop eigenstructure closely matches some desirable target eigenstructure. This method may be viewed as a multivariable extension of the classical root locus method.

The closed loop eigenvalues of a linear dynamic system

$$\dot{x} = Ax + B_0 u, \quad y = C_0 x, \quad z = C_1 x \tag{4.1}$$

may be placed arbitrarily to any self-conjugate set providing (A, B_0) is controllable [111]. For SISO systems, the state feedback gain is uniquely determined by the desired eigenvalue pattern so it is not possible to specify the closed loop eigenvectors independent of the closed loop eigenvalues. However for MIMO systems, the desired eigenvalue pattern may not uniquely determine a state feedback controller and typically there is substantial freedom in selecting the controller parameters [62]. This extra design freedom can be exploited to partially specify the eigenvectors [86].

To explain the extent to which eigenstructure assignment is possible, consider an m input, p output system described by equation (4.1), with (A, B_0) controllable, (C_0, A) observable and some constant output feedback controller. (Note that state feedback is a special case of constant output feedback with $C_0 = I$. Note also that the dynamic compensation problem can be reformulated as a constant output feedback problem [50], so there is no loss of generality by considering the constant output feedback case.) It is possible to arbitrarily specify $\max(m, p)$ closed loop eigenvalues and to partially specify $\max(m, p)$ closed loop eigenvectors with $\min(m, p)$ elements in each eigenvector arbitrarily chosen [96]. To ensure that the resulting eigenvectors are in some sense close to the desired eigenvectors, the standard approach is first to form a new approximate set of target eigenvectors by projecting the desired eigenvectors onto the achievable eigenspace and then to perform an optimisation such that the closed loop eigenvectors are close to the new approximate set in a weighted least squares sense.

This base-line technique can also be extended to account for certain parameter variations and unmodelled dynamics.

There are a number of issues that limit the usefulness of eigenstructure assignment for vehicle roll controller design. As described in section 3.5.4, even vehicles fitted with active anti-roll bars at each axle group are typically input deficient, so the number of elements that can be arbitrarily chosen in each eigenvector is limited. Thus it may be difficult to achieve a closed loop eigenstructure that is reasonably close to the target eigenstructure. However the more fundamental and difficult problem is how to select the target eigenvalues and eigenvectors and tune the optimisation weightings to produce a closed loop system with satisfactory performance. For some simple physical systems, it is possible to specify a desirable set of eigenvalues and eigenvectors by inspection [94]. The yaw-roll dynamics of articulated heavy vehicles are complicated and strongly coupled, however, and it is unclear what the optimal target eigenstructure should be to ensure maximum roll stability, acceptably small degradation in handling and reasonable actuator force and bandwidth requirements. Thus the technique of eigenstructure assignment is not well suited to heavy vehicle roll controller design.

4.4.4 Decoupling by inverse-based control

A conceptually simple alternative approach to dealing with off-diagonal plant interactions is to use the following two step design procedure [94]. First, design a precompensator $W_1(s)$ for the non-diagonal multivariable plant $G(s)$ such that the new shaped plant $G_s(s) = G(s)W_1(s)$ is more diagonal and easier to control than the original plant. Then, design a diagonal controller $K_s(s)$ for the shaped plant using classical methods applicable to SISO systems. The overall controller for the real plant $G(s)$ is then given by $K(s) = W_1(s)K_s(s)$.

Unfortunately the resulting *inverse-based* controller typically features a number of undesirable properties [19, 94]. Systems with inverse-based controllers may be expected to produce impractically large demand signals at the actuators and may even

be internally unstable. Furthermore, it can be difficult to design a physically realisable inverse-based controller if the plant has a pole deficit of two or more. Inverse-based controllers feature poor robustness against modelling errors and may possess poor disturbance rejection performance [94]. Since the problem of roll controller design for heavy vehicles is essentially a problem of disturbance rejection, the use of an inverse-based controller would not be expected to yield satisfactory performance.

4.4.5 Control using SISO loop closures

In some cases, it is possible to control a multivariable plant effectively using a series of nested SISO controllers. One state variable is controlled by an inner SISO feedback loop and each subsequent state variable is controlled by another SISO loop surrounding the previous loops. Classical techniques can be used to shape each of these SISO loops.

To work best, this technique requires a large separation of timescales between different loops (typically a fast inner loop within a slow outer loop), a nearly diagonal system and a comparable number of control inputs and controlled outputs [86, 94]. However the problem of vehicle roll control is strongly nondiagonal, the timescales of the variables to be controlled (the load transfers and the roll angles) are similar and the system is input deficient. Therefore it is not obvious how SISO loop closures can be performed for this system.

4.4.6 Alternatives to classical control system design techniques

Clearly there are significant difficulties in using classical-based techniques for solving strongly multivariable control problems such as vehicle roll control. The alternative approach is to directly synthesise an optimal multivariable controller based on minimising some objective function. This approach is discussed in subsequent sections.

4.5 $\mathcal{H}_2$ control techniques

The $\mathcal{H}_2$ or linear quadratic optimisation is the fundamental technique in optimal control theory. The $\mathcal{H}_2$ controller design method is a signal-based approach that enables an explicit trade-off between performance and level of control activity for MIMO systems [50]. Roll control system design can be cast as a problem of load trasfer regulation in the presence of steering disturbances.

The suitability of using several variations of the basic linear quadratic optimal control problem for heavy vehicle roll controller design will be explored in the following sections. An important variation of the basic problem, the linear quadratic regulator (LQR) problem, has been used to design active roll control systems to improve the roll stability of single unit heavy vehicles [51, 55, 77]. However it will be shown that the standard LQR approach must be extended to provide optimal disturbance rejection.

4.5.1 Linear quadratic regulator problem

The linear quadratic regulator (LQR) problem is the infinite horizon, time invariant linear quadratic optimal control problem. Consider a strictly proper system

$$\dot{x} = Ax + B_0 u, \qquad z = C_1 x. \tag{4.2}$$

The LQR problem is to find the control $u(t)$ that minimises the quadratic performance index

$$J \;=\; \int_0^\infty \left(z^T Q z + u^T R u \right) dt \tag{4.3}$$

where the matrices Q and R are design parameters representing the relative weighting of the performance output trajectory z and the control input u respectively. For practical problems, Q is positive semidefinite, R is positive definite and (A, B_0) is controllable.

The solution is found using the calculus of variations, as detailed by Bryson and

Ho [8]. The optimal control law is provided by a state feedback controller

$$u(t) = K_{FB}x(t) \tag{4.4}$$

where

$$K_{FB} = -R^{-1}B_0^T S \tag{4.5}$$

and where S is a symmetric, positive semidefinite matrix satisfying the Riccati equation

$$SA^T + A^T S - SB_0R^{-1}B_0^T S + C_1^T QC_1 = 0. \tag{4.6}$$

The controller configuration is shown in figure 4.2.

If (A, B_0) is controllable and (C_1, A) is observable, then equation (4.6) has a unique solution S in the class of symmetric, positive semidefinite matrices [113]. Furthermore, it can be shown that the closed-loop system

$$\dot{x} = \left(A - B_0R^{-1}B_0^T S\right) x \tag{4.7}$$

is asymptotically stable [113].

4.5.2 Linear quadratic regulator with constant disturbance

The standard LQR approach is used to synthesise an optimal controller for the special case of zero input disturbance, as described by equation (4.2). However the problem of vehicle roll control is a problem of optimal disturbance rejection. The aim is to regulate load transfers in response to steering inputs from the driver. To demonstrate that the optimal control law for disturbance rejection is more involved than that given by equation (4.4), consider first the problem of optimal regulation in the presence of a constant deterministic disturbance $r(t)$. (In section 4.5.3, the design of a controller to provide optimal regulation in the presence of a stochastic input disturbance will be detailed.) Assume that the disturbance is measured and therefore can be included in

the optimal control law if necessary.

Consider a strictly proper linear dynamic system

$$\dot{x} = Ax + B_0 u + B_r r, \qquad z = C_1 x. \tag{4.8}$$

The problem is to find the control $u(t)$ to minimise the quadratic performance index

$$J = \int_0^\infty \left(z^T Q z + u^T R u \right) dt \tag{4.9}$$

where the matrices Q and R are design parameters representing the relative weighting of the performance output trajectory z and the control input u respectively.

The optimal control law is provided by a feedback controller K_{FB} *plus* a feedforward controller K_{FF} [50],

$$u(t) = K_{FB} x(t) + K_{FF} r(t), \tag{4.10}$$

where

$$K_{FB} = -R^{-1} B_0^T S, \qquad K_{FF} = R^{-1} B_0^T \left(A^T - S B_0 R^{-1} B_0^T \right)^{-1} S B_r, \tag{4.11}$$

and S satisfies the Riccati equation (4.6).

The controller configuration is shown in figure 4.3. Clearly the standard LQR problem from section 4.5.1 is the special case of the constant input disturbance problem with $r(t) = 0$.

4.5.3 Optimal disturbance rejection system design

The vehicle is subject to an exogeneous input in the form of the steering input. In section 4.5.2, it was shown that the optimal control law for a linear dynamic system with an input disturbance consists of a feedback controller on the vehicle states *plus* a feedforward controller on the input disturbance.

It is always possible to optimise a controller for one particular transient input, for example steady state cornering or a specific lane change manoeuvre. However in reality a vehicle is subjected to a range of different transient steering inputs which may all be equally likely and it is important to design a controller that is optimised over this range of disturbances [51, 55].

Effective disturbance rejection can be achieved if the dynamic properties of the disturbance are modelled and included in the controller design [50]. *For an optimal disturbance rejection law, the states of the disturbance inputs must be measured or estimated such that the feedback of the disturbance states to the controller becomes part of the feedback law.*

The steering input to a vehicle can be modelled as a zero-mean coloured stochastic process. That is, while it is not possible to predict the value of the steering input at any specific instant during a day of normal driving, it is possible to describe the typical frequency content in the form of a power spectral density function.

The steering input is described by a shaping filter (A_D, B_D, C_D, D_D) such that a zero-mean white noise source w at the input to the filter produces an appropriately time correlated stochastic steering disturbance δ at the output:

$$\dot{x}_D = A_D x_D + B_D w, \quad \delta = C_D x_D + D_D w. \tag{4.12}$$

Note that the shaping filter required to describe typical steering inputs is in the form of a low-pass filter (with $D = 0$), usually of first or second order [51, 54]. This form is convenient since the disturbance states x_D can be reconstructed from the filter output δ without knowledge of the white noise input w. A block diagram of such a shaping filter is shown in figure 4.4.

This steering disturbance δ then acts as the input to the vehicle system through the input injection node described by the matrix B_1 such that the dynamics of the system

are described by

$$\begin{aligned} \dot{x} &= Ax + B_0 u + B_1 \delta \\ &= Ax + B_0 u + B_1 C_D x_D + B_1 D_D w, \end{aligned} \tag{4.13}$$

as shown in figure 4.5(a).

Equation (4.13) can be rewritten by forming an augmented state vector $\underline{x}$ including the system states x and the disturbance state x_D such that the dynamics of the system are described by

$$\dot{\underline{x}} = \underline{A}\,\underline{x} + \underline{B}_0 u + \underline{B}_1 w \tag{4.14}$$

where

$$\underline{x} = \begin{bmatrix} x \\ x_D \end{bmatrix}, \quad \underline{A} = \begin{bmatrix} A & B_1 C_D \\ 0 & A_D \end{bmatrix}, \quad \underline{B}_0 = \begin{bmatrix} B_0 \\ 0 \end{bmatrix}, \quad \underline{B}_1 = \begin{bmatrix} B_1 D_D \\ B_D \end{bmatrix}.$$

Since x_D is a disturbance state, the optimal control is chosen to minimise the performance index described in equation (4.9). The optimal controller is a feedback controller K_{FB} operating on $\underline{x}$, and the optimal control law is given by

$$u(t) = K_{FB}\underline{x}(t) \tag{4.15}$$

where

$$K_{FB} = -R^{-1}\underline{B}_0^T S \tag{4.16}$$

and where S is the solution to the appropriate Riccati equation. The controller configuration is shown in figure 4.5(b).

Partitioning the feedback controller $K_{FB} = \begin{bmatrix} K_{FB,1} & K_{FB,2} \end{bmatrix}$ such that $K_{FB,1}$ denotes the gain on x and $K_{FB,2}$ denotes the gain on x_D, the closed loop system is

described by

$$\begin{bmatrix} \dot{x} \\ \dot{x}_D \end{bmatrix} = \begin{bmatrix} A + B_0 K_{FB,1} & B_1 C_D + B_0 K_{FB,2} \\ 0 & A_D \end{bmatrix} \begin{bmatrix} x \\ x_D \end{bmatrix} + \begin{bmatrix} B_1 D_D \\ B_D \end{bmatrix} w. \quad (4.17)$$

The term $B_0 K_{FB,2}$ acts as a feedforward control on the disturbance states x_D. This feedforward action reduces the response of the closed loop system to stochastic disturbances, as in section 4.5.2. However the stability of the closed loop system is unaffected by this feedforward control since the closed loop eigenvalues of the system are simply the eigenvalues of $A + B_0 K_{FB,1}$ and A_D. By contrast, for the case where x_D is estimated from the system response rather than measured, $K_{FB,2}$ becomes part of the feedback loop and therefore can affect the stability.

4.5.4 Robustness properties of LQR control

An LQR-controlled system with no stochastic process noise or measurement noise has favourable guaranteed stability margins: a gain margin of infinity, a gain reduction margin of 0.5, and a phase margin of at least 60° at each control input [37, 75]. (A necessary condition is that the weight R is chosen to be diagonal.)

4.5.5 Linear quadratic Gaussian problem

The LQR designs presented in sections 4.5.1–4.5.3 require that all the internal states of the system and all the disturbance states are available for feedback (and, in some cases, feedforward). Typically this is not practical because it may be difficult or prohibitively expensive to measure certain states, for example, sideslip angle. Furthermore the sensor output signals will be corrupted to some extent by noise, so to accurately deduce the states even from a complete set of measured outputs is not straightforward.

A more realistic system model is

$$\underline{\dot{x}} = \underline{A}\,\underline{x} + \underline{B}_0 u + \underline{B}_1 w, \quad \underline{y} = \underline{C}_0 \underline{x} + v, \quad (4.18)$$

where w and v are vectors representing the process noise and measurement noise respectively. The process noise w in this case is due to steering inputs from the driver, although it is also possible to model certain plant uncertainties as process noise. The measurement noise v is due to sensor inaccuracies and electrical interference. Both w and v are assumed to be uncorrelated zero-mean Gaussian stochastic processes with constant covariance matrices W and V such that

$$E\left\{w(t)w(\tau)^T\right\} = W\hat{\delta}(t-\tau), \tag{4.19}$$

$$E\left\{v(t)v(\tau)^T\right\} = V\hat{\delta}(t-\tau), \tag{4.20}$$

$$E\left\{w(t)v(\tau)^T\right\} = 0, \tag{4.21}$$

$$E\left\{v(t)w(\tau)^T\right\} = 0, \tag{4.22}$$

where $E\{\cdot\}$ is the *mean value operator* (also known as the *expectation operator*) and $\hat{\delta}(t-\tau)$ is a Dirac delta function (not to be confused with the steering input, δ).

The linear quadratic Gaussian (LQG) problem is to find the control $u(t)$ that minimises

$$J = E\left\{\int_0^\infty \left(x^T Q x + u^T R u\right) dt\right\} \tag{4.23}$$

where the matrices Q and R are design parameters as described in section 4.5.2 [113]. The name LQG is used because the problem involves a linear system, a quadratic cost function and Gaussian white process and measurement noise.

It is possible to incorporate coloured noise inputs into the LQG framework by augmenting the vehicle system model with shaping filters at the disturbance inputs. Thus white noise inputs to the augmented plant appear as coloured noise inputs to the vehicle system model. The characterisation of measurement noise is a less straightforward problem and is discussed in section 4.5.7.

By the *separation principle*, the solution to the LQG problem is surprisingly simple and elegant and consists of an optimal state estimator and an optimal state feedback controller that are designed independently [49].

The optimal state feedback controller is a linear quadratic regulator as described in section 4.5.3.

The optimal state estimator under additive process and measurement noise is a Kalman filter. The state estimator uses noisy measurements $\underline{y}$ and plant control inputs u to generate estimates $\underline{\hat{x}}$ of $\underline{x}$ (that is, both the system states x and the disturbance states x_D) according to

$$\dot{\underline{\hat{x}}} = A\underline{\hat{x}} + \underline{B}_0 u + H(\underline{y} - \underline{C}_0\underline{\hat{x}}), \tag{4.24}$$

and the problem is to find H to minimise the estimation error $E\left\{(\underline{x} - \underline{\hat{x}})^T (\underline{x} - \underline{\hat{x}})\right\}$. The controller configuration is shown in figure 4.6. This problem is a dual of the linear quadratic regulator problem, and in the time invariant case, the optimal choice of H is given by

$$H = P\underline{C}_0^T V^{-1} \tag{4.25}$$

where P is the unique solution of the Riccati equation

$$P\underline{A}^T + \underline{A}P - P\underline{C}_0^T V^{-1}\underline{C}_0 P + W = 0, \quad P = P^T \geq 0. \tag{4.26}$$

Trade-offs between speed of estimation and measurement noise attenuation are accomplished by varying the design parameters W and V, in much the same way as trade-offs between performance and control effort are affected by varying Q and R in the LQR design. As $V \to 0$ (or equivalently as $W \to \infty$), the estimation speed of the Kalman filter improves but the measurement noise rejection capability worsens.

Dual arguments to those presented in section 4.5.4 can be used to show that a Kalman filter with a diagonal measurement noise weighting matrix V has an infinite gain margin, a gain reduction margin of 0.5 and a phase margin of at least 60° at each filter input.

The optimal state feedback controller and the optimal state estimator may be combined as shown in figure 4.6 to form an LQG controller. This controller uses a set of

noisy output measurements, control signal measurements and an internal model of the system dynamics to provide optimal regulation of the plant.

4.5.6 Robustness properties of LQG control

Guaranteed stability margins for the LQR controller and the Kalman filter were detailed individually in sections 4.5.4 and 4.5.5 respectively. Referring to figure 4.6, there are guaranteed stability margins at the Kalman filter input (3) and at the controller output (4), where robustness is not particularly important. However there are no guaranteed stability margins at the plant input (1) and the plant output (2), where good robustness is required. Indeed there exist LQG combinations with arbitrarily small gain margins [20]. Thus a Kalman filter design must be carried out very carefully to ensure that the resulting LQG controller has similar robustness properties and transient performance as the full-state LQR design. A suitable design technique is described in the following section.

4.5.7 Loop transfer recovery

The *loop transfer recovery* (LTR) method is a technique for indirectly shaping the singular values of the LQG loop transfer function with the aim of recovering the favourable guaranteed stability margins of LQR control [20]. The technique is restricted to minimum phase plants and the matrices W and V must be chosen such that $V > 0$ is diagonal and $W \geq 0$ is symmetric.

The design of the Kalman filter in an LQG controller requires statistical information about the process and measurement noise (in the form of the matrices W and V) which is typically unavailable and is often impractical to attain. However the LQG design parameters Q, R, W and V strongly affect the performance of the system. The usual approach then is to use W and V as tuning parameters to improve system performance.

The two step LQG-LTR control design procedure consists of a *loopshaping* step

and a *recovery* step. In the loopshaping step, the regulator design parameters Q and R are varied to design a full-state linear quadratic regulator with favourable time domain and frequency domain characteristics. The LQR loop transfer function then becomes the *target feedback loop* transfer function. In the recovery step, the filter design parameters W and V are varied until the full LQG loop transfer function is acceptably close to the target feedback loop transfer function. As $V \to 0$ (or equivalently as $W \to \infty$), the LQG loop transfer function will asymptotically approach the target feedback loop transfer function.

Full loop transfer recovery is inadvisable in practice since, as $V \to 0$, the increase in the Kalman filter gain reduces measurement noise attenuation and can cause a lack of robustness to unmodelled dynamics [21]. Instead V is reduced until an acceptable balance between transient performance, adequate stability margins and measurement noise attenuation characteristics is reached.

4.6 Control of a torsionally rigid single unit vehicle

The design of an active roll control system for a torsionally rigid single unit vehicle is considered first. The effect of torsional flexibility of the vehicle frame is investigated in section 4.7.

4.6.1 Design of a full-state feedback controller

The design of a full-state active roll controller is a problem of optimal disturbance rejection system design.

It is desirable to optimise the active roll control system across the range of possible steering inputs rather than simply in response to a single manoeuvre. Since the steering input is to be modelled as a coloured noise process, it is necessary to specify an appropriate shaping filter (A_D, B_D, C_D, D_D) as described in (4.12). Lin developed a suitable steering spectrum by combining a low frequency steering spectrum from UK road alignment data with a higher frequency steering spectrum to represent lane change

manoeuvres [51, 55]. Combining the spectral densities from these low and high frequency sources, he found that, for a very active level of driver input on a typical road, the steering input spectrum could be modelled approximately by

$$S_\delta(\omega) = \frac{0.00014}{\omega^2 + 4}\,\mathrm{rad}^2/(\mathrm{rad/s}) \tag{4.27}$$

This corresponds to white noise filtered with a first order filter with a cut-off frequency of 4 rad/s:

$$\dot{x}_D = -4x_D + 2w, \qquad \delta = 2x_D. \tag{4.28}$$

An optimal control system means only that the control law minimises some performance index. The challenge is to choose an appropriate performance index, through selecting weighting matrices Q and R, to ensure that the control system meets the design objectives. Since the torsionally rigid single unit vehicle is input deficient, the active roll control system design is a trade-off between reducing lateral load transfers, constraining suspension roll angles and limiting energy requirements.

The weighting matrices Q and R penalise the performance output z and the control input u respectively. In order to simplify the selection of these matrices, the elements of Q are chosen to penalise only the unsprung mass roll angle terms (since the load transfer at an axle is equal to the unsprung mass roll angle multiplied by the effective roll stiffness of the tyres),

$$z = \begin{bmatrix} \phi_{t,f} & \phi_{t,r} \end{bmatrix}^T. \tag{4.29}$$

The constraint on suspension roll angles is handled implicitly by selecting the elements of R to be sufficiently large to limit the roll moments from the active anti-roll bars, since excessive roll moments lead to excessive inward roll angles. A useful starting point for selecting the elements of the weighting matrices is to choose Q and R as diagonal matrices

$$Q = \begin{bmatrix} q_1 & 0 \\ 0 & q_2 \end{bmatrix}, \qquad q_i = (z_{\mathrm{i,max}})^{-2} \tag{4.30}$$

and

$$R = \begin{bmatrix} r_1 & 0 \\ 0 & r_2 \end{bmatrix}, \qquad r_i = (u_{\mathrm{i,max}})^{-2} \tag{4.31}$$

where $z_{\mathrm{i,max}}$ and $u_{\mathrm{i,max}}$ are respectively the maximum acceptable values of the ith elements of the performance output vector and control input vector [8]. From this starting point, an iterative design process follows in which the elements of Q and R are tuned to produce a controller with acceptable performance across a range of manoeuvres. The following tuning procedure was used for the range of vehicles investigated in this report, and produced good performance with a reasonably limited number of design iterations:

1. Adjust the elements of Q and R to tune the steady-state performance of the system such that the normalised load transfers at all critical axles are balanced and the maximum inward suspension roll angle at roll-over is around 4°. Although this may seem conservative, the largest steady-state suspension roll angle should be less than the maximum allowable angle to leave space for overshoot in severe transient manoeuvres; otherwise the axles will strike the bump stops.

2. Simulate the performance of the vehicle for a range of severe transient manoeuvres including step steering inputs and lane changes.

3. If the maximum suspension roll angle in response to any critical* transient manoeuvre is greater than the maximum allowable angle, then the step 1 should be repeated with the largest steady-state inward suspension roll angle at roll-over reduced.

4. If the peak normalised load transfer responses among the axles are poorly balanced in severe transient manoeuvres, it is necessary to adjust the elements of Q and R. This will necessarily require a compromise in the steady-state balance. The compromise required is typically small for torsionally rigid single

*A manoeuvre is described as *critical* when the size of the steering input is just sufficient to induce roll-over.

unit vehicles. A greater compromise is required for articulated vehicles, particularly when a high level of rearward amplification is present, for example at high speed or where pintle hitch couplings are used.

For a speed of 60 km/h, the weighting matrices were chosen to be

$$Q = \begin{bmatrix} 1.000 & 0 \\ 0 & 1.850 \end{bmatrix} \mathrm{rad}^{-2}, \tag{4.32}$$

$$R = 1.246 \times 10^{-14} \begin{bmatrix} 1 & 0 \\ 0 & 1 \end{bmatrix} \mathrm{N}^{-2}.\mathrm{m}^{-2}. \tag{4.33}$$

This produced a full-state feedback controller

$$K_{FB} = \begin{bmatrix} -4.006 \times 10^5 & -3.282 \times 10^5 \\ -3.124 \times 10^5 & -3.650 \times 10^5 \\ -2.032 \times 10^6 & -2.299 \times 10^6 \\ 3.553 \times 10^5 & 3.441 \times 10^5 \\ 6.886 \times 10^6 & 4.411 \times 10^6 \\ 7.279 \times 10^4 & 8.898 \times 10^6 \\ 2.184 \times 10^6 & 3.145 \times 10^6 \end{bmatrix}^T \begin{matrix} \mathrm{N.m/rad} \\ \mathrm{N.m.s/rad} \\ \mathrm{N.m/rad} \\ \mathrm{N.m.s/rad} \\ \mathrm{N.m/rad} \\ \mathrm{N.m/rad} \\ \mathrm{N.m/rad} \end{matrix} \tag{4.34}$$

acting on the augmented state vector

$$\underline{x} = \begin{bmatrix} \phi & \dot{\phi} & \beta & \dot{\psi} & \phi_{t,f} & \phi_{t,r} & \delta/2 \end{bmatrix}^T. \tag{4.35}$$

The performance of this controller is examined in detail in sections 4.6.2–4.6.5.

4.6.2 Steady-state cornering response

From section 1.1, there is a strong link between steady-state roll stability and the probability of a vehicle being involved in a roll-over accident. The response of the linear,

torsionally rigid single unit vehicle model with a full-state feedback controller to a steady-state steering input at 60 km/h is shown in figure 4.7.

With passive suspension, the vehicle rolls out of the corner (that is, negative roll angle). Since the vehicle frame is torsionally rigid, the absolute roll angles at the front and rear are identical. However, the *suspension* roll angles (that is, the relative roll angles between the sprung and unsprung masses) differ due to the small difference in the unsprung mass roll angles at the steer and drive axles. The roll motion of the sprung mass generates a *destabilising* lateral displacement moment. As lateral acceleration increases, the normalised load transfer builds up more quickly at the drive axle than at the steer axle, since the ratio of effective roll stiffness to vertical load is greater at the drive axle. The drive axle lifts off at 0.42 g (point A), at which point the normalised load transfer at the steer axle is 0.82 (point B). As lateral acceleration continues to increase, the drive axle is unable to contribute any additional restoring moment and the slopes of the suspension roll angle and normalised load transfer curves increase, as described in section 3.3.3. The normalised load transfer at the steer axle reaches 1 at 0.43 g (point C), and the vehicle rolls over.

By contrast, with active roll control, the vehicle rolls into the corner (that is, positive roll angle). This motion of the sprung mass generates a *stabilising* lateral displacement moment. The total roll moment from the active anti-roll bars is distributed between the drive and steer axles so that, as lateral acceleration increases, the normalised load transfers at the two axles increase in a balanced fashion, reaching the maximum value of 1 simultaneously at 0.53 g (point D). The suspension roll angle at the steer axle at roll-over is 3.2° inward. For clarity, only the maximum suspension roll angles in the passive and active cases are shown in figure 4.7(a) and similar figures throughout chapters 4, 5 and 6. This is because the key purpose of the plot is to show how much of the available suspension travel is used. The relative magnitudes of *all* steady-state suspension roll angles are shown elsewhere, in the steady-state section of the plot of suspension roll angle response to a step steering input (in this case, figure 4.9(c)).

The roll-over threshold of the torsionally rigid single unit vehicle is increased by 23% and the lateral acceleration at which axle lift-off first occurs is increased by 28% due to the action of the active roll control system. This represents a significant increase in steady-state roll stability.

4.6.3 Response to a step steering input

A rapid transition from straightline running to constant radius cornering requires a step-like steering input.

An instantaneous change in steering input is unrealistic because the curvature of highways changes continuously and the frequency response of a driver is limited, even in rapid avoidance manoeuvres [107]. To generate a severe but feasible step-like input, the steering angle was ramped from zero to the maximum value over a period of 0.5 s and this curve was then filtered at a frequency of 4 rad/s to represent the finite bandwidth of the driver [51, 84]. The resulting input is shown in figure 4.8. The magnitude of the steering input is scaled to give a maximum normalised load transfer of 1 in the following simulations. The response of the linear, torsionally rigid single unit vehicle model with a full-state feedback controller to this step-like steering input at 60 km/h is shown in figure 4.9.

The trajectory and lateral acceleration responses are shown in figures 4.9(a) and 4.9(b) respectively. Both with and without active roll control, the vehicle quickly settles into a constant turn of radius 74 m in response to the steering input of 3.1°. The corresponding lateral acceleration is 0.38 g. For the linear vehicle model, the steady-state handling performance is decoupled from the roll-plane motion, so the action of the active roll control system does not alter the steady-state lateral acceleration. However there is some difference in transient lateral acceleration response due to the dynamic coupling of yaw and roll motions.

The suspension roll angle responses are shown in figure 4.9(c). Without active roll control, the vehicle rolls out of the corner with a steady-state roll angle of 4.3°,

whereas with active roll control, it rolls into the corner at an angle of approximately 2.3°. The suspension roll angles must be constrained to limits set by the available wheel travel. The suspension roll angle responses for the vehicle equipped with the active roll control system overshoot the steady-state values by 36%. Overshoot reduces the maximum achievable inward steady-state roll angle, and thus the achievable roll-over threshold, because the controller is tuned to avoid the axles striking the bump stops, even momentarily, in severe transient manoeuvres. However, there is a trade-off between roll angle and load transfer such that, to reduce the roll angle overshoot, it is necessary to reduce the speed of response of the controller, thus increasing the peak load transfer response in severe transient manoeuvres.

The normalised load transfer responses are shown in figure 4.9(d). Without active roll control, the normalised load transfer builds up more quickly at the drive axle than at the steer axle, as in the steady-state cornering case. The load transfer responses feature small overshoots before settling at final values of 0.76 and 0.93 for the steer and drive axles respectively. In contrast, the load transfer responses for the vehicle fitted with an active roll control system are overdamped and rise monotonically to a value of 0.72 at *both* the steer and drive axles for the same manoeuvre. (The performance benefits of delaying the rise of load transfer will be demonstrated more clearly in section 4.6.4.) The active roll control system reduces the peak load transfer by 11% at the steer axle and by 28% at the drive axle.

Steady-state results from section 4.6.2 show that, without active roll control, the roll-over threshold for this vehicle is only marginally (5%) higher than the lateral acceleration at which axle lift-off first occurs. However, since the peak normalised load transfer for the vehicle with active roll control is 0.72, this vehicle could remain stable with up to 39% additional lateral acceleration (that is, up to 0.53 g). The peak inward roll angle in response to such an input is 4.3°, which is within the allowable range. Therefore it is clear that the active roll control system provides a significant increase in dynamic roll stability in response to a step steering input.

In order to balance the normalised load transfers between the two axles, the active

roll control system produces significant roll moments at both axles, with the majority of the roll moment (59%) applied at the drive axle (see figure 4.9(e)). Since the peak roll moment is 65 kN.m at the drive axle and the peak normalised load transfer is 0.72, the peak roll moment at the drive axle in response to a critical step steering input is 90 kN.m. This is below the maximum active roll moment of 120 kN.m recommended by McKevitt, who performed a preliminary hardware design for the active roll control system using reasonably priced standard components [59].

The fluid flow rates through the servo-valves are proportional to the relative roll rates between the sprung and unsprung masses at the steer and drive axles. (The geometry of active anti-roll bar systems at the two axles is assumed to be identical; this may or may not be true in practice.) Since the vehicle frame is torsionally rigid, the relative roll angles, roll rates and fluid flow rates at the two axles vary only due to differences in small axle roll motions, as shown in figure 4.9(c). The positive half of figure 4.9(f) shows the flow rates supplied through the left side servo-valves and the negative half of the plot shows the flow rates supplied through the right side servo-valves. When the roll angle is increasing, the left side valve is supplying oil to the (larger) piston side of the left actuator and the right side valve is supplying oil to the (smaller) rod side of the right actuator, and vice versa. Therefore the two parts of the figure always vary by the ratio of areas on the piston and rod sides of the actuators. Since the peak roll flow rate is 0.73 l/s and the peak normalised load transfer is 0.72, the peak roll moment at the drive axle in response to a critical step steering input is 1.02 l/s, which is below McKevitt's maximum recommended flow rate of 2.2 l/s [59].

Since the active anti-roll bars are very stiff, the power supplied to the system (neglecting losses in the hydraulics) can be calculated approximately as the sum of the products of active roll moment and suspension roll rate at each axle. The peak power supplied to the system in response to a critical step steering input is 7.2 kW. A practical active roll control system would most likely operate intermittently so as not to consume power when the vehicle is running in a straight line. Therefore the peak power consumed by a continuously operating system is a more useful metric than the

average power, which was discussed in detail by Lin [51, 54, 55].

4.6.4 Response to a double lane change steering input

A double lane change manoeuvre is often used to avoid an obstacle in an emergency. The double lane change is a popular test manoeuvre for heavy vehicles since it can be used to measure rearward amplification.

The double lane change manoeuvre used here features a 5 m path deviation over a 120 m test section. The size of path deviation is chosen to ensure moderately high peak values of lateral acceleration at 60 km/h. The steering input, which is shown in figure 4.10, consists of two full sine waves, back-to-back and filtered at 4 rad/s to represent the finite bandwidth of the driver. Figure 4.11 shows the response of the linear, torsionally rigid single unit vehicle model with a full-state feedback controller to this double lane change steering input at 60 km/h.

The trajectory and lateral acceleration responses are shown in figures 4.11(a) and 4.11(b) respectively. The simulations of the vehicle with and without the active roll control system share a common open loop steering input rather than a common trajectory, so there are differences between the trajectory and lateral acceleration responses. In general, the yaw response of the vehicle with active roll control is less oscillatory and the peak lateral acceleration of this vehicle is therefore slightly lower.

The suspension roll angle responses are shown in figure 4.11(c). The vehicle with passive suspension rolls out of the corners, whereas the vehicle with active roll control rolls into the corners.

The normalised load transfer responses are shown in figure 4.11(d). With passive suspension, the normalised load transfer is again higher at the drive axle than at the steer axle. The peak normalised steer axle load transfer is 0.47, compared to 0.61 at the drive axle. When equipped with the active roll control system, the normalised load transfer responses at the steer and drive axles are again balanced, both with a peak value of 0.38. Thus the peak load transfer is reduced by 20% at the steer axle and by

38% at the drive axle.

The active roll control reduces load transfers even more significantly for this double lane change manoeuvre than for the steady-state or step steering inputs. This is because the system is able to slow the build-up of load transfers (as noted in section 4.6.3) to such an extent that, before the load transfers rise to the steady-state values, the steering input is already bringing the vehicle back in the other direction. It should be noted that this manoeuvre generates larger suspension roll angles per normalised load transfer than the steady-state or step manoeuvres. If the path deviation is increased to take the active vehicle to the point of roll-over, the peak suspension roll angle is 5.9°.

Figure 4.11(e) shows that the majority of the total roll moment is again generated at the drive axle. The peak roll moment generated at the drive axle is 40 kN.m, so that when the manoeuvre is scaled to increase the severity to the point of roll-over, the peak moment is 105 kN.m. The flow rates through the servo-valves, as shown in figure 4.11(f), vary rapidly as the steering input switches from left to right and then back from right to left. The peak flow rate for the manoeuvre described in figure 4.11 is 0.63 l/s, which corresponds to 1.68 l/s for a critical double lane change manoeuvre. The peak power required, neglecting losses in the hydraulic system, is 2.3 kW, so the peak power for the critical manoeuvre is 16.5 kW.

4.6.5 Frequency response

A sample of the closed loop frequency response of the linear, torsionally rigid single unit vehicle model with a full-state feedback controller at 60 km/h is shown in figure 4.12. The frequency response includes a 4 rad/s pre-filter on the steering input to represent the limited bandwidth of the driver, and the plots are used to identify any resonances in the response that may be excited by the driver. (This pre-filter affects both the magnitude *and* the phase plots in figure 4.12.)

Figure 4.12(a) illustrates the frequency response from steering input to suspension roll angles. At low frequencies, the suspension roll angles are in phase with the steering

input for the active case (that is, the active vehicle rolls into corners), whereas the roll angles are 180° out of phase for the passive case (that is, the passive vehicle rolls out of corners). There are no large high-frequency resonances in the active response, due in part to the fact that the pre-filter causes the magnitude of the steering input to roll off sharply above 4 rad/s.

Figure 4.12(b) shows the response from steering input to normalised load transfers. At low frequencies, the load transfers are in phase with the steering input for both the passive and active cases. Active roll control reduces the normalised load transfers at both the steer and drive axles throughout the majority of the frequency range shown. Like the suspension roll angle responses, the normalised load transfer responses roll off above 4 rad/s.

The corresponding closed loop frequency response plots without the steering input pre-filter are included for comparison in figure 4.13.

4.6.6 Design of a partial-state feedback controller

It is impractical to measure all vehicle states in order to implement a full-state feedback controller, as discussed in section 4.5.5. A more practical proposition is to measure selected vehicle states and to implement a partial-state feedback controller. Such a controller uses the control law developed for the full-state feedback case and a state estimator to calculate the unmeasured states and filter measurement noise. The partial-state feedback controller here uses measurements of suspension roll angles, body roll rate, yaw rate and steering input. The unmeasured vehicle states are sideslip angle and the lateral load transfers at the steer and drive axles.

The LQG-LTR design procedure described in section 4.5.7 is used to design the partial-state feedback controller. The loopshaping step, consisting of designing the full-state feedback controller, was detailed in section 4.6.1. The recovery step is to design a state estimator by varying weighting matrices W and V. The aim is to tune the closed loop frequency response of the LQG-controlled system to be acceptably close

to that of the LQR-controlled system. This ensures that the robustness properties of the partial-state feedback system are comparable to the guaranteed robustness properties of the full-state feedback system (see section 4.5.6).

Since there are four measurements and one exogeneous input to the system, the measurement noise weighting matrix W is a 4×4 matrix and the process noise weighting matrix V is a 1×1 matrix, that is, a scalar. W was chosen to be diagonal, with the on-diagonal terms inversely proportional to the estimated expected variances of measurement noise on the four channels of the measurement vector. For the measurement vector

$$y = \begin{bmatrix} \phi - \phi_{t,f} & \dot{\phi} & \dot{\psi} & \delta/2 \end{bmatrix}^T, \tag{4.36}$$

the measurement noise weighting matrix was chosen to be

$$W = \begin{bmatrix} 1.000 & 0 & 0 & 0 \\ 0 & 1.000 & 0 & 0 \\ 0 & 0 & 0.500 & 0 \\ 0 & 0 & 0 & 1.291 \end{bmatrix}^T \begin{matrix} \text{rad}^{-2} \\ \text{rad}^{-2}.\text{s}^2 \\ \text{rad}^{-2}.\text{s}^2 \\ \text{rad}^{-2} \end{matrix} \tag{4.37}$$

The process noise weighting V was then used as a tuning parameter and was varied from 1 rad^{-2} down to 0.001 rad^{-2} and beyond.

Figure 4.14 shows frequency response functions of a series of LQG designs ranging from $V = 1$ rad^{-2} to $V = 0.001$ rad^{-2}. As V decreases, the frequency response functions converge to the target (full-state feedback) response. For $V = 1$ rad^{-2} and $V = 0.1$ rad^{-2}, the low frequency suspension roll angle performances of the LQG design are noticeably different from that of the target response and the LQG phase plots on all channels break away from the target response around 4 rad/s. The response is considered to be acceptable for $V = 0.001$ rad^{-2}, since both the magnitude and phase responses of the partial-state feedback controller closely match those of the target filter loop up to 50 rad/s.

The transient responses of the different LQG-controlled designs to a step steering

input are compared in figure 4.15. Random, uncorrelated white measurement noise, with a root mean square (RMS) average of 5% of the peak response of the LQR-controlled system, is introduced to each channel. As V is reduced relative to W, the Kalman filter places more confidence in the measurements, reducing the filtering action and increasing the filter speed at the expense of measurement noise attenuation. However there appears to be little variation in the noise attenuation performance for the range of V considered here. Figure 4.15(a) shows that, for $V = 1$ rad^{-2}, there is a 3.3° difference between the steady-state roll angle responses of the LQR-controlled and LQG-based systems. However figures 4.15(b) and 4.15(c) indicate that there is no improvement in steer axle load transfer and a noticeably reduced improvement in drive axle load transfer for this design. Conversely, for $V = 0.001$ rad^{-2}, there is less than 0.5° difference in roll angle responses and no significant difference in load transfer responses compared to the LQR-controlled system. Measurement noise attenuation is satisfactory for this design, since 5% RMS noise on all four measurement channels produces an RMS variation of less than 2% on the load transfer responses of the system. Clearly it is possible to achieve significant improvements in roll stability with a partial-state feedback controller.

4.6.7 Effect of actuator performance limitations

The results presented up to this point have assumed that the active roll control system can provide a roll moment instantaneously in response to a demand signal from the controller. However, in practice the effective bandwidth of the active roll control system is limited by: (1) the maximum flow rate of hydraulic fluid through the servo-valves; (2) the frequency response characteristics of the servo-valves; and (3) the speed of the local controller loops, which may be restricted to ensure internal stability and smooth response. It is important to incorporate these limitations into the control system design procedure to minimse the resulting reduction in achievable dynamic roll stability of the vehicle. There are potentially several different ways to accomplish this.

One possibility for representing the limitations to the dynamic response of the active roll control system is to use a low-pass filter on the demand roll moment, as described in section 2.5.4. The filter cut-off frequency represents the effective bandwidth of the active roll control system and depends on the speed of the local control loop and the maximum flow rate through the servo-valves. If the speed of the local control loop is the main factor limiting the dynamic response of the active roll control system, then the cut-off frequency of the filter is the bandwidth of the local loop. However, if it is the servo-valve throughput capacity that limits the dynamic response (as is most likely), then the filter cut-off frequency can be used as a tuning parameter to adjust the flow rates through the servo-valves.

Figure 4.16 illustrates how this technique can be used to accomplish a trade off between flow rates through the servo-valves and dynamic performance. The dynamics of the active roll control system were represented by a first-order low-pass filter with a cut-off frequency of 0.5 Hz. Such a low-pass filter was added to each of the active roll moment inputs to the plant so that the filter input represents the roll moment *demanded* of the actuators by the controller and the filter output represents the roll moment *supplied* to the vehicle. A new controller was then synthesised to give the same steady-state performance as described in section 4.6.2. This requires a different choice of Q and R, with R now penalising the roll moments demanded of the active roll control system rather than the roll moments supplied by the system[†]. The new Q and R matrices were

$$Q = \begin{bmatrix} 1.000 & 0 \\ 0 & 1.768 \end{bmatrix} \mathrm{rad}^{-2}, \tag{4.38}$$

$$R = 4.297 \times 10^{-15} \begin{bmatrix} 1 & 0 \\ 0 & 1 \end{bmatrix} \mathrm{N}^{-2}.\mathrm{m}^{-2}. \tag{4.39}$$

Figure 4.16(a) shows that limiting the bandwidth of the active roll control system

[†]Otherwise the controller would attempt to compensate for the poor response of the actuators by performing a dynamic inversion of the actuator model. This would lead to unreasonably large and rapidly varying demand roll moments.

increases the rise time of the roll angle responses to a double lane change input. This is because the rise time in the roll moment responses delivered by the active roll control system is increased, as shown in figure 4.16(d). The performance costs of the limited bandwidth are increases of around 3% to the peak normalised load transfers at the steer and drive axles, as shown in figures 4.16(b) and 4.16(c). Figure 4.16(e) shows that the reduced suspension roll rates lead to an 11% decrease in the peak flow rates through the servo-valves for this manoeuvre.

By altering the effective bandwidth of the active roll control system and synthesising a new controller, it is possible to trade off servo-valve flow rates against roll stability. The key benefit of this approach is that the performance limitations of the active roll control system can be included during the design stage. This is preferable to the alternative, which is to design a controller assuming perfect response of the active roll control system and then to analyse the effect of limited bandwidth on the system performance a posteriori. While the former approach allows good control over performance and stability robustness properties of the system through the choice of the weighting matrices, the latter does not.

4.6.8 Stability robustness to vehicle parameter uncertainty

The properties of vehicle components vary with different operating conditions. For example, tyre cornering stiffness varies with vertical load, and the height of the vehicle's centre of gravity depends on the payload configuration. In order to design a practical active roll control system, it is necessary to use a simplified vehicle model with some estimates of vehicle parameters and some simplifications of component response characteristics. However, the controlled system should remain stable even when the vehicle parameters vary within reasonable bounds from the nominal values. Although the linear quadratic regulator has guaranteed stability margins in the form of gain margin, gain reduction margin and phase margin, it is also necessary to verify that the stability of a controlled vehicle is robust in the presence of model uncertainties.

The following is a list of important vehicle parameters that were assumed to vary from the nominal values used in the linear vehicle model:

- The vehicle sprung mass and the sprung mass height were assumed to both vary by $\pm$15%, to represent uncertainty in payload configuration for a fully loaded vehicle.

- The average coefficient of friction between the tyres and the road (and therefore the tyre cornering stiffnesses) was assumed to vary between the nominal value and 0.65 of this value, to represent the effects of variations in road conditions.

- The front-to-rear balance in tyre cornering stiffness was assumed to vary by $\pm$15% from the nominal balance, to account for changes in handling characteristics due to lateral load transfers during severe manoeuvres.

- Both suspension roll stiffnesses were varied between the nominal value and a value 15% lower, to account for the nonlinear response of air springs and geometric nonlinearities in the suspension system.

- An additional phase lag represented by a first-order filter with bandwidth as low as 2 Hz was introduced at each active anti-roll bar, to represent unforeseen actuator performance limitations.

- The vehicle speed was assumed to vary about the design set point by $\pm$10%, that is, $\pm$6 km/h. A practical active roll control system would schedule controller gains according to vehicle speed.

Robust stability to parameter variations was examined by performing an exhaustive simulation of all combinations (approximately 10^5 cases) of these possible parameter values. Figure 4.17 shows the variation of the closed loop poles of the vehicle system across the full range of parameter values. The nominal system poles, denoted by the symbol ($\circ$), are located at $-1.81 \pm j1.05$, -4, -12.4, -19.2, -1917 and -2290 rad/s. Since the yaw and roll modes are coupled, there is no roll-only or yaw-only mode, but

the poles at $-1.81 \pm j1.05$ rad/s are primarily associated with handling performance and the poles at -12.4 and -19.2 rad/s are primarily associated with roll-plane performance. The pole at -4 rad/s comes from the filter used to represent the driver's limited frequency response.

The main effect of increasing the sprung mass is to reduce the roll stability of the system. Increasing the height of the centre of mass has a similar effect. Reducing the rear tyre cornering stiffness relative to the front generates a reduction in understeer that reduces handling stability. The primary effect of reducing the coefficient of friction between the tyres and the road or increasing vehicle speed is also to reduce handling stability. A 15% reduction of the suspension roll stiffnesses has little effect on the roll or yaw stability of the active vehicle. The actuator phase lag reduces the stability of the roll and yaw modes.

Stability is drastically reduced when vehicle speed is increased by 10%, overall tyre grip is reduced by 35% and the handling bias changes by 15% towards the front from the nominal values. However this combination reduces stability both with and without active roll control, that is, the active roll control system does not reduce the handling stability per se. (This issue is discussed in more detail in section 4.6.9.)

For all combinations of possible parameter variations, the closed loop poles of the system remain in the open left half plane and the system is stable.

4.6.9 Effect on handling performance

Although the active roll control system was designed solely to increase the roll stability of the vehicle, it is important to analyse the effect of such a system on handling performance.

Handling performance is determined by the balance of tyre cornering stiffness among the axles of a vehicle. Due to the nonlinear relationship between tyre cornering stiffness and vertical load, as described in (2.42), the combined cornering stiffness of the tyres on a given axle decreases with an increase in lateral load transfer.

The effect of active roll control on the handling performance of the torsionally rigid single unit vehicle model at 60 km/h is shown in figure 4.18. The *handling diagram* is the plot of a_y against $\delta - L_1/R$, where δ, L, R and a_y are respectively the steering angle, the wheelbase, the radius of curvature and the lateral acceleration [84]. Negative slope indicates understeer and positive slope indicates oversteer.

First, consider the response of the vehicle with passive suspension. At low levels of lateral acceleration, the vehicle understeers mildly. Understeer is a stable handling regime. As lateral acceleration increases, the normalised load transfer builds up more quickly at the drive axle than at the steer axle and a reduction in the cornering stiffness at the rear relative to the front could be anticipated. However, each of the twin tyres at the rear is more lightly loaded than the front tyres, so from figure 2.5, the rear tyres will lose less cornering stiffness for a given normalised load transfer. These two effects negate each other so the understeer gradient does not change significantly until the drive axle lifts off at 0.42 g.

The active roll control system causes the normalised load transfers at the steer and drive axles to build up in a balanced fashion. However, because the rear tyres are comparatively lightly loaded, these tyres lose less cornering stiffness than the front tyres. Therefore the understeer gradient of the vehicle with active roll control increases with lateral acceleration and the vehicle understeers particularly strongly above 0.4 g. Incidentally, this increase in understeer may alert the driver to the high level of lateral acceleration.

From section 3.3.3, most heavy vehicles feature a higher ratio of roll stiffness to vertical load at the drive axle than at the steer axle, so normalised load transfers typically build up in an unbalanced fashion, that is, more quickly at the drive axle. By redressing this imbalance, an active roll control system can generally be expected to increase understeer.

4.7 Control of a torsionally flexible single unit vehicle

4.7.1 Design of a full-state feedback controller

The design of a full-state roll controller for a torsionally flexible single unit vehicle is again a problem of optimal disturbance rejection system design. The steering input spectrum (4.28) is used. Like the torsionally rigid single unit vehicle, the torsionally flexible single unit vehicle is input deficient, so the active roll control system design is again a trade-off between reducing lateral load transfers, constraining suspension roll angles and limiting energy requirements. The problem is to tune the weighting matrices Q and R to penalise the performance output vector

$$z = \begin{bmatrix} \phi_{t,f} & \phi_{t,r} \end{bmatrix}^T \tag{4.40}$$

and the control input u respectively.

Without active roll control, the presence of torsional flexibility in the vehicle frame further accentuates the imbalance in the rate of build up of normalised load transfers between the steer and drive axles. If the front and rear sections of the vehicle were torsionally decoupled, then the normalised lateral load transfer would typically be higher at the drive axle than at the steer axle because the majority of the sprung mass is located high and to the rear.

The active roll control system must balance the normalised load transfers between the steer and drive axles. To achieve this balance, a twisting moment must be transmitted from the drive axle through the vehicle frame to the steer axle. Since the vehicle frame is flexible, this moment will generate a relative roll angle between the front and rear sections of the vehicle, typically with the front section rolling into the corner more than the rear section. To ensure that the steer axle suspension roll angle remains within the required range, the penalty on the control inputs relative to the performance output must be increased. Further tuning of the elements of Q using the procedure outlined in section 4.6.1 is then required.

For a speed of 60 km/h, the weighting matrices were chosen to be

$$Q = \begin{bmatrix} 1.000 & 0 \\ 0 & 2.076 \end{bmatrix} \mathrm{rad}^{-2}, \tag{4.41}$$

$$R = 3.352 \times 10^{-14} \begin{bmatrix} 1 & 0 \\ 0 & 1 \end{bmatrix} \mathrm{N}^{-2}.\mathrm{m}^{-2}. \tag{4.42}$$

This produced a full-state feedback controller

$$K_{FB} = \begin{bmatrix} 1.870 \times 10^5 & -1.145 \times 10^4 \\ -7.232 \times 10^3 & -5.413 \times 10^3 \\ -4.387 \times 10^5 & -1.161 \times 10^5 \\ -1.841 \times 10^5 & -2.168 \times 10^5 \\ -1.244 \times 10^6 & -1.352 \times 10^6 \\ 2.133 \times 10^5 & 2.065 \times 10^5 \\ 3.569 \times 10^6 & 3.272 \times 10^4 \\ 5.399 \times 10^4 & 4.901 \times 10^6 \\ 1.192 \times 10^6 & 1.739 \times 10^6 \end{bmatrix}^T \begin{matrix} \mathrm{N.m/rad} \\ \mathrm{N.m.s/rad} \\ \mathrm{N.m/rad} \\ \mathrm{N.m.s/rad} \\ \mathrm{N.m/rad} \\ \mathrm{N.m.s/rad} \\ \mathrm{N.m/rad} \\ \mathrm{N.m/rad} \\ \mathrm{N.m/rad} \end{matrix} \tag{4.43}$$

acting on the augmented state vector

$$\underline{x} = \begin{bmatrix} \phi_f & \dot{\phi}_f & \phi_r & \dot{\phi}_r & \beta & \dot{\psi} & \phi_{t,f} & \phi_{t,r} & \delta/2 \end{bmatrix}^T. \tag{4.44}$$

The performance of this controller is examined in detail in sections 4.7.2–4.7.5.

4.7.2 Steady-state cornering response

The response of the linear, torsionally flexible single unit vehicle model to a steady-state steering input at 60 km/h is shown in figure 4.19.

Without active roll control, the vehicle rolls out of the corner. As with the rigid vehicle from section 4.6, the normalised load transfer builds up more quickly at the

drive axle than at the steer axle, although this effect becomes more pronounced as torsional flexibility of the frame increases. The drive axle lifts off at 0.38 g (point A), at which point the normalised load transfer at the steer axle is 0.67 (point B). As lateral acceleration continues to increase, the slopes of the suspension roll angle and normalised load transfer curves increase, and the normalised load transfer at the steer axle reaches the critical value of 1 at 0.40 g (point C). Thus the torsional flexibility of the vehicle frame reduces the roll-over threshold by 7%.

With active roll control, the vehicle rolls into the corner. The total roll moment is distributed between the active anti-roll bars so that the normalised load transfers at the two axles increase in a balanced fashion as lateral acceleration increases. This requires a relative angle between the front and rear sections of the vehicle of 5.7°/g, with the front section rolling into the corner more than the rear. As the flexibility of the vehicle frame increases, the relative roll angle required to balance the normalised load transfers also increases. The normalised load transfers at both axles reach the critical value of 1 at 0.51 g (point D), at which point the steer axle suspension roll angle is 3.4° inward. This represents a 5% reduction in roll-over threshold compared to the torsionally rigid vehicle described in section 4.6.2.

Active roll control increases the roll-over threshold of the torsionally flexible single unit vehicle by 26% and the lateral acceleration at which axle lift-off first occurs by 33%. This is a substantial improvement in steady-state roll stability and suggests that the achievable improvements to roll stability offered by active roll control systems are even greater for torsionally flexible vehicles than for torsionally rigid vehicles.

4.7.3 Response to a step steering input

The response of the linear, torsionally flexible single unit vehicle model to a step steering input is shown in figure 4.20. The step input is scaled to give a maximum normalised load transfer of 1 in the following simulations and is therefore 10% smaller than the input to the torsionally rigid single unit vehicle in section 4.6.3 and figure 4.9.

The lateral acceleration response is shown in figure 4.20(a). The steady-state lateral acceleration is 0.34 g. The active roll control system eliminates the small lateral acceleration overshoot that is present in the passive response.

The suspension roll angle responses are shown in figure 4.20(b). Without active roll control, the vehicle rolls out of the corner by 3.2° and 4.3° at the steer and drive axles respectively. There is a small overshoot in both traces. The roll angle at the drive axle exceeds that at the steer axle because the majority of the vehicle mass is high at the rear and so the moment of the inertial force due to cornering there is very large. With active roll control, the vehicle rolls into the corner by 2.3° at the steer axle and 0.2° at the drive axle, with peak values of 3.0° and 1.4° respectively. While the overshoot of the steer axle suspension roll angle response is undesirable, a reduction in overshoot would lead to an increase in load transfer. The difference between the front and rear roll angles is generated in order to transfer some overturning moment from the rear to the front, balancing the normalised load transfers and minimising the performance index described in equation (4.9).

The normalised load transfer responses are shown in figure 4.20(c). Without active roll control, the normalised load transfer builds up more quickly at the drive axle than at the steer axle, and this trend becomes more apparent as the flexibility of the vehicle frame increases; that is, frame flexibility reduces the ability of the steer axle to carry its share of the total lateral load transfer. The normalised load transfer responses feature moderate overshoots before settling at final values of 0.60 and 0.91 for the steer and drive axles respectively. In addition to reducing the total lateral load transfer by rolling the vehicle into the turn, the active roll control system redistributes the load transfer in a balanced fashion between the axles so that both show a peak normalised value of 0.68. The system reduces the peak load transfer at the drive axle by 32%. The load transfer at the steer axle increases, although this is because, in the passive case, the steer axle carries much less than its fair share of the total load transfer.

The results in section 4.7.2 show that the roll-over threshold of the vehicle with passive suspension is just 6% higher than the level of lateral acceleration at which the

drive axle lifts off. By contrast, the active roll control system can retain roll stability with up to 46% additional lateral acceleration (that is, up to 0.51 g). This represents a significant enhancement in roll stability.

Figure 4.20(d) shows that, for the torsionally flexible vehicle, 46% of the total active roll moment is generated at the drive axle. (For the torsionally rigid vehicle, 59% of the total roll moment is generated at the drive axle.) The peak roll moment in response to a critical steering input is 63 kN.m at the steer axle.

Frame flexibility increases the peak steer axle suspension roll rate relative to the drive axle suspension roll rate, so the fluid flow rate through the servo-valves at the steer axle is larger than at the drive axle (see figure 4.20(e)). The peak fluid flow rates in response to a critical steering manoeuvre are 1.17 l/s at the steer axle and 0.62 l/s at the drive axle. The peak power supplied to the system in response to a critical step input is 5.9 kW (neglecting losses).

4.7.4 Response to a double lane change steering input

The response of the linear, torsionally flexible single unit vehicle model to a double lane change steering input at 60 km/h is illustrated in figure 4.21. The path deviation is again 5 m over a 120 m test section, with a peak lateral acceleration of just under 0.2 g (see figure 4.21(a)).

The suspension roll angle responses are shown in figure 4.21(b). The patterns from sections 4.7.2 and 4.7.3 are again evident. The vehicle without active roll control rolls out of the corner while the vehicle with active roll control rolls into the corner. There is a relative roll angle between the front and rear sections of the vehicle both with and without the active roll control system, with the front section always rolling more towards the inside of the corner.

The normalised load transfer responses are shown in figure 4.21(c). The active roll control system balances the normalised load transfers between the axles effectively, reducing the peak normalised drive axle load transfer by 43% (from 0.68 to 0.39) with

little change in the peak normalised steer axle load transfer. That is, the vehicle with active roll control could remain stable even if the steering input was scaled up by 157%. This represents a greater relative improvement in roll stability than was achieved for the torsionally rigid vehicle, although the ultimate roll stability of the rigid vehicle is higher.

The ratio of peak suspension roll angle to peak normalised load transfer is again higher for the double lane change steering input than for the step input. The peak inward roll angle at the steer axle in response to a critical steering input is 6.2°, which is at the limit of the available suspension travel.

Figure 4.21(d) shows that the peak active anti-roll bar moments at the steer and drive axles are of comparable magnitude, with the roll moment at the drive axle slightly higher. The peak roll moment in response to a critical double lane change steering input is 82 kN.m

The servo-valve flow rate responses are shown in figure 4.21(e). The peak flow rates in response to a critical double lane change manoeuvre are 1.82 l/s and 1.18 l/s at the steer axle and drive axle respectively. When compared with the peak flow rates for the torsionally rigid vehicle described in section 4.6.4, the required servo-valve capacity is similar at the steer axle and is significantly lower at the drive axle because the roll angle and roll rate responses are reduced. The forced oscillation frequency of the vehicle body in roll is dictated by the steering input and the maximum roll angle is set by the suspension travel. This means that the axles with the largest amplitude of suspension roll should be expected on average to have the highest roll rates and therefore the highest fluid flow rates. The peak power supplied to the system in response to a critical step input is 14.7 kW (neglecting losses).

4.7.5 Frequency response

Frequency response functions from steering input to suspension roll angles and normalised load transfers are shown in figures 4.22(a) and 4.22(b) respectively. The sys-

tem again includes a 4 rad/s pre-filter on the steering input to represent the limited bandwidth of the driver.

Active roll control reduces the normalised load transfer at the drive axle throughout the majority of the frequency range up to 10 rad/s. There is a 180° phase difference between active and passive roll angle responses since, with active roll control, the vehicle rolls into the corner whereas, without active roll control, it rolls out of the corner. The roll angle and load transfer responses roll off above 4 rad/s.

4.7.6 Design of a partial-state feedback controller

A partial-state feedback controller was designed using the LQG-LTR procedure. The controller uses measurements of the suspension roll angles at both the steer and drive axles, plus the body roll rate at the rear, the yaw rate and the steering input,

$$y = \left[\begin{array}{ccccc} \phi_f - \phi_{t,f} & \phi_r - \phi_{t,r} & \dot{\phi}_r & \dot{\psi} & \delta/2 \end{array} \right]^T . \tag{4.45}$$

This is one measurement more than for the torsionally rigid single unit vehicle in section 4.6.6: the suspension roll angles at *both* the steer and drive axles are now measured. The unmeasured vehicle states are the body roll rate at the front, the sideslip angle and the lateral load transfers at the steer and drive axles.

For the Kalman filter design, the elements of the measurement noise weighting matrix W were chosen to be

$$W = \left[\begin{array}{ccccc} 1.000 & 0 & 0 & 0 & 0 \\ 0 & 1.000 & 0 & 0 & 0 \\ 0 & 0 & 1.000 & 0 & 0 \\ 0 & 0 & 0 & 0.500 & 0 \\ 0 & 0 & 0 & 0 & 1.291 \end{array} \right]^T \begin{array}{l} \mathrm{rad}^{-2} \\ \mathrm{rad}^{-2} \\ \mathrm{rad}^{-2}.\mathrm{s}^2 \\ \mathrm{rad}^{-2}.\mathrm{s}^2 \\ \mathrm{rad}^{-2} \end{array} \tag{4.46}$$

and the process noise weighting V was varied as a tuning parameter from 1 rad^{-2} down

to 0.001 rad^{-2}. The target feedback loop is that of the full-state feedback controller described in section 4.7.2.

The frequency responses of the steer axle suspension roll angle, steer axle load transfer and drive axle load transfer to a steering input are shown as a function of V in figure 4.23. The results are similar to those presented for the torsionally rigid single unit vehicle in section 4.6.6. For $V = 1$ rad^{-2} and $V = 0.1$ rad^{-2}, there are significant differences from the target response in the magnitude of the suspension roll angles at low frequency and in the phase of the drive axle load transfer above 4 rad/s. As V is reduced, the frequency responses converge towards the target response.

The transient performances of several LQG-controlled designs to a step steering input are compared in figure 4.24. The load transfer performance of the system improves as V is reduced from 1 rad^{-2}, and by $V = 0.001$ rad^{-2} there is little difference in the performance of the LQR-controlled and LQG-controlled systems. Random, uncorrelated white measurement noise of 5% RMS on each measurement channel is effectively attenuated. The improvements to roll stability offered by a full-state feedback controller are also available using a partial-state feedback controller.

4.7.7 Effect of actuator performance limitations

Figure 4.25 illustrates the effect of the limited bandwidth of the active roll control system on the response of the linear, torsionally flexible single unit vehicle model to a step steering input. The active roll control system was represented with a 0.5 Hz first order low-pass filter and a new controller was synthesised to give the same steady-state performance as in section 4.7.2. The new Q and R matrices were

$$Q = \begin{bmatrix} 1.000 & 0 \\ 0 & 1.846 \end{bmatrix} \text{rad}^{-2}, \tag{4.47}$$

$$R = 1.179 \times 10^{-14} \begin{bmatrix} 1 & 0 \\ 0 & 1 \end{bmatrix} \text{N}^{-2}.\text{m}^{-2}. \tag{4.48}$$

Limiting the bandwidth of the active roll control system increases the rise time of the roll angle responses (see figure 4.25(a)). For this particular manoeuvre, however, the increases in peak normalised load transfers at both axles are negligible, as illustrated in figures 4.25(b) and 4.25(c). The peak flow rates through the servo-valves are reduced by 8% and 23% at the steer and drive axles respectively, as shown in figure 4.25(e).

4.7.8 Stability robustness to vehicle parameter uncertainty

The effect of vehicle parameter uncertainty on the closed loop stability of the torsionally flexible single unit vehicle model is shown in figure 4.26.

The range of variation in vehicle parameters from the nominal values is as described in section 4.6.8. The nominal system poles, denoted by the symbol ($\circ$), are located at $-1.87 \pm j1.52$, -12.9, -23.0, $-4.10 \pm j17.6$, -4, -1317 and -1474 rad/s. The mode shapes associated with these poles are similar to those described in section 4.6.8, and there is an additional lightly damped pair of poles at $-4.10 \pm j17.6$ rad/s associated with the torsional resonance of the vehicle frame at approximately 3 Hz.

The closed loop poles of the system remain in the open left half plane for all combinations of possible parameter variations, so the system is robustly stable in the presence of model uncertainty.

4.7.9 Effect on handling performance

The effect of active roll control on the handling performance of the torsionally flexible single unit vehicle model at 60 km/h is shown in figure 4.27.

First, consider the response of the vehicle without active roll control. At low levels of lateral acceleration, the vehicle understeers mildly. As lateral acceleration increases, the normalised load transfer builds up more quickly at the drive axle than at the steer axle. This effect becomes more pronounced as the torsional flexibility of the vehicle frame increases. There is a reduction in the cornering stiffness of the rear relative

to the front and the handling changes from neutral steer to strong oversteer by 0.3 g. The drive axle lifts off at 0.38 g, by which point the yaw stability of the vehicle is significantly reduced.

Despite the presence of torsional compliance in the vehicle frame, the active roll control system balances the build up of normalised load transfer evenly between the steer and drive axles. Therefore the handling performance of the torsionally flexible vehicle equipped with an active roll control system is similar to that of the torsionally rigid active vehicle in figure 4.18. The understeer gradient builds up as lateral acceleration increases. The active roll control system significantly increases the level of yaw stability at high levels of lateral acceleration.

4.8 Conclusions

1. Active roll control is a strongly multivariable problem. The $\mathcal{H}_2$ controller design method enables an explicit trade-off between performance and control energy for MIMO systems.

2. Active roll control is a problem of optimal disturbance rejection, which is an extension of the standard LQR problem. The steering disturbance must be measured or estimated and incorporated into the feedback law to maximise roll stability.

3. A partial-state LQG feedback controller consisting of a linear quadratic regulator and a Kalman filter is more practical than a full-state feedback controller. The loop transfer recovery method can be used to shape the singular values of the LQG transfer function to ensure adequate stability.

4. Simulations show that active roll control can increase the roll-over threshold of a torsionally rigid single unit vehicle by 23%. The improvements in roll stability in severe transient manoeuvres can be even greater. Given the accident

statistics presented in section 1.1, these figures suggest a possible reduction in the frequency of roll-over accidents of up to 50%.

5. Without active roll control, the roll-over threshold of a single unit vehicle decreases significantly with increasing torsional flexibility of the vehicle frame. However, the *relative* improvement to achievable roll stability offered by active roll control increases (up to a point) with the torsional flexibility of the vehicle frame, so the *absolute* reduction in stability is limited. Simulations show that active roll control can increase the roll-over threshold of a typical torsionally flexible single unit vehicle by 26%.

6. A partial-state LQG feedback controller, using measurements of suspension roll angles, body roll rate, yaw rate and steering input, is a practical controller design that can significantly improve the roll stability of a single unit vehicle without significant sensitivity to measurement noise. The loop transfer recovery design procedure can be used to ensure sufficient stability robustness of the controller.

7. The limited effective bandwidth of the active roll control system causes a degradation in the achievable dynamic roll stability. However it is possible to minimise this performance reduction and retain adequate stability margins if the effective bandwidth limitation is incorporated into the vehicle model during the control system design stage.

8. The actuator forces and hydraulic fluid flow rates required for good performance are achievable using the practical, reasonably priced hardware recommended by McKevitt.

9. By distributing the total normalised load transfer between the steer and drive axles in a balanced fashion, active roll control tends to increase understeer for a typical single unit vehicle.

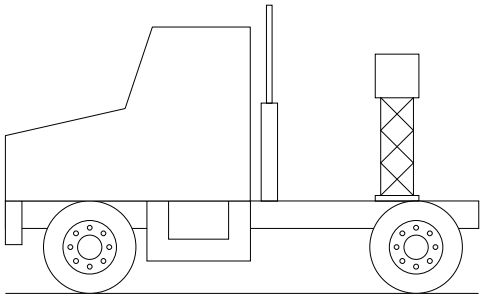

(a) Schematic.

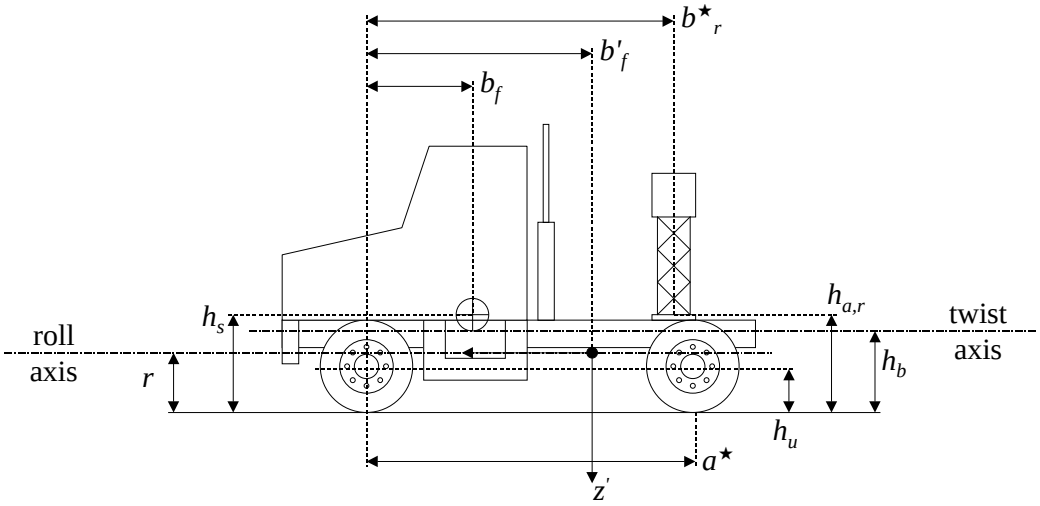

(b) Dimensions.

Figure 4.1: Single unit vehicle with lumped mass.

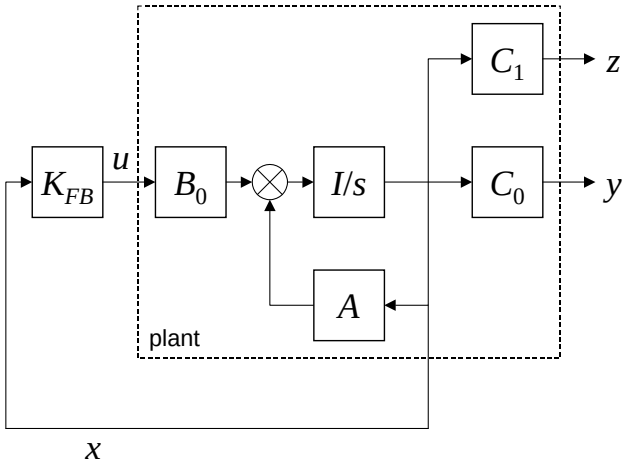

Figure 4.2: Linear quadratic regulator.

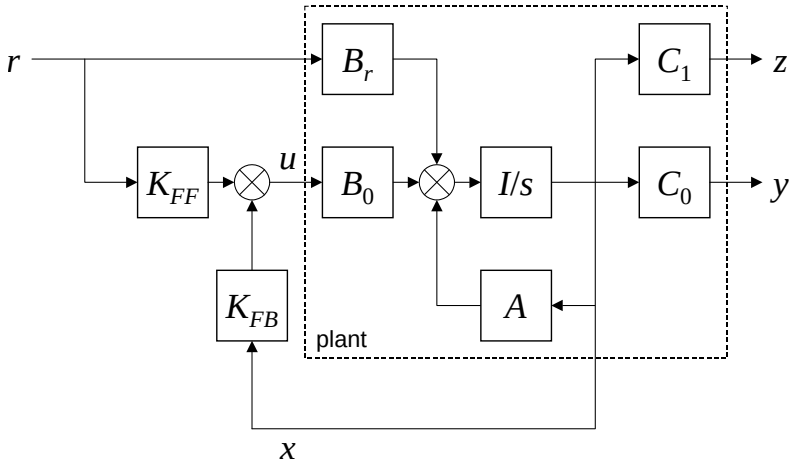

Figure 4.3: Linear quadratic regulator with constant disturbance.

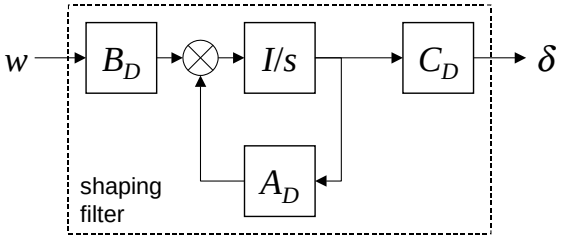

Figure 4.4: Generating a stochastic steering input by filtering white noise.

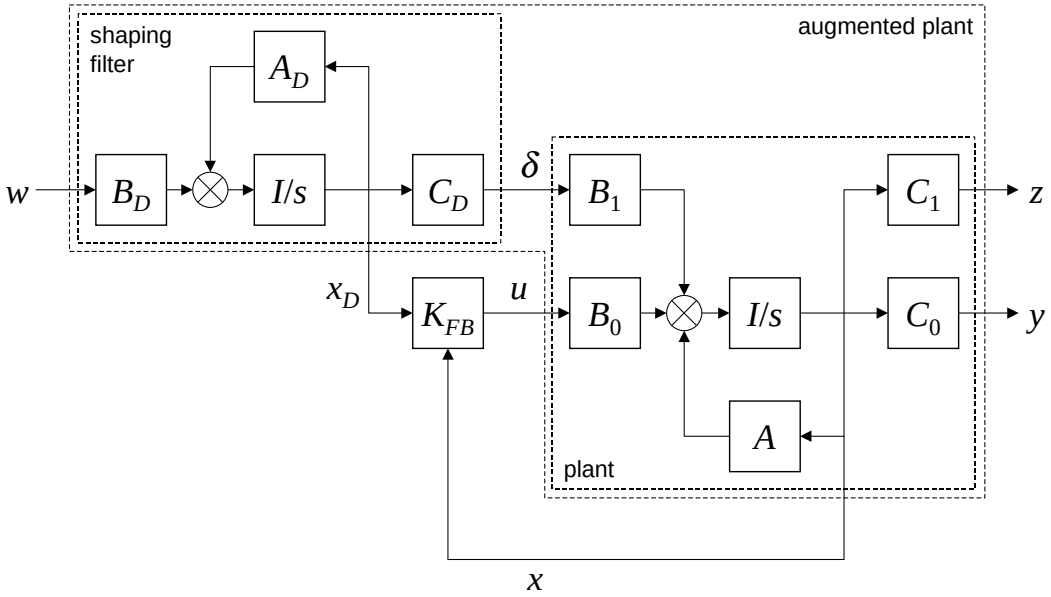

(a) Detailed model showing the shaping filter and the plant.

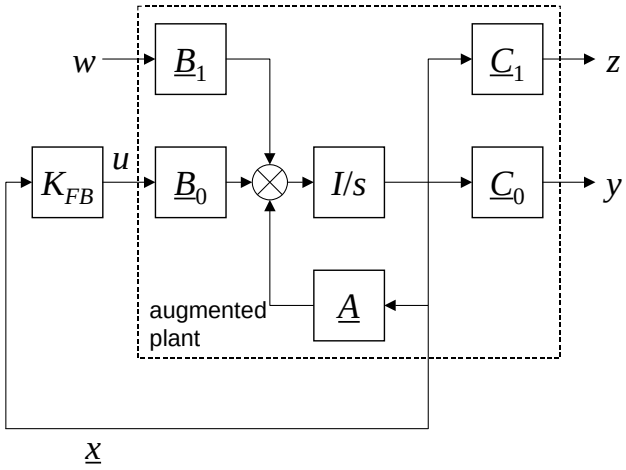

(b) Simplified model showing the augmented plant.

Figure 4.5: Optimal disturbance rejection.

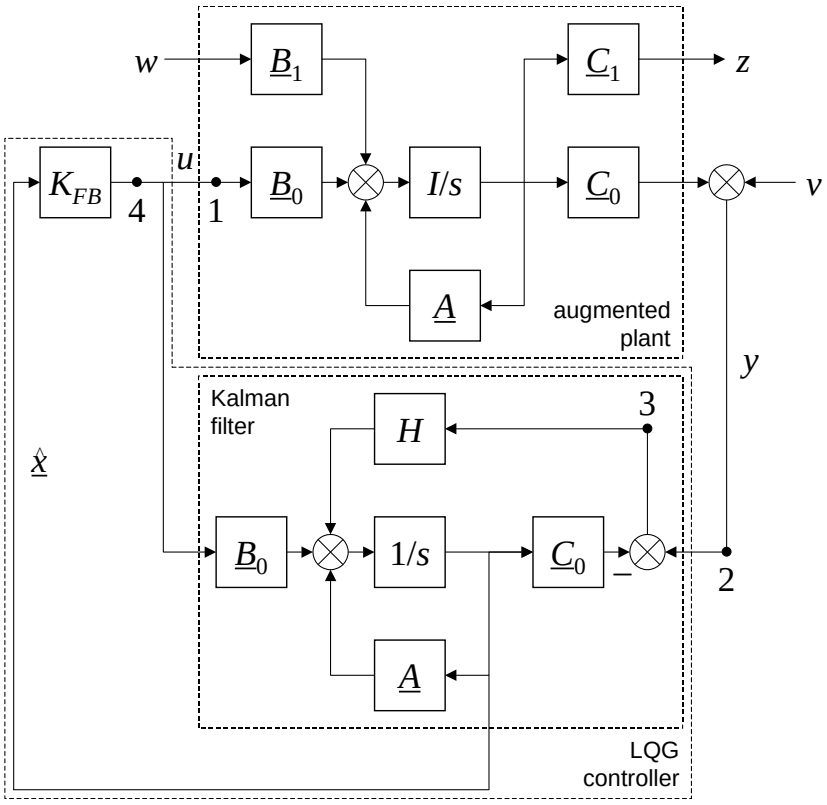

Figure 4.6: Linear quadratic Gaussian controller.

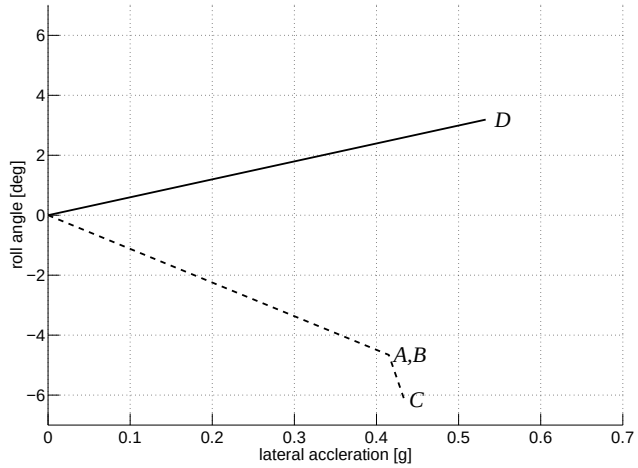

(a) Suspension roll angles. Active roll control: *steer axle (——)*; passive suspension: *steer axle (– – –).*

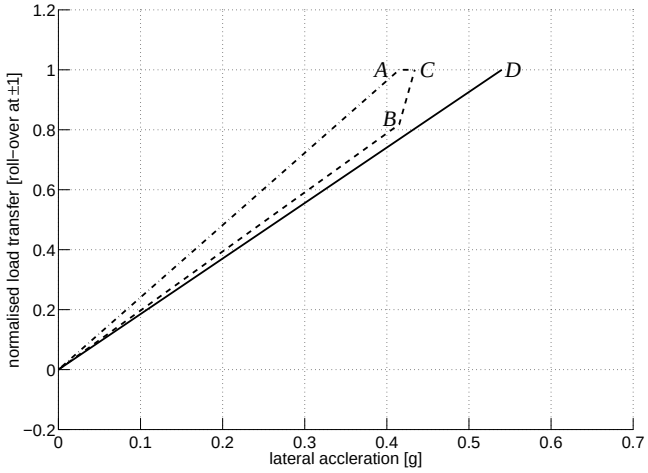

(b) Normalised load transfers. Active roll control: *steer axle and drive axle (——)*; passive suspension: *steer axle (– – –), drive axle (· – · – ·).*

Figure 4.7: Response of the linear, torsionally rigid single unit vehicle model with a full-state feedback controller to a steady-state steering input.

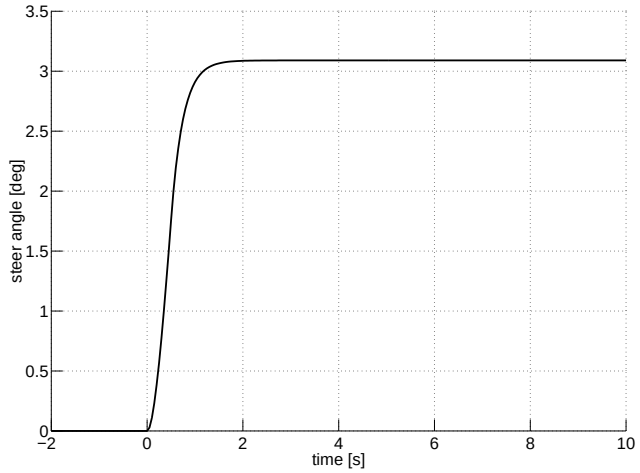

Figure 4.8: Step steering input to the linear, torsionally rigid single unit vehicle model.

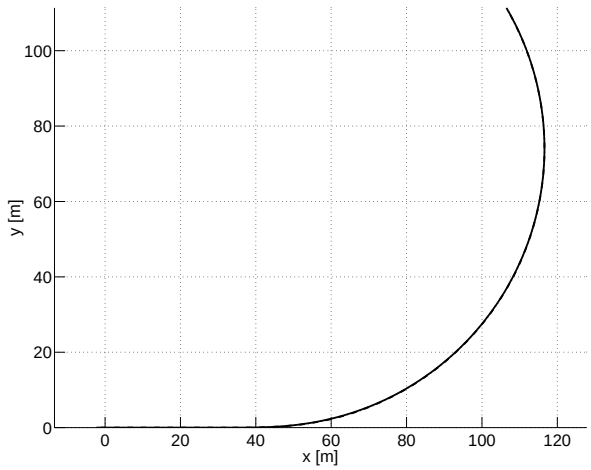

(a) Trajectory. *Active roll control (——), passive suspension (· – · – ·).*

Figure 4.9: Response of the linear, torsionally rigid single unit vehicle model with a full-state feedback controller to a step steering input.

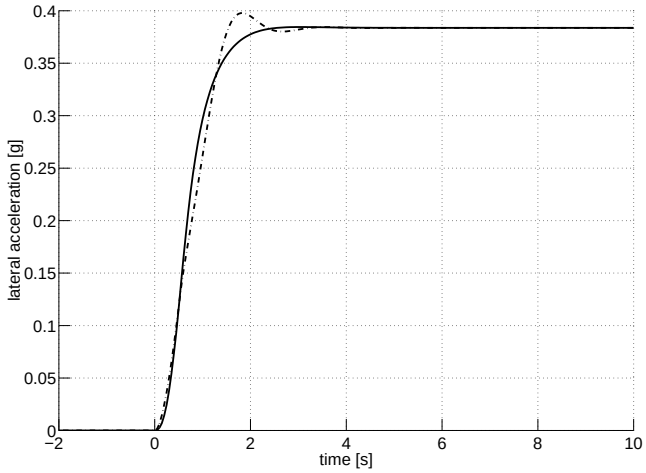

(b) Lateral acceleration. *Active roll control (——), passive suspension (· – · – ·).*

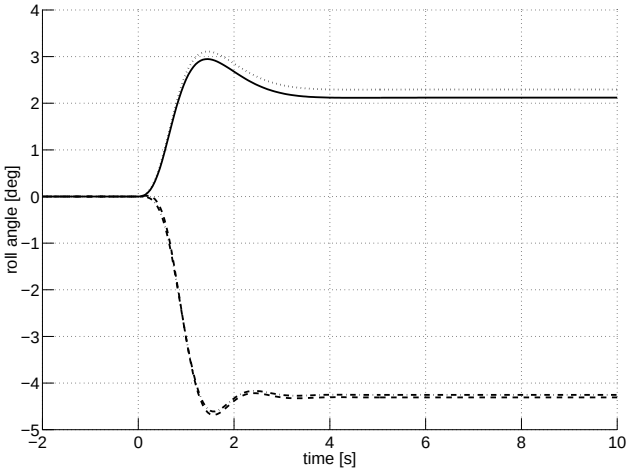

(c) Suspension roll angles. Active roll control: *steer axle (· · · · · ·), drive axle (——)*; passive suspension: *steer axle (– – –), drive axle (· – · – ·).*

Figure 4.9: Continued.

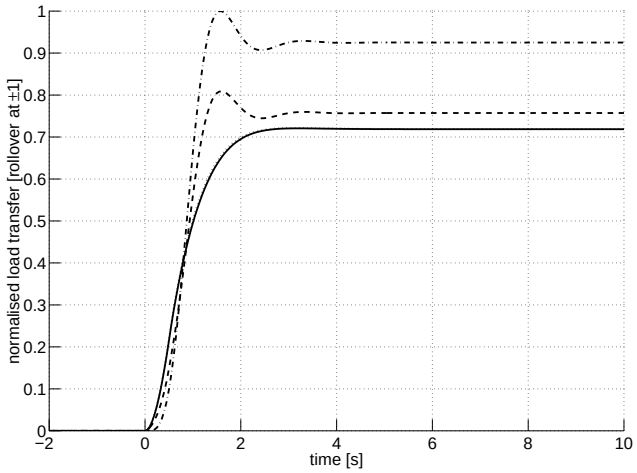

(d) Normalised load transfers. Active roll control: *steer axle (· · · · · ·), drive axle (——)*; passive suspension: *steer axle (– – –), drive axle (· – · – ·).*

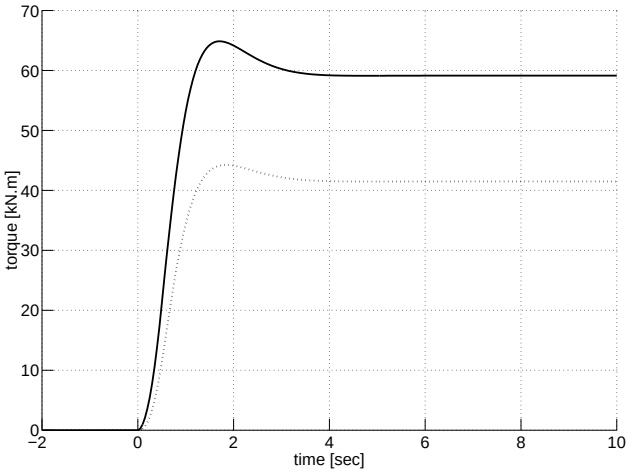

(e) Active anti-roll bar moments. Active roll control: *steer axle (· · · · · ·), drive axle (——).*

Figure 4.9: Continued.

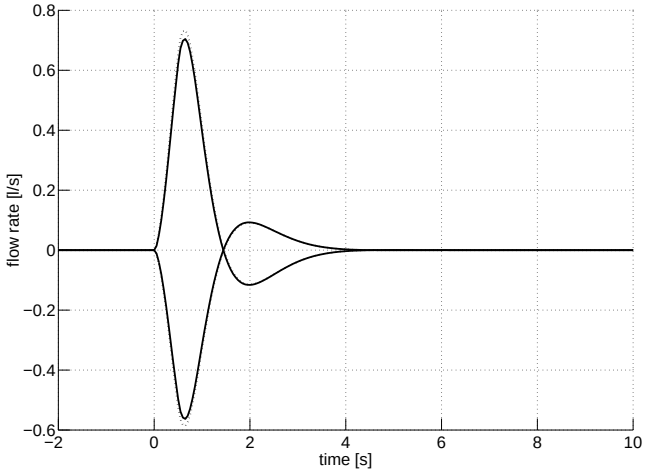

(f) Servo-valve flow rates. Active roll control: *steer axle (· · · · · ·), drive axle (——).*

Figure 4.9: Continued.

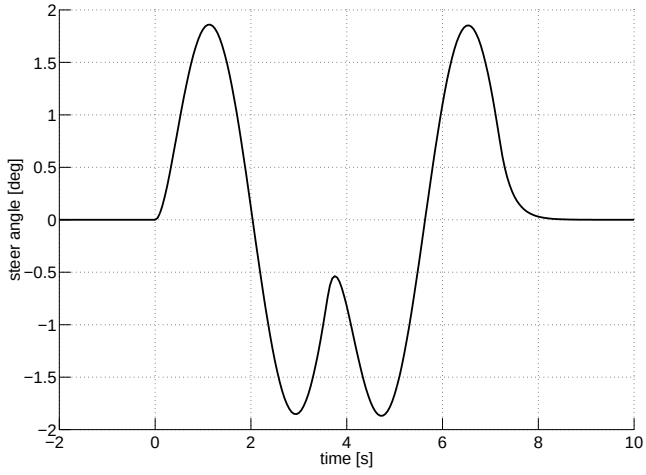

Figure 4.10: Double lane change steering input to the linear, torsionally rigid single unit vehicle model.

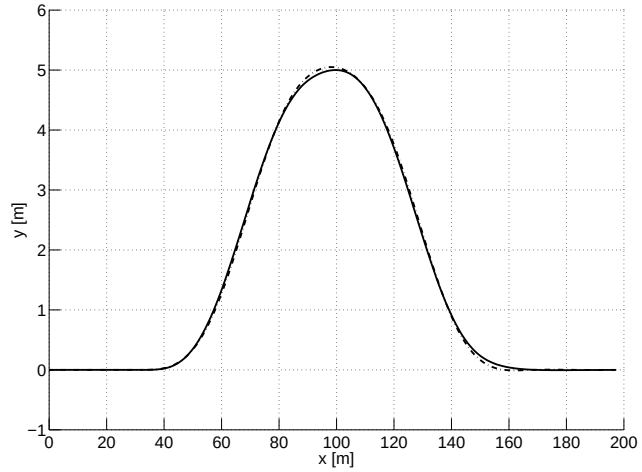

(a) Trajectory (not to scale). *Active roll control (——), passive suspension (· – · – ·).*

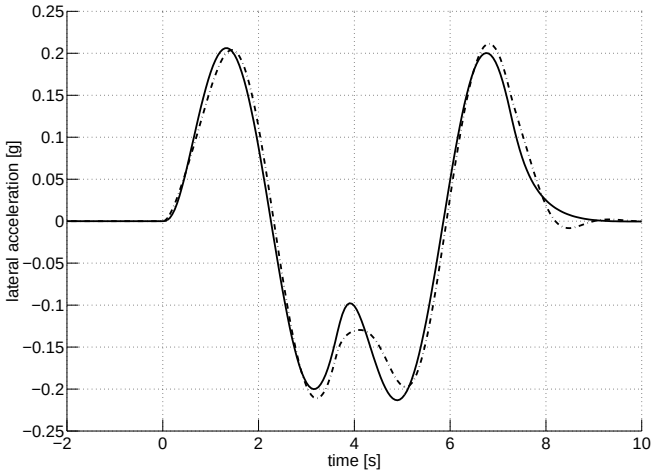

(b) Lateral acceleration. *Active roll control (——), passive suspension (· – · – ·).*

Figure 4.11: Response of the linear, torsionally rigid single unit vehicle model with a full-state feedback controller to a double lane change steering input.

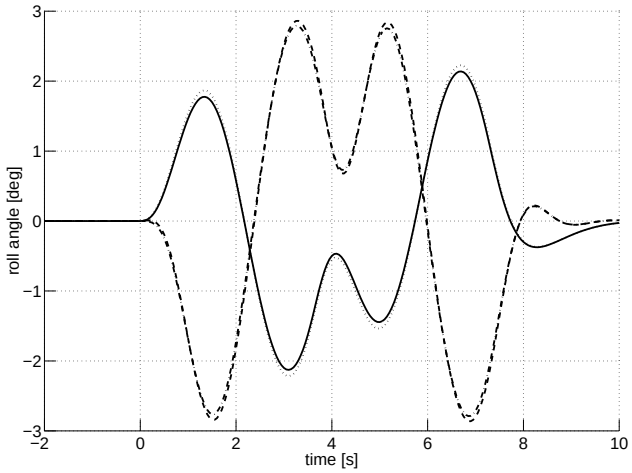

(c) Suspension roll angles. Active roll control: *steer axle (· · · · · ·), drive axle (——)*; passive suspension: *steer axle (– – –), drive axle (· – · – ·).*

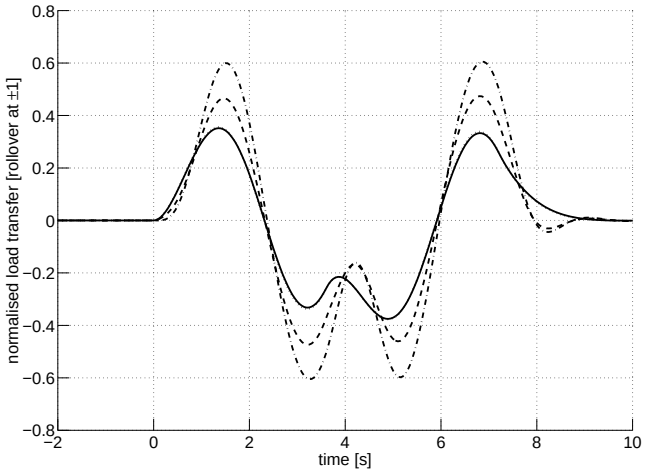

(d) Normalised load transfers. Active roll control: *steer axle (· · · · · ·), drive axle (——)*; passive suspension: *steer axle (– – –), drive axle (· – · – ·).*

Figure 4.11: Continued.

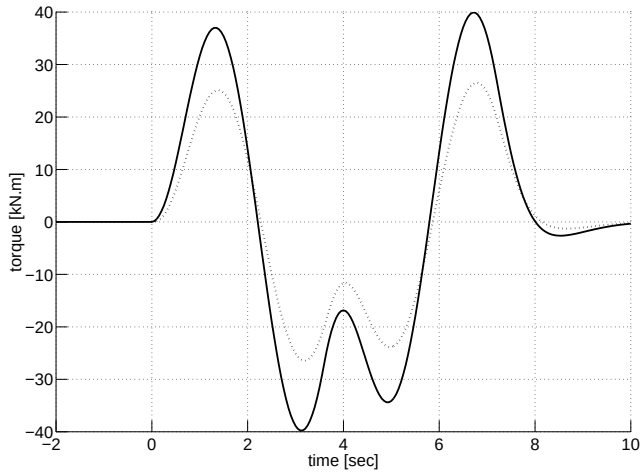

(e) Active anti-roll bar moments. Active roll control: *steer axle (· · · · · ·), drive axle (——).*

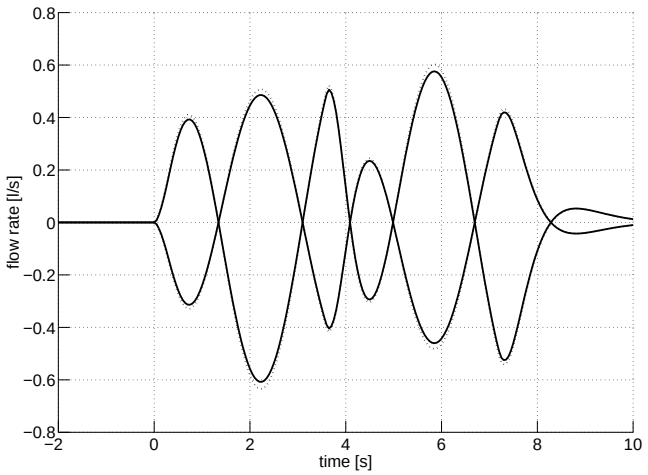

(f) Servo-valve flow rates. Active roll control: *steer axle (· · · · · ·), drive axle (——).*

Figure 4.11: Continued.

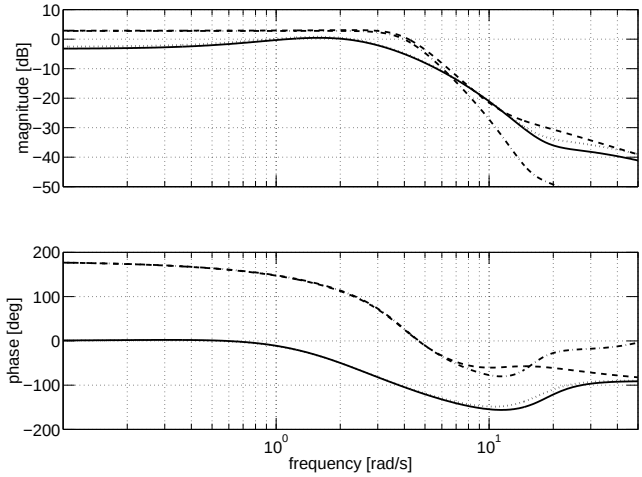

(a) From steering input [deg] to suspension roll angles [deg]. Active roll control: *steer axle (· · · · · ·), drive axle (——)*; passive suspension: *steer axle (– – –), drive axle (· – · – ·).*

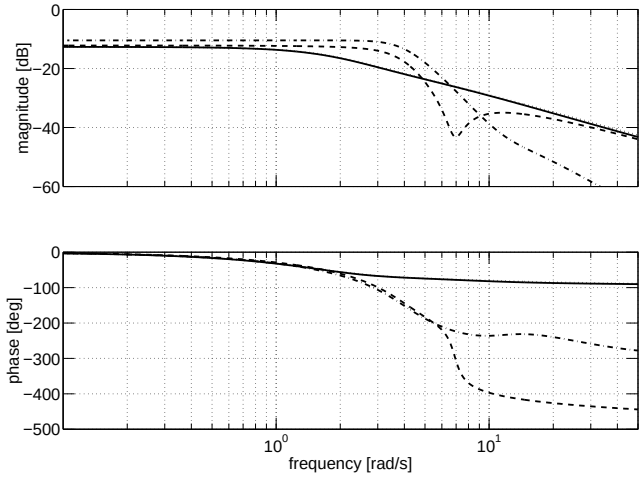

(b) From steering input [deg] to normalised load transfers [roll-over at ± 1]. Active roll control: *steer axle (· · · · · ·), drive axle (——)*; passive suspension: *steer axle (– – –), drive axle (· – · – ·).*

Figure 4.12: Frequency response of the linear, torsionally rigid single unit vehicle model with a full-state feedback controller.

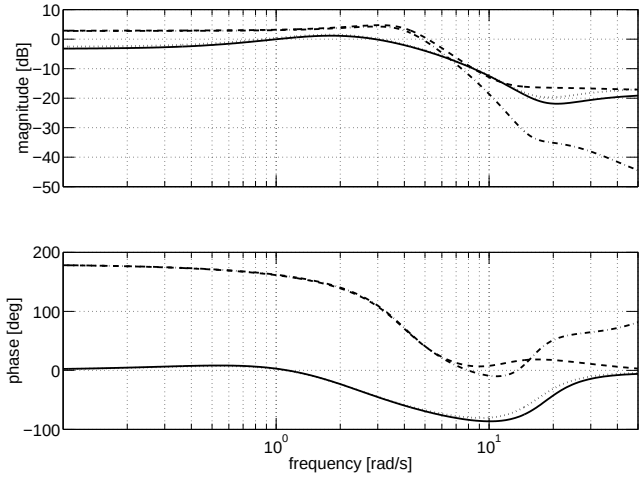

(a) From steering input [deg] to suspension roll angles [deg]. Active roll control: *steer axle (· · · · · ·), drive axle (——)*; passive suspension: *steer axle (– – –), drive axle (· – · – ·).*

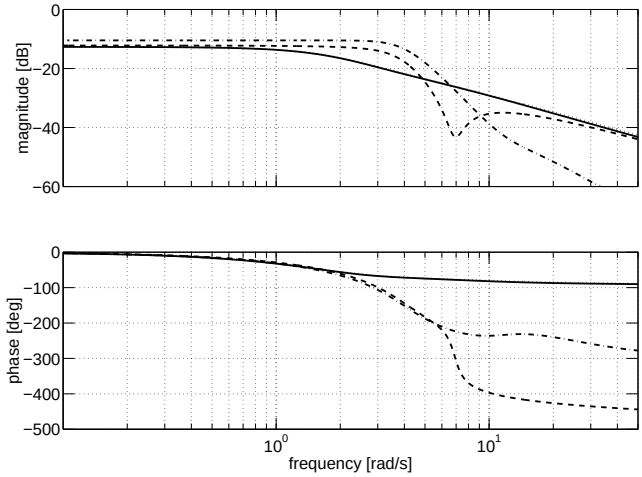

(b) From steering input [deg] to normalised load transfers [roll-over at ± 1]. Active roll control: *steer axle (· · · · · ·), drive axle (——)*; passive suspension: *steer axle (– – –), drive axle (· – · – ·).*

Figure 4.13: Frequency response of the linear, torsionally rigid single unit vehicle model with a full-state feedback controller and without the driver model.

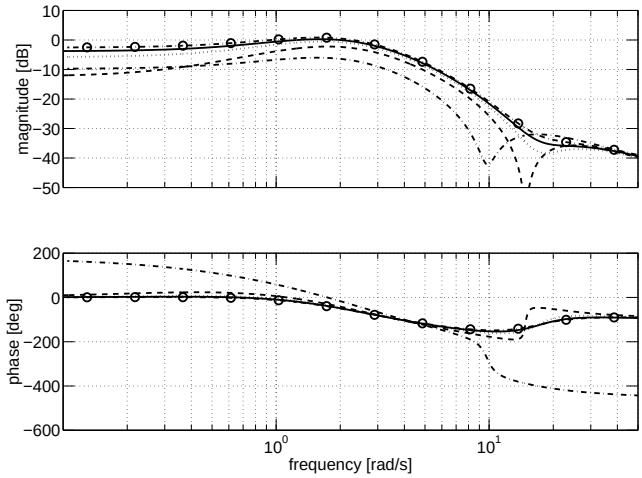

(a) From steering input [deg] to steer axle suspension roll angle [deg]. Partial-state feedback control: $V = 0.001$ (——), 0.01 ($\cdots\cdots$), 0.1 (– – –), 1 ($-\cdot-\cdot-\cdot$); full-state feedback control: ($-\cdot\circ-\cdot$).

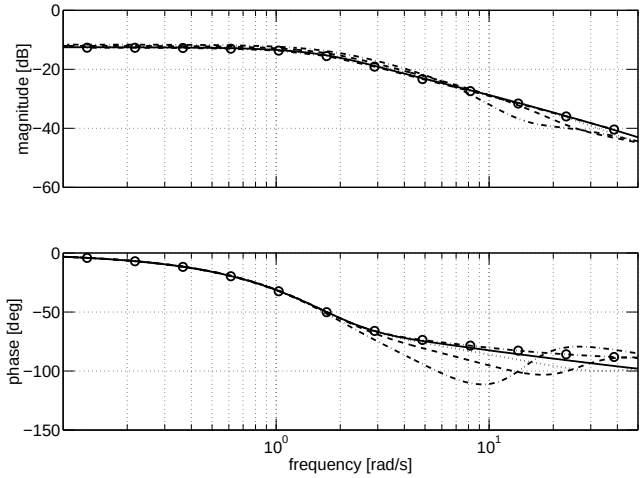

(b) From steering input [deg] to normalised steer axle load transfer [roll-over at ± 1]. Partial-state feedback control: $V = 0.001$ (——), 0.01 ($\cdots\cdots$), 0.1 (– – –), 1 ($-\cdot-\cdot-\cdot$); full-state feedback control: ($-\cdot\circ-\cdot$).

Figure 4.14: Variation with Kalman filter design weights of the frequency response of the linear, torsionally rigid single unit vehicle model with a partial-state feedback controller.

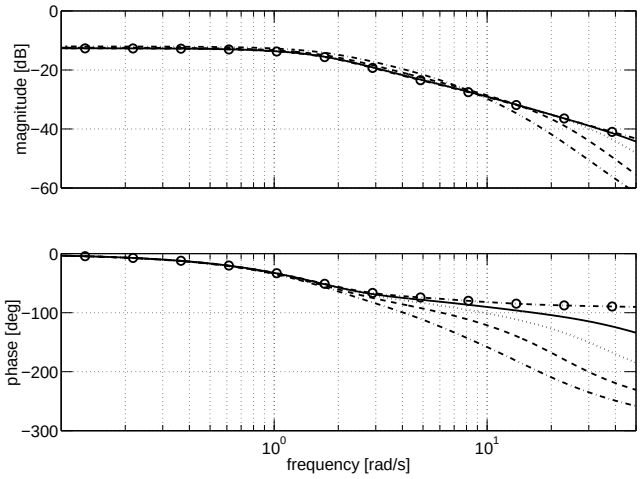

(c) From steering [deg] to normalised drive axle load transfer. Partial-state feedback control: $V = 0.001$ *(——), 0.01 (· · · · · ·), 0.1 (– – –), 1 (· – · – ·)*; full-state feedback control: *(· – ○ – ·).*

Figure 4.14: Continued.

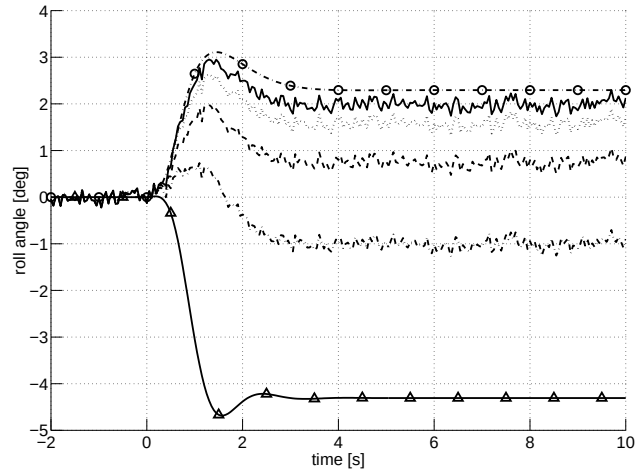

(a) Steer axle suspension roll angle [deg]. Partial-state feedback control: $V = 0.001$ *(——), 0.01 (· · · · · ·), 0.1 (– – –), 1 (· – · – ·)*; full-state feedback control: *(· – ○ – ·); passive control: (—△—).*

Figure 4.15: Variation with Kalman filter design weights of the response of the linear, torsionally rigid single unit vehicle model with a partial-state feedback controller.

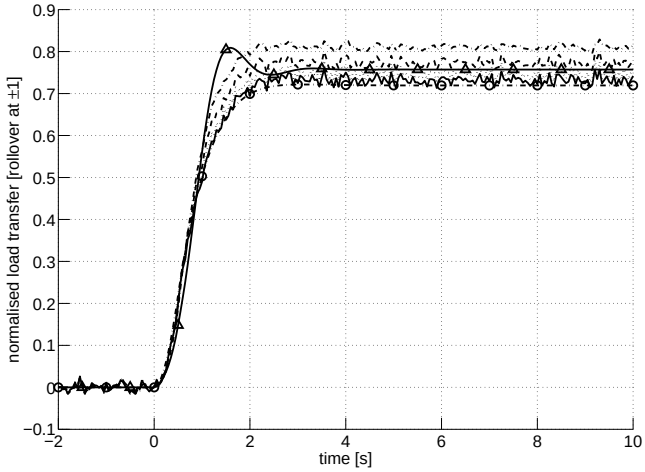

(b) Normalised steer axle load transfer. Partial-state feedback control: $V = 0.001$ (——), *0.01* (· · · · · ·), *0.1* (– – –), *1* (· – · – ·); full-state feedback control: (· – ○ – ·); *passive control:* (—△—).

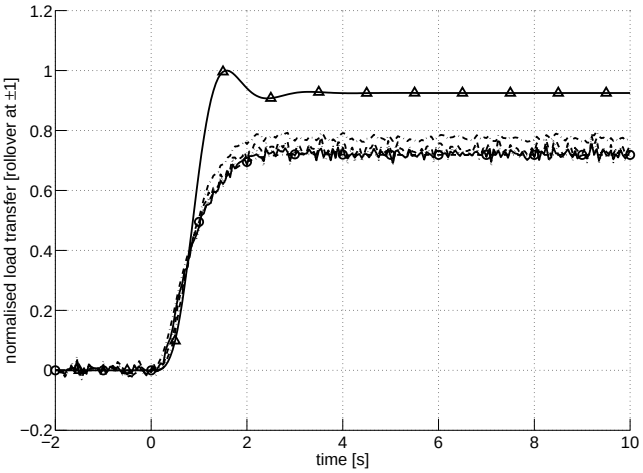

(c) Normalised drive axle load transfer. Partial-state feedback control: $V = 0.001$ (——), *0.01* (· · · · · ·), *0.1* (– – –), *1* (· – · – ·); full-state feedback control: (· – ○ – ·); *passive control:* (—△—).

Figure 4.15: Continued.

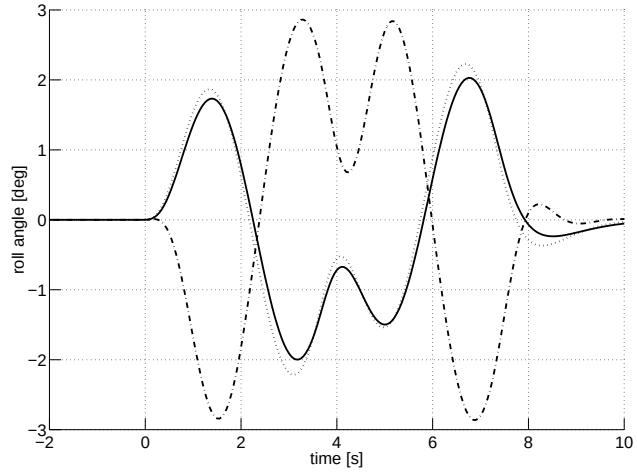

(a) Steer axle suspension roll angle. Full-state feedback control: ∞ *bandwidth (· · · · · ·), 0.5 Hz bandwidth (——); passive control: (· – · – ·).*

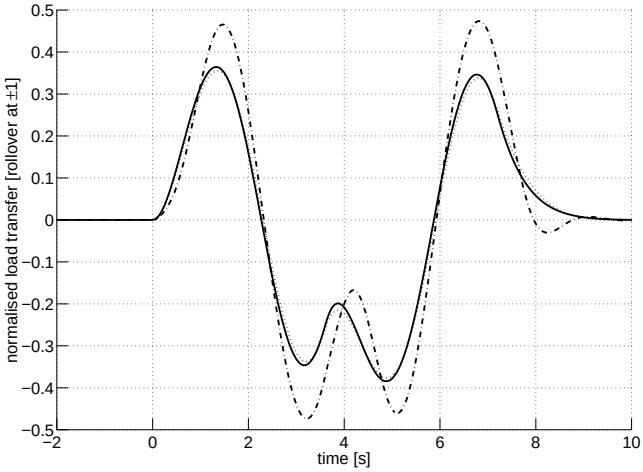

(b) Normalised steer axle load transfer. Full-state feedback control: ∞ *bandwidth (· · · · · ·), 0.5 Hz bandwidth (——); passive control: (· – · – ·).*

Figure 4.16: Effect of limited actuator bandwidth on the response of the linear, torsionally rigid single unit vehicle model with a full-state feedback controller to a double lane change steering input.

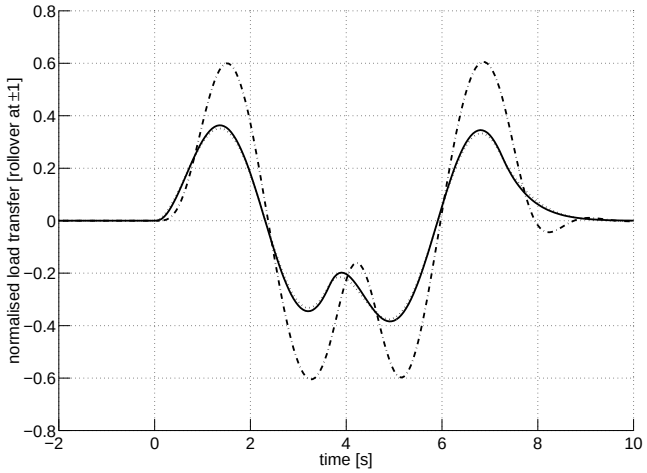

(c) Normalised drive axle load transfer. Full-state feedback control: ∞ *bandwidth (· · · · · ·), 0.5 Hz bandwidth (——); passive control: (· – · – ·).*

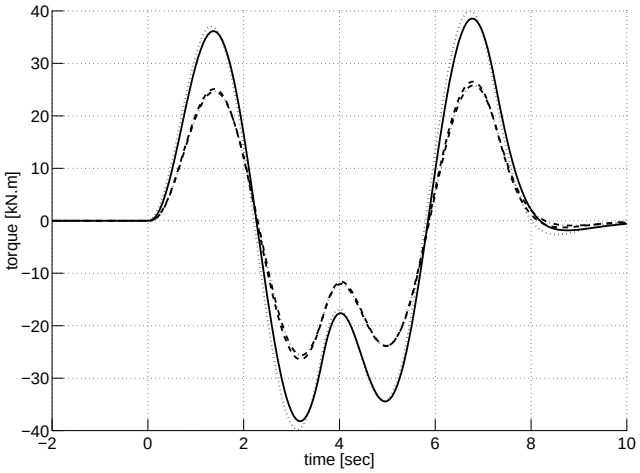

(d) Active anti-roll bar moments. ∞ bandwidth: *steer axle (· · · · · ·), drive axle (– – –)*; 0.5 Hz bandwidth: *steer axle (——), drive axle (· – · – ·).*

Figure 4.16: Continued.

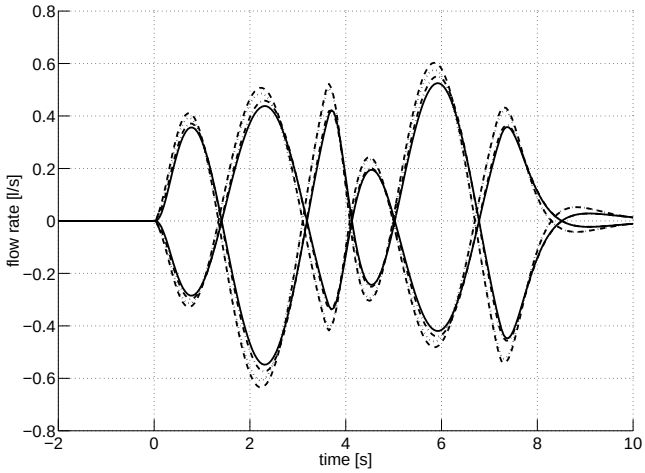

(e) Servo-valve flow rates. ∞ bandwidth: *steer axle (· · · · · ·), drive axle (– – –)*; 0.5 Hz bandwidth: *steer axle (——), drive axle (· – · – ·).*

Figure 4.16: Continued.

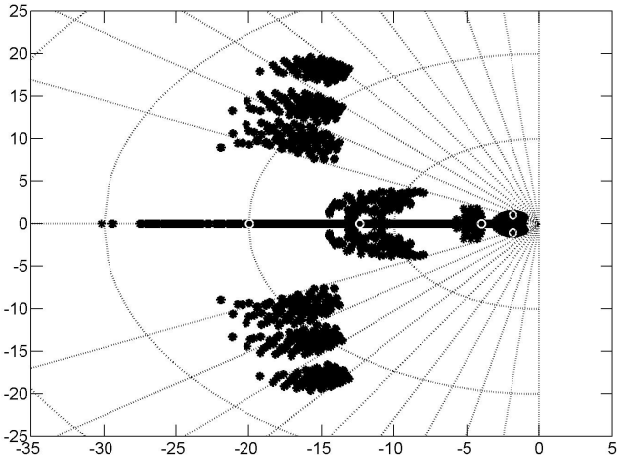

Figure 4.17: Variation with selected vehicle parameters of the closed-loop poles of the torsionally rigid single unit vehicle with a full-state feedback controller.

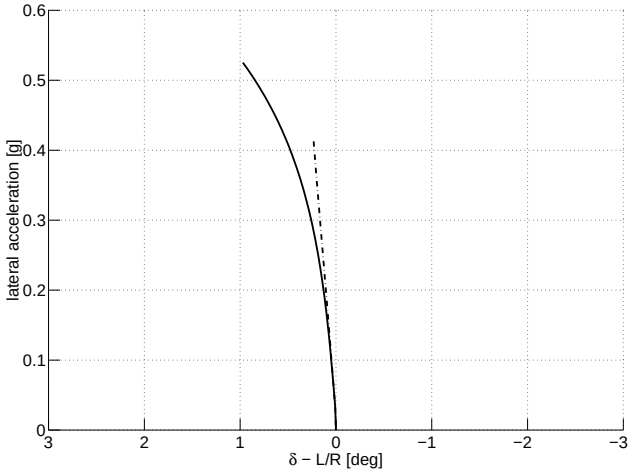

Active roll control (——), passive suspension (· – · – ·).

Figure 4.18: Handling diagram for the torsionally rigid single unit vehicle with a full-state feedback controller.

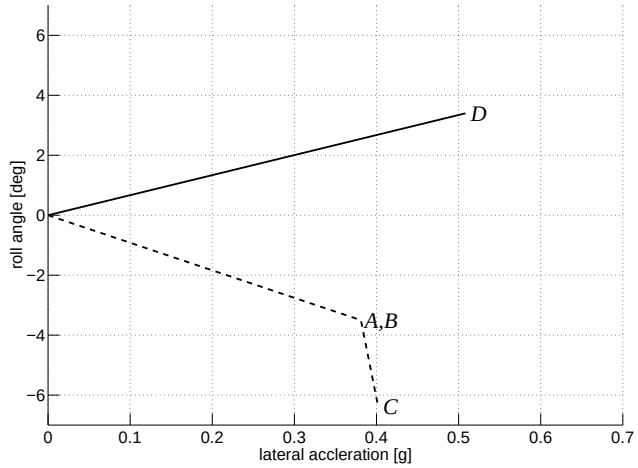

(a) Suspension roll angles. Active roll control: *steer axle (——)*; passive suspension: *steer axle (– – –).*

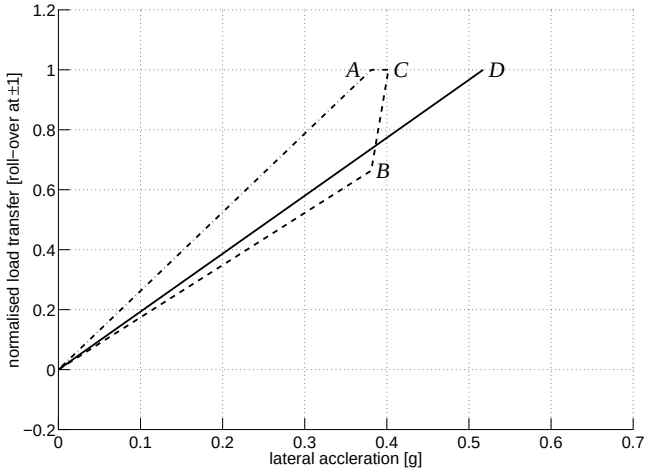

(b) Normalised load transfers. Active roll control: *steer axle and drive axle (——)*; passive suspension: *steer axle (– – –), drive axle (· – · – ·).*

Figure 4.19: Response of the linear, torsionally flexible single unit vehicle model with a full-state feedback controller to a steady-state steering input.

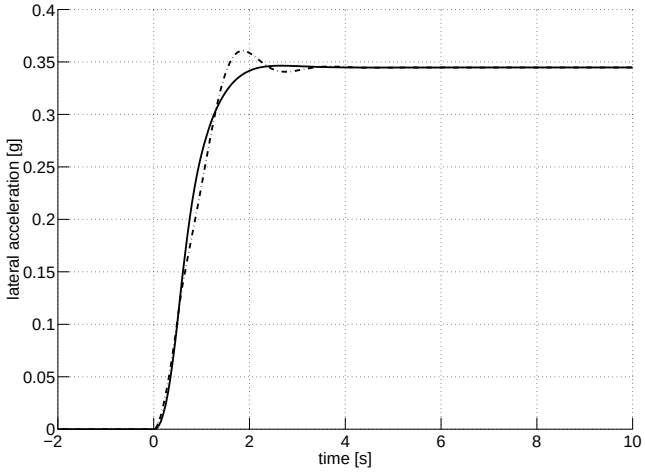

(a) Lateral acceleration. *Active roll control (——), passive suspension (· – · – ·).*

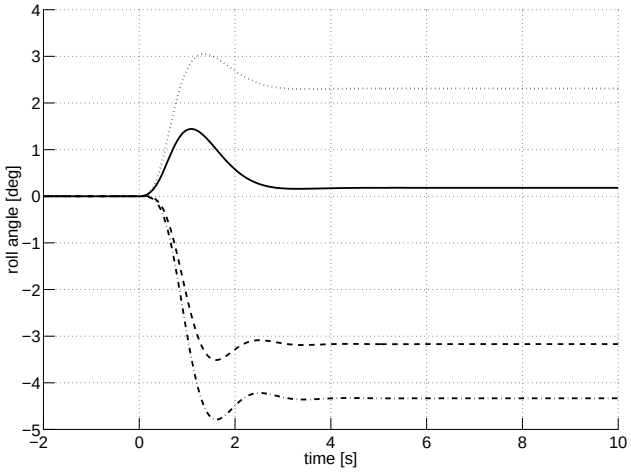

(b) Suspension roll angles. Active roll control: *steer axle (· · · · · ·), drive axle (——)*; passive suspension: *steer axle (– – –), drive axle (· – · – ·).*

Figure 4.20: Response of the linear, torsionally flexible single unit vehicle model with a full-state feedback controller to a step steering input.

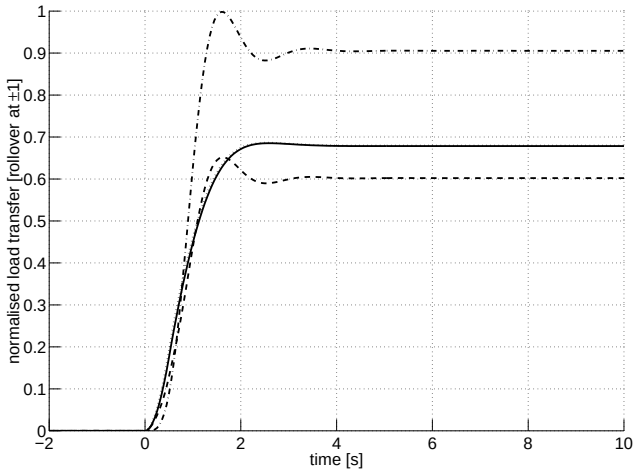

(c) Normalised load transfers. Active roll control: *steer axle (· · · · · ·), drive axle (——)*; passive suspension: *steer axle (– – –), drive axle (· – · – ·).*

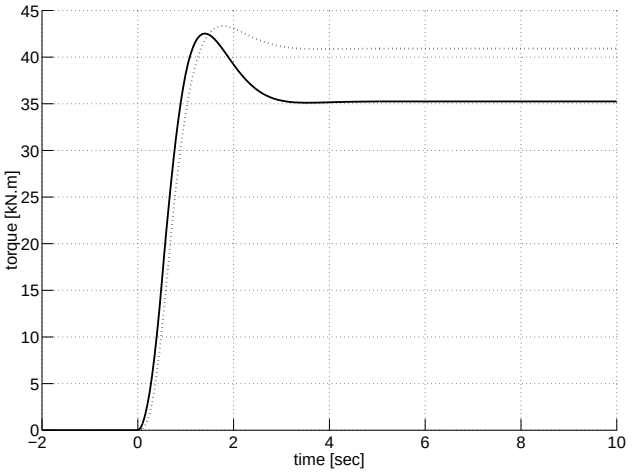

(d) Active anti-roll bar moments. Active roll control: *steer axle (· · · · · ·), drive axle (——).*

Figure 4.20: Continued.

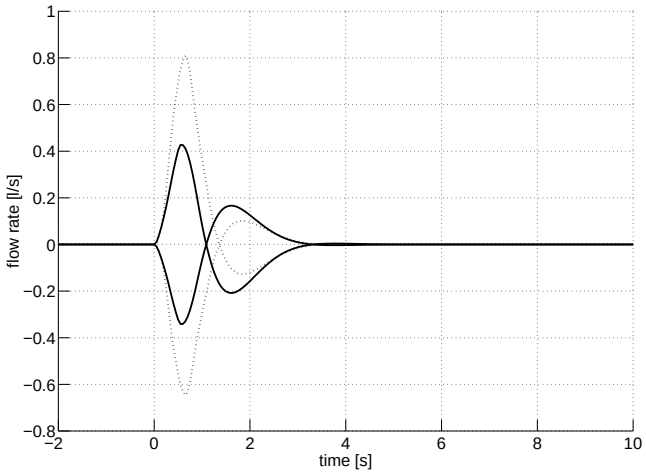

(e) Servo-valve flow rates. Active roll control: *steer axle (· · · · · ·), drive axle (——).*

Figure 4.20: Continued.

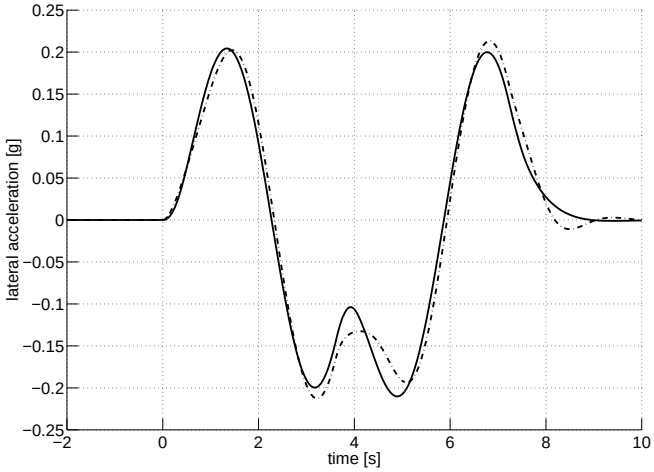

(a) Lateral acceleration. *Active roll control (——), passive suspension (· – · – ·).*

Figure 4.21: Response of the linear, torsionally flexible single unit vehicle model with a full-state feedback controller to a double lane change steering input.

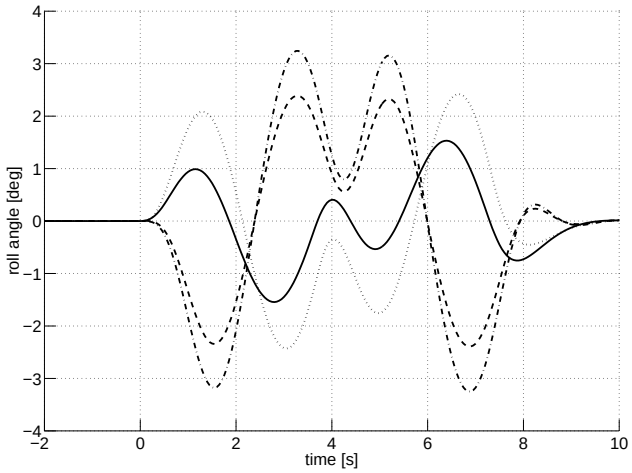

(b) Suspension roll angles. Active roll control: *steer axle (· · · · · ·), drive axle (——)*; passive suspension: *steer axle (– – –), drive axle (· – · – ·).*

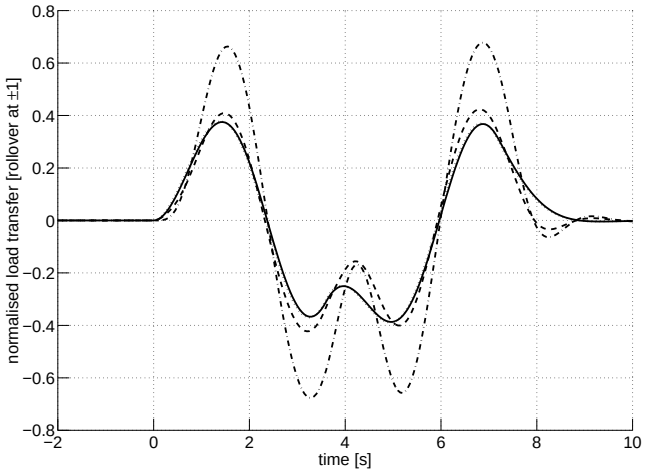

(c) Normalised load transfers. Active roll control: *steer axle (· · · · · ·), drive axle (——)*; passive suspension: *steer axle (– – –), drive axle (· – · – ·).*

Figure 4.21: Continued.

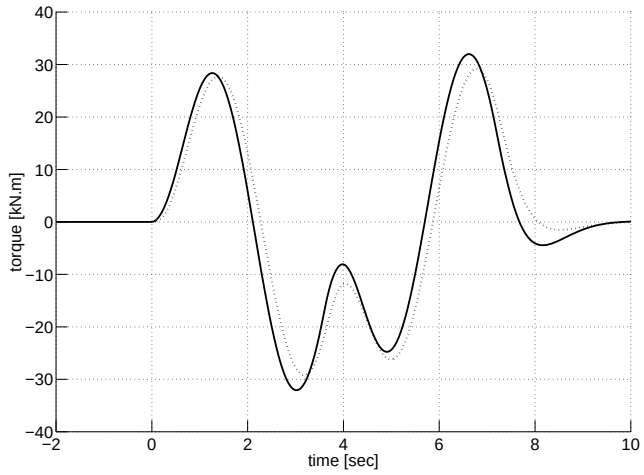

(d) Active anti-roll bar moments. Active roll control: *steer axle (· · · · · ·), drive axle (——).*

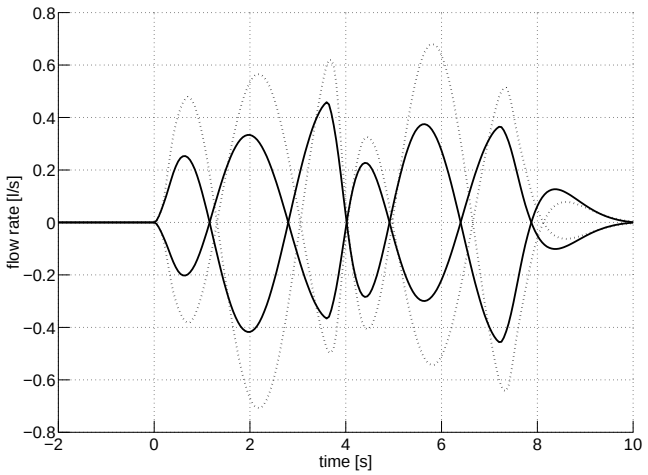

(e) Servo-valve flow rates. Active roll control: *steer axle (· · · · · ·), drive axle (——).*

Figure 4.21: Continued.

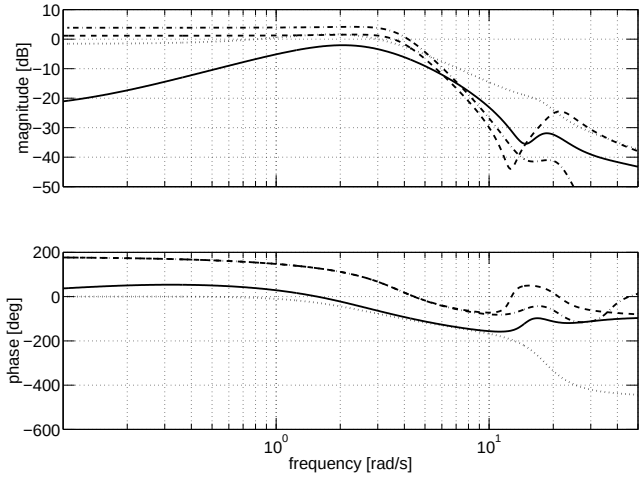

(a) From steering input [deg] to suspension roll angles [deg]. Active roll control: *steer axle (· · · · · ·), drive axle (——)*; passive suspension: *steer axle (– – –), drive axle (· – · – ·).*

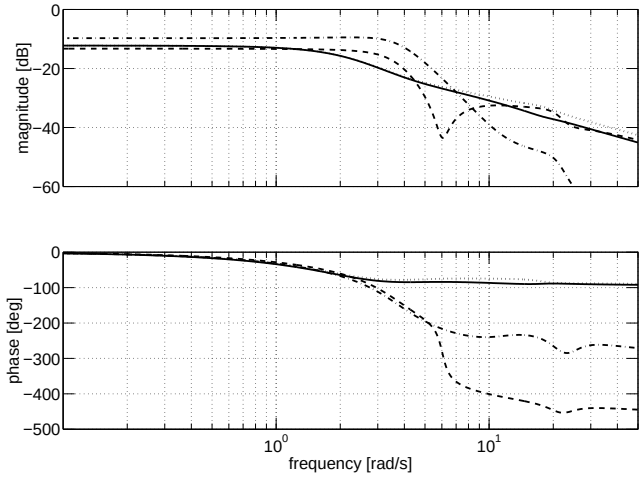

(b) From steering input [deg] to normalised load transfers [roll-over at ± 1]. Active roll control: *steer axle (· · · · · ·), drive axle (——)*; passive suspension: *steer axle (– – –), drive axle (· – · – ·).*

Figure 4.22: Frequency response of the linear, torsionally flexible single unit vehicle model with a full-state feedback controller.

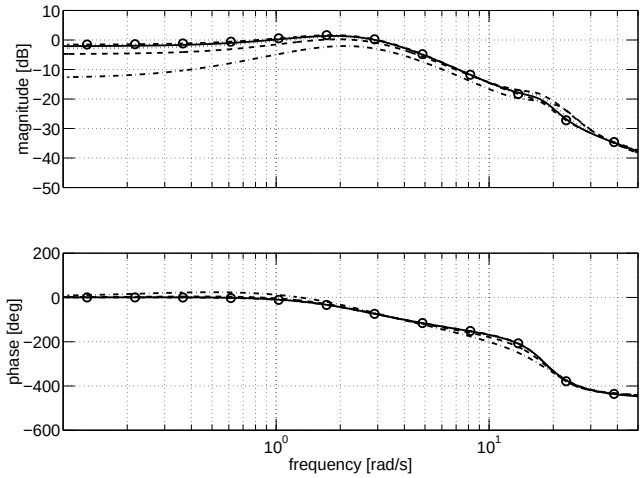

(a) From steering input [deg] to steer axle suspension roll angle [deg]. Partial-state feedback control: $V = 0.001$ (——), 0.01 ($\cdots\cdots$), 0.1 (– – –), 1 ($-\cdot-\cdot-\cdot$); full-state feedback control: ($-\cdot\circ-\cdot$).

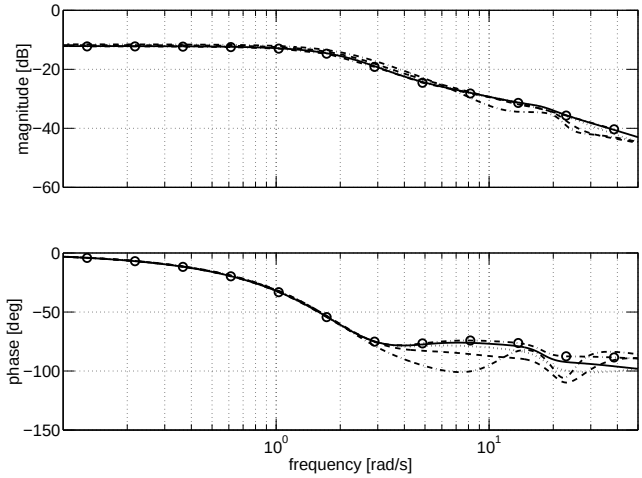

(b) From steering input [deg] to normalised steer axle load transfer [roll-over at ± 1]. Partial-state feedback control: $V = 0.001$ (——), 0.01 ($\cdots\cdots$), 0.1 (– – –), 1 ($-\cdot-\cdot-\cdot$); full-state feedback control: ($-\cdot\circ-\cdot$).

Figure 4.23: Variation with Kalman filter design weights of the frequency response of the linear, torsionally flexible single unit vehicle model with a partial-state feedback controller.

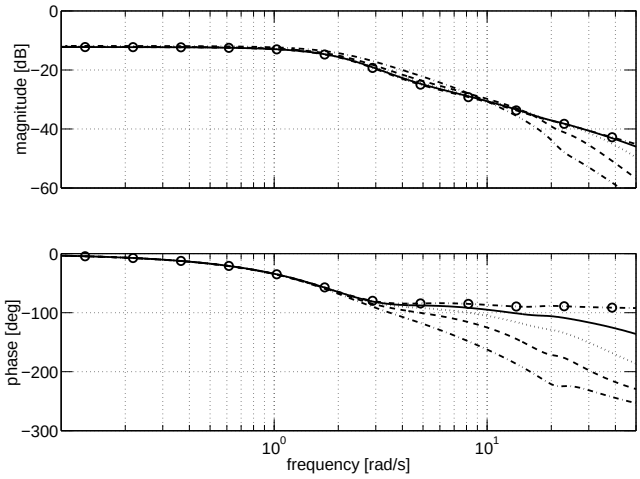

(c) From steering [deg] to normalised drive axle load transfer. Partial-state feedback control: $V = 0.001$ *(——), 0.01 (· · · · · ·), 0.1 (– – –), 1 (· – · – ·)*; full-state feedback control: *(· – ○ – ·).*

Figure 4.23: Continued.

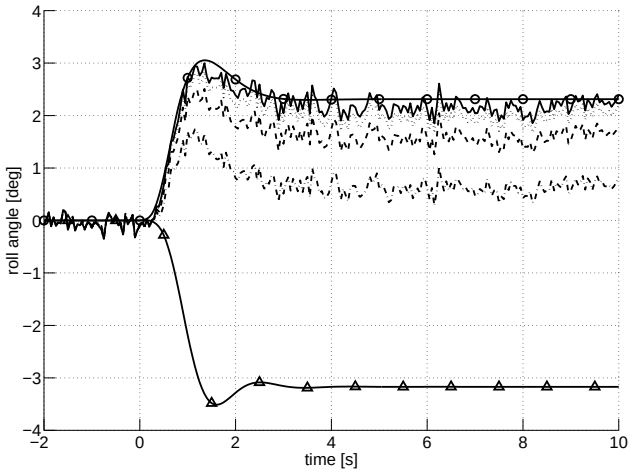

(a) Steer axle suspension roll angle [deg]. Partial-state feedback control: $V = 0.001$ *(——), 0.01 (· · · · · ·), 0.1 (– – –), 1 (· – · – ·)*; full-state feedback control: *(· – ○ – ·); passive control: (—△—).*

Figure 4.24: Variation with Kalman filter design weights of the response of the linear, torsionally flexible single unit vehicle model with a partial-state feedback controller.

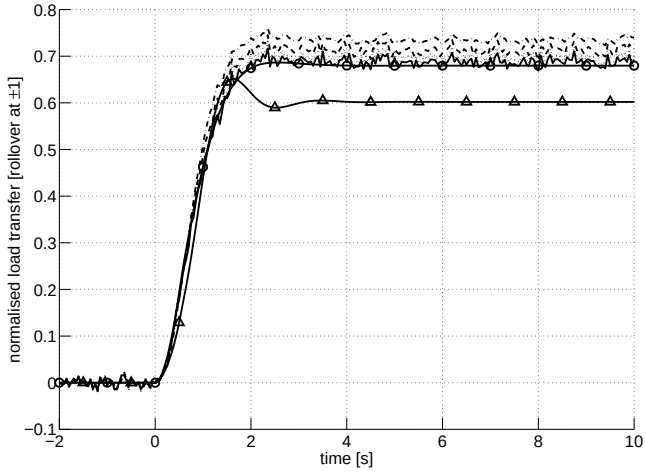

(b) Normalised steer axle load transfer. Partial-state feedback control: $V = 0.001$ (——), *0.01* (· · · · · ·), *0.1* (– – –), *1* (· – · – ·); full-state feedback control: (· – ○ – ·); *passive control:* (—△—).

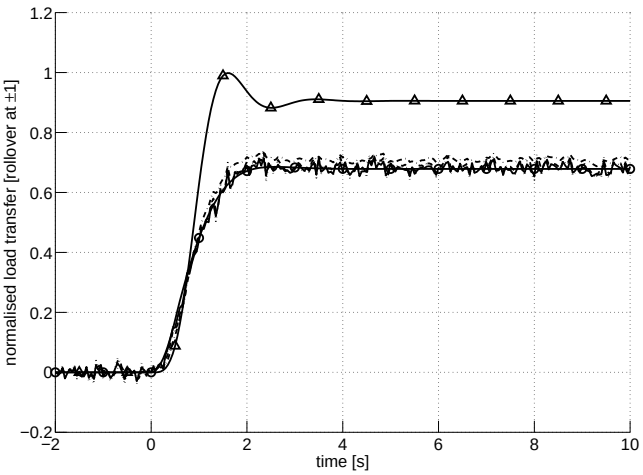

(c) Normalised drive axle load transfer. Partial-state feedback control: $V = 0.001$ (——), *0.01* (· · · · · ·), *0.1* (– – –), *1* (· – · – ·); full-state feedback control: (· – ○ – ·); *passive control:* (—△—).

Figure 4.24: Continued.

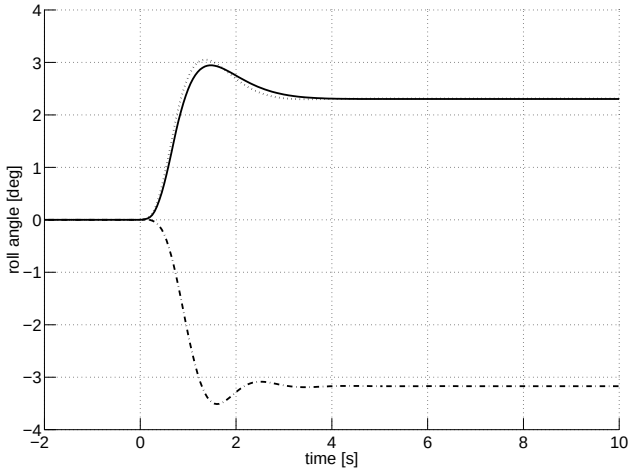

(a) Steer axle suspension roll angle. Full-state feedback control: ∞ *bandwidth (· · · · · ·), 0.5 Hz bandwidth (——); passive control: (· – · – ·).*

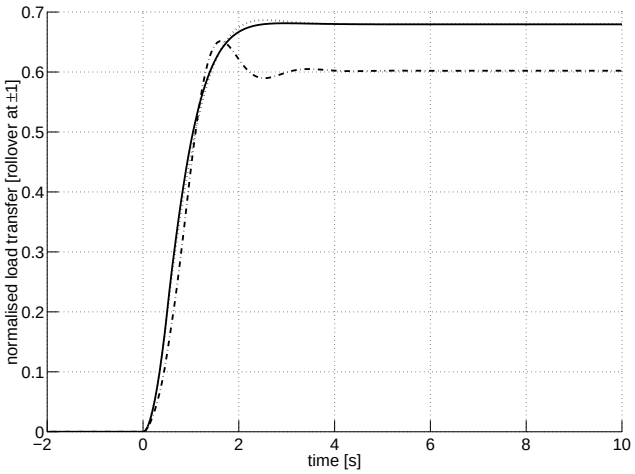

(b) Normalised steer axle load transfer. Full-state feedback control: ∞ *bandwidth (· · · · · ·), 0.5 Hz bandwidth (——); passive control: (· – · – ·).*

Figure 4.25: Effect of limited actuator bandwidth on the response of the linear, torsionally flexible single unit vehicle model with a full-state feedback controller to a step steering input.

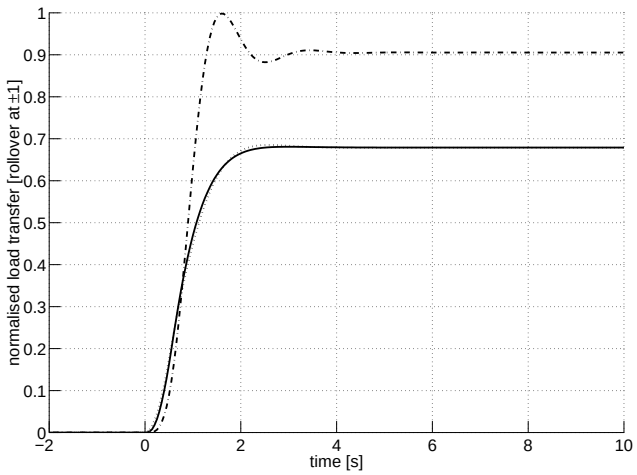

(c) Normalised drive axle load transfer. Full-state feedback control: ∞ *bandwidth (· · · · · ·), 0.5 Hz bandwidth (——); passive control: (· – · – ·).*

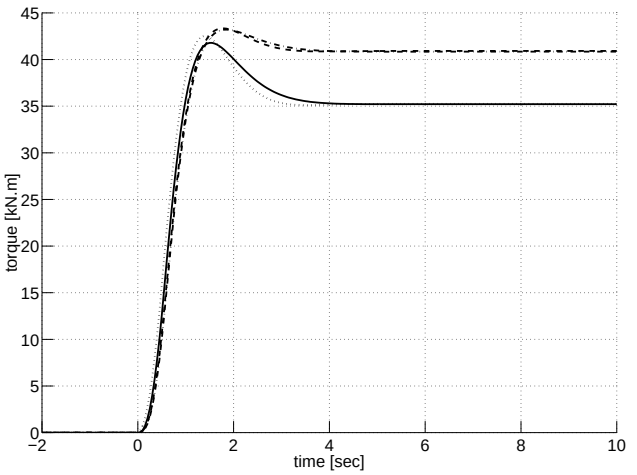

(d) Active anti-roll bar moments. ∞ bandwidth: *steer axle (· · · · · ·), drive axle (– – –)*; 0.5 Hz bandwidth: *steer axle (——), drive axle (· – · – ·).*

Figure 4.25: Continued.

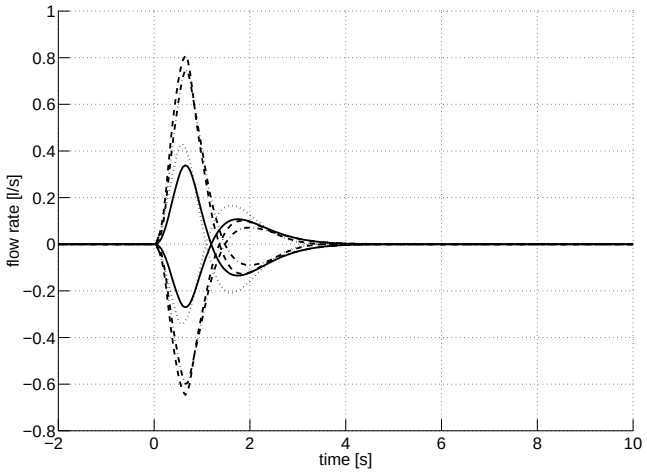

(e) Servo-valve flow rates. ∞ bandwidth: *steer axle (· · · · · ·), drive axle (– – –)*; 0.5 Hz bandwidth: *steer axle (——), drive axle (· – · – ·).*

Figure 4.25: Continued.

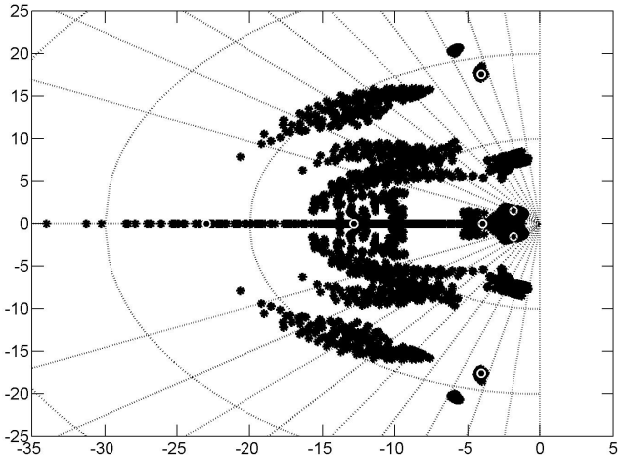

Figure 4.26: Variation with selected vehicle parameters of the closed-loop poles of the torsionally flexible single unit vehicle with a full-state feedback controller.

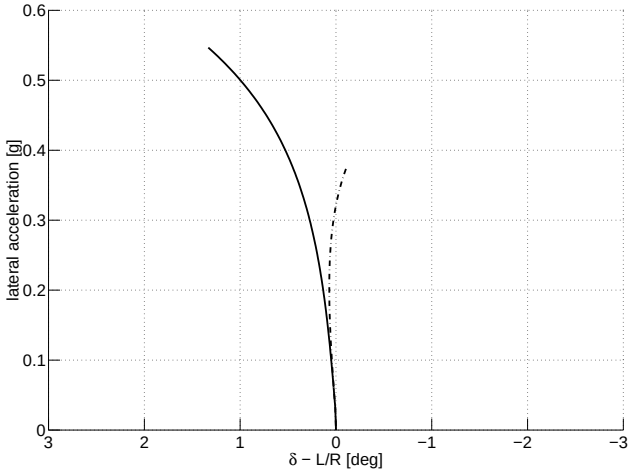

Active roll control (——), passive suspension (· – · – ·).

Figure 4.27: Handling diagram for the torsionally flexible single unit vehicle with a full-state feedback controller.

Chapter 5

Active roll control of a tractor semi-trailer

5.1 Introduction

This chapter considers the problem of designing an active roll control system for a tractor semi-trailer. The aim is to extend the application of the control system design techniques from section 4.5 to an articulated vehicle.

5.2 Vehicle description

The tractor semi-trailer combination, which is illustrated in figure 5.1, consists of the two axle tractor unit described in section 4.2 joined to a three axle tanker semi-trailer by a fifth wheel coupling. The tractor and semi-trailer parameters are from an experimental vehicle that is currently being designed and built at the University of Cambridge. The control strategies developed here will be implemented and tested on this prototype vehicle.

The semi-trailer is shown in detail in figure 5.2. The three axles of the semi-trailer are spaced evenly at 1.31 m intervals, and the distance from the front axle centreline to the fifth wheel coupling is 6.39 m. A pair of single tyres is fitted to each axle. The

tanker frame is more rigid than the tractor frame, and the combined torsional stiffness of the tanker frame and the fifth wheel coupling is 3000 kN.m/rad. The unladen mass of the semi-trailer is 5420 kg, and the unladen axle weights are 1400 kg on each axle.

To avoid slosh, the tank is divided into four 7600 l compartments and two 5000 l compartments. The tanker can transport up to 40400 l (30300 kg) of petrol but may also be used to transport other liquids. As it is not advisable to conduct testing of the system with a flammable payload, water will be used for the testing of the prototype vehicle. Filling the second, third, fourth and sixth compartments from the front with water gives a similar payload mass and mass distribution to filling all six tanks with petrol. Therefore this configuration will be used for the simulations presented in this chapter and the upcoming field tests.

The total mass of the laden semi-trailer is 33220 kg (including 27800 l of water), and the laden axle weights are 8131 kg on each axle. The complete set of vehicle parameters is given in appendix B.

5.3 Control system design objectives

First consider the case of the tractor semi-trailer combination with a torsionally rigid tractor unit. The vehicle is modelled using the techniques described in chapter 2. There are five roll outputs (the body roll angles of the tractor and semi-trailer units and the load transfers at the tractor steer, tractor drive and semi-trailer axles). Since the semi-trailer axles are identical and are connected by a load levelling system, these three axles are considered to be a single axle group with a single roll angle and load transfer. There are three roll control inputs (the roll moments from the active anti-roll bars at the tractor steer, tractor drive and semi-trailer axles). Without active roll control, the system is stable (with poles at $-1.70 \pm j3.59$, $-7.02 \pm j2.26$, $-5.12 \pm j37.9$, -2.88, -9.86, -112, -594 and -601 rad/s) and minimum phase. By the controllability analysis from section 3.5.4, the system is input deficient. An eigenvalue analysis as described in section 3.5.5 yields the following significant results. Without active roll control, the

vehicle is unstable once the tractor drive axle and semi-trailer axles lift off. That is, the tractor steer axle is not sufficiently stiff to provide a restoring moment to balance the lateral displacement moment (see section 3.3.3). This means that the vehicle rolls over without the restoring moment at the tractor steer axle reaching the maximum level. However it is possible for an active roll control system to provide additional net restoring moment through the tractor steer axle beyond this point. Therefore, when formulating a set of control system design objectives, it is important to control the load transfer at all axles. By section 3.6, the achievable design objective that maximises the vehicle roll stability is to balance the normalised load transfers at all axles while taking the maximum suspension roll angle to the maximum allowable inward angle.

Next consider the case of the tractor semi-trailer combination with a torsionally flexible tractor unit. There are now six roll outputs (the front and rear body roll angles of the tractor, the body roll angle of the semi-trailer, and the load transfer at the tractor steer, tractor drive and semi-trailer axles) and three roll control inputs (the roll moments from the active anti-roll bars at the tractor steer, tractor drive and semi-trailer axles). Without active roll control, the system is minimum phase and stable (with poles at $-1.66 \pm j3.53$, $-7.34 \pm j1.78$, $-7.19 \pm j53.9$, $-1.39 \pm j19.4$, -2.95, -9.47, -112, -596 and -604 rad/s). Without active roll control, the vehicle is again unstable once the tractor drive and semi-trailer axles lift off. In fact, the introduction of torsional flexibility of the tractor frame reduces the ability of the steer axle to stabilise the vehicle once the other axles lift off. However, even when the torsional stiffness of the vehicle is reduced to 629 kN.m/rad, it is still possible for an active roll control system to provide additional net restoring moment through the tractor steer axle beyond this point. By section 3.6, the achievable design objective that maximises the vehicle roll stability is again to balance the normalised load transfers at all axles while taking the maximum suspension roll angle to the maximum allowable inward angle.

5.4 Control of a torsionally rigid tractor semi-trailer

The design of an active roll control system for a torsionally rigid* tractor semi-trailer is considered first. The effect of torsional flexibility of the tractor frame is investigated in section 5.5.

5.4.1 Design of a full-state feedback controller

The tractor semi-trailer combination has more degrees of freedom, more inputs and outputs, more internal states and therefore more complicated dynamics than the single unit vehicle considered in chapter 4. However the roll control of a tractor semi-trailer, like the roll control of a single unit vehicle, is fundamentally a problem of optimal disturbance rejection system design, so the design framework used in sections 4.6 and 4.7 is still applicable. However there are more factors to consider when selecting the weighting matrices Q and R.

The coloured noise steering input specified by the filter (4.28) is used. The elements of the performance output z are chosen to penalise only the unsprung mass roll angles (since these are proportional to load transfer),

$$z = \begin{bmatrix} \phi_{t,f,1} & \phi_{t,r,1} & \phi_{t,r,2} \end{bmatrix}^T . \tag{5.1}$$

The constraint on suspension roll angles is handled implicitly by selecting the elements of R to limit the roll moments from the anti-roll bars. Q and R were chosen to be diagonal matrices. An initial estimate of the elements of Q and R was made by taking the inverse squares of the corresponding states' maximum expected values. The elements of Q and R were subsequently tuned according to the procedure outlined in section 4.6.1 to give acceptable performance across a wide range of manoeuvres. For

*For brevity, *torsionally rigid* or *torsionally flexible* here refers specifically to the tractor frame. The torsional flexibilities of the tanker semi-trailer and the fifth-wheel coupling, which are typically significantly lower than that of the tractor unit, are included in all models.

a speed of 60 km/h, the weighting matrices

$$Q = \begin{bmatrix} 1.000 & 0 & 0 \\ 0 & 1.641 & 0 \\ 0 & 0 & 1.762 \end{bmatrix} \mathrm{rad}^{-2}, \tag{5.2}$$

$$R = 7.225 \times 10^{-14} \begin{bmatrix} 1 & 0 & 0 \\ 0 & 1 & 0 \\ 0 & 0 & 1 \end{bmatrix} \mathrm{N}^{-2}.\mathrm{m}^{-2}, \tag{5.3}$$

produced a full-state feedback controller

$$K_{FB} = \begin{bmatrix} 1.0158 \times 10^5 & 1.6520 \times 10^5 & -9.4448 \times 10^4 \\ -1.9875 \times 10^4 & -2.2633 \times 10^4 & -4.0026 \times 10^4 \\ -2.6015 \times 10^5 & -2.8325 \times 10^5 & -7.5283 \times 10^5 \\ 7.9171 \times 10^4 & 5.6237 \times 10^4 & 1.4744 \times 10^5 \\ 2.0233 \times 10^6 & 1.4382 \times 10^4 & 5.3792 \times 10^3 \\ 2.3732 \times 10^4 & 2.2422 \times 10^6 & 1.0333 \times 10^4 \\ -2.6453 \times 10^5 & -3.0853 \times 10^5 & -1.4998 \times 10^5 \\ -9.1789 \times 10^4 & -1.0609 \times 10^5 & -2.0218 \times 10^5 \\ -4.5706 \times 10^5 & -5.2830 \times 10^5 & -9.9916 \times 10^5 \\ 1.5985 \times 10^5 & 1.8478 \times 10^5 & 3.5216 \times 10^5 \\ 3.1691 \times 10^4 & 3.6892 \times 10^4 & 3.0056 \times 10^6 \\ 3.5659 \times 10^4 & 3.3340 \times 10^5 & 5.6887 \times 10^5 \end{bmatrix}^T \begin{array}{l} \mathrm{N.m/rad} \\ \mathrm{N.m.s/rad} \\ \mathrm{N.m/rad} \\ \mathrm{N.m.s/rad} \\ \mathrm{N.m/rad} \\ \mathrm{N.m/rad} \\ \mathrm{N.m/rad} \\ \mathrm{N.m.s/rad} \\ \mathrm{N.m/rad} \\ \mathrm{N.m.s/rad} \\ \mathrm{N.m/rad} \\ \mathrm{N.m/rad} \end{array} \tag{5.4}$$

acting on the augmented state vector

$$\underline{x} = \begin{bmatrix} \phi_1 & \dot{\phi}_1 & \beta_1 & \dot{\psi}_1 & \phi_{t,f,1} & \phi_{t,r,1} & \phi_2 & \dot{\phi}_2 & \beta_2 & \dot{\psi}_2 & \phi_{t,r,2} & \delta/2 \end{bmatrix}^T. \tag{5.5}$$

The performance of this controller is examined in sections 5.4.2–5.4.5.

5.4.2 Steady-state cornering response

The response of the linear, torsionally rigid tractor semi-trailer model with a full-state feedback controller to a steady-state steering input at 60 km/h is shown in figure 5.3.

Without active roll control, the vehicle rolls out of the corner (that is, negative roll angle). As lateral acceleration increases, the normalised load transfer builds up most quickly at the tractor drive axle and most slowly at the tractor steer axle. From section 3.3.3, the semi-trailer axles would typically be expected to have the highest effective stiffness-to-load ratio, so the normalised load transfer would be expected to build up faster there than at the tractor drive axle. However, the effective stiffness-to-load ratio of the semi-trailer axles here is particularly low because the tyres are relatively compliant in roll and the roll centre of the suspension is very low. The tractor drive axle lifts off at 0.43 g (point C), at which point the normalised load transfer is 0.80 at the tractor steer axle (point A) and is 0.86 at the semi-trailer axles (point B). As lateral acceleration continues to increase, the tractor drive axle is unable to contribute any additional restoring moment, and the slopes of the other normalised load transfer curves and of the suspension roll angle curves increase. The semi-trailer axles lift off at 0.48 g (point E), at which point the normalised load transfer at the steer axle is 0.95 (point D). Beyond this point, the steer axle is unable to provide sufficient additional restoring moment to stabilise the vehicle, and roll-over occurs.

With active roll control, the vehicle rolls into the corner (that is, positive roll angle). The roll moments from the active anti-roll bars are distributed among the axles so that the normalised load transfers increase in a balanced fashion, reaching the maximum value of 1 simultaneously at 0.62 g (point F). The maximum suspension roll angle is 3.3° at the semi-trailer axles. A relative roll angle between the tractor and trailer of 1.0°/g, with the tractor rolling into the corner more than the trailer, is required to ensure that the normalised load transfers are balanced. Surprisingly, despite the greater absolute roll angle of the tractor body, the suspension roll angle at roll-over is greater at the semi-trailer axles than at the tractor drive axle. This is because the semi-trailer tyres are significantly more compliant in roll than the tractor drive axle tyres and the

difference between the unsprung mass roll angles is greater than the difference between the absolute body roll angles.

Active roll control increases the roll-over threshold of the torsionally rigid tractor semi-trailer combination by 29% and the lateral acceleration at which axle lift-off first occurs by 45%. This represents a significant improvement in vehicle safety.

5.4.3 Response to a step steering input

The response of the linear, torsionally rigid tractor semi-trailer model to a step steering input is shown in figure 5.4. The step input is scaled to give a maximum normalised lateral load transfer of 1 in the following simulations.

The vehicle quickly settles into a constant turn of radius 68 m (see figure 5.4(a)). The lateral acceleration responses are shown in figure 5.4(b). Lateral acceleration builds up to the steady-state value of 0.43 g much more quickly at the tractor than at the semi-trailer. The active roll control system causes the transient lateral acceleration responses to be less oscillatory.

The suspension roll angle responses are shown in figure 5.4(c). With passive suspension, the vehicle rolls out of the corner with suspension roll angles of approximately 4.8° at all axles. There is a small overshoot in all three traces. The active roll control causes the vehicle to roll into the corner. Although the maximum suspension roll angle is 2.3° at the semi-trailer axles, the tractor body actually rolls into the corner more than the semi-trailer body. The suspension roll angles overshoot the steady-state values by 0.5°. As noted in section 4.6.3, suspension roll angle overshoot is undesirable because it limits the maximum achievable inward steady-state roll angle, assuming that the controller is tuned to avoid striking the bump stops.

The normalised load transfer responses are shown in figure 5.4(d). With passive suspension, the normalised load transfer builds up most quickly at the tractor drive axle and most slowly at the tractor steer axle, as in the steady-state steering case. The load transfer traces feature small overshoots before settling at 0.80, 1.00 and 0.86 at

the tractor steer, tractor drive and semi-trailer axles respectively. Note that there is a delay between the load transfer building up at the tractor axles and the semi-trailer axles. By contrast, the normalised load transfer response of the vehicle fitted with the active roll control system is more heavily damped and rises to a value of 0.69 at *all* axles. There is no delay before the load transfer begins to build up at the semi-trailer axles. The active roll control system reduces the peak load transfer by 14%, 31% and 19% at the tractor steer, tractor drive and semi-trailer axles respectively.

The steady-state results in section 5.4.2 show that, in the passive case, the roll-over threshold for this vehicle is 12% higher than the lateral acceleration at which axle lift-off first occurs. However, with active roll control, the vehicle can remain stable with up to 44% additional lateral acceleration (that is, up to 0.62 g). The peak inward suspension roll angle in response to such a critical manoeuvre is 4.1°, which is within the allowable limit. Clearly, active roll control significantly improves the roll stability of the vehicle in response to a step steering input.

The active anti-roll bar moment responses are shown in figure 5.4(e). The peak roll moment in response to a critical manoeuvre is 77 kN.m at the tractor drive axle. Since the roll moment applied to the semi-trailer is distributed among three axles, the peak roll moment there in response to a critical step steering input is just 42 kN.m. The roll moment builds up fastest at the tractor drive and semi-trailer axles. This is necessary to distribute the total load transfer evenly among the axles throughout the early part of this severe manoeuvre.

Since the torsional flexibility of the vehicle is limited to the fifth wheel and the tanker frame, the suspension roll rates and therefore the fluid flow rates through the servo-valves are similar at all axles. The peak flow rate in response to a critical step manoeuvre is 0.70 l/s (see figure 5.4(f)). The peak power supplied to the system in response to a critical step steering input is 8.8 kW (neglecting losses).

5.4.4 Response to a double lane change steering input

The response of the linear, torsionally rigid tractor semi-trailer model to A double lane change steering input is shown in figure 5.5. Figure 5.5(a) shows that the path deviation over the 120 m test section is 5.05 m for the tractor and 5.2 m for the semi-trailer. The peak lateral acceleration is 0.21 g (see figure 5.5(b)).

The suspension roll angle responses are shown in figure 5.5(c). The trends discussed in sections 5.4.2 and 5.4.3 are again apparent. Active roll control causes the vehicle to roll into the corners, with the tractor unit rolling more towards the inside than the semi-trailer.

Figure 5.5(d) shows the normalised load transfer responses. Without active roll control, the normalised load transfers are unbalanced, with the tractor drive axle bearing significantly more than its share of the total load transfer. The peak load transfers are 0.35 at the tractor steer axle, 0.46 at the tractor drive axle and 0.42 at the semi-trailer axles. When equipped with the active roll control system, the normalised load transfer responses are better balanced. The peak normalised load transfers are 0.29 at the tractor drive, tractor steer and semi-trailer axles. The vehicle with active roll control could remain stable even if the steering input was increased by a factor of 3.50. Peak normalised load transfer is substantially reduced at all axles: 17% at the tractor steer axle, 38% at the tractor drive axle and 32% at the semi-trailer axles.

The peak inward roll angle at the semi-trailer axles in response to a critical steering input is 6.0°. This is close to the maximum available suspension travel.

Figure 5.5(e) illustrates that the largest active anti-roll bar moment for this manoeuvre is 24 kN.m at the tractor drive axle. The roll moment in response to a critical double lane change steering input is therefore 84 kN.m.

The peak flow rate through the servo-valves is 0.50 *l*/s at the semi-trailer axles, as shown in figure 5.5(f). There is little variation in the flow rates among the axles because the vehicle is almost completely torsionally rigid. The peak power supplied to the system during a critical double lane change, neglecting losses, is 28 kW.

5.4.5 Frequency response

Frequency response functions from steering input to suspension roll angles and normalised load transfers are shown in figures 5.6(a) and 5.6(b) respectively. The frequency responses include the 4 rad/s pre-filter to represent the limited bandwidth of the driver.

The active roll control causes both the tractor and semi-trailer to roll into corners, so the roll angle responses are in phase with the steering input at low frequencies. This is by contrast with the roll responses for the passive case, which are 180° out of phase with the steering input at low frequencies. The normalised load transfers are reduced throughout the majority of the frequency range shown. The suspension roll angle and load transfer frequency responses roll off above 4 rad/s.

5.4.6 Design of a partial-state feedback controller

A partial state feedback controller was designed using the LQG-LTR procedure. The controller uses measurements of the suspension roll angles at the tractor steer axle and the semi-trailer axles, the body roll rates of the tractor and semi-trailer, the yaw rates of the tractor and semi-trailer and the steering input,

$$y = \left[\begin{array}{cccccccc} \phi_1 - \phi_{t,f,1} & \dot{\phi}_1 & \dot{\psi}_1 & \phi_2 - \phi_{t,r,2} & \dot{\phi}_2 & \dot{\psi}_2 & \delta/2 \end{array} \right]^T . \tag{5.6}$$

The unmeasured states are the sideslip angles of the tractor and semi-trailer, the suspension roll angle at the tractor drive axle and the load transfers at all axles. The

measurement noise weighting matrix for the Kalman filter design was chosen to be

$$W = \begin{bmatrix} 1.000 & 0 & 0 & 0 & 0 & 0 & 0 \\ 0 & 1.000 & 0 & 0 & 0 & 0 & 0 \\ 0 & 0 & 0.500 & 0 & 0 & 0 & 0 \\ 0 & 0 & 0 & 1.000 & 0 & 0 & 0 \\ 0 & 0 & 0 & 0 & 1.000 & 0 & 0 \\ 0 & 0 & 0 & 0 & 0 & 0.500 & 0 \\ 0 & 0 & 0 & 0 & 0 & 0 & 1.291 \end{bmatrix}^T \begin{matrix} \mathrm{rad}^{-2} \\ \mathrm{rad}^{-2}.\mathrm{s}^2 \\ \mathrm{rad}^{-2}.\mathrm{s}^2 \\ \mathrm{rad}^{-2} \\ \mathrm{rad}^{-2}.\mathrm{s}^2 \\ \mathrm{rad}^{-2}.\mathrm{s}^2 \\ \mathrm{rad}^{-2} \end{matrix} \tag{5.7}$$

and the process noise weighting V was varied as a tuning parameter from 1 rad^{-2} to 0.001 rad^{-2}.

The target feedback loop is that of the full-state feedback controller in section 5.4.1. The results are again similar to those presented for the torsionally rigid single unit vehicle in section 4.6.6. At $V = 1$ rad^{-2}, there are significant differences from the target response in the magnitude of the suspension roll angles at low frequency and in the phase of the drive axle load transfer above 4 rad/s. As V is reduced, the frequency responses converge towards the target response, and by $V = 0.001$ rad^{-2}, there is little difference between the LQR and LQG loop transfer functions.

The transient performances of various LQG designs in response to a step steering input are shown in figure 5.7. As V is reduced, the suspension roll angle and load transfer responses converge towards the response of the vehicle with the full-state feedback controller. Measurement noise attenuation is satisfactory, since 5% random, uncorrelated white noise on all measurements produces less than 2% noise on the load transfer responses in particular (see figures 5.7(b), 5.7(c) and 5.7(d)). It is clear that the improvements in roll stability offered by the full-state feedback controller can also be achieved using a partial-state feedback controller.

5.4.7 Effect of actuator performance limitations

Figure 5.8 shows the effect of the limited bandwidth of the active roll control system on the response of the linear, torsionally flexible tractor semi-trailer model to a double lane change steering input. The active roll control system was represented with a 0.5 Hz first order low-pass filter, and a new controller was synthesised to give the same steady-state performance as in section 5.4.2. The new Q and R matrices were

$$Q = \begin{bmatrix} 1.000 & 0 & 0 \\ 0 & 1.531 & 0 \\ 0 & 0 & 1.600 \end{bmatrix} \mathrm{rad}^{-2}, \tag{5.8}$$

$$R = 5.563 \times 10^{-14} \begin{bmatrix} 1 & 0 & 0 \\ 0 & 1 & 0 \\ 0 & 0 & 1 \end{bmatrix} \mathrm{N}^{-2}.\mathrm{m}^{-2}. \tag{5.9}$$

Limiting the bandwidth of the active roll control system delays the rise of roll moment in the active anti-roll bars (see figure 5.8(f)) which increases the rise time of the roll angle responses (see figures 5.8(a) and 5.8(b)). Thus the capacity of the active roll control system to reduce transient load transfer is compromised, although the changes in peak normalised load transfer at all axles are negligible, as illustrated in figures 5.8(c), 5.8(d) and 5.8(e). The peak flow rates through the servo-valves are reduced by 13%, 14% and 12% at the tractor steer, tractor drive and semi-trailer axles respectively, as shown in figure 5.8(g). Peak roll moments in the active anti-roll bars are reduced by around 8%.

By including the limitations of the active roll control system in the vehicle model at the control system design stage, it is possible to maintain stability robustness and reduce servo-valve flow rate requirements with minimal effect on system performance.

5.4.8 Stability robustness to vehicle parameter uncertainty

Stability robustness to parameter variation is important for reasons outlined in section 4.6.8. To investigate the stability robustness, the following vehicle parameters were varied from their nominal values:

- The sprung mass and the sprung mass height of both the tractor and semi-trailer were varied by $\pm 15\%$, to represent uncertainty in payload configuration.
- The average coefficient of friction between the tyres and the road (and therefore the tyre cornering stiffnesses) was varied between the nominal value and 0.65 of this value, to represent the effects of wet weather and variations in road surfaces.
- The ratios of the tyre cornering stiffnesses on the tractor drive and semi-trailer axles to those on the tractor steer axle were varied by $\pm 15\%$ from the nominal balance, to account for changes in handling characteristics due to lateral load transfers.
- Each suspension roll stiffnesses was varied between the nominal value and a value 15% lower, to account for the nonlinear response of air springs and geometric nonlinearities in the suspension system.
- An additional phase lag represented by a first-order filter with bandwidth as low as 2 Hz can be introduced at each active anti-roll bar, to represent unforeseen actuator performance limitations.
- The vehicle speed can vary about the design set point by $\pm 10\%$, that is ± 6 km/h.

Figure 5.9 shows the variation of the closed loop poles of the vehicle system across the full range of parameters described above. The nominal system poles are located at $-1.94 \pm j1.81$, -6.52 ± 2.92, $-6.50 \pm j34.8$, -2.74, -14.8, -235, -930, -1096 and -4 rad/s. These are denoted by the symbol $(\circ)$ in the figure. Although all fundamental modes of the system feature both yaw-plane and roll-plane components, the

poles at $-1.94 \pm j1.81$ and $-6.52 \pm j2.92$ are primarily associated with handling performance. The closed loop poles of the system remain in the open left half plane for all combinations of possible parameter values, so the system is robustly stable in the presence of model uncertainty.

5.4.9 Effect on handling performance

The effect of active roll control on the handling performance of the torsionally rigid tractor unit in the tractor semi-trailer combination at 60 km/h is shown in figure 5.10. The handling responses of both the tractor and semi-trailer are included in the figure. The handling diagram for the tractor unit is the plot of a_y against $\delta - L_1/R$, where δ, L_1, R and a_y are respectively the steering angle, the wheelbase, the radius of curvature and the lateral acceleration [84]. The handling diagram for the semi-trailer unit is the plot of $\Gamma - L_2/R$ against a_y, where Γ and L_2 are respectively the articulation angle and the effective wheelbase [106]. The effective wheelbase is approximately equal to the distance from the fifth wheel coupling to the mid-point of the semi-trailer axle group.

As outlined in section 1.3.1, the yaw stability of the tractor semi-trailer combination is determined by the handling performances of both the tractor and the semi-trailer. Four handling regimes are possible [84]:

1. If the tractor and the semi-trailer both understeer, the vehicle is always stable in yaw.

2. If the tractor understeers and the semi-trailer oversteers, the vehicle is always stable in yaw.

3. If the tractor oversteers and the semi-trailer understeers, the vehicle is unstable in yaw above a critical speed. The mode of instability in this case is jack-knifing.

4. If the tractor and the semi-trailer both oversteer, the vehicle is unstable in yaw above a critical speed. The mode of instability in this case depends on the ratio

of the understeer gradients and can be either jack-knifing or trailer swing.

The focus here is on whether active roll control increases or decreases the yaw stability of the vehicle.

First, consider the response of the vehicle with passive suspension. At low levels of lateral acceleration, the tractor unit understeers mildly. As lateral acceleration increases, the handling performance (as quantified by the understeer gradient) of the tractor does not change significantly for the same reasons as the single unit vehicle (see section 4.6.9). The semi-trailer oversteers with increasing severity as lateral acceleration builds. However, as long as the tractor unit understeers, the combination is stable in yaw.

The active roll control system causes the normalised load transfers at all axles to build up with lateral acceleration in a balanced fashion. As described in section 4.6.9, this results in a reduction in the cornering stiffness of the steer axle tyres relative to the drive axle tyres. The drive axle tyres are relatively lightly loaded, so the understeer gradient of the tractor unit increases with lateral acceleration. The semi-trailer oversteers increasingly as lateral acceleration builds up. However the oversteer gradient for a given level of lateral acceleration is reduced relative to the passive case because the load transfer at the semi-trailer axles is reduced. Clearly active roll control increases the understeer of both the tractor and semi-trailer and therefore increases yaw stability.

5.5 Control of a torsionally flexible tractor semi-trailer

5.5.1 Design of a full-state feedback controller

The design of a full-state roll controller for a torsionally flexible tractor semi-trailer is again a problem of optimal disturbance rejection system design. The steering input spectrum (4.28) is used. Since the system is input deficient, the active roll control system design is again a trade-off between reducing load transfers, constraining suspension roll angles and limiting energy requirements. The problem is to tune Q and R

to penalise the performance output vector

$$z = \begin{bmatrix} \phi_{t,f,1} & \phi_{t,r,1} & \phi_{t,r,2} \end{bmatrix}^T \tag{5.10}$$

and the control input u respectively.

Without active roll control, torsional flexibility of the tractor frame accentuates the unbalanced build up of normalised load transfers among the axles. An important aim of active roll control is to balance these load transfers, and this is achieved by appropriate choices of Q and R. However, since the tractor and semi-trailer frames are not perfectly rigid, achieving this balance requires the active anti-roll bars to twist the vehicle frames. Suspension roll angles are constrained and power consumption is limited by choosing R to be large enough relative to Q.

For a speed of 60 km/h, the weighting matrices

$$Q = \begin{bmatrix} 1.000 & 0 & 0 \\ 0 & 2.457 & 0 \\ 0 & 0 & 2.630 \end{bmatrix} \mathrm{rad}^{-2}, \tag{5.11}$$

$$R = 1.254 \times 10^{-13} \begin{bmatrix} 1 & 0 & 0 \\ 0 & 1 & 0 \\ 0 & 0 & 1 \end{bmatrix} \mathrm{N}^{-2}.\mathrm{m}^{-2}, \tag{5.12}$$

produce a full-state feedback controller

$$K_{FB} = \begin{bmatrix} 1.0325 \times 10^5 & -2.7201 \times 10^3 & -1.0680 \times 10^3 \\ -1.0209 \times 10^4 & -1.4757 \times 10^3 & 1.9068 \times 10^2 \\ -7.4218 \times 10^4 & 1.6270 \times 10^5 & -7.1742 \times 10^4 \\ -1.5811 \times 10^4 & -1.8235 \times 10^4 & -3.5054 \times 10^4 \\ -2.8207 \times 10^5 & -2.2639 \times 10^5 & -6.3888 \times 10^5 \\ 5.8797 \times 10^4 & 4.7504 \times 10^4 & 1.2992 \times 10^5 \\ 1.3105 \times 10^6 & 1.0321 \times 10^4 & 3.1853 \times 10^3 \\ 1.7030 \times 10^4 & 1.9900 \times 10^6 & 1.2411 \times 10^4 \\ -2.2109 \times 10^5 & -2.6930 \times 10^5 & -1.1766 \times 10^5 \\ -7.2990 \times 10^4 & -9.4483 \times 10^4 & -1.8436 \times 10^5 \\ -3.6958 \times 10^5 & -4.7462 \times 10^5 & -9.2325 \times 10^5 \\ 1.3048 \times 10^5 & 1.6284 \times 10^5 & 3.1767 \times 10^5 \\ 1.8766 \times 10^4 & 4.4310 \times 10^4 & 2.6901 \times 10^6 \\ 1.4252 \times 10^5 & 2.5284 \times 10^5 & 4.2828 \times 10^5 \end{bmatrix}^T \begin{matrix} \mathrm{N.m/rad} \\ \mathrm{N.m.s/rad} \\ \mathrm{N.m/rad} \\ \mathrm{N.m.s/rad} \\ \mathrm{N.m/rad} \\ \mathrm{N.m.s/rad} \\ \mathrm{N.m/rad} \\ \mathrm{N.m/rad} \\ \mathrm{N.m/rad} \\ \mathrm{N.m.s/rad} \\ \mathrm{N.m/rad} \\ \mathrm{N.m.s/rad} \\ \mathrm{N.m/rad} \end{matrix} \tag{5.13}$$

acting on the augmented state vector

$$\underline{x} = \begin{bmatrix} \phi_{f,1} & \dot{\phi}_{f,1} & \phi_{r,1} & \dot{\phi}_{r,1} & \beta_1 & \dot{\psi}_1 & \phi_{t,f,1} & \phi_{t,r,1} & \phi_2 & \dot{\phi}_2 & \beta_2 & \dot{\psi}_2 & \phi_{t,r,2} & \delta/2 \end{bmatrix}^T. \tag{5.14}$$

The performance of this controller is examined in sections 5.5.2–5.5.5.

5.5.2 Steady-state cornering response

The response of the linear, torsionally flexible tractor semi-trailer with a full-state feedback controller to a steady-state steering input at 60 km/h is shown in figure 5.11.

Without active roll control, the vehicle rolls out of the corner. As with the rigid vehicle from section 5.4, the normalised load transfer builds up most quickly at the tractor drive axle and most slowly at the tractor steer axle, although this effect be-

comes more pronounced as torsional flexibility of the tractor frame increases. The drive axle lifts off at 0.41 g (point C), at which point the normalised load transfer is 0.67 at the tractor steer axle (point A) and is 0.85 at the semi-trailer axles (point B). As lateral acceleration continues to increase, the slopes of the suspension roll angle and normalised load transfer curves increase. The semi-trailer axles lift off at 0.46 g (point E), at which point the normalised load transfer at the steer axle is 0.76 (point F). Beyond this point, the steer axle is unable to stabilise the vehicle, and roll-over occurs. Comparing these results with those from figure 5.3, the torsional flexibility of the vehicle frame reduces the roll-over threshold by 3%.

With active roll control, the vehicle rolls into the corner. The total roll moment is distributed among the active anti-roll bars so that the normalised load transfers at all axles increase in a balanced fashion with lateral acceleration. This requires a relative roll angle of 4.0°/g between the front and rear sections of the tractor unit (with the front section rolling into the corner more than the rear) and a relative roll angle between the rear section of the tractor unit and the rear section of the semi-trailer of 1.2°/g (with the tractor rolling into the corner more than the semi-trailer). As the flexibilities of the tractor and semi-trailer frames increase, the relative roll angles required to balance the normalised load transfers also increase. The normalised load transfers at all axles reach the critical value of 1 simultaneously at 0.60 g (point F), at which point the maximum inward suspension roll angle is 4.0° at the tractor steer axle. This represents a 3% reduction in roll-over threshold compared to the torsionally rigid vehicle described in section 5.4.2.

Active roll control increases the roll-over threshold of the torsionally flexible tractor semi-trailer by 29% and the lateral acceleration at which axle lift-off first occurs by 45%. This is a significant improvement in steady-state roll stability. The achievable improvement in roll stability offered by active roll control is greater for the torsionally flexible vehicle than for the torsionally rigid vehicle in section 5.4.2. A similar trend for single unit vehicles was demonstrated in section 4.7.2.

5.5.3 Response to a step steering input

The response of the linear, torsionally flexible tractor semi-trailer model to a step steering input is shown in figure 5.12. The step input is scaled to give a maximum normalised load transfer of 1 in the following simulations and is therefore 3% smaller than the input to the torsionally rigid tractor semi-trailer in section 5.4.3 and figure 5.4. The lateral acceleration response is shown in figure 5.12(a). The steady-state lateral acceleration is 0.41 g.

The suspension roll angle responses are shown in figure 5.11(b). Without active roll control, the vehicle rolls out of the corner, with peak suspension roll angles of 3.7° at the tractor steer axle and 4.8° at the tractor drive and semi-trailer axles. The active roll control system causes the vehicle to roll into the corner, with peak suspension roll angles of 3.0° at the tractor steer axle, 1.6° at the tractor drive axle and 2.2° at the semi-trailer axles. The corresponding steady-state suspension roll angles are 2.8°, 0.9° and 1.4°. Although the *suspension* roll angle is greater at the semi-trailer axles than at the tractor drive axle, the *absolute* inward roll angle of the tractor's rear section is again actually greater than that of the semi-trailer, the difference being due to the higher stiffness of the tractor tyres.

The normalised load transfer responses are shown in figure 5.12(c). For the passive suspension, the normalised load transfer again builds up fastest at the tractor drive axle and slowest at the tractor steer axle. This trend becomes more apparent as the flexibility of the vehicle frame increases; that is, frame flexibility reduces the ability of the tractor steer axle, in particular, to carry its share of the total lateral load transfer. The normalised load transfer responses feature small overshoots before settling at final values of 0.67, 1.00 and 0.85 at the tractor steer, tractor drive and semi-trailer axles respectively. In addition to reducing the total lateral load transfer by rolling the vehicle units into the turn, the active roll control system redistributes the load transfer in a balanced fashion among the axles so that all show a peak normalised value of 0.69 at all axles. The system reduces the peak load transfer by 31% at the tractor drive axle and by 19% at the semi-trailer axles. The load transfer at the tractor steer axle remains

essentially unchanged. However, rather than indicating poor controller performance, this emphasises that the tractor steer axle carries much less than its fair share of the total load transfer in the passive case.

The steady-state results in section 5.5.2 show that, with passive suspension, the roll-over threshold for this vehicle is 12% higher than the lateral acceleration at which axle lift-off first occurs. However, with active roll control, the vehicle can remain stable with up to 45% additional lateral acceleration (that is, up to 0.60 g). This represents a significant improvement in roll stability. The peak inward suspension roll angle in response to such a critical manoeuvre is 4.3°, which is within the allowable limits.

The active anti-roll bar moment responses are shown in figure 5.12(d). The peak roll moment in response to a critical manoeuvre is 64 kN.m at the drive axle. The roll moment builds up most quickly at the tractor drive and semi-trailer axles to distribute the total load transfer evenly among the axles throughout the early part of this severe manoeuvre.

The peak flow rate in response to a critical step manoeuvre is 0.78 *l*/s (see figure 5.12(e)). The peak power supplied to the system in response to a critical step steering input, neglecting losses, is 6.9 kW.

5.5.4 Response to a double lane change steering input

The response of the linear, torsionally flexible tractor semi-trailer model to a double lane change steering input at 60 km/h is illustrated in figure 5.13. The path deviation over a 120 m test section is again 5.05 m for the tractor and 5.2 m for the semi-trailer. The peak lateral acceleration is 0.21 g (see figure 5.13(a)).

The suspension roll angle responses are shown in figure 5.13(b). The trends discussed in sections 5.5.2 and 5.5.3 are again apparent. Active roll control causes the vehicle to roll into the corners, with the tractor unit rolling more towards the inside than the semi-trailer.

The normalised load transfer responses are shown in figure 5.13(c). In the passive

case, the normalised load transfers are unbalanced, with the tractor drive axle bearing significantly more than its share of the total load transfer and the tractor steer axle bearing significantly less than its share. The peak load transfers are 0.28 at the tractor steer axle, 0.48 at the tractor drive axle and 0.43 at the semi-trailer axles. When equipped with the active roll control system, the normalised load transfer responses are better balanced, with peak values of 0.30 at all axles. The vehicle with active roll control could remain stable with up to 233% additional steering angle. Peak normalised load transfer is reduced by 39% at the tractor drive axle and 31% at the semi-trailer axles.

The peak inward roll angle at the semi-trailer axles in response to a critical double lane change steering input is 5.8°. This is within the available suspension travel.

Figure 5.13(d) illustrates that the largest active anti-roll moment for this manoeuvre is 22 kN.m at the tractor drive axle. The roll moment in response to a critical double lane change steering input is therefore 73 kN.m.

The peak flow rate through the servo-valves is 0.51 l/s at the tractor steer axle, as shown in figure 5.13(e). There is a substantial variation in the flow rates among the axles because, in order to balance the normalised load transfers, the active roll control system must oscillate different parts of the vehicle at different rates. The peak power supplied to the system during a critical double lane change, neglecting losses, is 25 kW.

5.5.5 Frequency response

Frequency response functions from steering input to suspension roll angles and normalised load transfers are shown in figures 5.14(a) and 5.14(b) respectively. The frequency responses again include the 4 rad/s pre-filter to represent the limited bandwidth of the driver.

The active roll control causes both the tractor and semi-trailer to roll into corners. The normalised load transfers are reduced throughout the majority of the frequency range shown.

5.5.6 Design of a partial-state feedback controller

A partial state feedback controller was designed using the LQG-LTR procedure. The controller uses measurements of the suspension roll angles at the tractor steer axle and the semi-trailer axles, the body roll rates of the tractor and semi-trailer, the yaw rates of the tractor and semi-trailer and the steering input,

$$y = \left[\begin{array}{cccccccc} \phi_{f,1} - \phi_{t,f,1} & \phi_{r,1} - \phi_{t,r,1} & \dot{\phi}_{r,1} & \dot{\psi}_1 & \phi_2 - \phi_{t,r,2} & \dot{\phi}_2 & \dot{\psi}_2 & \delta/2 \end{array} \right]^T. \quad (5.15)$$

This is one measurement more than for the torsionally rigid tractor semi-trailer in section 5.4.6: the suspension roll angles at *both* the tractor steer and tractor drive axles are now measured. The unmeasured states are the sideslip angles of the tractor and semi-trailer, the body roll rate at the front of the tractor unit and the load transfers at all axles. The Kalman filter measurement noise weighting matrix was chosen to be

$$W = \left[\begin{array}{cccccccc} 1.000 & 0 & 0 & 0 & 0 & 0 & 0 & 0 \\ 0 & 1.000 & 0 & 0 & 0 & 0 & 0 & 0 \\ 0 & 0 & 1.000 & 0 & 0 & 0 & 0 & 0 \\ 0 & 0 & 0 & 0.500 & 0 & 0 & 0 & 0 \\ 0 & 0 & 0 & 0 & 1.000 & 0 & 0 & 0 \\ 0 & 0 & 0 & 0 & 0 & 1.000 & 0 & 0 \\ 0 & 0 & 0 & 0 & 0 & 0 & 0.500 & 0 \\ 0 & 0 & 0 & 0 & 0 & 0 & 0 & 1.291 \end{array} \right]^T \begin{array}{l} \mathrm{rad}^{-2} \\ \mathrm{rad}^{-2}.\mathrm{s}^2 \\ \mathrm{rad}^{-2}.\mathrm{s}^2 \\ \mathrm{rad}^{-2}.\mathrm{s}^2 \\ \mathrm{rad}^{-2} \\ \mathrm{rad}^{-2}.\mathrm{s}^2 \\ \mathrm{rad}^{-2}.\mathrm{s}^2 \\ \mathrm{rad}^{-2} \end{array} \quad (5.16)$$

and the process noise weighting V was varied as a tuning parameter from 1 rad^{-2} to 0.001 rad^{-2}. The target feedback loop is that of the full-state feedback controller described in section 5.4.1.

Results of the loop transfer recovery procedure are again similar to those presented in section 4.6.6. As V is reduced, the frequency responses converge towards the target response.

The transient responses of several LQG-controlled designs to a step steering input are shown in figure 5.15. As V is reduced from 1 rad^{-2}, the load transfer performance of the system improves until, by $V = 0.001$ rad^{-2}, there is little difference in performance between the LQG-controlled and LQR-controlled systems. Random, uncorrelated white measurement noise of 5% RMS on each channel is again effectively attenuated. Clearly the improvements to roll stability offered by a full-state feedback controller are also available using a partial-state feedback controller.

5.5.7 Effect of actuator performance limitations

Figure 5.16 shows the effect of the limited active roll control system bandwidth on the response of the linear, torsionally flexible tractor semi-trailer model to a step steering input. The active roll control system was represented with a 0.5 Hz first order low-pass filter, and a new controller was synthesised to give the same steady-state performance as in section 5.5.2. The new Q and R matrices were

$$Q = \begin{bmatrix} 1.000 & 0 & 0 \\ 0 & 2.208 & 0 \\ 0 & 0 & 2.300 \end{bmatrix} \text{rad}^{-2}, \tag{5.17}$$

$$R = 9.295 \times 10^{-14} \begin{bmatrix} 1 & 0 & 0 \\ 0 & 1 & 0 \\ 0 & 0 & 1 \end{bmatrix} \text{N}^{-2}.\text{m}^{-2}. \tag{5.18}$$

Figures 5.16(a) and 5.16(b) show how limiting the bandwidth of the active roll control system increases the rise time of the suspension roll angle responses. The peak flow rates through the servo-valves are reduced by 14%, 8% and 11% at the tractor steer, tractor drive and semi-trailer axles respectively, as shown in figure 5.16(g). However the increases in peak normalised load transfer for this manoeuvre are negligible (see figures 5.16(c), 5.16(d) and 5.16(e)).

5.5.8 Stability robustness to vehicle parameter uncertainty

The effect of vehicle parameter uncertainty on the closed loop stability of the torsionally flexible tractor semi-trailer model is shown in figure 5.17.

The range of variation in vehicle parameters from the nominal values is as described in section 5.4.8. The nominal system poles, denoted by the symbol ($\circ$), are located at $-1.91 \pm j1.88$, $-6.74 \pm j2.72$, -2.80, -14.5, $-2.76 \pm j17.0$, $-8.85 \pm j51.6$, -222, -894, -919 and -4 rad/s. The mode shapes associated with these poles are similar to those described in section 5.4.8, for example, the poles at $-1.91 \pm j1.88$ and $-6.74 \pm j2.72$ rad/s are primarily associated with handling performance. The two lightly damped pairs of poles at $-2.76 \pm j17.0$ and $-8.85 \pm j51.6$ rad/s are associated with the torsional resonances of the tractor and semi-trailer frames respectively.

The closed loop poles of the system remain in the open left half plane for all combinations of possible parameter variations, so the system is robustly stable in the presence of model uncertainty.

5.5.9 Effect on handling performance

The effect of active roll control on the handling performance of the torsionally flexible tractor semi-trailer model at 60 km/h is shown in figure 5.18. The handling responses of both the tractor and semi-trailer are included on the figure because, as outlined in section 5.4.9, the yaw stability of the combination is determined by the handling characteristics of both vehicle units.

First, consider the response of the vehicle without active roll control. At low levels of lateral acceleration, the tractor unit understeers mildly. As lateral acceleration increases, the normalised load transfer builds up more quickly at the drive axle than at the steer axle, an effect that is accentuated by reducing the torsional rigidity of the tractor frame. The handling balance of the tractor changes to mild oversteer by 0.2 g. The tractor oversteers with increasing severity as lateral acceleration builds up. From the results quoted in section 5.4.9, yaw stability will be lost at high speed and high

lateral acceleration if both the tractor and semi-trailer are oversteering.

Despite the presence of torsional flexibility in the tractor and semi-trailer frames and in the fifth wheel coupling, the active roll control system balances the build up of normalised load transfer evenly between all the axles. Therefore, the handling performance of the torsionally flexible tractor semi-trailer with active roll control is similar to that of the torsionally rigid active vehicle described in section 5.4.9. The active roll control system causes the understeer gradient of the tractor to increase with lateral acceleration and also reduces the severity of oversteer at the semi-trailer. As long as the tractor unit understeers, the combination cannot be unstable in yaw. Therefore, the active roll control system significantly increases yaw stability at high levels of lateral acceleration.

5.6 Conclusions

1. Active roll control of a tractor semi-trailer, like active roll control of a single unit vehicle, is a problem of optimal disturbance rejection system design. Therefore, the same control system design techniques are appropriate in both cases.

2. Simulations show that active roll control can increase the roll-over threshold of a torsionally rigid tractor semi-trailer by 29%. Such an improvement in roll stability represents a significant increase in vehicle safety.

3. Without active roll control, the roll-over threshold of a tractor semi-trailer decreases significantly with increasing torsional flexibility of the tractor and semi-trailer frames. However, with active roll control, this sensitivity of achievable roll stability to torsional flexibility is reduced. Simulations show that active roll control can increase the roll-over threshold of a typical torsionally flexible tractor semi-trailer by 29%.

4. A partial-state LQG feedback controller, using measurements of suspension roll angles, body roll rates and body yaw rates at both the tractor and semi-trailer,

in addition to the steering input, is a practical controller design that can significantly improve the roll stability of a tractor semi-trailer. The loop transfer recovery design procedure can be used to synthesise a robust controller that also features favourable measurement noise attenuation characteristics.

5. The actuator forces and hydraulic fluid flow rates required for good performance are again achievable using practical, reasonably priced hardware.

6. The yaw stability of a tractor semi-trailer depends on the levels of understeer or oversteer at both the tractor and semi-trailer. By distributing the total normalised load transfer among all axles in a balanced fashion, active roll control tends to increase understeer for both units of a typical tractor semi-trailer, thus increasing yaw stability.

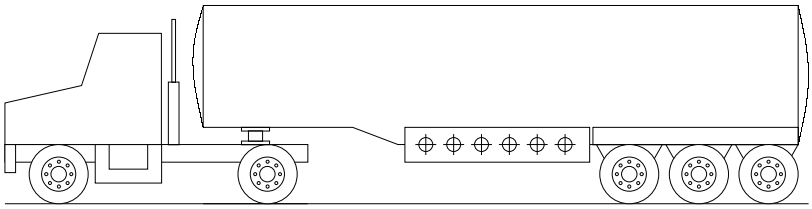

Figure 5.1: Tractor semi-trailer combination.

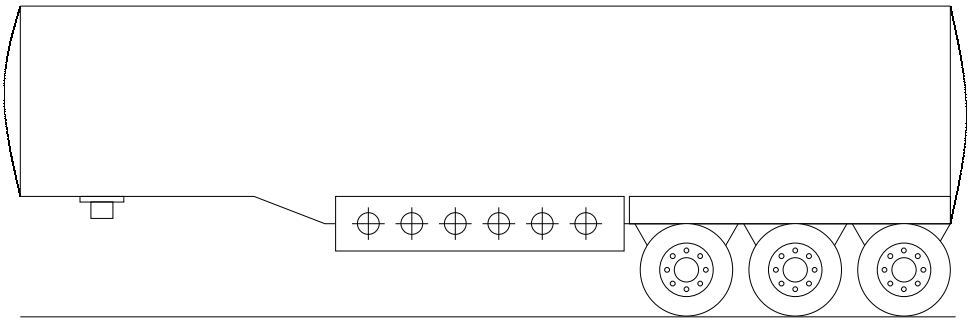

(a) Schematic.

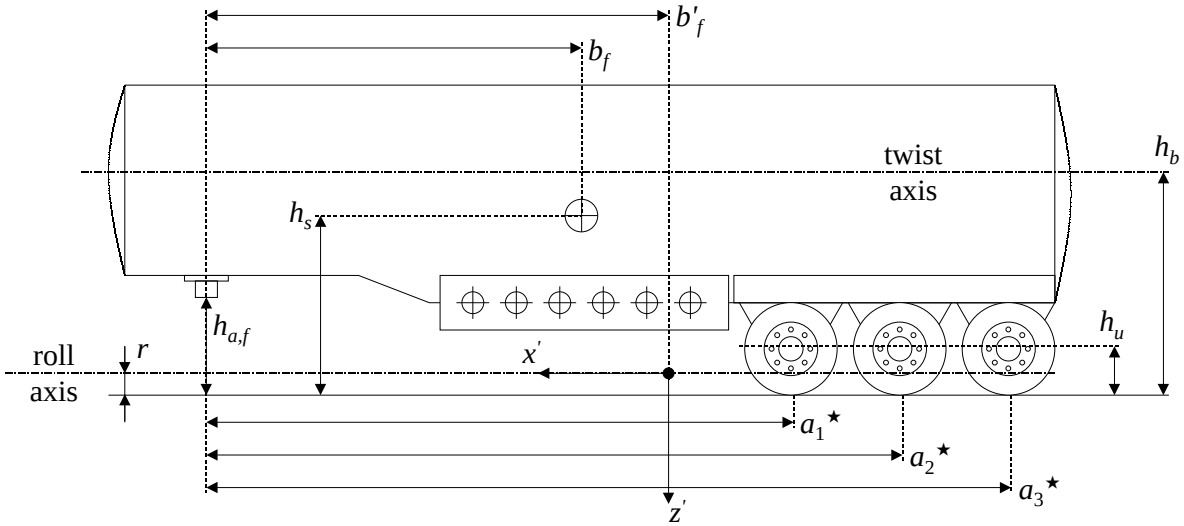

(b) Dimensions.

Figure 5.2: Semi-trailer.

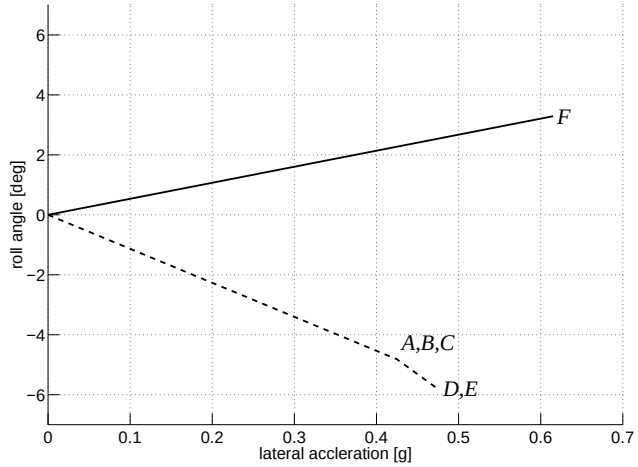

(a) Suspension roll angles. Active roll control: *semi-trailer axles (——)*; passive suspension: *steer axle (– – –).*

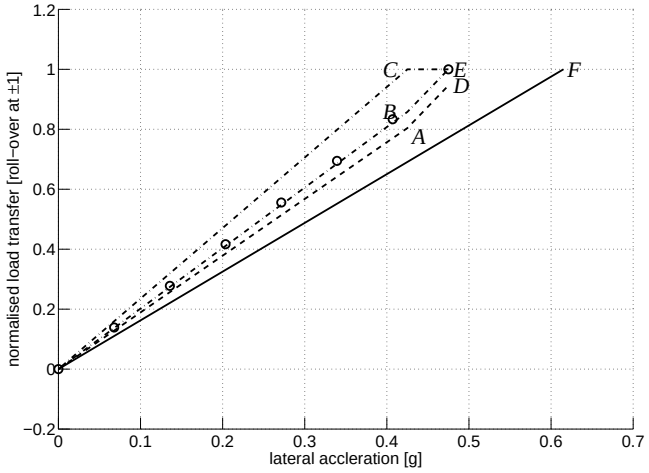

(b) Normalised load transfers. Active roll control: *steer axle, drive axle and semi-trailer axles (——)*; passive suspension: *steer axle (– – –), drive axle (· – · – ·) and semi-trailer axles (· – ○ – ·).*

Figure 5.3: Response of the linear, torsionally rigid tractor semi-trailer model with a full-state feedback controller to a steady-state steering input.

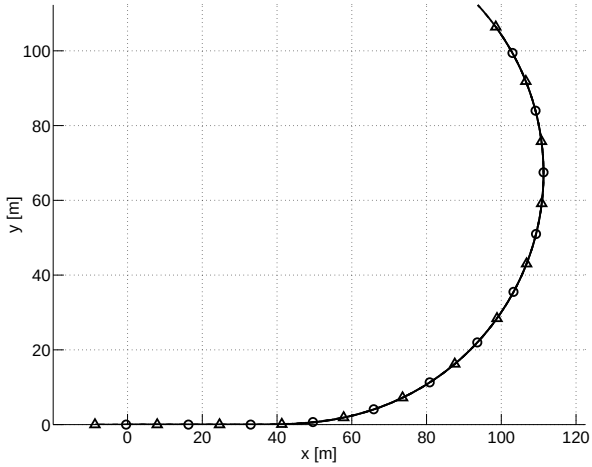

(a) Trajectories. Active roll control: *tractor (——), semi-trailer (—△—)*; passive suspension: *tractor (· – · – ·), semi-trailer (· – ○ – ·).*

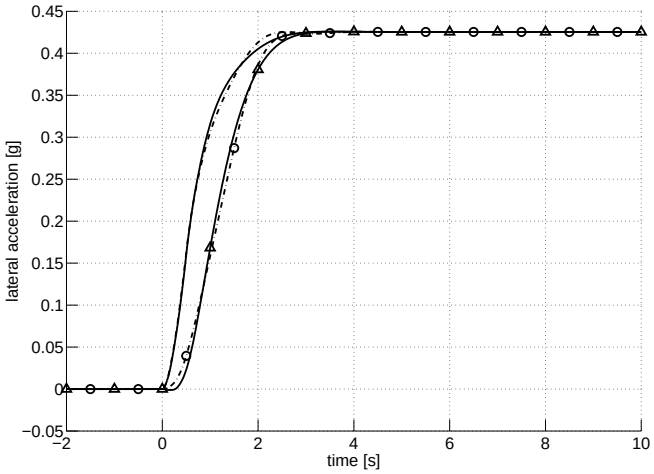

(b) Lateral accelerations. Active roll control: *tractor (——), semi-trailer (—△—)*; passive suspension: *tractor (· – · – ·), semi-trailer (· – ○ – ·).*

Figure 5.4: Response of the linear, torsionally rigid tractor semi-trailer model with a full-state feedback controller to a step steering input.

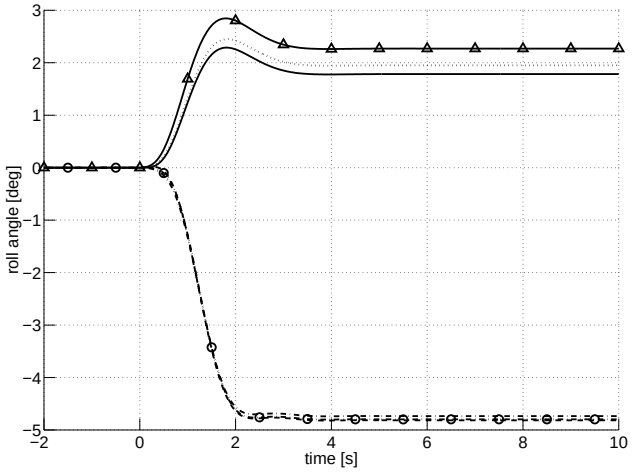

(c) Suspension roll angles. Active roll control: *steer axle (· · · · · ·), drive axle (——), semi-trailer axles (—△—)*; passive suspension: *steer axle (– – –), drive axle (· – · – ·), semi-trailer axles (· – ○ – ·).*

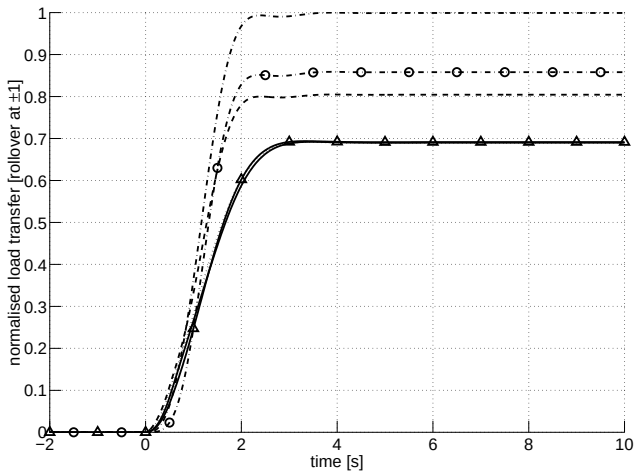

(d) Normalised load transfers. Active roll control: *steer axle (· · · · · ·), drive axle (——), semi-trailer axles (—△—)*; passive suspension: *steer axle (– – –), drive axle (· – · – ·), semi-trailer axles (· – ○ – ·).*

Figure 5.4: Continued.

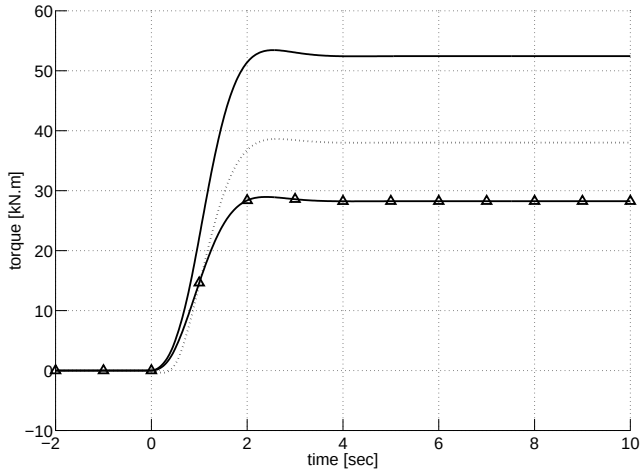

(e) Active anti-roll bar moments. Active roll control: *steer axle (· · · · · ·), drive axle (——), semi-trailer axles (—△—).*

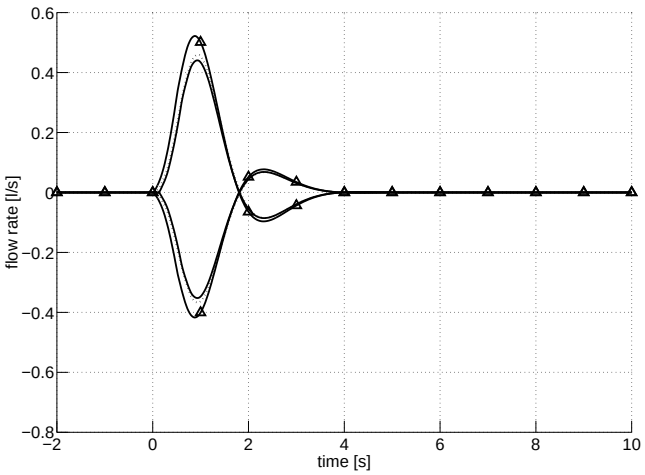

(f) Servo-valve flow rates. Active roll control: *steer axle (· · · · · ·), drive axle (——), semi-trailer axles (—△—).*

Figure 5.4: Continued.

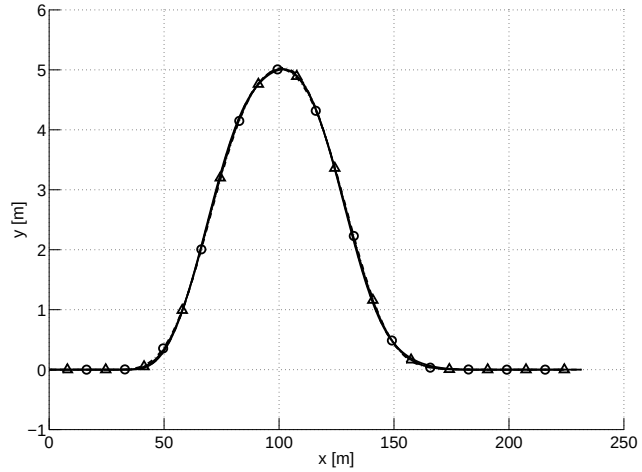

(a) Trajectories. Active roll control: *tractor (——), semi-trailer (—△—)*; passive suspension: *tractor (· – · – ·), semi-trailer (· – ○ – ·).*

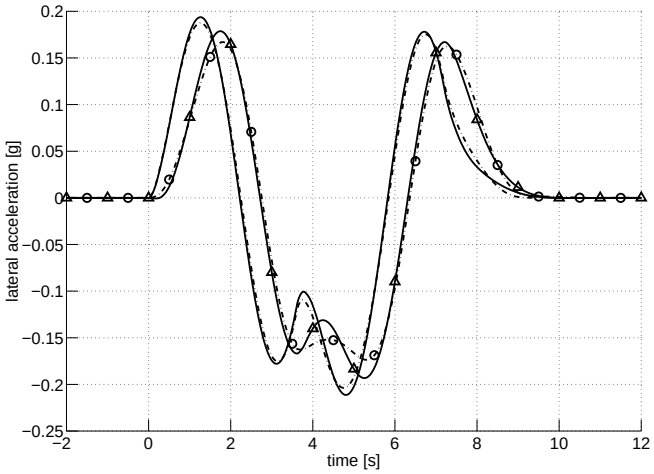

(b) Lateral accelerations. Active roll control: *tractor (——), semi-trailer (—△—)*; passive suspension: *tractor (· – · – ·), semi-trailer (· – ○ – ·).*

Figure 5.5: Response of the linear, torsionally rigid tractor semi-trailer model with a full-state feedback controller to a double lane change steering input.

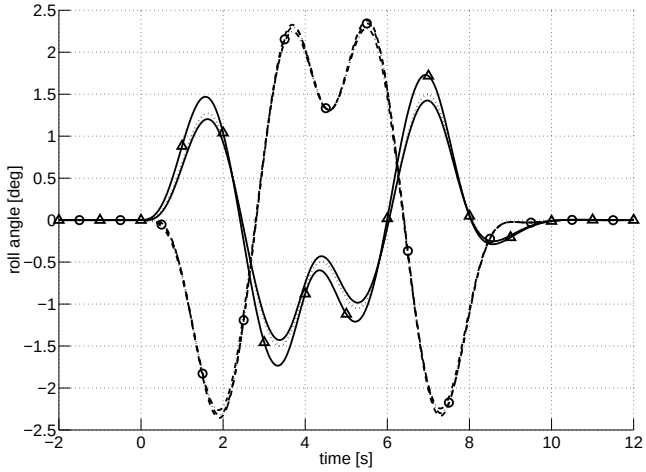

(c) Suspension roll angles. Active roll control: *steer axle (· · · · · ·), drive axle (——), semi-trailer axles (—△—)*; passive suspension: *steer axle (– – –), drive axle (· – · – ·), semi-trailer axles (· – ○ – ·).*

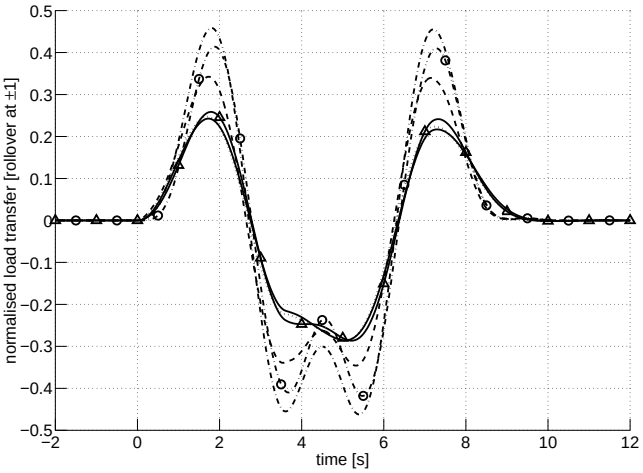

(d) Normalised load transfers. Active roll control: *steer axle (· · · · · ·), drive axle (——), semi-trailer axles (—△—)*; passive suspension: *steer axle (– – –), drive axle (· – · – ·), semi-trailer axles (· – ○ – ·).*

Figure 5.5: Continued.

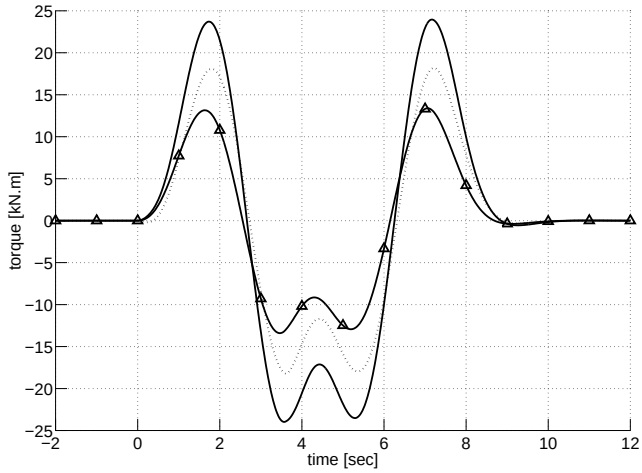

(e) Active anti-roll bar moments. Active roll control: *steer axle (· · · · · ·), drive axle (——), semi-trailer axles(—△—).*

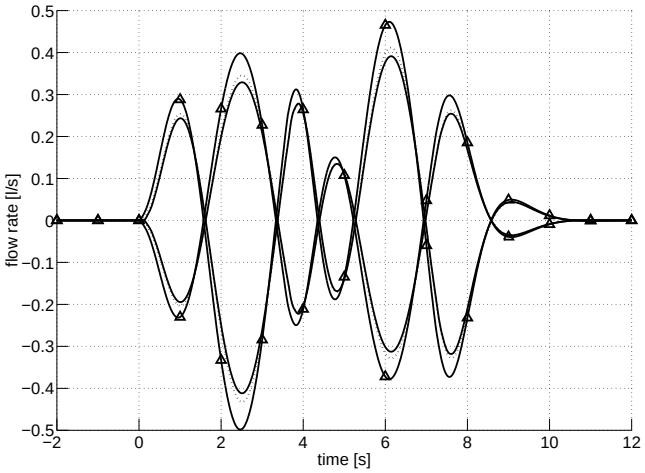

(f) Servo-valve flow rates. Active roll control: *steer axle (· · · · · ·), drive axle (——), semi-trailer axles (—△—).*

Figure 5.5: Continued.

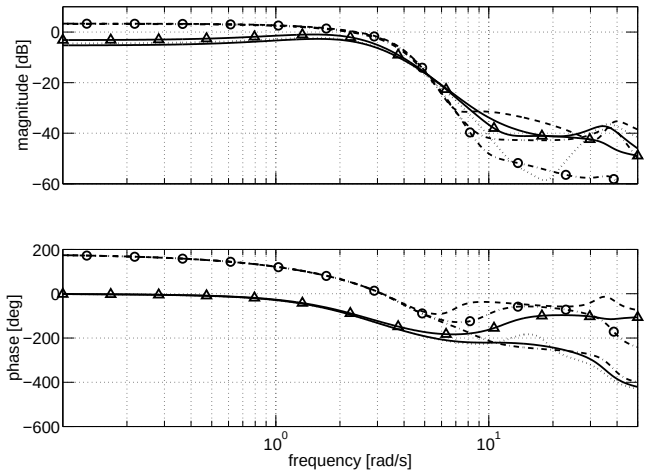

(a) From steering input [deg] to suspension roll angles [deg]. Active roll control: *steer axle (· · · · · ·), drive axle (——), semi-trailer axles (—△—)*; passive suspension: *steer axle (– – –), drive axle (· – · – ·), semi-trailer axles (· – ○ – ·).*

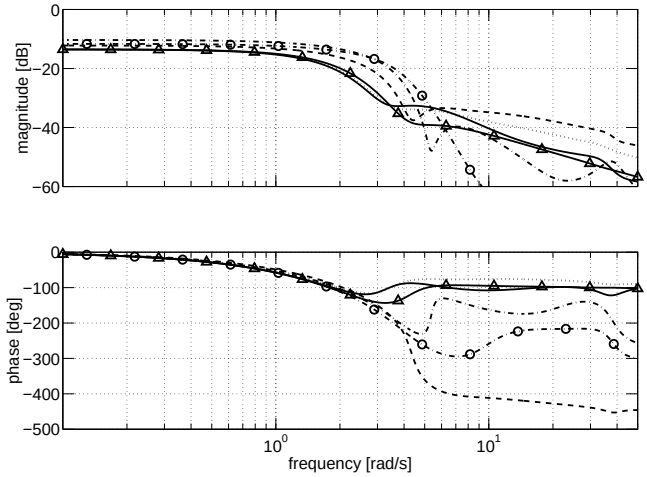

(b) From steering input [deg] to normalised load transfers [roll-over at ± 1]. Active roll control: *steer axle (· · · · · ·), drive axle (——), semi-trailer axles (—△—)*; passive suspension: *steer axle (– – –), drive axle (· – · – ·), semi-trailer axles (· – ○ – ·).*

Figure 5.6: Frequency response of the linear, torsionally rigid tractor semi-trailer model with a full-state feedback controller.

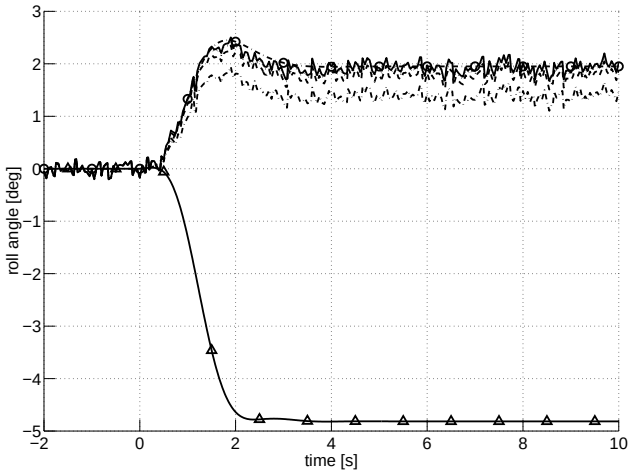

(a) Steer axle suspension roll angle [deg]. Partial-state feedback control: $V = 0.001$ (——), *0.01* (· · · · · ·), *0.1* (– – –), *1* (· – · – ·); full-state feedback control: (· – ○ – ·); *passive control:* (—△—).

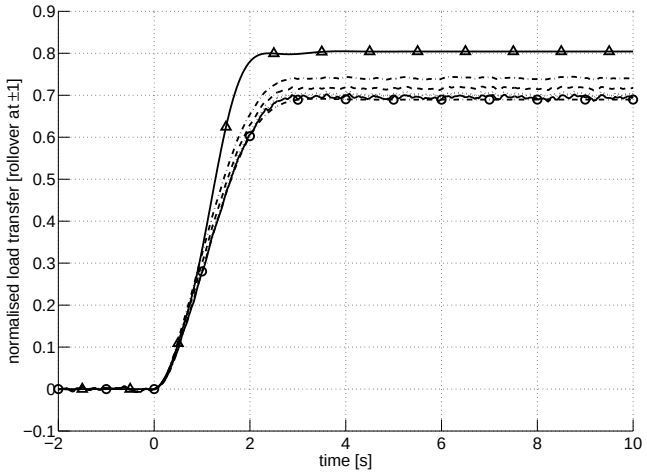

(b) Normalised steer axle load transfer. Partial-state feedback control: $V = 0.001$ (——), *0.01* (· · · · · ·), *0.1* (– – –), *1* (· – · – ·); full-state feedback control: (· – ○ – ·); *passive control:* (—△—).

Figure 5.7: Variation with Kalman filter design weights of the response of the linear, torsionally rigid tractor semi-trailer model with a partial-state feedback controller.

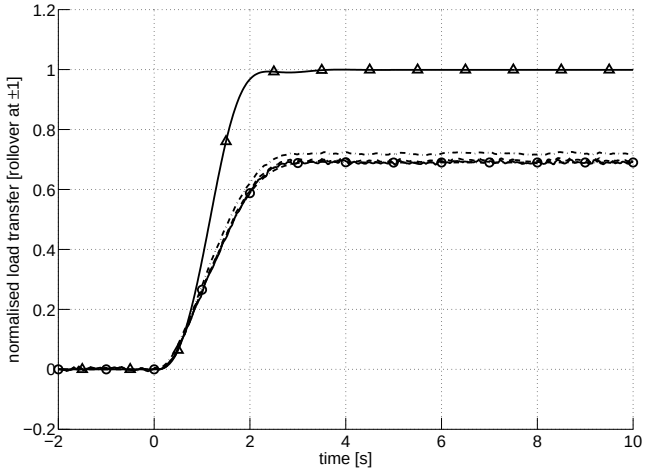

(c) Normalised drive axle load transfer. Partial-state feedback control: $V = 0.001$ (——), *0.01* (· · · · · ·), *0.1* (– – –), *1* (· – · – ·); full-state feedback control: (· – ○ – ·); *passive control:* (—△—).

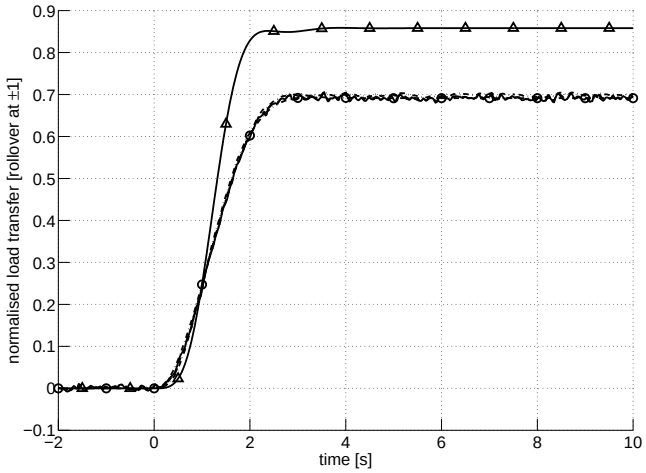

(d) Normalised semi-trailer axle load transfer. Partial-state feedback control: $V = 0.001$ (——), *0.01* (· · · · · ·), *0.1* (– – –), *1* (· – · – ·); full-state feedback control: (· – ○ – ·); *passive control:* (—△—).

Figure 5.7: Continued.

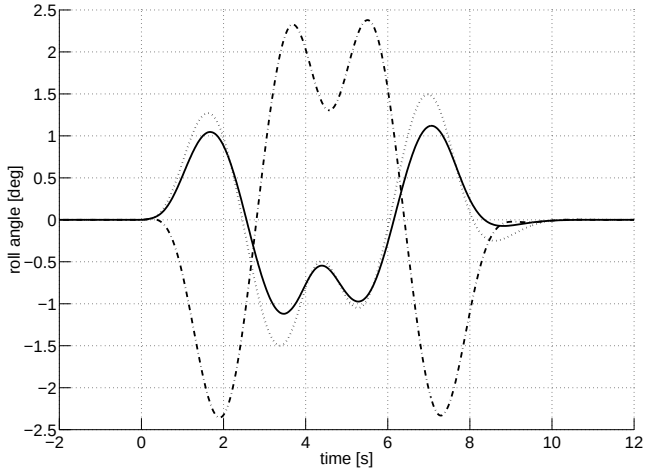

(a) Steer axle suspension roll angle. Full-state feedback control: ∞ *bandwidth (· · · · · ·), 0.5 Hz bandwidth (——); passive control: (· – · – ·).*

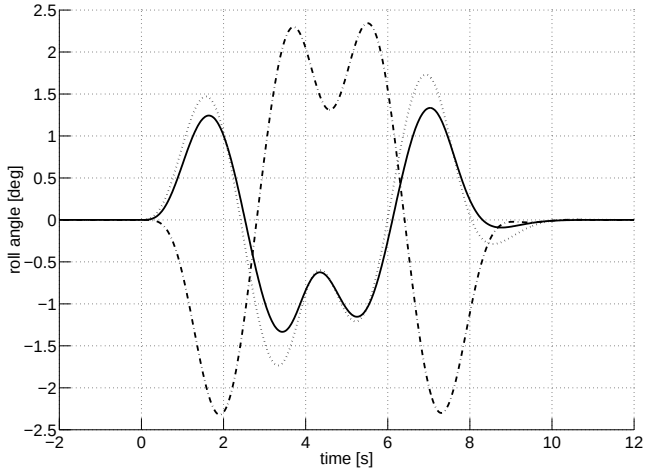

(b) Semi-trailer axle suspension roll angle. Full-state feedback control: ∞ *bandwidth (· · · · · ·), 0.5 Hz bandwidth (——); passive control: (· – · – ·).*

Figure 5.8: Effect of limited actuator bandwidth on the response of the linear, torsionally rigid tractor semi-trailer model with a full-state feedback controller to a double lane change steering input.

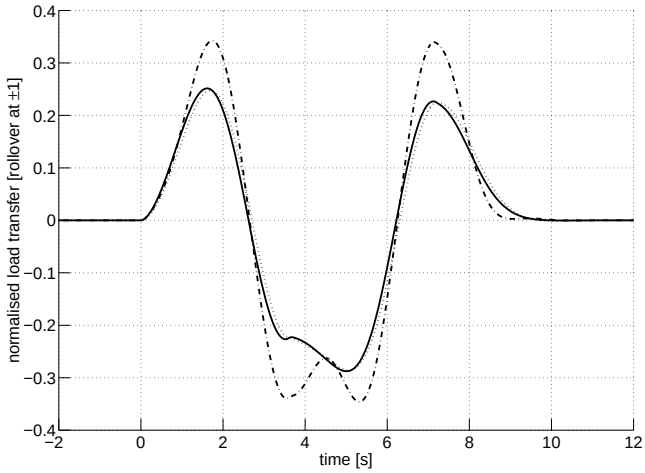

(c) Normalised steer axle load transfer. Full-state feedback control: ∞ *bandwidth (· · · · · ·), 0.5 Hz bandwidth (——); passive control: (· – · – ·).*

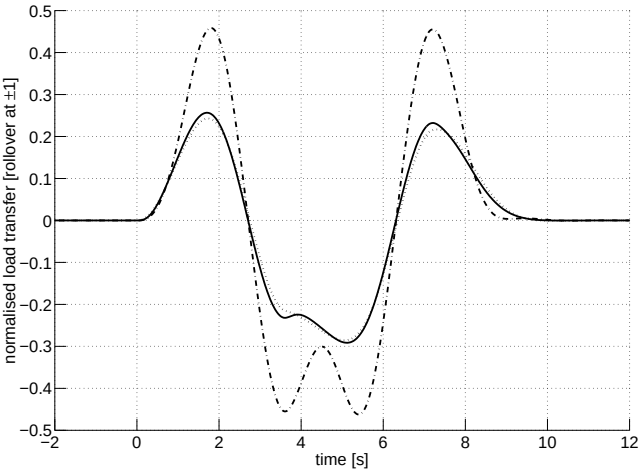

(d) Normalised drive axle load transfer. Full-state feedback control: ∞ *bandwidth (· · · · · ·), 0.5 Hz bandwidth (——); passive control: (· – · – ·).*

Figure 5.8: Continued.

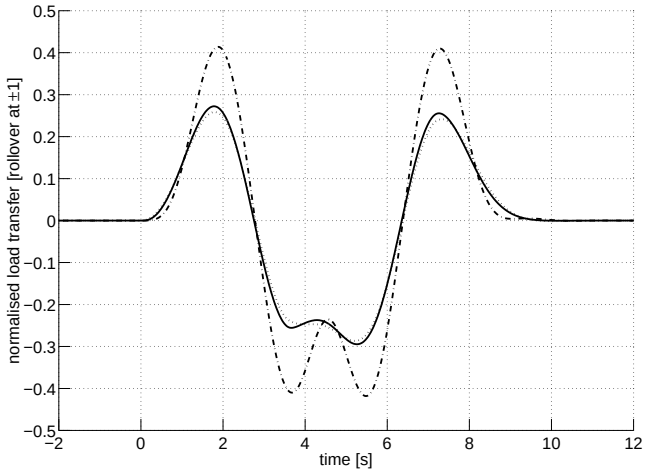

(e) Normalised semi-trailer axle load transfer. Full-state feedback control: ∞ *bandwidth (· · · · · ·), 0.5 Hz bandwidth (——); passive control: (· – · – ·).*

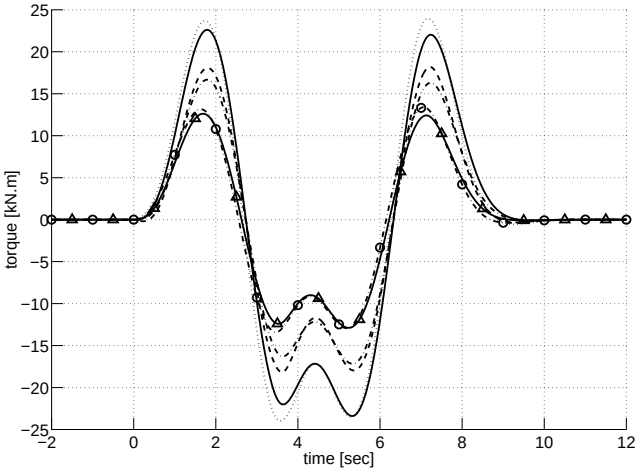

(f) Active anti-roll bar moments. ∞ bandwidth: *steer axle (· · · · · ·), drive axle (– – –), semi-trailer axles (· – ○ – ·)*; 0.5 Hz bandwidth: *steer axle (——), drive axle (· – · – ·), semi-trailer axles (—△—).*

Figure 5.8: Continued.

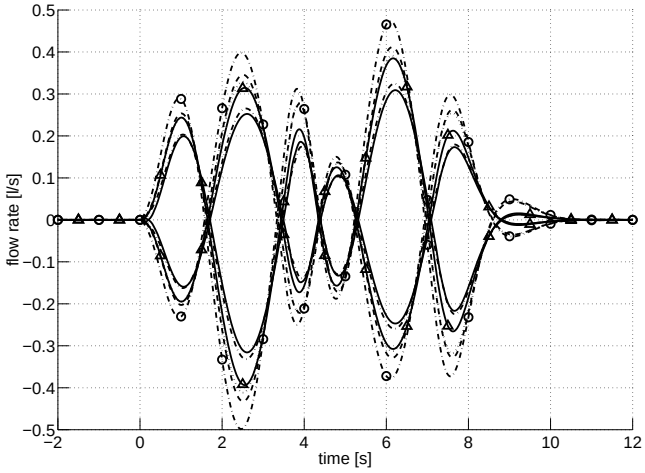

(g) Servo-valve flow rates. ∞ bandwidth: *steer axle (· · · · · ·), drive axle (– – –), semi-trailer axles (· – ○ – ·)*; 0.5 Hz bandwidth: *steer axle (——), drive axle (· – · – ·), semi-trailer axles (—△—).*

Figure 5.8: Continued.

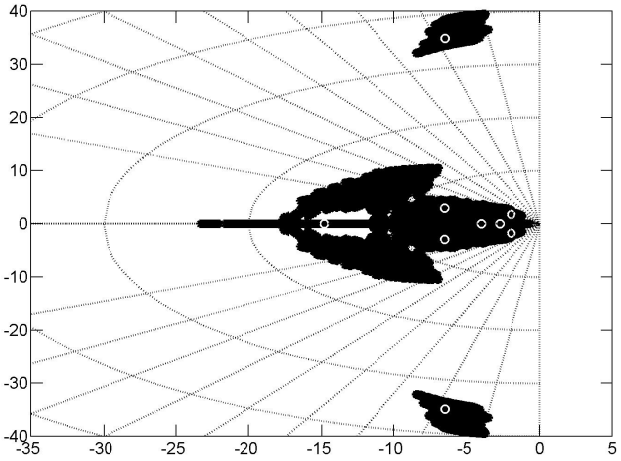

Figure 5.9: Variation with selected vehicle parameters of the closed-loop poles of the torsionally rigid tractor semi-trailer with a full-state feedback controller.

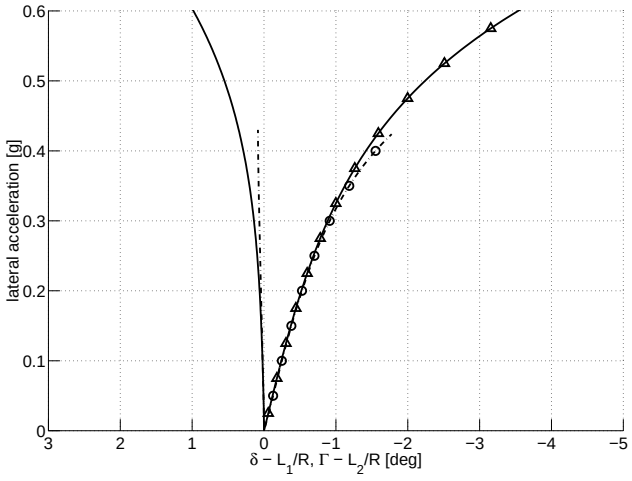

Active roll control: *tractor (——)*, *semi-trailer (—△—)*; passive suspension: *tractor (· – · – ·)*, *semi-trailer (· – ○ – ·).*

Figure 5.10: Handling diagram of the torsionally rigid tractor semi-trailer with a full-state feedback controller.

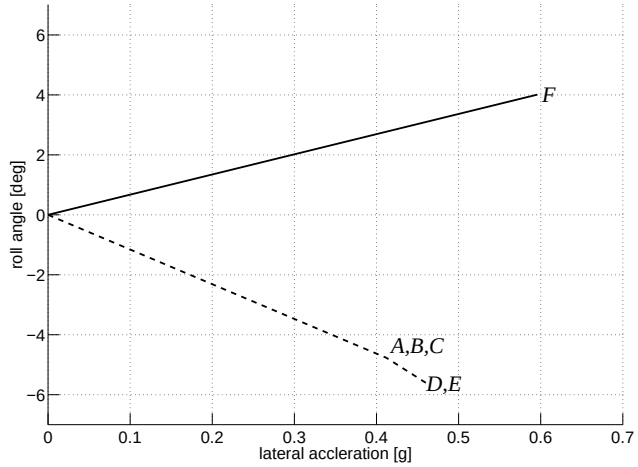

(a) Suspension roll angles. Active roll control: *steer axle (——)*; passive suspension: *semi-trailer axles (– – –).*

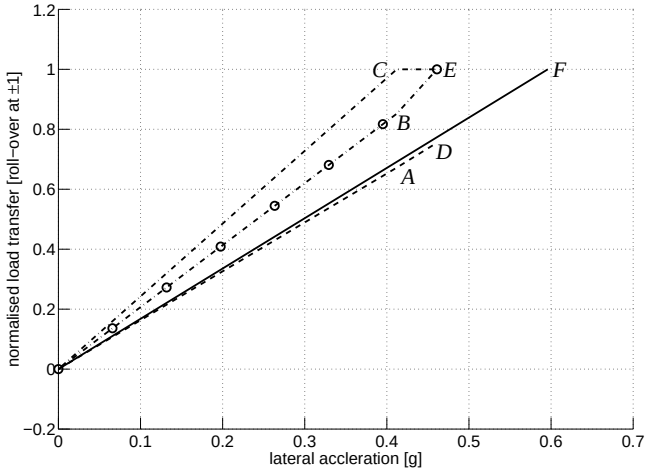

(b) Normalised load transfers. Active roll control: *steer axle, drive axle and semi-trailer axles (——)*; passive suspension: *steer axle (– – –), drive axle (· – · – ·) and semi-trailer axles (· – ○ – ·).*

Figure 5.11: Response of the linear, torsionally flexible tractor semi-trailer model with a full-state feedback controller to a steady-state steering input.

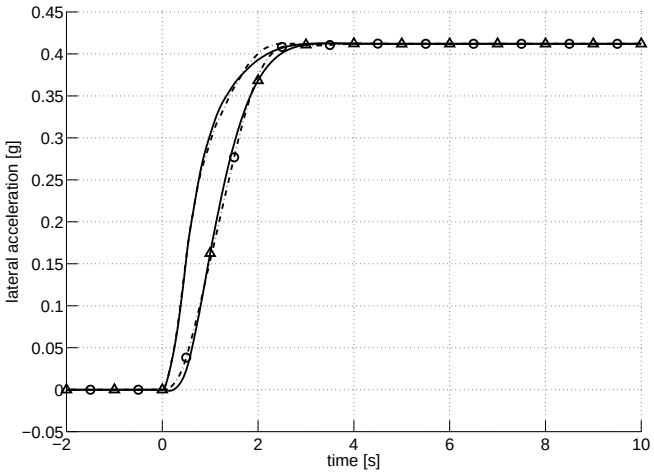

(a) Lateral accelerations. Active roll control: *tractor (——), semi-trailer (—△—)*; passive suspension: *tractor (· – · – ·), semi-trailer (· – ○ – ·).*

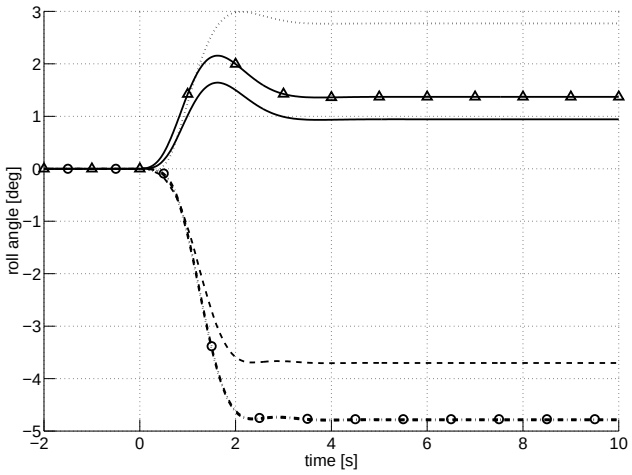

(b) Suspension roll angles. Active roll control: *steer axle (· · · · · ·), drive axle (——), semi-trailer axles (—△—)*; passive suspension: *steer axle (– – –), drive axle (· – · – ·), semi-trailer axles (· – ○ – ·).*

Figure 5.12: Response of the linear, torsionally flexible tractor semi-trailer model with a full-state feedback controller to a step steering input.

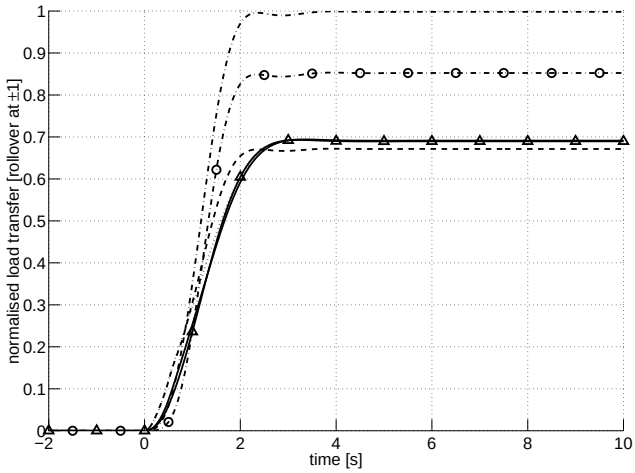

(c) Normalised load transfers. Active roll control: *steer axle (· · · · · ·), drive axle (——), semi-trailer axles (—△—)*; passive suspension: *steer axle (– – –), drive axle (· – · – ·), semi-trailer axles (· – ○ – ·).*

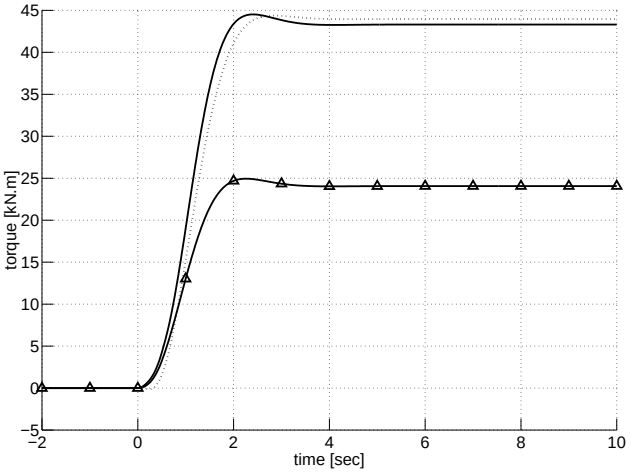

(d) Active anti-roll bar moments. Active roll control: *steer axle (· · · · · ·), drive axle (——), semi-trailer axles (—△—).*

Figure 5.12: Continued.

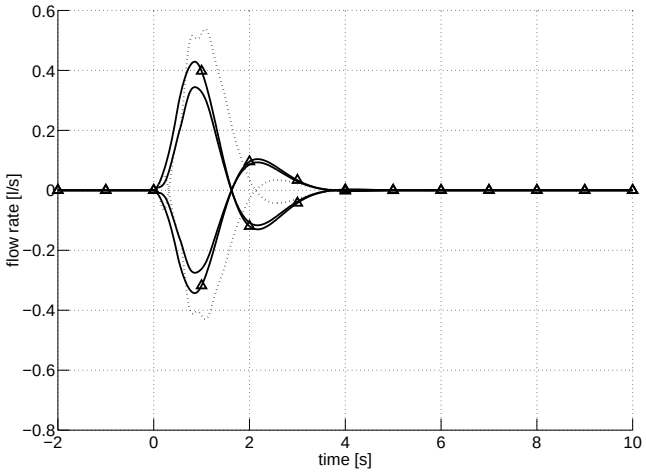

(e) Servo-valve flow rates. Active roll control: *steer axle (· · · · · ·), drive axle (——), semi-trailer axles (—△—).*

Figure 5.12: Continued.

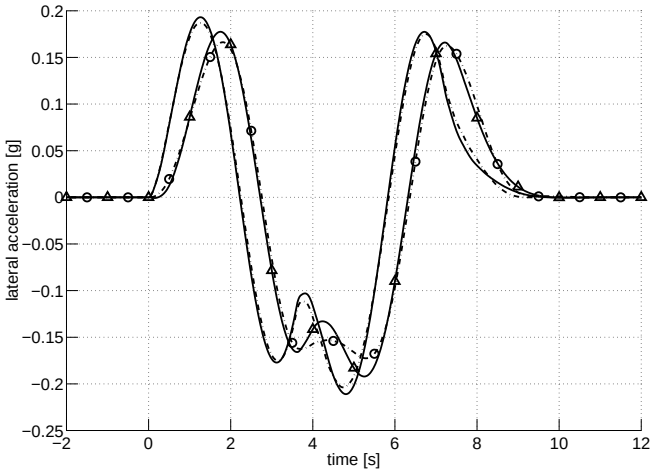

(a) Lateral accelerations. Active roll control: *tractor (——), semi-trailer (—△—)*; passive suspension: *tractor (· – · – ·), semi-trailer (· – ○ – ·).*

Figure 5.13: Response of the linear, torsionally flexible tractor semi-trailer model with a full-state feedback controller to a double lane change steering input.

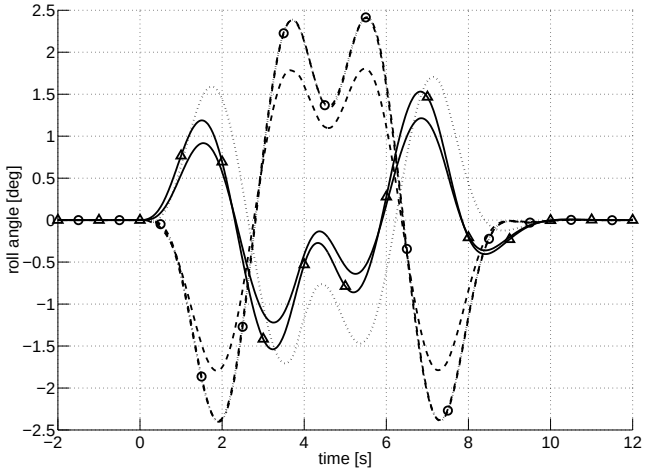

(b) Suspension roll angles. Active roll control: *steer axle (· · · · · ·), drive axle (——), semi-trailer axles (—△—)*; passive suspension: *steer axle (– – –), drive axle (· – · – ·), semi-trailer axles (· – ○ – ·).*

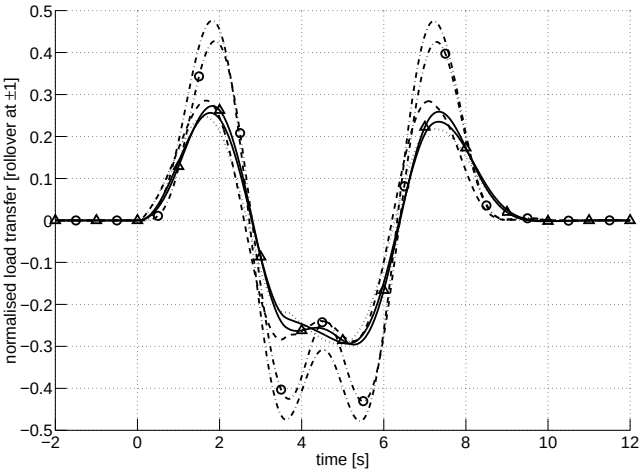

(c) Normalised load transfers. Active roll control: *steer axle (· · · · · ·), drive axle (——), semi-trailer axles (—△—)*; passive suspension: *steer axle (– – –), drive axle (· – · – ·), semi-trailer axles (· – ○ – ·).*

Figure 5.13: Continued.

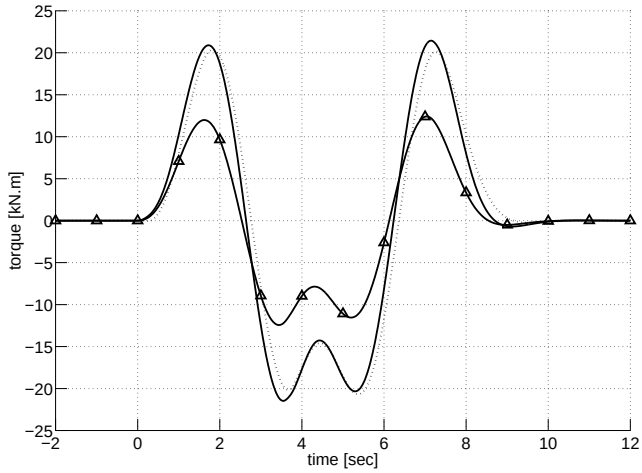

(d) Active anti-roll bar moments. Active roll control: *steer axle (· · · · · ·), drive axle (——), semi-trailer axles(—△—).*

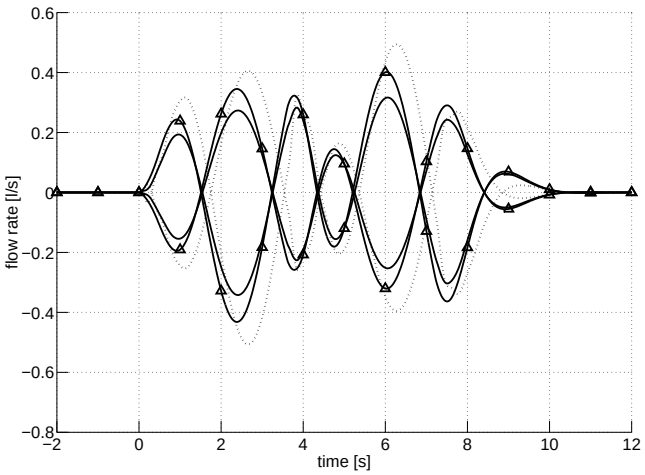

(e) Servo-valve flow rates. Active roll control: *steer axle (· · · · · ·), drive axle (——), semi-trailer axles (—△—).*

Figure 5.13: Continued.

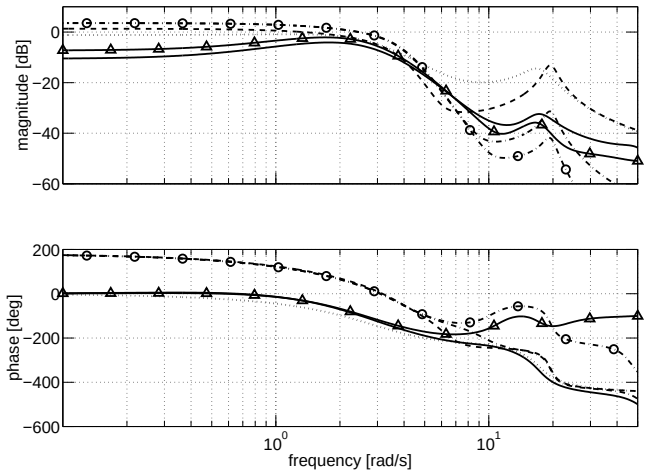

(a) From steering input [deg] to suspension roll angles [deg]. Active roll control: *steer axle (· · · · · ·), drive axle (——), semi-trailer axles (—△—)*; passive suspension: *steer axle (– – –), drive axle (· – · – ·), semi-trailer axles (· – ○ – ·).*

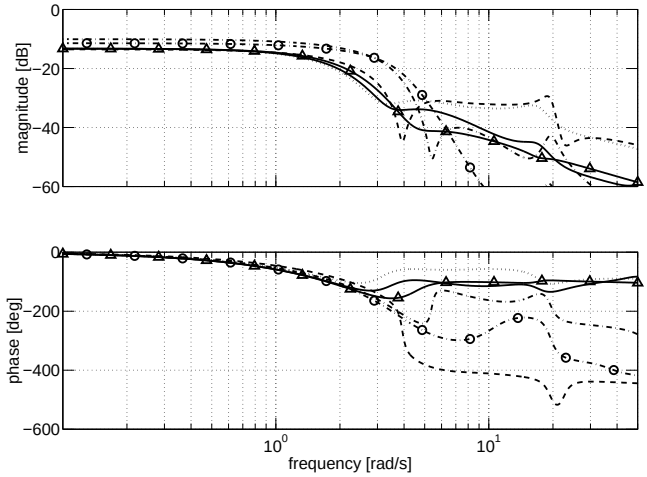

(b) From steering input [deg] to normalised load transfers [roll-over at ±1]. Active roll control: *steer axle (· · · · · ·), drive axle (——), semi-trailer axles (—△—)*; passive suspension: *steer axle (– – –), drive axle (· – · – ·), semi-trailer axles (· – ○ – ·).*

Figure 5.14: Frequency response of the linear, torsionally flexible tractor semi-trailer model with a full-state feedback controller.

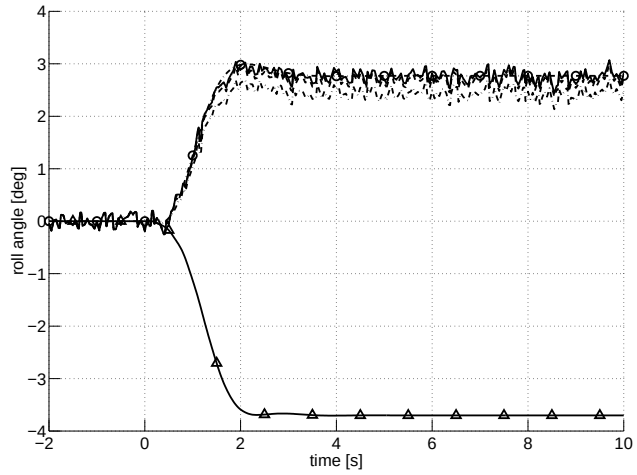

(a) Steer axle suspension roll angle [deg]. Partial-state feedback control: $V = 0.001$ (——), *0.01* (· · · · · ·), *0.1* (– – –), *1* (· – · – ·); full-state feedback control: (· – ○ – ·); *passive control:* (—△—).

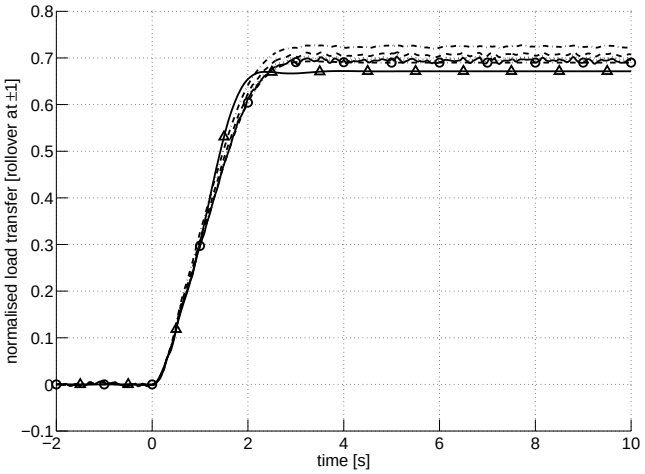

(b) Normalised steer axle load transfer. Partial-state feedback control: $V = 0.001$ (——), *0.01* (· · · · · ·), *0.1* (– – –), *1* (· – · – ·); full-state feedback control: (· – ○ – ·); *passive control:* (—△—).

Figure 5.15: Variation with Kalman filter design weights of the response of the linear, torsionally flexible tractor semi-trailer model with a partial-state feedback controller.

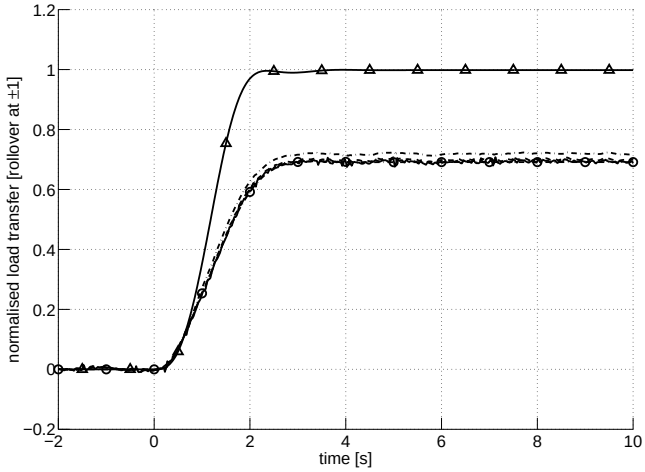

(c) Normalised drive axle load transfer. Partial-state feedback control: $V = 0.001$ (——), *0.01* (· · · · · ·), *0.1* (– – –), *1* (· – · – ·); full-state feedback control: (· – ○ – ·); *passive control:* (—△—).

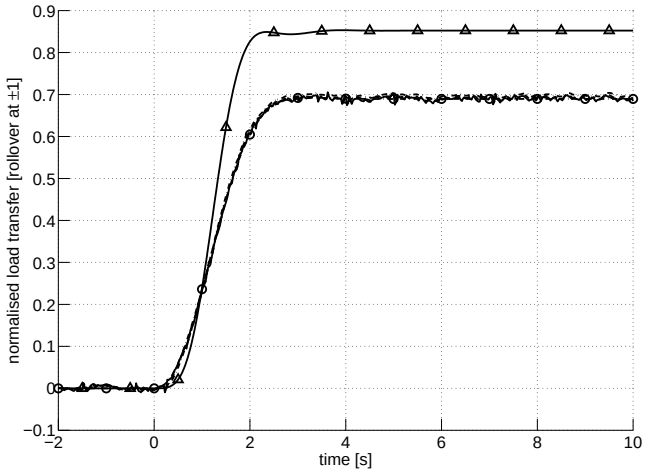

(d) Normalised semi-trailer axle load transfer. Partial-state feedback control: $V = 0.001$ (——), *0.01* (· · · · · ·), *0.1* (– – –), *1* (· – · – ·); full-state feedback control: (· – ○ – ·); *passive control:* (—△—).

Figure 5.15: Continued.

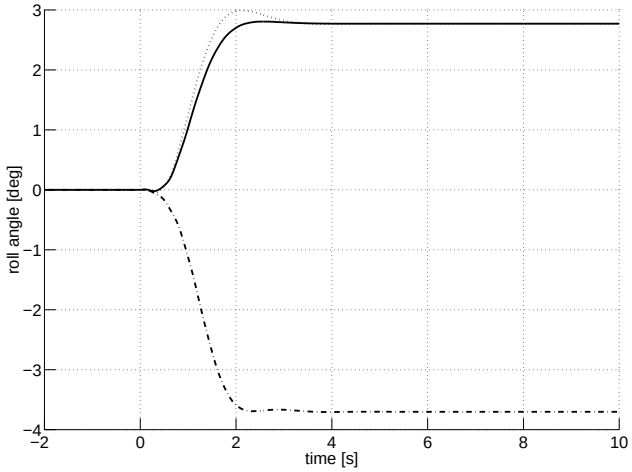

(a) Steer axle suspension roll angle. Full-state feedback control: ∞ *bandwidth (· · · · · ·), 0.5 Hz bandwidth (——); passive control: (· – · – ·).*

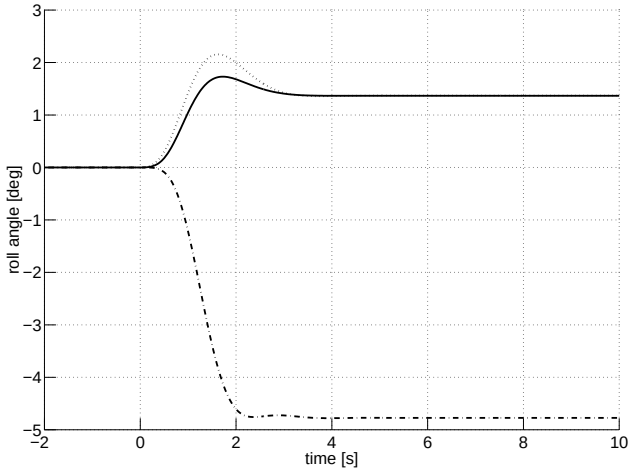

(b) Semi-trailer axle suspension roll angle. Full-state feedback control: ∞ *bandwidth (· · · · · ·), 0.5 Hz bandwidth (——); passive control: (· – · – ·).*

Figure 5.16: Effect of limited actuator bandwidth on the response of the linear, torsionally flexible tractor semi-trailer model with a full-state feedback controller to a double lane change steering input.

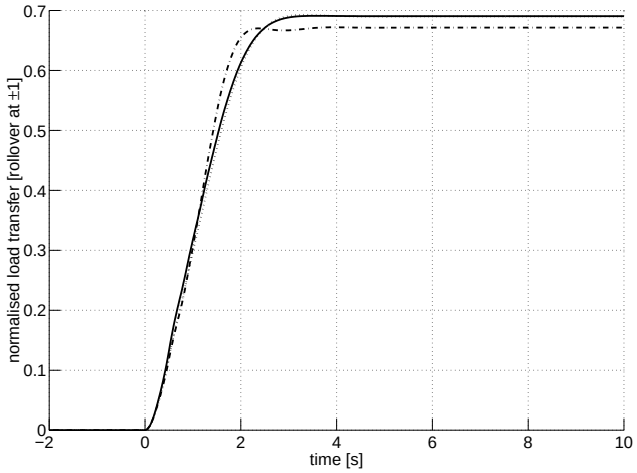

(c) Normalised steer axle load transfer. Full-state feedback control: ∞ *bandwidth (· · · · · ·), 0.5 Hz bandwidth (——); passive control: (· – · – ·).*

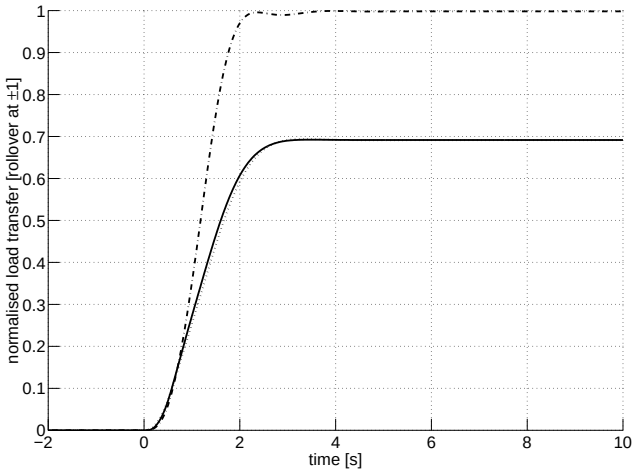

(d) Normalised drive axle load transfer. Full-state feedback control: ∞ *bandwidth (· · · · · ·), 0.5 Hz bandwidth (——); passive control: (· – · – ·).*

Figure 5.16: Continued.

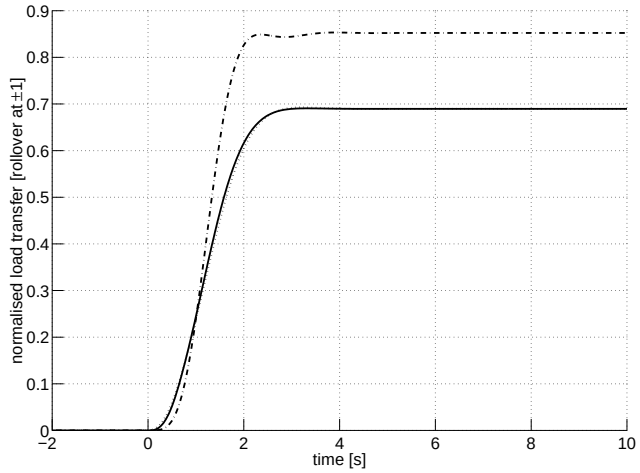

(e) Normalised semi-trailer axle load transfer. Full-state feedback control: ∞ *bandwidth (· · · · · ·), 0.5 Hz bandwidth (——); passive control: (· – · – ·).*

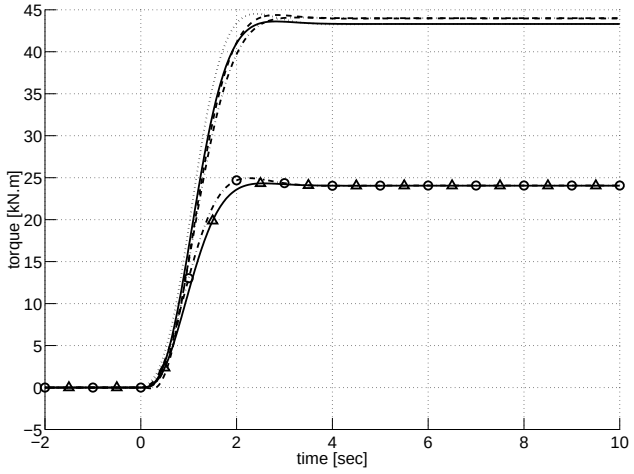

(f) Active anti-roll bar moments. ∞ bandwidth: *steer axle (· · · · · ·), drive axle (– – –), semi-trailer axles (· – ○ – ·)*; 0.5 Hz bandwidth: *steer axle (——), drive axle (· – · – ·), semi-trailer axles (—△—).*

Figure 5.16: Continued.

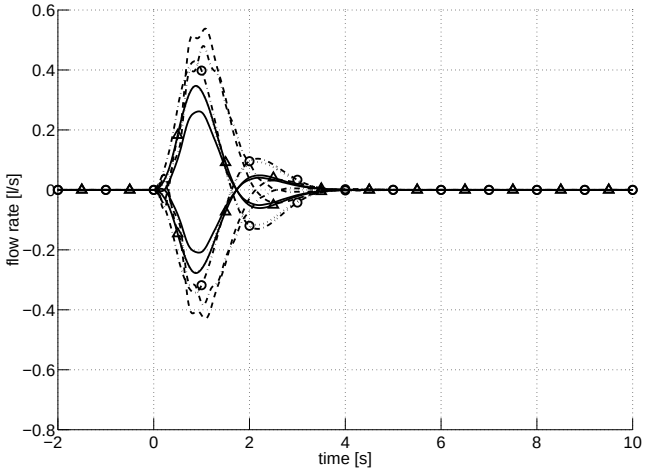

(g) Servo-valve flow rates. ∞ bandwidth: *steer axle (· · · · · ·), drive axle (– – –), semi-trailer axles (· – ○ – ·)*; 0.5 Hz bandwidth: *steer axle (——), drive axle (· – · – ·), semi-trailer axles (—△—).*

Figure 5.16: Continued.

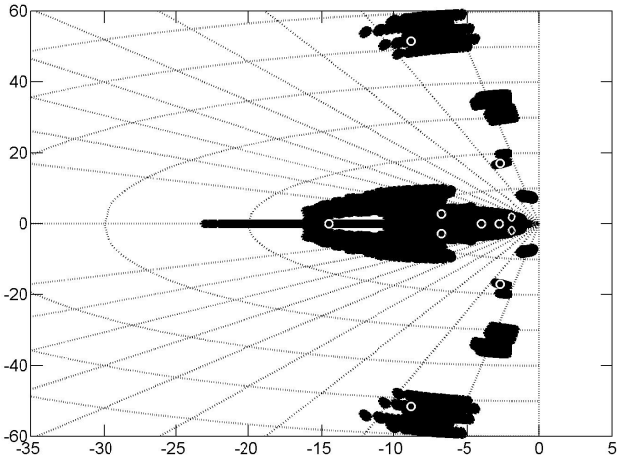

Figure 5.17: Variation with selected vehicle parameters of the closed-loop poles of the torsionally flexible tractor semi-trailer with a full-state feedback controller.

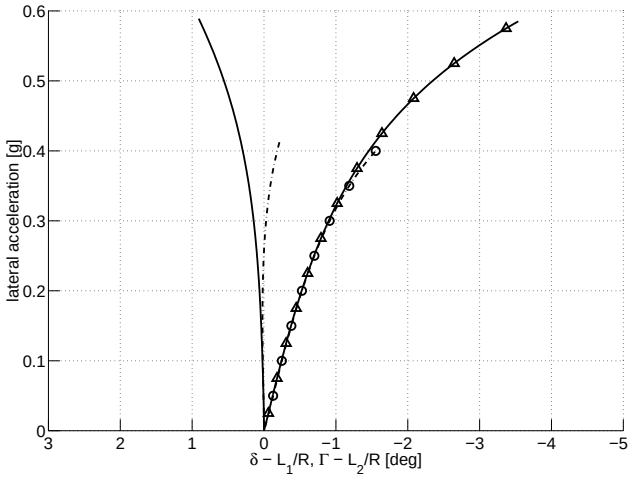

Active roll control: *tractor (——)*, *semi-trailer (—△—)*; passive suspension: *tractor (· – · – ·)*, *semi-trailer (· – ○ – ·).*

Figure 5.18: Handling diagram of the torsionally flexible tractor semi-trailer with a full-state feedback controller.

Chapter 6

Active roll control of long combination vehicles

6.1 Introduction

This chapter considers the problem of designing active roll control systems for a selection of long combination vehicles: a *B-double*, a *truck full-trailer* and an *A-double*. The aim is to investigate how the full-state feedback control system design techniques detailed in section 4.5.3 may be applied to multiple-unit articulated vehicles, including vehicles with highly flexible couplings.

6.2 Control of a B-double

6.2.1 Vehicle description

The B-double combination, which consists of a tractor unit and two semi-trailer units joined using fifth wheel couplings, is illustrated in figure 6.1. B-doubles typically have very good dynamic yaw-roll behaviour, and are widely used in Australia, Canada and some parts of the United States [57].

The tractor unit is as described in section 4.2. The first semi-trailer is similar in size

to that described in section 5.2, except that the two rearward tanks are removed and a fifth wheel coupling is mounted in their place. The laden mass of the first semi-trailer is 24175 kg but, since this unit also supports 8828 kg of the second semi-trailer at the fifth wheel coupling, the laden axle weights are 8541 kg at each axle. The second semi-trailer is identical to that described in section 5.2.

The complete set of parameters is given in appendix C.1.

6.2.2 Control system design objectives

The B-double vehicle model consists of three units and is assembled using the techniques detailed in chapter 2. There are eight roll outputs (two body roll angles for the torsionally flexible tractor unit, one body roll angle for each semi-trailer, and one load transfer at each of the four axle groups) and four roll control inputs (the active anti-roll bar moments at each of the four axle groups), so the system is input deficient.

The eigenvalue analysis described in section 3.5.5 yields results similar to those presented for the tractor semi-trailer in section 5.3. Without active roll control, the system is stable and minimum phase, and the vehicle can retain roll stability until the tractor drive axle and all semi-trailer axles lift off. After this, the tractor steer axle is not sufficiently stiff in roll to stabilise the vehicle. However it is possible for an active roll control system to provide additional net restoring moment through the tractor steer axle beyond this point. Therefore it is important to control the load transfer at all axles when formulating a set of control system design objectives. By section 3.6, the achievable design objective that maximises the vehicle roll stability is to balance the normalised load transfers at all axles while taking the maximum suspension roll angle to the maximum allowable inward angle.

6.2.3 Design of a full-state feedback controller

A full-state roll controller was synthesised using the optimal disturbance rejection system design technique detailed in section 4.5.3. The steering input spectrum (4.28) was

used. The design problem is to tune the weighting matrices Q and R to penalise the performance output vector

$$z = \begin{bmatrix} \phi_{t,f,1} & \phi_{t,r,1} & \phi_{t,r,2} & \phi_{t,r,3} \end{bmatrix}^T \tag{6.1}$$

and the control input u respectively. The aim is to balance the normalised load transfers among the axles without exceeding the maximum allowable suspension roll angles. Using the tuning procedure outlined in section 4.6.1, a full-state feedback controller was synthesised for a speed of 60 km/h using the weighting matrices

$$Q = \begin{bmatrix} 1.000 & 0 & 0 & 0 \\ 0 & 2.540 & 0 & 0 \\ 0 & 0 & 2.795 & 0 \\ 0 & 0 & 0 & 3.457 \end{bmatrix} \mathrm{rad}^{-2}, \tag{6.2}$$

$$R = 1.572 \times 10^{-13} \begin{bmatrix} 1 & 0 & 0 & 0 \\ 0 & 1 & 0 & 0 \\ 0 & 0 & 1 & 0 \\ 0 & 0 & 0 & 1 \end{bmatrix} \mathrm{N}^{-2}.\mathrm{m}^{-2}. \tag{6.3}$$

The performance of this controller is examined in sections 6.2.4–6.2.6.

Note that a practical, partial-state feedback controller, using measurements of suspension roll angles, body roll rates, yaw rates and the steering input, consists of a full-state feedback controller and a Kalman filter. Only the design of the full-state feedback controller is considered here; the Kalman filter may be designed using the techniques demonstrated in section 4.6.6.

6.2.4 Steady-state cornering response

The response of the linear B-double model with a full-state feedback controller to a steady-state steering input at 60 km/h is shown in figure 6.4.

Without active roll control, the vehicle rolls out of the corner (that is, negative roll angle). Since the roll stiffnesses of the vehicle couplings are high, normalised load transfer builds with lateral acceleration in an unbalanced fashion that is approximately proportional to the effective stiffness-to-load ratios of the axle groups, that is, fastest at the tractor drive axle and slowest at the tractor steer axle. The tractor drive axle lifts off at 0.43 g (point D), at which point the normalised load transfer is 0.95 at the axles of the second semi-trailer (point C), 0.83 at the axles of the first semi-trailer (point B) and 0.68 at the tractor steer axle (point A). As lateral acceleration continues to increase, the tractor drive axle is unable to contribute any additional restoring moment, and there is a small increase in the slopes of the normalised load transfer and suspension roll angle curves. The axles of the second semi-trailer are the next to lift off, at 0.46 g (point G). The axles at the first semi-trailer (point F) and the tractor steer axle (point E) remain on the ground at this point, with normalised load transfers of 0.87 and 0.72 respectively. Despite the fact that two of the four axle groups have lifted off, the vehicle combination can maintain roll stability until 0.46 g when the axles of the first semi-trailer lift off (point I). Beyond this point, the steer axle is unable to provide sufficient restoring moment to stabilise the vehicle, and roll-over occurs.

The active roll control system rolls the vehicle units towards the inside of the corner (that is, positive roll angle). The roll moments from the active anti-roll bars are distributed among the axles so that the normalised load transfers build up in a balanced fashion, reaching the maximum value of 1 simultaneously at 0.61 g (point J). The maximum suspension roll angle is 4.5° at the tractor steer axle. A tractor twist angle of 3.9°/g and relative roll angles of 1.2°/g between the tractor and the first semi-trailer and 1.4°/g between the two semi-trailers are required to ensure that the normalised load transfers are balanced. As noted in sections 4.7.2 and 5.5.2, torsional flexibility of vehicle frames and couplings reduces the achievable roll stability.

Active roll control increases the roll-over threshold of the B-double combination by 32% and the lateral acceleration at which lift-off first occurs by 42%. This represents a useful improvement in vehicle safety.

6.2.5 Response to a step steering input

The response of the linear B-double model with a full-state feedback controller to a step steering input at 60 km/h is shown in figure 6.5. The step input is scaled to give a maximum normalised load transfer of 1 in the following simulations.

The lateral acceleration responses are shown in figure 6.5(a). Lateral acceleration builds up first at the tractor unit, then at the first semi-trailer and finally at the second semi-trailer. The significant overshoot in the lateral acceleration response of the second semi-trailer is evidence of rearward amplification. The steady-state lateral acceleration is 0.42 g.

The suspension roll angle responses are shown in figure 6.5(b). Without active roll control, the vehicle rolls out of the corner with peak suspension roll angles of 5.4° at the second semi-trailer, 4.9° at both the first semi-trailer and the tractor drive axle, and 3.8° at the tractor steer axle. With active roll control, all suspension roll angles are towards the inside of the corner. The peak suspension roll angles are 3.4° at the tractor steer axle, 1.7° at the tractor drive axle, 2.3° at the first semi-trailer and 2.1° at the second semi-trailer. The corresponding steady-state values are 3.1°, 1.3°, 1.8° and 1.1°. The peak absolute roll angles are 2.0° into the corner at the front of the tractor unit, 0.3° into the corner at the rear of the tractor unit, and 0.2° and 0.8° out of the turn at the first and second semi-trailers respectively. If the vehicle frames and couplings were less torsionally compliant, it would be possible to balance the normalised load transfers among the axles and roll all units into the corner simultaneously.

The normalised load transfer responses are shown in figure 6.5(c). Without active roll control, the normalised load transfer builds up most quickly at the tractor drive axle and most slowly at the tractor steer axle, as described in section 6.2.4. In addition to significantly reducing the total lateral load transfer by rolling the vehicle units towards the inside of the corner, the active roll control redistributes the total normalised load transfer among the axles in a balanced fashion, with peak responses of 0.69, 0.69, 0.70 and 0.70 at the tractor steer, tractor drive, first semi-trailer and second semi-trailer axles respectively. The system reduces the peak lateral load transfer by 30%, 15% and 26%

at the tractor drive axle and the axles at the first and second semi-trailers respectively. The steer axle load transfer is increased, although this simply indicates that this axle does not support its fair share of the total load transfer in the passive case.

The steady-state results in section 6.2.4 indicate that, without active roll control, the roll-over threshold of the vehicle is 8% higher than the lateral acceleration at which axle lift-off first occurs. However, with active roll control, the B-double can remain stable with up to 43% additional steering input, that is, with up to 0.61 g lateral acceleration. This represents a significant increase in roll stability. The peak inward suspension roll angle in response to a critical manoeuvre is 4.5° at the tractor steer axle, which is within the allowable limits.

The active anti-roll bar moment responses are shown in figure 6.5(d). The peak roll moment in response to a critical manoeuvre is 72 kN.m at the tractor drive axle. Note that the roll moments shown are per anti-roll bar, so the total roll moments at the semi-trailer axle groups are three times the values shown.

6.2.6 Response to a double lane change steering input

The response of the linear B-double model with a full-state feedback controller to a double lane change steering input at 60 km/h is shown in figure 6.6. The path deviation is 5 m. The peak lateral acceleration is 0.19 g (see figure 6.6(a)), and some rearward amplification is evident at the last semi-trailer.

The suspension roll angle responses are shown in figure 6.6(b). The trends discussed in sections 6.2.4 and 6.2.5 are again apparent.

The normalised load transfer responses are shown in figure 6.9(c). Without active roll control, the normalised load transfers are poorly balanced, with peak values of 0.26, 0.36, 0.32 and 0.38 at the tractor steer axle, tractor drive axle, first semi-trailer axles and second semi-trailer axles respectively. Active roll control reduces the total lateral load transfer and significantly improves the balance of the normalised load transfers among the axle groups, with peak values of 0.27, 0.27, 0.26 and 0.25 at the

tractor steer axle, tractor drive axle, first semi-trailer axles and second semi-trailer axles respectively.

The peak inward roll angle for a critical double lane change manoeuvre is 5.7° at the tractor steer axle, which is again within the allowable range.

The active anti-roll bar moment responses are shown in figure 6.6(d). The maximum anti-roll bar moment in response to a critical double lane change steering input is 74 kN.m.

6.3 Control of a truck full-trailer

6.3.1 Vehicle description

The truck full-trailer, which consists of a three axle truck and a full-trailer joined using a pintle hitch, is illustrated in figure 6.2. The truck full trailer is widely used throughout Europe and the United States, and is one of three configurations included in the new European Weight and Dimension Directive 96/53 for 60 tonne heavy vehicles [4].

The truck tandem drive axles are located 4.625 m and 5.935 m respectively behind the steer axle. The steer axle geometries, inertias and suspension properties are identical to those of the tractor steer axle in section 4.2, and the tandem drive axle geometries, inertias and suspension properties are equal to those of the tractor drive axle from the same section. The truck payload is 15000 l of water. The total mass of the laden truck is 22925 kg, and the laden axle weights are 6053 kg on the steer axle and 8436 kg each on the tandem drive axles. The truck frame is considerably stiffer than the tractor frame despite its greater length because the tank significantly increases the torsional rigidity. The truck features a pintle hitch 1.400 m behind the drive axle centreline.

The full-trailer actually consists of two distinct units coupled by a fifth wheel: a dolly and a semi-trailer*. The dolly axle is located 2 m behind the hitch point, and

*The *dolly* and *trailer* axle groups are respectively the front and rear axle groups of the full-trailer.

the centre of the fifth wheel coupling is directly above the axle centreline. The total mass of the dolly is 1300 kg, 800 kg of which is unsprung. The geometry of the semi-trailer section of the full-trailer is similar to that of the semi-trailer detailed in section 5.2, but the payload configuration is modified to limit the axle weights at the dolly and trailer axles to 7108 kg and 8271 kg respectively. The dolly and trailer axle geometries, inertias and suspension properties are identical to those of the semi-trailer axles described in section 5.2. The combined torsional stiffness of the trailer tanker frame and the fifth wheel is 3000 kN.m/rad.

The complete set of parameters is given in appendix C.2.

6.3.2 Control system design objectives

Although the truck full-trailer is ostensibly a two unit vehicle, the vehicle model uses three units because the full-trailer actually consists of a dolly and a semi-trailer. There are eight roll outputs (two body roll angles for the torsionally flexible truck, one body roll angle each for the dolly and the trailer, and one load transfer at each of the four axle groups) and four roll control inputs (the active anti-roll bar moments at each of the four axle groups), so the system is input deficient.

Since a pintle hitch has no roll stiffness, it is not possible to transfer roll moment between the truck and the dolly by generating a relative roll angle between these two units. An eigenvalue analysis as described in section 3.5.5 reveals that this static roll decoupling has an important effect on the achievable roll stability of the vehicle combination. The vehicle (both with and without active roll control) is unstable in roll if *either* the truck rolls over *or* the full-trailer rolls over. As a consequence, the roll-over threshold of the vehicle combination is determined by the roll-over threshold of either the truck subsystem or the full-trailer subsystem, whichever is lower.

If the achievable roll-over threshold of the full-trailer with active roll control is still well below the passive roll-over threshold of the truck, then there is no benefit (from a roll stability perspective) in applying active roll control to the truck axles. In this case,

all control effort should be directed towards controlling the load transfers at the dolly axle and the trailer axles. Since it is not possible for active anti-roll bars on the truck to enhance the roll stability of the full-trailer, active anti-roll bars should only be fitted to the dolly and trailer axles in this case.

The roll-over thresholds of the truck and the full-trailer for the vehicle parameters presented here are comparable. Although the roll-over threshold of the passive vehicle combination is governed by the roll-over of the full-trailer, it is possible to increase the roll stability of the full-trailer using active anti-roll bars to the point where the truck and full-trailer are equally stable in roll. Any further increase in the roll stability of the vehicle combination requires improvements at *both* the truck and the full-trailer. Therefore, when formulating a set of control system design objectives, most benefit can be obtained in this case by controlling the load transfer at all axles. By section 3.6, the achievable design objective that maximises the vehicle roll stability is to balance the normalised load transfers at all axles while taking the maximum suspension roll angle to the maximum allowable inward angle. This requires that active anti-roll bars are fitted to all axles.

6.3.3 Design of a full-state feedback controller

A full-state roll controller was again synthesised using the optimal disturbance rejection system design technique detailed in section 4.5.3. The problem is to tune the weighting matrices Q and R to penalise the performance output vector

$$z = \begin{bmatrix} \phi_{t,f,1} & \phi_{t,r,1} & \phi_{t,r,2} & \phi_{t,r,3} \end{bmatrix}^T \tag{6.4}$$

and the control input u respectively. The aim is to balance the normalised load transfers among the axles without exceeding the maximum allowable suspension roll angles. The tuning process was simplified in practice by the fact that the elements of Q and R corresponding to the truck states and inputs have little effect on the roll stability of the full-trailer, and vice versa.

When tuning the controller performance, it is important to realise that there is no performance benefit in increasing the roll-over threshold of the truck beyond the maximum achievable roll-over threshold of the full-trailer, and vice versa.

A full-state feedback controller was designed for a speed of 60 km/h using the weighting matrices

$$Q = \begin{bmatrix} 1.000 & 0 & 0 & 0 \\ 0 & 4.438 & 0 & 0 \\ 0 & 0 & 0.462 & 0 \\ 0 & 0 & 0 & 2.434 \end{bmatrix} \mathrm{rad}^{-2}, \tag{6.5}$$

$$R = 4.978 \times 10^{-14} \begin{bmatrix} 1.000 & 0 & 0 & 0 \\ 0 & 1.000 & 0 & 0 \\ 0 & 0 & 2.186 & 0 \\ 0 & 0 & 0 & 2.186 \end{bmatrix} \mathrm{N}^{-2}.\mathrm{m}^{-2}. \tag{6.6}$$

The performance of this controller is examined in sections 6.3.4–6.3.6.

6.3.4 Steady-state cornering response

The response of the linear truck full-trailer model with a full-state feedback controller to a steady-state steering input at 60 km/h is shown in figure 6.7.

Without active roll control, the vehicle rolls out of the corner. The truck and the full-trailer are not coupled torsionally because the pintle hitch between them has no roll stiffness. The normalised load transfer builds up more quickly at the full-trailer than at the truck. The dolly axle is the first to lift off, at 0.44 g (point D). At this point, the normalised load transfers at the truck steer axle, truck tandem drive axles and trailer axles are 0.71 (point A), 0.86 (point B) and 0.93 (point C) respectively. As lateral acceleration continues to increase, the dolly axle is unable to contribute any additional restoring moment, but the trailer axles provide sufficient restoring moment to stabilise the full-trailer in roll. However, at 0.47 g the trailer axles also lift off (point G), and

the full-trailer rolls over. At this point, the available load transfers at the truck axles are somewhat underutilised (points E and F).

The active roll control system rolls the truck and the full-trailer towards the inside of the corner to reduce the total load transfer. The roll moments from the active anti-roll bars are distributed among the axles so that the normalised load transfers build up in a balanced fashion, simultaneously reaching the maximum value of 1 at 0.58 g (point H). Since the roll stability of the truck is higher than that of the full-trailer in the passive case, the active roll control system must increase roll stability more at the full-trailer than at the truck in order to balance the steady-state normalised load transfers at all axles. The maximum inward suspension roll angle is 1.2° at the trailer axles.

Active roll control increases the roll-over threshold of the truck full-trailer combination by 25% and the lateral acceleration at which lift-off first occurs by 31%. These are substantial gains in roll stability.

6.3.5 Response to a step steering input

The response of the linear truck full-trailer model with a full-state feedback controller to a step steering input at 60 km/h is shown in figure 6.8. The step input is scaled to give a maximum normalised load transfer of 1 in the following simulations.

The lateral acceleration responses are shown in figure 6.8(a). Lateral acceleration builds up at the truck before the full-trailer. There is a significant level of rearward amplification, as would be expected for a vehicle featuring an A-coupling [26, 84]. The steady-state lateral acceleration is 0.37g.

The suspension roll angle responses are shown in figure 6.8(b). Without active roll control, the vehicle rolls out of the corner. The roll angle responses of the full-trailer axles feature significant levels of overshoot that are driven by the overshoot in the trailer lateral acceleration response. This does not affect the roll motion of the truck because no roll moment can be transferred through the pintle hitch. With active roll

control, all suspension roll angles are towards the inside of the corner, although body roll angles are actually slightly towards the outside of the turn. The peak suspension roll angles are around 2.0° at all axles. The steady-state suspension roll angles are 0.8° at the truck steer axle, 0.5° at the truck tandem drive axles, and 1.1° at the dolly and trailer axles.

The normalised load transfer responses are shown in figure 6.8(c). Without active roll control, the normalised load transfers at the full-trailer axles feature significant levels of overshoot. The active roll control system reduces the total lateral load transfer at both the truck and the full-trailer by rolling both vehicle units towards the inside of the corner. For long combination vehicles with flexible couplings, such as the truck full-trailer, it is neither feasible nor advisable to balance the normalised load transfers among the axles throughout a severe transient manoeuvre. This is because there is a time lag in the build up of lateral acceleration down the vehicle that is approximately proportional to the length of the vehicle units and inversely proportional to the vehicle speed. However, the active roll control is able to effectively balance the peak load transfers at the truck and the full-trailer. The effect of rearward amplification on load transfer is also attenuated. The peak values of normalised load transfer are 0.66 at the truck axles, 0.67 at the dolly axle and 0.67 at the trailer axles.

From the steady-state results in section 6.3.4, the roll-over threshold of the vehicle with passive suspension is 5% higher than the lateral acceleration at which axle lift-off first occurs. However, with active roll control, the truck full-trailer can remain stable with up to 49% additional steering input, that is, with up to 0.58 g lateral acceleration. This is a worthwhile improvement in roll stability. The peak inward suspension roll angle in response to a critical manoeuvre is 3.4°, which is within the allowable limits.

The active anti-roll bar moment responses are shown in figure 6.8(d). The peak roll moment in response to a critical step steering input is 95 kN.m at the dolly axle. Note that the roll moments shown are per anti-roll bar, so the total roll moments at the truck drive and trailer axle groups are respectively two and three times the values shown.

6.3.6 Response to a double lane change steering input

The response of the linear truck full-trailer model with a full-state feedback controller to a double lane change steering input at 60 km/h is shown in figure 6.9. The path deviation is 5 m. The peak lateral acceleration is 0.26 g (see figure 6.9(a)), and a significant level of rearward amplification is evident.

The suspension roll angle responses are shown in figure 6.9(b). The trends discussed in sections 6.3.4 and 6.3.5 are again apparent.

The normalised load transfer responses are shown in figure 6.9(c). Without active roll control, the normalised load transfers are much lower at the truck (with peak values of 0.33 at the steer axle and 0.42 at the drive axle group) than at the full-trailer (with peak values 0.66 and 0.63 at the dolly axle and trailer axles respectively).

The active roll control system again reduces the total lateral load transfer at the tractor and full-trailer by rolling both vehicle units towards the inside of the corner. The system is able to effectively balance the peak load transfers at the truck and the full-trailer and attenuate the effect of rearward amplification on load transfer. With active roll control, the peak values of normalised load transfer are 0.33 at the truck axles and 0.33 at the full-trailer axles.

The peak inward roll angle for a critical double lane change manoeuvre is calculated to be 6.2° at the truck steer axle, which is near the limit of the allowable range.

The active anti-roll bar moment responses are shown in figure 6.9(d). The maximum anti-roll bar moment in response to a critical double lane change steering input is calculated to be 114 kN.m at the dolly axle. In practice, a tandem axle dolly would most likely be used in order to share this large roll moment between two axles.

6.4 Control of an A-double

6.4.1 Vehicle description

The A-double combination, which consists of a tractor semi-trailer and a full-trailer joined using a pintle hitch, is illustrated in figure 6.3. A-doubles are widely used throughout the United States and Australia [26], and tend to exhibit severe rearward amplification, compromising roll stability in avoidance manoeuvres such as the double lane change. The tractor semi-trailer is as described in section 4.2. The full-trailer is as described in section 6.3.1.

6.4.2 Control system design objectives

The A-double vehicle model consists of four units: the tractor unit, the semi-trailer, the dolly and the semi-trailer section of the full-trailer. There are ten roll outputs (two body roll angles for the torsionally flexible tractor, one body roll angle each for the semi-trailer, the dolly and the trailer, and one load transfer at each of the five axle groups) and five roll control inputs (the active anti-roll bar moments at each of the five axle groups), so the system is input deficient.

The roll motions of the tractor semi-trailer and full-trailer subsystems are statically decoupled because the pintle hitch that joins them has no roll stiffness. An eigenvalue analysis as described in section 3.5.5 reveals that, without active roll control, the vehicle combination is unstable in roll if *either* the tractor drive axle and the semi-trailer axles lift off (that is, the tractor semi-trailer rolls over) *or* the dolly and trailer axles lift off (that is, the full-trailer rolls over). The tractor steer axle is not sufficiently stiff in roll to stabilise the vehicle. (This was also true for the tractor semi-trailer considered in section 5.3 and the B-double considered in section 6.2.2.) However it is possible for an active roll control system to provide additional net restoring moment through the tractor steer axle beyond this point.

Since the roll-over thresholds of the tractor semi-trailer and the full-trailer are com-

parable in this case, it is necessary to improve the roll stability of *both* the tractor semi-trailer and the full-trailer to achieve a significant increase in the roll stability of the combination vehicle. Therefore the load transfer at all axles must be controlled. By section 3.6, the achievable control system design objective that maximises the vehicle roll stability is again to balance the normalised load transfers at all axles while taking the maximum suspension roll angle to the maximum allowable inward angle. This requires that active anti-roll bars are fitted to all axles.

6.4.3 Design of a full-state feedback controller

A full-state roll controller was again synthesised using the optimal disturbance rejection system design technique detailed in section 4.5.3. The problem is to tune the weighting matrices Q and R to penalise the performance output vector

$$z = \begin{bmatrix} \phi_{t,f,1} & \phi_{t,r,1} & \phi_{t,r,2} & \phi_{t,r,3} & \phi_{t,r,4} \end{bmatrix}^T \tag{6.7}$$

and the control input u respectively. The aim is to balance the normalised load transfers among the axles without exceeding the maximum allowable suspension roll angles. The elements of Q and R corresponding to the tractor semi-trailer states and inputs have little effect on the roll stability of the full-trailer, and vice versa. There is no performance benefit in increasing the roll-over threshold of the tractor semi-trailer beyond the maximum achievable roll-over threshold of the full-trailer, and vice versa.

Using the tuning procedure outlined in section 4.6.1, a full-state feedback controller was synthesised for a speed of 60 km/h using the weighting matrices

$$Q = \begin{bmatrix} 1.000 & 0 & 0 & 0 & 0 \\ 0 & 3.583 & 0 & 0 & 0 \\ 0 & 0 & 3.719 & 0 & 0 \\ 0 & 0 & 0 & 1.110 & 0 \\ 0 & 0 & 0 & 0 & 4.903 \end{bmatrix} \text{rad}^{-2}, \tag{6.8}$$

$$R = 2.819 \times 10^{-13} \begin{bmatrix} 1.000 & 0 & 0 & 0 & 0 \\ 0 & 1.000 & 0 & 0 & 0 \\ 0 & 0 & 1.000 & 0 & 0 \\ 0 & 0 & 0 & 0.724 & 0 \\ 0 & 0 & 0 & 0 & 0.724 \end{bmatrix} \mathrm{N}^{-2}.\mathrm{m}^{-2}. \quad (6.9)$$

The performance of this controller is examined in sections 6.4.4–6.4.6.

6.4.4 Steady-state cornering response

The response of the linear A-double model with a full-state feedback controller to a steady-state steering input at 60 km/h is shown in figure 6.10.

Without active roll control, the vehicle rolls out of the corner. The tractor semi-trailer and the full-trailer are not coupled in roll because the pintle hitch that joins them cannot transmit any roll moment. The tractor semi-trailer and the full-trailer have similar roll-over thresholds. As lateral acceleration increases, the first axle to lift off is the tractor drive axle, at 0.41 g (point E). At this point, the normalised load transfer is 0.67 at the tractor steer axle (point A), 0.85 at the semi-trailer axles (point B), 0.94 at the dolly axle (point D) and 0.87 at the trailer axles (point C). As lateral acceleration continues to increase, the dolly axle is the next to lift off, at 0.44 g (point I). At this point, the normalised load transfer is 0.74 at the tractor steer axle (point F), 0.94 at the semi-trailer axles (point H) and 0.93 at the trailer axle group (point G). An additional lateral acceleration of less than 0.02 g causes the semi-trailer axles to lift off and the tractor semi-trailer to roll over. The full-trailer is also very close to roll over at this point.

The active roll control system rolls the tractor semi-trailer and the full-trailer into the corner to increase the roll stability. The roll moments from the active anti-roll bars are distributed among the axles such that the normalised load transfers build up in a more balanced fashion, increasing the roll-over threshold to 0.57 g. The maximum inward suspension roll angle is 2.3° at the tractor steer axle.

Active roll control improves the roll stability of the A-double combination significantly, increasing the roll-over threshold by 23% and the lateral acceleration at which axle lift off first occurs by 37%.

6.4.5 Response to a step steering input

The response of the linear A-double model with a full-state feedback controller to a step steering input at 60 km/h is shown in figure 6.11. The step input is scaled to give a maximum normalised load transfer of 1 in the following simulations.

The lateral acceleration responses are shown in figure 6.11(a). Rearward amplification is not a factor at the semi-trailer but is significant at the full-trailer. The steady-state lateral acceleration is 0.39 g.

The suspension roll angle responses are shown in figure 6.11(b). Without active roll control, the vehicle rolls out of the corner. The peak suspension roll angles at the full-trailer axles are particularly large, driven by the large peak lateral accelerations at that unit. The active roll control system rolls all vehicle units towards the inside of the turn to increase roll stability. The peak inward suspension roll angle at the tractor semi-trailer is 2.1° at the tractor steer axle, while the largest roll angle at the full-trailer is 1.4° at the trailer axles.

The normalised load transfer responses are shown in figure 6.11(c). Without active roll control, the normalised load transfers at the full-trailer axles feature significant levels of overshoot. This effect was also observed for the truck full-trailer in section 6.3.5. The active roll control system reduces the total lateral load transfer at the tractor semi-trailer and the full-trailer by rolling both vehicle units towards the inside of the corner. The peak load transfers are 0.70 at the tractor semi-trailer axles and 0.71 at the full-trailer axles. The peak at the full-trailer axles lags the peak at the tractor semi-trailer axles for reasons detailed in section 6.3.5.

The steady-state results in section 6.4.4 indicate that, without active roll control, the roll-over threshold of the vehicle is 12% higher than the lateral acceleration at which

axle lift-off first occurs. However, with active roll control, the A-double can remain stable with up to 40% additional steering input, which is an important increase in roll stability. The peak inward suspension roll angle in response to a critical manoeuvre is 4.2° at the tractor steer axle. This is within the allowable limits.

The peak inward roll angle for a critical step steering input is 2.9° at the tractor steer axle, which is within the allowable range.

The active anti-roll bar moment responses are shown in figure 6.11(d). The peak roll moment in response to a critical step steering input is 83 kN.m at the dolly axle.

6.4.6 Response to a double lane change steering input

The response of the linear A-double model with a full-state feedback controller to a double lane change steering input at 60 km/h is shown in figure 6.12. The path deviation is 5 m. The lateral acceleration responses in figure 6.12(a) show a significant level of rearward amplification at the full-trailer.

The suspension roll angle responses are shown in figure 6.12(b). The trends discussed in sections 6.4.4 and 6.4.5 are again apparent.

The normalised load transfer responses are shown in figure 6.11(c). The active roll control system reduces the total lateral load transfers at both the tractor semi-trailer and the full-trailer by rolling both vehicle units towards the inside of the corner. The peak load transfers are 0.31 at the tractor semi-trailer axles and 0.32 at the full-trailer axles. The peak at the full-trailer axles again lags the peak at the tractor semi-trailer axles.

The peak inward roll angle for a critical double lane change manoeuvre is calculated to be 5.3° at the trailer axles, which is on the limit of the allowable range.

The active anti-roll bar moment responses are shown in figure 6.12(d). The maximum anti-roll bar moment in response to a critical double lane change steering input is calculated to be 108 kN.m at the dolly axle. In practice, a tandem axle dolly would most likely be used in order to share this large roll moment between two axles.

6.5 Conclusions

1. Active roll control system design for long combination vehicles is a problem of optimal disturbance rejection system design. The control system design techniques developed in chapter 4 are suitable for arbitrarily long combination vehicles.

2. For vehicles with torsionally flexible couplings, the roll-over threshold of the combination is governed by the stability of the least stable set of torsionally decoupled vehicle units. This has important implications for the control objectives and actuator placement.

3. Simulations show that active roll control can increase the roll-over threshold by 32% for a B-double. This represents a significant increase in vehicle safety.

4. Truck full-trailers and A-doubles typically exhibit significant levels of rearward amplification that substantially increase lateral load transfer (and therefore reduce roll stability) in severe avoidance manoeuvres such as a double lane change. Active roll control can increase the roll-over threshold by 25% for a truck full-trailer and by 23% for an A-double, and can also significantly attenuate the effect of rearward amplification on load transfer.

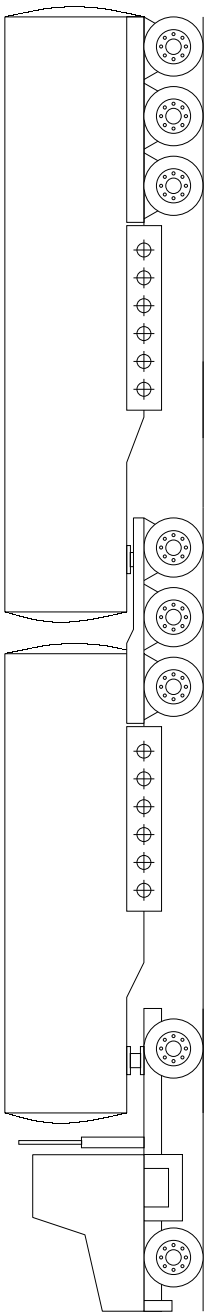

Figure 6.1: B-double combination.

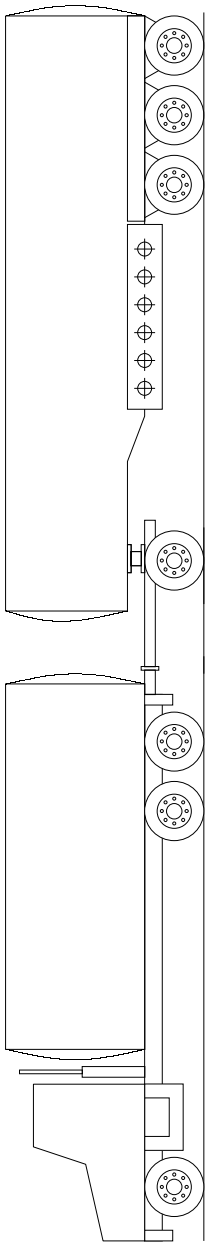

Figure 6.2: Truck full-trailer combination.

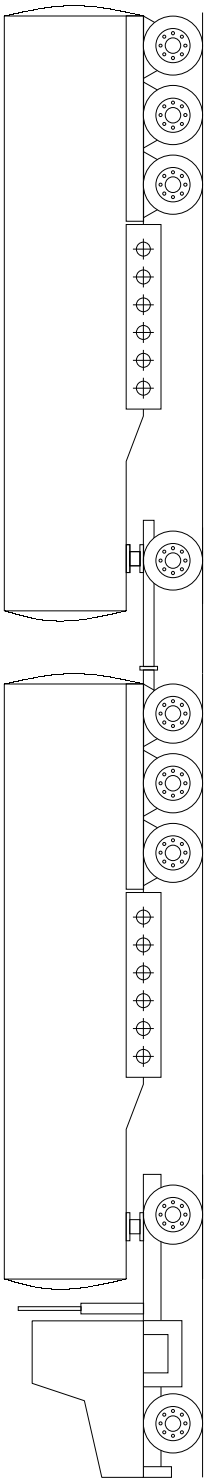

Figure 6.3: A-double combination.

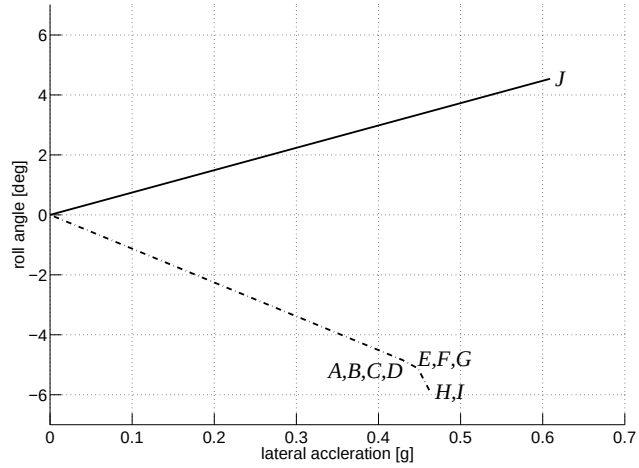

(a) Suspension roll angles. Active roll control: *steer axle (——)*; passive suspension: *semi-trailer #1 axles (· – · – ·).*

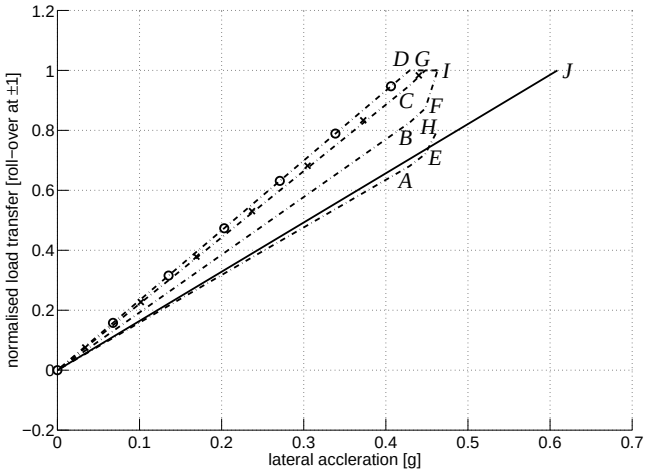

(b) Normalised load transfers. Active roll control: *steer axle, drive axle and semi-trailer axles (——)*; passive suspension: *steer axle (– – –), drive axle (· – ○ – ·), semi-trailer #1 axles (· – · – ·), semi-trailer #2 axles (· – × – ·).*

Figure 6.4: Response of the linear B-double model with a full-state feedback controller to a steady-state steering input.

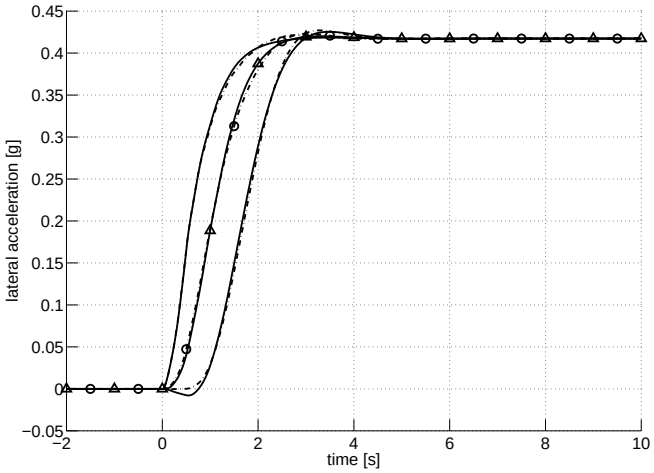

(a) Lateral accelerations. Active roll control: *tractor (· · · · · ·), semi-trailer #1 (—△—), semi-trailer #2 (——)*; passive suspension: *tractor (– – –), semi-trailer #1 (· – ○ – ·), semi-trailer #2 (· – · – ·).*

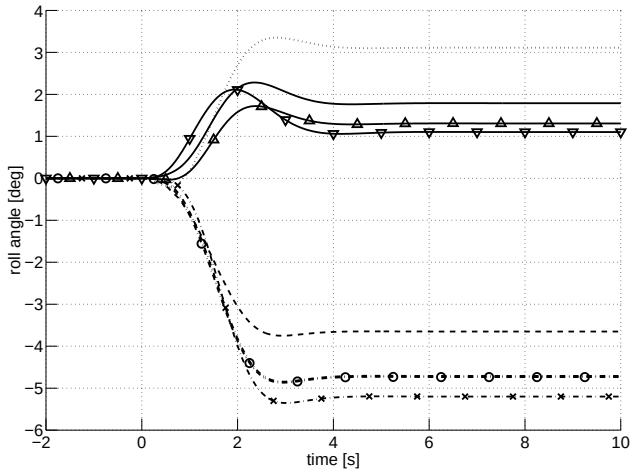

(b) Suspension roll angles. Active roll control: *steer axle (· · · · · ·), drive axle (—△—), semi-trailer #1 axles (——), semi-trailer #2 axles (—▽—)*; passive suspension: *steer axle (– – –), drive axle (· – ○ – ·), semi-trailer #1 axles (· – · – ·), semi-trailer #2 axles (· – × – ·).*

Figure 6.5: Response of the linear B-double model with a full-state feedback controller to a step steering input.

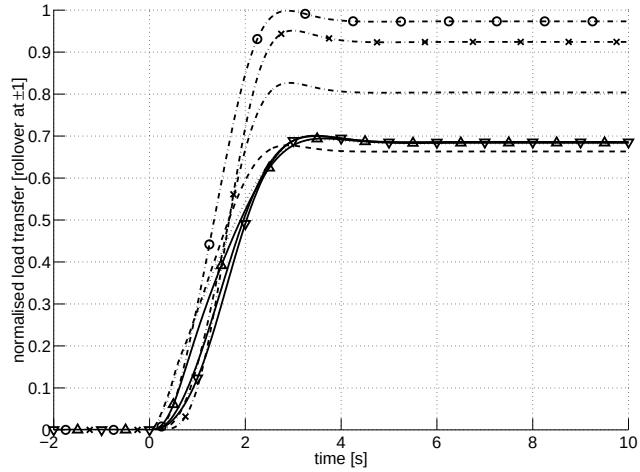

(c) Normalised load transfers. Active roll control: *steer axle (· · · · · ·), drive axle (—△—), semi-trailer #1 axles (——), semi-trailer #2 axles (—▽—)*; passive suspension: *steer axle (– – –), drive axle (· – ○ – ·), semi-trailer #1 axles (· – · – ·), semi-trailer #2 axles (· – × – ·).*

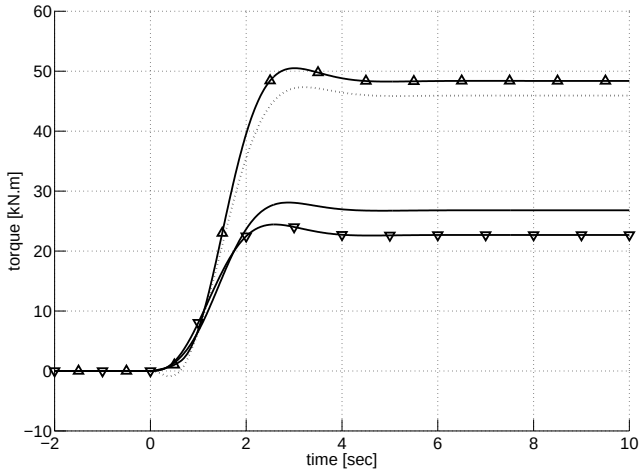

(d) Active anti-roll bar moments. Active roll control: *steer axle (· · · · · ·), drive axle (—△—), semi-trailer #1 axles (——), semi-trailer #2 axles (—▽—).*

Figure 6.5: Continued.

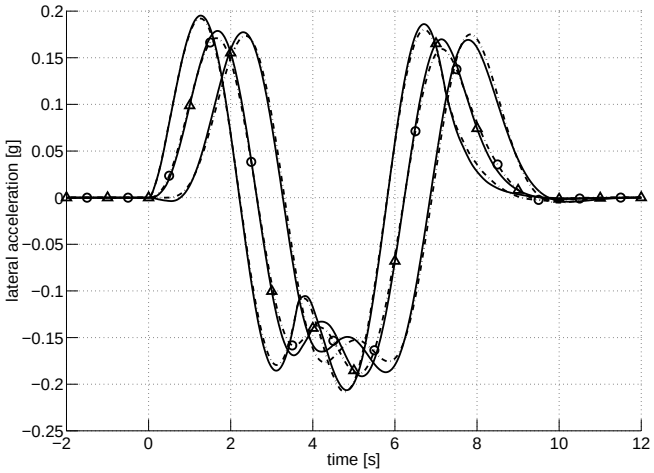

(a) Lateral accelerations. Active roll control: *tractor (· · · · · ·), semi-trailer #1 (—△—), semi-trailer #2 (——)*; passive suspension: *tractor (– – –), semi-trailer #1 (· – ○ – ·), semi-trailer #2 (· – · – ·).*

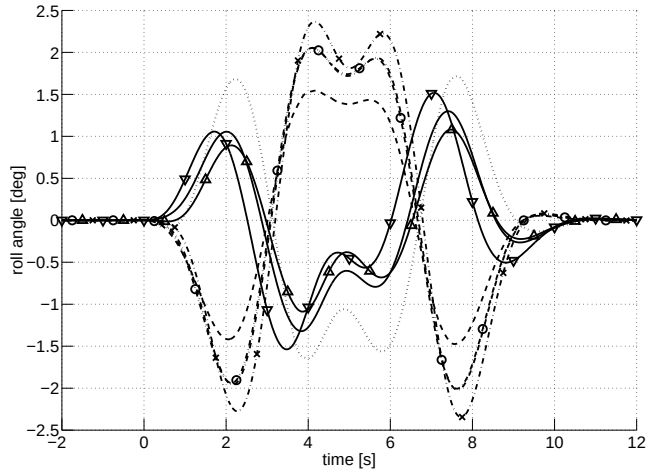

(b) Suspension roll angles. Active roll control: *steer axle (· · · · · ·), drive axle (—△—), semi-trailer #1 axles (——), semi-trailer #2 axles (—▽—)*; passive suspension: *steer axle (– – –), drive axle (· – ○ – ·), semi-trailer #1 axles (· – · – ·), semi-trailer #2 axles (· – × – ·).*

Figure 6.6: Response of the linear B-double model with a full-state feedback controller to a double lane change steering input.

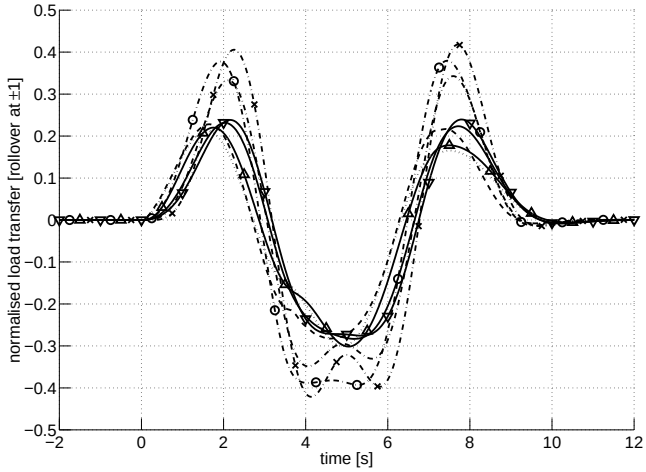

(c) Normalised load transfers. Active roll control: *steer axle (· · · · · ·), drive axle (—△—), semi-trailer #1 axles (——), semi-trailer #2 axles (—▽—)*; passive suspension: *steer axle (– – –), drive axle (· – ○ – ·), semi-trailer #1 axles (· – · – ·), semi-trailer #2 axles (· – × – ·).*

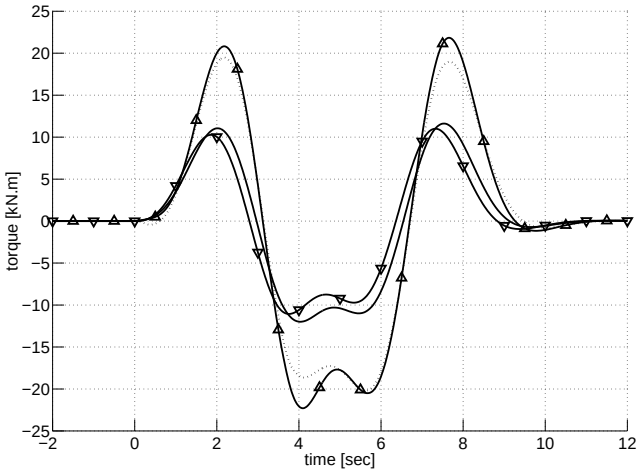

(d) Active anti-roll bar moments. Active roll control: *steer axle (· · · · · ·), drive axle (—△—), semi-trailer #1 axles (——), semi-trailer #2 axles (—▽—).*

Figure 6.6: Continued.

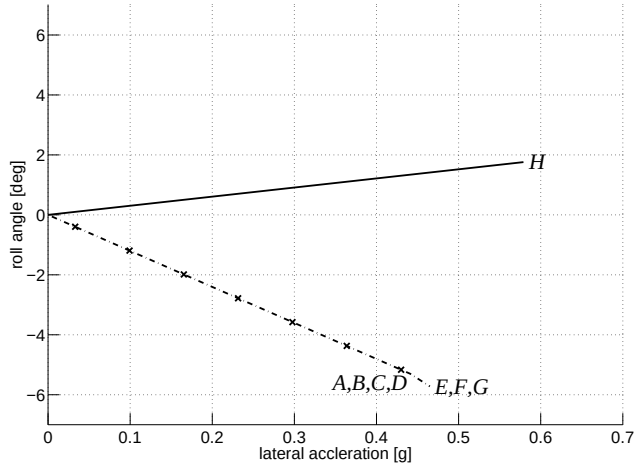

(a) Suspension roll angles. Active roll control: *dolly axle (——)*; passive suspension: *trailer axles (· – × – ·).*

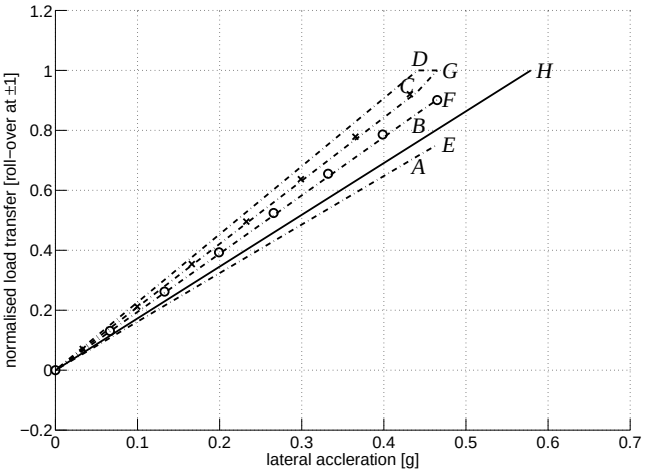

(b) Normalised load transfers. Active roll control: *steer axle, tandem drive axles, dolly axle and trailer axles (——)*; passive suspension: *steer axle (– – –), tandem drive axles (· – ○ – ·), dolly axle (· – · – ·), trailer axles (· – × – ·).*

Figure 6.7: Response of the linear truck full-trailer model with a full-state feedback controller to a steady-state steering input.

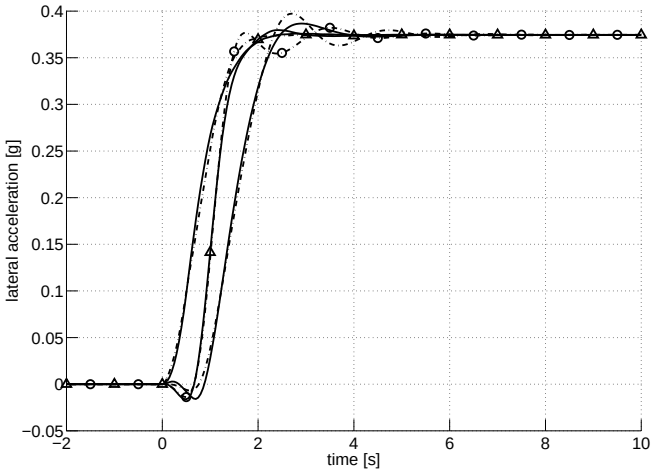

(a) Lateral accelerations. Active roll control: *truck* (· · · · · ·), *dolly* (—△—), *trailer* (——); passive suspension: *truck* (– – –), *dolly* (· – ○ – ·), *trailer* (· – · – ·).

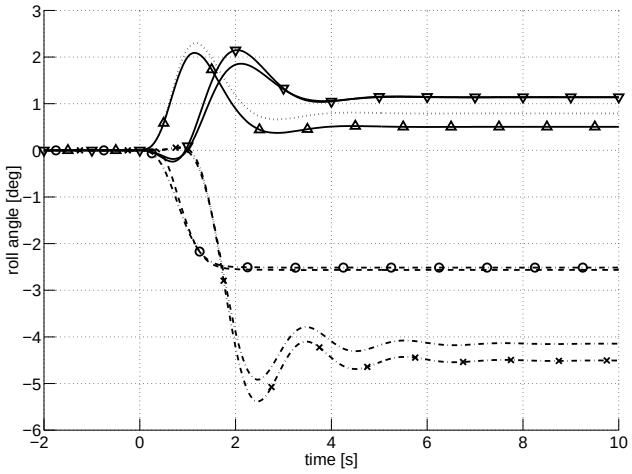

(b) Suspension roll angles. Active roll control: *steer axle* (· · · · · ·), *tandem drive axles* (—△—), *dolly axle* (——), *trailer axles* (—▽—); passive suspension: *steer axle* (– – –), *tandem drive axles* (· – ○ – ·), *dolly axle* (· – · – ·), *trailer axles* (· – × – ·).

Figure 6.8: Response of the linear truck full-trailer model with a full-state feedback controller to a step steering input.

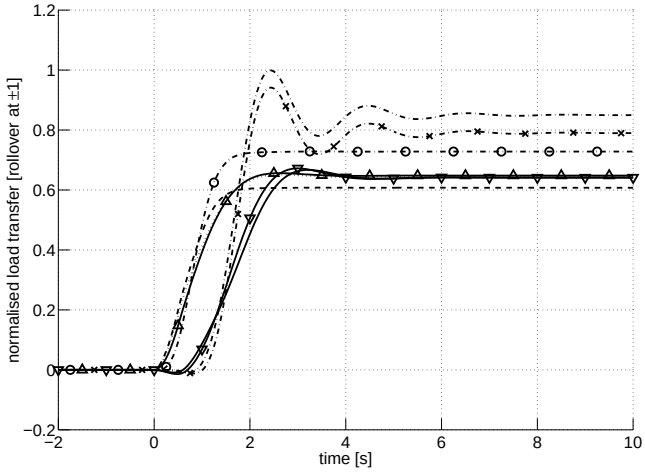

(c) Normalised load transfers. Active roll control: *steer axle (· · · · · ·), tandem drive axles (—△—), dolly axle (——), trailer axles (—▽—)*; passive suspension: *steer axle (– – –), tandem drive axles (· – ○ – ·), dolly axle (· – · – ·), trailer axles (· – × – ·).*

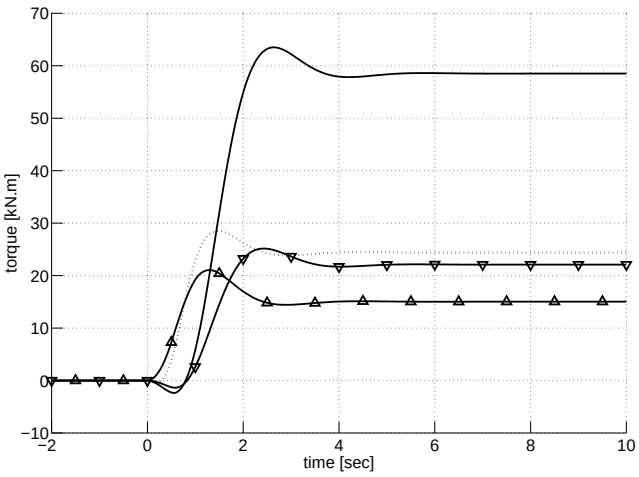

(d) Active anti-roll bar moments. Active roll control: *steer axle (· · · · · ·), tandem drive axles (—△—), dolly axle (——), trailer axles (—▽—).*

Figure 6.8: Continued.

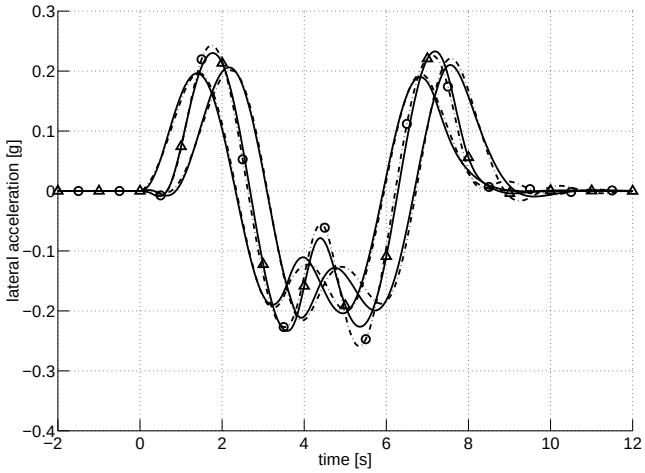

(a) Lateral accelerations. Active roll control: *truck* (· · · · · ·), *dolly* (—△—), *trailer* (——); passive suspension: *truck* (– – –), *dolly* (· – ○ – ·), *trailer* (· – · – ·).

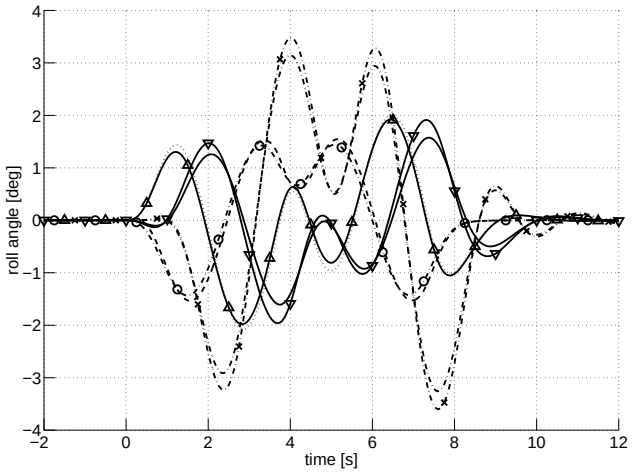

(b) Suspension roll angles. Active roll control: *steer axle* (· · · · · ·), *tandem drive axles* (—△—), *dolly axle* (——), *trailer axles* (—▽—); passive suspension: *steer axle* (– – –), *tandem drive axles* (· – ○ – ·), *dolly axle* (· – · – ·), *trailer axles* (· – × – ·).

Figure 6.9: Response of the linear truck full-trailer model with a full-state feedback controller to a double lane change steering input.

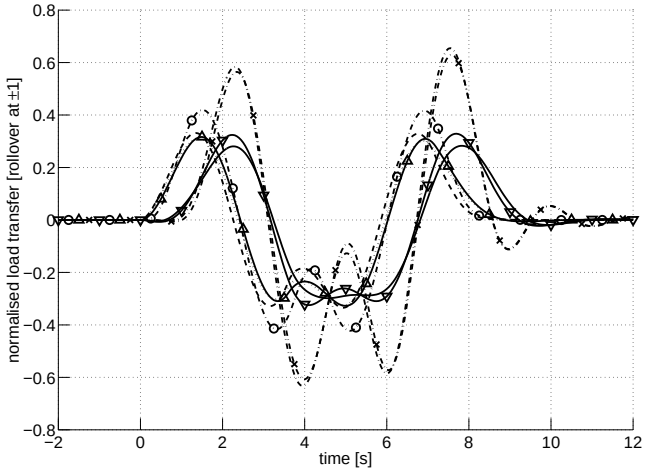

(c) Normalised load transfers. Active roll control: *steer axle (· · · · · ·), tandem drive axles (—△—), dolly axle (——), trailer axles (—▽—)*; passive suspension: *steer axle (– – –), tandem drive axles (· – ○ – ·), dolly axle (· – · – ·), trailer axles (· – × – ·).*

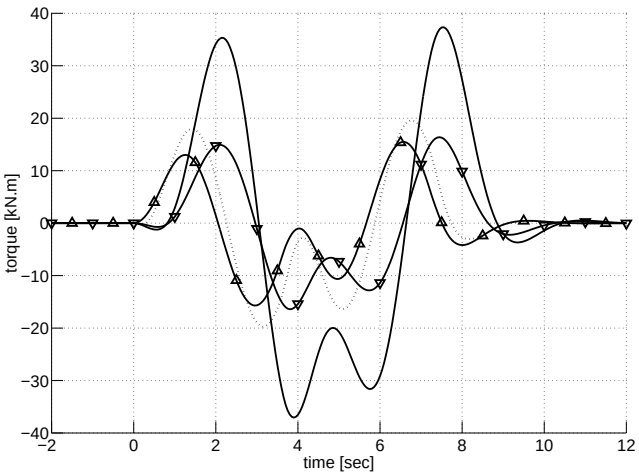

(d) Active anti-roll bar moments. Active roll control: *steer axle (· · · · · ·), tandem drive axles (—△—), dolly axle (——), trailer axles (—▽—).*

Figure 6.9: Continued.

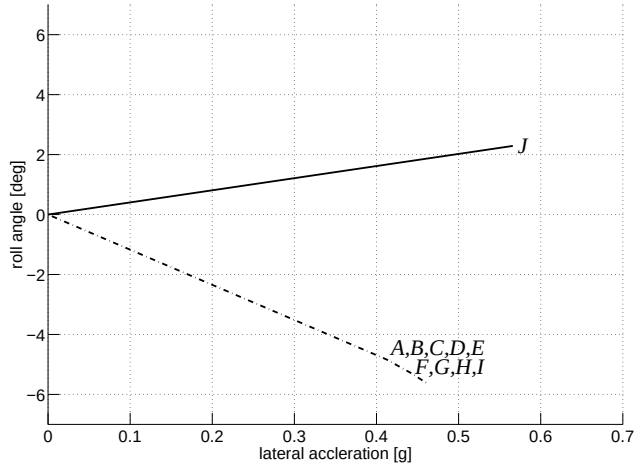

(a) Suspension roll angles. Active roll control: *steer axle (· · · · · ·)*; passive suspension: *semi-trailer axles (· – · – ·).*

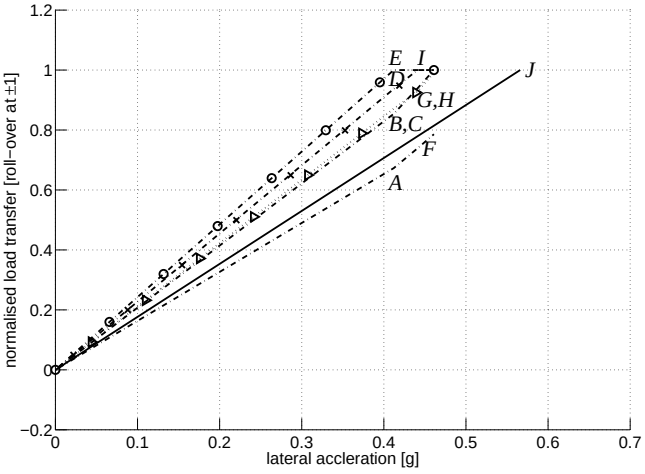

(b) Normalised load transfers. Active roll control: *steer axle, drive axle, semi-trailer axles, dolly axle and trailer axles (——)*; passive suspension: *steer axle (– – –), drive axle (· – ○ – ·), semi-trailer axles (· – · – ·), dolly axle (· – × – ·), trailer axles (· · ▷ · ·).*

Figure 6.10: Response of the linear A-double model with a full-state feedback controller to a steady-state steering input.

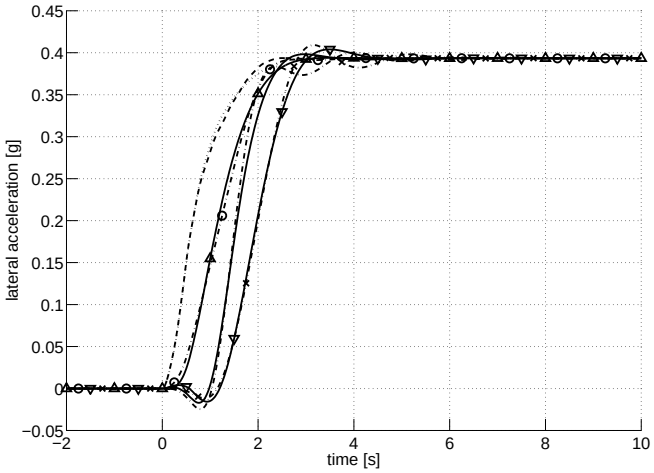

(a) Lateral accelerations. Active roll control: *tractor (· · · · · ·), semi-trailer (—△—), dolly (——), trailer (—▽—)*; passive suspension: *tractor (– – –), semi-trailer (· – ○ – ·), dolly (· – · – ·), trailer (· – × – ·).*

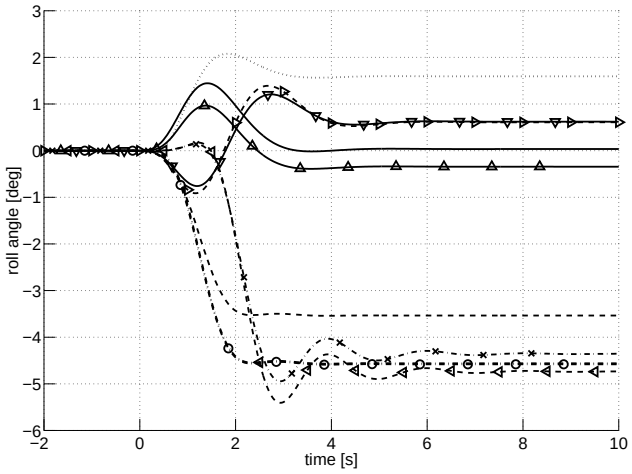

(b) Suspension roll angles. Active roll control: *steer axle (· · · · · ·), drive axle (—△—), semi-trailer axles (——), dolly axle (—▽—), trailer axles (– ◁ –)*; passive suspension: *steer axle (– – –), drive axle (· – ○ – ·), semi-trailer axles (· – · – ·), dolly axle (· – × – ·), trailer axles (· · ▷ · ·).*

Figure 6.11: Response of the linear A-double model with a full-state feedback controller to a step steering input.

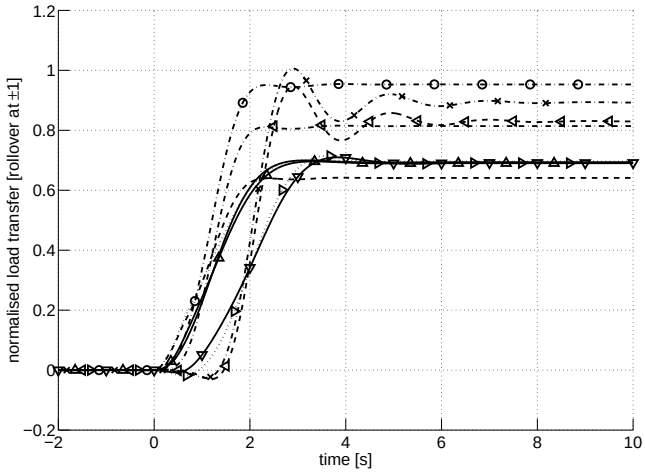

(c) Normalised load transfers. Active roll control: *steer axle (· · · · · ·), drive axle (—△—), semi-trailer axles (——), dolly axle (—▽—), trailer axles (– ◁ –)*; passive suspension: *steer axle (– – –), drive axle (· – ○ – ·), semi-trailer axles (· – · – ·), dolly axle (· – × – ·), trailer axles (· · ▷ · ·).*

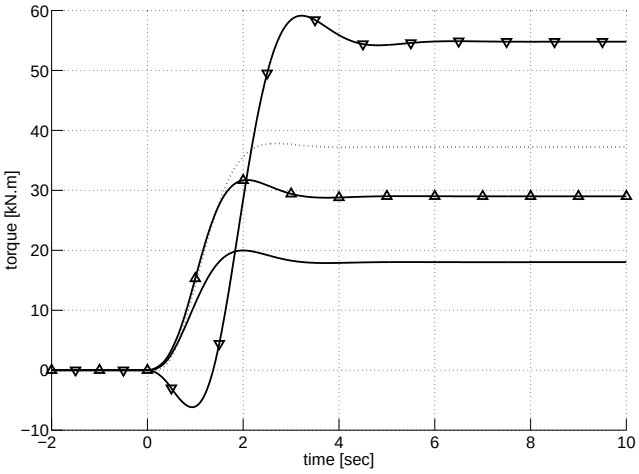

(d) Active anti-roll bar moments. Active roll control: *steer axle (· · · · · ·), drive axle (—△—), semi-trailer axles (——), dolly axle (—▽—), trailer axles (– ◁ –).*

Figure 6.11: Continued.

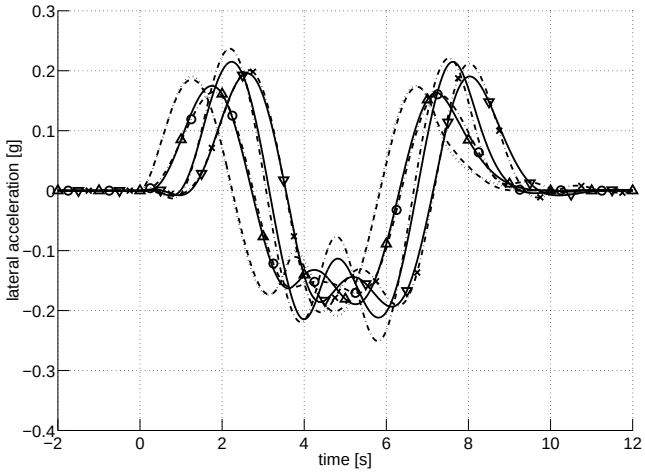

(a) Lateral accelerations. Active roll control: *tractor (· · · · · ·), semi-trailer (—△—), dolly (——), trailer (—▽—)*; passive suspension: *tractor (– – –), semi-trailer (· – ○ – ·), dolly (· – · – ·), trailer (· – × – ·).*

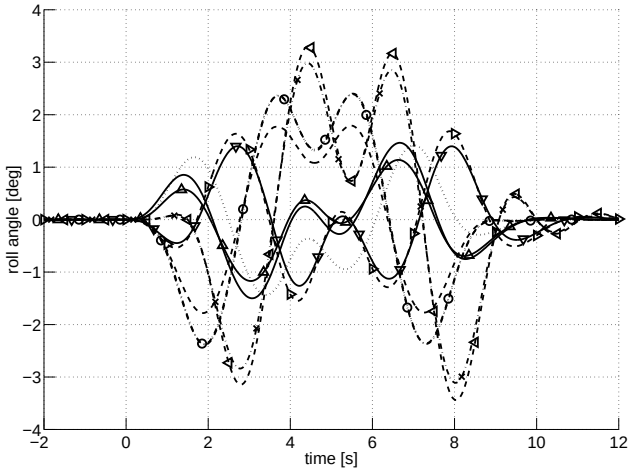

(b) Suspension roll angles. Active roll control: *steer axle (· · · · · ·), drive axle (—△—), semi-trailer axles (——), dolly axle (—▽—), trailer axles (– ◁ –)*; passive suspension: *steer axle (– – –), drive axle (· – ○ – ·), semi-trailer axles (· – · – ·), dolly axle (· – × – ·), trailer axles (· · ▷ · ·).*

Figure 6.12: Response of the linear A-double model with a full-state feedback controller to a double lane change steering input.

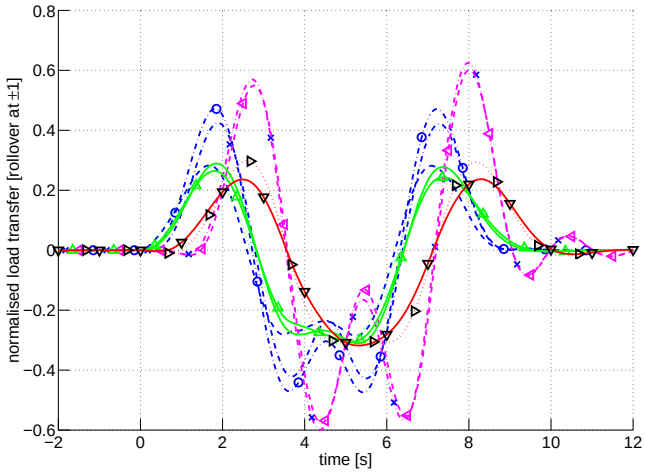

(c) Normalised load transfers. Active roll control: *steer axle (· · · · · ·), drive axle (—△—), semi-trailer axles (——), dolly axle (—▽—), trailer axles (– ◁ –)*; passive suspension: *steer axle (– – –), drive axle (· – ○ – ·), semi-trailer axles (· – · – ·), dolly axle (· – × – ·), trailer axles (· · ▷ · ·).*

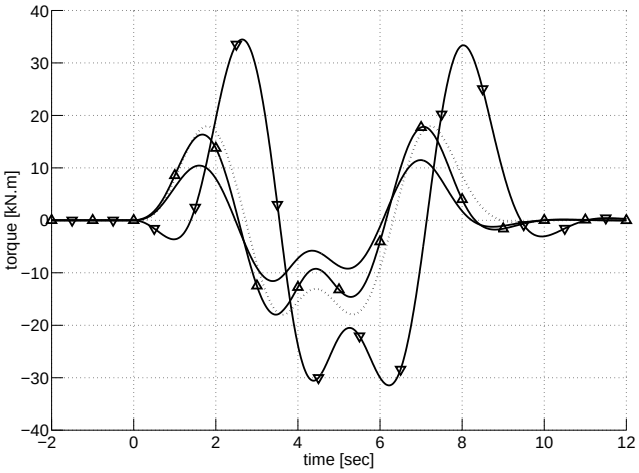

(d) Active anti-roll bar moments. Active roll control: *steer axle (· · · · · ·), drive axle (—△—), semi-trailer axles (——), dolly axle (—▽—), trailer axles (– ◁ –).*

Figure 6.12: Continued.

Chapter 7

Conclusions and recommendations

7.1 Summary of main conclusions

7.1.1 Vehicle modelling (chapter 2)

A simplified dynamic model for simulating the handling and roll performance of a torsionally flexible single unit vehicle was developed. A technique for coupling multiple single unit vehicle models to form a model of a long combination vehicle was detailed. A range of common vehicle couplings, including the pintle hitch, the fifth wheel and the draw bar, can be represented within this modelling framework.

7.1.2 Achievable roll stability (chapter 3)

Roll-over occurs when a vehicle is unable to provide a stabilising net restoring moment to balance an overturning moment. Wheel lift-off at a particular axle does not necessarily imply a loss of roll stability of the entire vehicle. A procedure for identifying critical axles whose lift-off determines the roll-over threshold was presented.

Functional controllability analysis can be used to verify that a candidate set of active anti-roll bars can exert some degree of control over a given set of roll-plane states (load transfers and roll angles). This has important implications for actuator placement.

Achievable roll stability is limited because it is not possible to control all axle load transfers and body roll angles independently using active anti-roll bars alone. The best achievable control objective for maximising roll stability was shown to be balancing the normalised load transfers at all critical axles while taking the largest inward suspension roll angle to the maximum allowable angle.

7.1.3 Active roll control of a single unit vehicle (chapter 4)

Active roll control is a problem of optimal disturbance rejection, which is an extension of the standard LQR problem. It was shown that, in order to maximise roll stability, the steering disturbance must be either measured or estimated and incorporated into the feedback law.

A more practical partial-state feedback controller, using measurements of suspension roll angles, body roll rate, yaw rate and steering input, can be designed using the linear quadratic Gaussian-loop transfer recovery technique.

Simulations showed that a system of active anti-roll bars incorporating moderately priced, low bandwidth hydraulic actuators and servo-valves and relatively simple instrumentation can improve steady-state roll stability of a rigid single unit vehicle by 23% and of a torsionally flexible single unit vehicle by 26%. Improvements in severe transient manoeuvres were even greater. These figures represent a significant increase in vehicle safety.

By distributing the total normalised load transfer between the steer and drive axles in a balanced fashion, active roll control tends to increase understeer for a typical single unit vehicle.

7.1.4 Active roll control of a tractor semi-trailer (chapter 5)

Simulations showed that active roll control systems can increase the roll-over threshold of a torsionally rigid tractor semi-trailer by 29% and of a torsionally flexible tractor semi-trailer by 29%. Such an improvement in roll stability represents a significant

increase in vehicle safety.

A partial-state LQG feedback controller, using measurements of suspension roll angles, body roll rates and body yaw rates at both the tractor and semi-trailer, in addition to the steering input, is a practical controller design that can significantly improve the roll stability of a tractor semi-trailer.

The actuator forces and hydraulic fluid flow rates required for good performance were again demonstrated to be achievable using practical, reasonably priced hardware.

The yaw stability of a tractor semi-trailer depends on the levels of understeer or oversteer at both the tractor and semi-trailer. By distributing the total normalised load transfer among all axles in a balanced fashion, active roll control tends to increase understeer for both units of a typical tractor semi-trailer, thus increasing yaw stability.

7.1.5 Active roll control of long combination vehicles (chapter 6)

Simulations showed that active roll control can increase the roll-over threshold by 32% for a B-double. This represents a significant increase in vehicle safety.

For vehicles with torsionally flexible couplings, such as truck full-trailers and A-doubles, the roll-over threshold of the combination is governed by the stability of the least stable set of torsionally decoupled vehicle units. This has important implications for the control objectives and actuator placement.

Truck full-trailers and A-doubles typically exhibit significant levels of rearward amplification that substantially increase lateral load transfer (and therefore reduce roll stability) in severe avoidance manoeuvres such as a double lane change. Active roll control was shown to increase the roll-over threshold by 25% for a truck full-trailer and by 23% for an A-double and also significantly attenuated the effect of rearward amplification on load transfer.

7.2 Recommendations for further work

7.2.1 Vehicle dynamics and control system simulation

The performance of the control strategies developed in chapters 4, 5 and 6 should be simulated using more detailed and authentic models of the vehicles and active roll control system components.

7.2.2 Experimental validation

The performance of a tractor semi-trailer with an active roll control system and the control strategies developed in chapter 5 should be validated using the experimental vehicle that is currently being developed at the University of Cambridge.

7.2.3 Roll control strategies

The use of intermittent rather than continuous active roll control action promises significant reductions in power consumption, and should be investigated in detail. For example, the advantages and disadvantages of signal threshold-based metrics [109] and "time-to-roll-over"-based metrics [11] for activating and deactivating the control system should be examined. The achievable roll stability of vehicles with semi-active roll control systems should also be studied. Finally, the potential performance benefits from nonlinear active roll controller synthesis should be assessed.

7.2.4 Driver feedback

The simulations in sections 4.7.9 and 5.5.9 showed that active roll control systems may be expected to cause significant, stable changes in vehicle handling at high levels of lateral acceleration. The use of this effect to improve the feedback of roll stability information to the driver is worthy of further investigation.

Appendix A

Single unit vehicle parameters

Dimensions are illustrated in figure 4.1(b).

Body geometry

Vehicle unit	b_f	h_s	b'_f	h_{cm}	$b^\star_r$	$h_{a,r}$	r	h_b
Tractor	0.742	1.058	1.115	0.920	3.074	1.250	0.742	0.776
Units	m	m	m	m	m	m	m	m

Body inertia

Vehicle unit	m_s	I_{xx}	I_{zz}	I_{xz}
Tractor	4819	2411	11383	1390
Units	kg	kg.m^2	kg.m^2	kg.m^2

Axle geometry

Vehicle unit	Axle	$a^\star$	h_u	d	Δd
Tractor	steer	0.000	0.530	2.000	—
Tractor	drive	3.700	0.530	1.800	0.429
Units		m	m	m	m

Axle inertia

Vehicle unit	Axle	m_u	I_{xx}	I_{zz}	I_{xz}
Tractor	steer	706	440	440	0
Tractor	drive	1000	563	563	0
Units		kg	kg.m^2	kg.m^2	kg.m^2

Additional lumped mass inertia

Vehicle unit	m_s	I_{xx}	I_{zz}	I_{xz}
Tractor	8828	792	792	0
Units	kg	kg.m^2	kg.m^2	kg.m^2

Frame and coupling properties

Vehicle unit	k_γ
Tractor	629
Units	kN.m/rad

Suspension properties

Vehicle unit	Axle	k	L
Tractor	steer	380	4.05
Tractor	drive	684	6.68
Units		kN.m/rad	kN.m.s/rad

Tyre properties

Vehicle unit	Axle	c_1	c_2	k_t	M^*
Tractor	steer	10.34	90.9	2060	6053
Tractor	drive	10.34	90.9	3337	9300
Units		rad^{-1}	$MN^{-1}.rad^{-1}$	kN.m/rad	kg

*Axle weight including the additional lumped mass.

Appendix B

Tractor semi-trailer parameters

Dimensions are illustrated in figure 5.2(b).

Body geometry

Vehicle unit	b_f	h_s	b'_f	h_{cm}	$b^\star_r$	$h_{a,r}$	r	h_b
Tractor	0.742	1.058	1.115	0.920	3.074	1.250	0.621	0.776
Semi-trailer	5.494	1.900	5.653	1.801	9.910	1.100	0.100	2.050
Units	m	m	m	m	m	m	m	m

Body inertia

Vehicle unit	m_s	I_{xx}	I_{zz}	I_{xz}
Tractor	4819	2411	11383	1390
Semi-trailer	30821	20164	223625	14577
Units	kg	kg.m^2	kg.m^2	kg.m^2

Axle geometry

Vehicle unit	Axle	$a^\star$	h_u	d	Δd
Tractor	steer	0.000	0.530	2.000	—
Tractor	drive	3.700	0.530	1.800	0.429
Semi-trailer	1	6.390	0.530	2.095	—
Semi-trailer	2	7.700	0.530	2.095	—
Semi-trailer	3	9.010	0.530	2.095	—
Units		m	m	m	m

Axle inertia

Vehicle unit	Axle	m_u	I_{xx}	I_{zz}	I_{xz}
Tractor	steer	706	440	440	0
Tractor	drive	1000	563	563	0
Semi-trailer	1,2,3	800	564	564	0
Units		kg	kg.m^2	kg.m^2	kg.m^2

Frame and coupling properties

Vehicle unit	k_γ †	k_ϕ †
Tractor	629	3000
Units	kN.m/rad	kN.m/rad

† For semi-trailers and dollies, the torsional flexibilities of the coupling and vehicle frame are lumped together into k_ϕ, and the vehicle frame is modelled as a rigid body.

Suspension properties

Vehicle unit	Axle	k	L
Tractor	steer	380	4.05
Tractor	drive	684	6.68
Semi-trailer	1,2,3	800	23.9
Units		kN.m/rad	kN.m.s/rad

Tyre properties

Vehicle unit	Axle	c_1	c_2	k_t	$M^{\ddagger}$
Tractor	steer	10.34	90.9	2060	6053
Tractor	drive	10.34	90.9	3337	9300
Semi-trailer	1,2,3	9.27	69.6	1776	8131
Units		rad^{-1}	$\text{MN}^{-1}.\text{rad}^{-1}$	kN.m/rad	kg

[‡]Axle weight in combination, as opposed to standalone.

Appendix C

Long combination vehicle parameters

C.1 B-double

Body geometry

Vehicle unit	b_f	h_s	b'_f	h_{cm}	$b^\star_r$	$h_{a,r}$	r	h_b
Tractor	0.742	1.058	1.115	0.920	3.074	1.250	0.621	0.776
Semi-trailer #1	4.286	1.870	4.625	1.737	8.890	1.250	0.100	2.050
Semi-trailer #2	5.494	1.900	5.653	1.801	9.910	1.100	0.100	2.050
Units	m	m	m	m	m	m	m	m

Body inertia

Vehicle unit	m_s	I_{xx}	I_{zz}	I_{xz}
Tractor	4819	2411	11383	1390
Semi-trailer #1	21755	15870	78199	6919
Semi-trailer #2	30821	20164	223625	14577
Units	kg	kg.m^2	kg.m^2	kg.m^2

Axle geometry

Vehicle unit	Axle	$a^\star$	h_u	d	Δd
Tractor	steer	0.000	0.530	2.000	—
Tractor	drive	3.700	0.530	1.800	0.429
Semi-trailer #1	1	6.390	0.530	2.095	—
Semi-trailer #1	2	7.700	0.530	2.095	—
Semi-trailer #1	3	9.010	0.530	2.095	—
Semi-trailer #2	1	6.390	0.530	2.095	—
Semi-trailer #2	2	7.700	0.530	2.095	—
Semi-trailer #2	3	9.010	0.530	2.095	—
Units		m	m	m	m

Axle inertia

Vehicle unit	Axle	m_u	I_{xx}	I_{zz}	I_{xz}
Tractor	steer	706	440	440	0
Tractor	drive	1000	563	563	0
Semi-trailer #1	1,2,3	800	564	564	0
Semi-trailer #2	1,2,3	800	564	564	0
Units		kg	kg.m^2	kg.m^2	kg.m^2

Frame and coupling properties

Vehicle unit	k_γ[†]	k_ϕ[†]
Tractor	629	3000
Semi-trailer #1	—	3000
Units	kN.m/rad	kN.m/rad

[†]For semi-trailers and dollies, the torsional flexibilities of the coupling and vehicle frame are lumped together into k_ϕ, and the vehicle frame is modelled as a rigid body.

Suspension properties

Vehicle unit	Axle	k	L
Tractor	steer	380	4.05
Tractor	drive	684	6.68
Semi-trailer #1	1,2,3	800	23.9
Semi-trailer #2	1,2,3	800	23.9
Units		kN.m/rad	kN.m.s/rad

Tyre properties

Vehicle unit	Axle	c_1	c_2	k_t	$M^{\ddagger}$
Tractor	steer	10.34	90.9	2060	6053
Tractor	drive	10.34	90.9	3337	9300
Semi-trailer #1	1,2,3	9.27	69.6	1776	8541
Semi-trailer #2	1,2,3	9.27	69.6	1776	8131
Units		rad^{-1}	$\text{MN}^{-1}.\text{rad}^{-1}$	kN.m/rad	kg

C.2 Truck full-trailer

Body geometry

Vehicle unit	b_f	h_s	b'_f	h_{cm}	$b^{\star}_r$	$h_{a,r}$	r	h_b
Truck	3.884	1.728	3.886	1.587	7.335	1.100	0.836	0.776
Dolly	2.000	1.100	2.000	0.749	2.000	1.250	0.100	1.100
Trailer	6.115	1.897	6.239	1.790	9.910	1.100	0.100	2.050
Units	m	m	m	m	m	m	m	m

[‡]Axle weight in combination, as opposed to standalone.

Body inertia

Vehicle unit	m_s	I_{xx}	I_{zz}	I_{xz}
Truck	20219	14396	122416	14714
Dolly	500	281	500	0
Trailer	28221	18596	224025	13670
Units	kg	kg.m^2	kg.m^2	kg.m^2

Axle geometry

Vehicle unit	Axle	$a^\star$	h_u	d	Δd
Truck	steer	0.000	0.530	2.000	—
Truck	push	4.625	0.530	1.800	0.429
Truck	drive	5.935	0.530	1.800	0.429
Dolly	1	2.000	0.530	2.095	—
Trailer	1	6.390	0.530	2.095	—
Trailer	2	7.700	0.530	2.095	—
Trailer	3	9.010	0.530	2.095	—
Units		m	m	m	m

Axle inertia

Vehicle unit	Axle	m_u	I_{xx}	I_{zz}	I_{xz}
Truck	steer	706	440	440	0
Truck	push	1000	563	563	0
Truck	drive	1000	563	563	0
Dolly	1	800	564	564	0
Trailer	1,2,3	800	564	564	0
Units		kg	kg.m^2	kg.m^2	kg.m^2

Frame and coupling properties

Vehicle unit	k_γ†	k_ϕ†
Truck	1573	0
Dolly	—	3000
Units	kN.m/rad	kN.m/rad

Suspension properties

Vehicle unit	Axle	k	L
Truck	steer	380	4.05
Truck	push	684	6.68
Truck	drive	684	6.68
Dolly	1	800	23.9
Trailer	1,2,3	800	23.9
Units		kN.m/rad	kN.m.s/rad

Tyre properties

Vehicle unit	Axle	c_1	c_2	k_t	M‡
Truck	steer	10.34	90.9	2060	6053
Truck	push	10.34	90.9	3337	8436
Truck	drive	10.34	90.9	3337	8436
Dolly	1	9.27	69.6	1776	7108
Trailer	1,2,3	9.27	69.6	1776	8271
Units		rad^{-1}	MN^{-1}.rad^{-1}	kN.m/rad	kg

†For semi-trailers and dollies, the torsional flexibilities of the coupling and vehicle frame are lumped together into k_ϕ, and the vehicle frame is modelled as a rigid body.

‡Axle weight in combination, as opposed to standalone.

References

[1] Abe, M. A study on effects of roll moment distribution control in active suspension on improvement of limit performance of vehicle handling. *International Journal of Vehicle Design*, 15(3–5):326–336, 1994.

[2] Anon. *The Allocation of Road Track Costs 1991/92*. Department of Transport, HMSO, UK, 1991.

[3] Anon. *Road Accidents in Great Britain*. Department of Transport, HMSO, UK, 1994.

[4] Aurell, J. 60 tonne truck proposal. Personal communication, 2000.

[5] Blow, P. W., Woodrooffe, J. H. F., and Sweatman, P. F. Vehicle stability and control research for US comprehensive truck size and weight (TS&W) study. *SAE Transactions*, 107(982819):617–623, 1998.

[6] Blower, D. and Pettis, L. Trucks involved in fatal accidents. Codebook 1996. Technical Report UMTRI-98-14, University of Michigan Transportation Research Institute, Ann Arbor, MI, USA, 1998.

[7] Blower, D. and Pettis, L. Trucks involved in fatal accidents. Codebook 1997. Technical Report UMTRI-99-18, University of Michigan Transportation Research Institute, Ann Arbor, MI, USA, 1999.

[8] Bryson, A. E. and Ho, Y. C. *Applied Optimal Control*. Blaisdell, Waltham, MA, USA, second edition, 1975.

[9] Cebon, D. Maximising roll-over stability of heavy road vehicles, 1996. Research Proposal to EPSRC: Case for Support.

[10] Cech, I. A slow-acting in-series active suspension. *Vehicle System Dynamics*, 16(1):17–26, 1987.

[11] Chen, B.-C. and Peng, H. Rollover prevention for sports utility vehicles with human-in-the-loop evaluations. In *Proc. 5th International Symposium on Advanced Vehicle Control*, number 35, Ann Arbor, MI, USA, 2000.

[12] Claar, P. W. and Vogel, J. M. A review of active suspension control for on and off-highway vehicles. *SAE Transactions*, 98(892482):557–568, 1989.

[13] Cooperrider, N. K., Thomas, T. M., and Hammoud, S. A. Testing and analysis of vehicle rollover behavior. *SAE Transactions*, 99(900366):518–527, 1990.

[14] Darling, J., Dorey, R. E., and Ross-Martin, T. J. Low cost active anti-roll suspension for passenger cars. In *Proc. ASME Winter Annual Meeting, Dynamic Systems and Control Division*, Dallas, TX, USA, 1990.

[15] Darling, J., Dorey, R. E., and Ross-Martin, T. J. A low cost active anti-roll suspension for passenger cars. *ASME Transactions, Journal of Dynamic Systems, Measurement and Control*, 114(4):599–605, 1992.

[16] Darling, J. and Ross-Martin, T. J. Theoretical investigation of a prototype active roll control system. *Proc. IMechE, Journal of Automobile Engineering*, 211(1):3–12, 1997.

[17] Dorling, R. J. Achievable dynamic response of active suspensions in bounce and roll. Technical Report CUED/C-MECH/TR 66, Department of Engineering, University of Cambridge, Cambridge, UK, 1995.

[18] Dorling, R. J. *Integrated Control of Road Vehicle Dynamics*. Ph.D. thesis, University of Cambridge, Cambridge, UK, 1996.

[19] Doyle, J. C., Francis, B. A., and Tannenbaum, A. R. *Feedback Control Theory*. Macmillan, New York, NY, USA, 1992.

[20] Doyle, J. C. and Stein, G. Robustness with observers. *IEEE Transactions on Automatic Control*, 24(2):607–611, 1979.

[21] Doyle, J. C. and Stein, G. Multivariable feedback design: Concepts for a classical/modern synthesis. *IEEE Transactions on Automatic Control*, 26(1):4–16, 1981.

[22] Dunwoody, A. B. and Froese, S. Active roll control of a semi-trailer. *SAE Transactions*, 102(933045):999–1004, 1993.

[23] Ellis, J. R. *Vehicle Handling Dynamics*. Mechanical Engineering Publications, London, UK, 1994.

[24] Ervin, R. D. Influence of size and weight variables on the stability and control properties of heavy trucks. *SAE Transactions*, 92(831163):629–654, 1983.

[25] Fancher, P. S., Ervin, R. D., Winkler, C. B., and Gillespie, T. D. A factbook of the mechanical properties of the components for single-unit and articulated heavy trucks. Technical Report UMTRI-86-12, University of Michigan Transportation Research Institute, Ann Arbor, MI, USA, 1986.

[26] Fancher, P. S. and Mathew, A. A vehicle dynamics handbook for single-unit and articulated heavy trucks. Technical Report UMTRI-86-37, University of Michigan Transportation Research Institute, Ann Arbor, MI, USA, 1987.

[27] Frank, P., Palkovics, L., and Gianone, P. Using wheel speed and wheel slip information for controlling vehicle chassis systems. In *Proc. 5th International Symposium on Advanced Vehicle Control*, number 35, Ann Arbor, MI, USA, 2000.

[28] Gillespie, T. D. *Fundamentals of Vehicle Dynamics*. SAE, Warrendale, PA, USA, 1992.

[29] Goodall, R. M. and Kortüm, W. Active controls in ground transportation – a review of the state-of-the-art and future potential. *Vehicle System Dynamics*, 12(4):225–257, 1983.

[30] Harris, R. J. W. Cost of roll-over accidents. Personal communication, 1995.

[31] Hedrick, J. K. and Butsuen, T. Invariant properties of automotive suspensions. *Proc. IMechE, Journal of Automobile Engineering*, 204(1):21–27, 1990.

[32] Hibbard, R. and Karnopp, D. Dynamics of small, relatively tall and narrow active tilting ground vehicles. In *Proc. ASME Winter Annual Meeting, Dynamic Systems and Control Division*, pages 397–416, New Orleans, LA, USA, 1993.

[33] Hibbard, R. and Karnopp, D. Methods of controlling the lean angle of tilting vehicles. In *Proc. ASME Winter Annual Meeting, Dynamic Systems and Control Division*, pages 311–320, New Orleans, LA, USA, 1993.

[34] Hibbard, R. and Karnopp, D. Twenty-first century transportation system solutions – a new type of small, relatively tall and narrow active tilting commuter vehicle. *Vehicle System Dynamics*, 25(5):321–347, 1996.

[35] Huang, P., Smakman, H., and Guldner, J. Design of a vehicle state observer for vehicle dynamics control systems. In *Proc. 5th International Symposium on Advanced Vehicle Control*, number 78, Ann Arbor, MI, USA, 2000.

[36] Hwang, S.-M. and Park, Y. Active roll moment distribution based on predictive control. *International Journal of Vehicle Design*, 16(1):15–28, 1995.

[37] Kalman, R. When is a linear control system optimal? *ASME Transactions, Journal of Basic Engineering*, 86:51–60, 1964.

[38] Karnopp, D. Are active suspensions really necessary? In *Proc. ASME Winter Annual Meeting, Dynamic Systems and Control Division*, pages 1–9, San Francisco, CA, USA, 1978.

[39] Karnopp, D. Theoretical limitations in active suspension. *Vehicle System Dynamics*, 15(1):41–54, 1986.

[40] Karnopp, D. Active suspensions based on fast load levelers. *Vehicle System Dynamics*, 16(5–6):355–380, 1987.

[41] Karnopp, D. and Hibbard, R. Optimum roll angle behavior for tilting ground vehicles. In *Proc. ASME Winter Annual Meeting, Dynamic Systems and Control Division*, pages 29–37, Anaheim, CA, USA, 1992.

[42] Kemp, R. N., Chinn, B. P., and Brock, G. Articulated vehicle roll stability: Method of assessment and effects of vehicle characteristics. Technical Report TRRL-788, Transport and Road Research Laboratory, UK, 1978.

[43] King, R. I. and Crolla, D. A. Flexible and efficient model development and analysis for road vehicle dynamics using a modular approach. In *Proc. 4th International Symposium on Advanced Vehicle Control*, pages 547–551, Nagoya, Japan, 1998.

[44] Kortüm, W. Review of multibody computer codes for vehicle system dynamics. In Kortüm, W. and Sharp, R. S., editors, *Multibody Computer Codes for Vehicle System Dynamics*, pages 3–31. Swets and Zeitlinger, Lisse, The Netherlands, 1993.

[45] Kusahara, Y., Li, X., Hata, N., and Watanabe, Y. Feasibility study of active roll stabilizer for reducing roll angle of an experimental medium-duty truck. In *Proc. 2nd International Symposium on Advanced Vehicle Control*, pages 343–348, Tsukuba, Japan, 1994.

[46] Kusters, L. J. J. Increasing roll-over safety of commercial vehicles by application of electronic systems. In Pauwelussen, J. P. and Pacejka, H. B., editors, *Smart Vehicles*, pages 362–377. Swets and Zeitlinger, Lisse, The Netherlands, 1995.

[47] Lang, R. and Walz, U. Active roll reduction. In *Proc. 3rd International Conference on Vehicle Dynamics and Power Train Engineering*, pages 88–92, Strasbourg, France, 1991.

[48] Li, Y. T., Meiry, J. L., and Roesler, W. G. An active roll mode suspension system for ground vehicles. *ASME Transactions, Journal of Basic Engineering*, 90:167–174, 1968.

[49] Lin, C.-F. *Modern Navigation, Guidance, and Control Processing*. Prentice Hall, Upper Saddle River, NJ, USA, 1991.

[50] Lin, C.-F. *Advanced Control Systems Design*. Prentice Hall, Upper Saddle River, NJ, USA, 1994.

[51] Lin, R. C. *An Investigation of Active Roll Control for Heavy Vehicle Suspensions*. Ph.D. thesis, University of Cambridge, Cambridge, UK, 1994.

[52] Lin, R. C., Cebon, D., and Cole, D. J. Investigation of active roll control of heavy road vehicles. In *Proc. 14th IAVSD Symposium on the Dynamics of Vehicles on Roads and Tracks*, pages 308–321, Chengdu, China, 1993.

[53] Lin, R. C., Cebon, D., and Cole, D. J. Validation of an articulated vehicle yaw/roll model. Technical Report CUED/C-MECH/TR 53, Department of Engineering, University of Cambridge, Cambridge, UK, 1993.

[54] Lin, R. C., Cebon, D., and Cole, D. J. Active roll control of articulated vehicles. *Vehicle System Dynamics*, 26(1):17–43, 1996.

[55] Lin, R. C., Cebon, D., and Cole, D. J. Optimal roll control of a single-unit lorry. *Proc. IMechE, Journal of Automobile Engineering*, 210(1):44–55, 1996.

[56] McFarlane, S. The integration of larger combination vehicles into the existing infrastructure using heavy vehicle simulations. *International Journal of Vehicle Design*, 7(1):96–110, 1997.

[57] McFarlane, S. and Sweatman, P. F. The development of high productivity combination vehicles using computer simulation. *SAE Transactions*, 106(973268):656–664, 1997.

[58] McFarlane, S., Sweatman, P. F., and Woodrooffe, J. H. F. The correlation of heavy vehicle performance measures. *SAE Transactions*, 106(973190):459–465, 1997.

[59] McKevitt, P. G. *Design of Roll Control Systems for Heavy Vehicles*. M.Phil. thesis, University of Cambridge, Cambridge, UK, 1999.

[60] Merritt, H. E. *Hydraulic Control Systems*. John Wiley & Sons, New York, NY, USA, 1967.

[61] Mizuno, M., Doi, S., Amano, Y., Matsunaga, T., Ishiguro, M., and Hayashi, Y. The adaption of active control technology to car chassis. In *Proc. 3rd International Conference on Vehicle Dynamics and Power Train Engineering*, pages 82–87, Strasbourg, France, 1991.

[62] Moore, B. C. On the flexibility offered by state feedback in multivariable systems beyond closed loop eigenvalue assignment. *IEEE Transactions on Automatic Control*, 21(4):689–692, 1976.

[63] Morari, M. Design of resilient processing plants. Part III: A general framework for the assessment of dynamic resilience. *Chemical Engineering Science*, 38:1881–1891, 1983.

[64] Nalecz, A. G. and Genin, J. Dynamic stability of articulated vehicles. *International Journal of Vehicle Design*, 5(4):417–426, 1984.

[65] Pacejka, H. B. Simplified analysis of steady turning behavior of motor vehicles. Part I: Handling diagrams of simple systems. *Vehicle System Dynamics*, 2(3):161–172, 1973.

[66] Pacejka, H. B. Simplified analysis of steady turning behavior of motor vehicles. Part II: Stability of the steady-state turn. *Vehicle System Dynamics*, 2(3):173–183, 1973.

[67] Pacejka, H. B. Simplified analysis of steady turning behavior of motor vehicles. Part III: More elaborate systems. *Vehicle System Dynamics*, 2(4):184–204, 1973.

[68] Palkovics, L., Semsey, À., and Gerum, E. Roll-over prevention system for vehicles – additional sensorless function of the electronic brake system. In *Proc. 4th International Symposium on Advanced Vehicle Control*, pages 643–647, Nagoya, Japan, 1998.

[69] Pflug, H. C., von Glasner, E.-Ch., and Povel, R. Improvement of commercial vehicles' handling and stability by smart chassis systems. In Pauwelussen, J. P. and Pacejka, H. B., editors, *Smart Vehicles*, pages 318–338. Swets and Zeitlinger, Lisse, The Netherlands, 1995.

[70] Pham, A. T. and Ugazio, P. Basic developments of an active air suspension for passenger cars. *SAE Transactions*, 98(890095):175–181, 1989.

[71] Pratt, I. Fundamental study into the design of an active anti-roll bar system for heavy trucks. Technical report, Department of Engineering, University of Cambridge, Cambridge, UK, 1997.

[72] Rakheja, S., Sankar, S., and Ranganthan, R. Roll plane analysis of articulated tank vehicles during steady turning. *Vehicle System Dynamics*, 17(2):81–104, 1987.

[73] Rakheja, S., Sankar, S., and Ranganthan, R. Influence of tank design factors on the roll-over threshold of partially filled tank vehicles. *SAE Transactions*, 98(892480):536–547, 1989.

[74] Rosenbrock, H. H. *State-Space and Multivariable Theory*. Nelson, London, UK, 1970.

[75] Safonov, M. G. and Athans, M. Gain and phase margin for multiloop LQG regulators. *IEEE Transactions on Automatic Control*, 22(2):173–179, 1977.

[76] Sampson, D. J. M. *Active Roll Control of Articulated Heavy Vehicles*. Ph.D. thesis, University of Cambridge, Cambridge, UK, 2000.

[77] Sampson, D. J. M. and Cebon, D. An investigation of roll control system design for articulated heavy vehicles. In *Proc. 4th International Symposium on Advanced Vehicle Control*, pages 311–316, Nagoya, Japan, 1998.

[78] Sampson, D. J. M., Jeppesen, B. P., and Cebon, D. The development of an active roll control system for heavy vehicles. In *Proc. 6th International Conference on Heavy Vehicle Weights and Dimensions*, Saskatoon, Canada, 2000. In press.

[79] Sampson, D. J. M., McKevitt, P. G., and Cebon, D. The development of an active roll control system for heavy vehicles. In *Proc. 16th IAVSD Symposium on the Dynamics of Vehicles on Roads and Tracks*, pages 704–715, Pretoria, South Africa, 1999.

[80] Sayers, M. W. *Symbolic Computer Methods to Automatically Formulate Vehicle Simulation Codes*. Ph.D. thesis, University of Michigan, Ann Arbor, MI, USA, 1990.

[81] Sayers, M. W. Vehicle models for RTS applications. In *Proc. 4th International Symposium on Advanced Vehicle Control*, pages 541–546, Nagoya, Japan, 1998.

[82] Sayers, M. W. and Riley, S. M. Modeling assumptions for realistic multibody simulations of the yaw and roll behavior of heavy trucks. *SAE Transactions*, 105(960173):72–83, 1996.

[83] Segel, L. Theoretical prediction and experimental substantiation of the response of an automobile to steering control. *Proc. IMechE, Automotive Division*, pages 310–330, 1956–57.

[84] Segel, L., editor. *Course on the Mechanics of Heavy-Duty Trucks and Truck Combinations*, Surfers Paradise, Qld, Australia, 1988. University of Michigan Transportation Research Institute.

[85] Segel, L. and Ervin, R. D. The influence of tire factors on the stability of trucks and truck-trailers. *Vehicle System Dynamics*, 10(1):39–59, 1981.

[86] Shahian, B. and Hassul, M. *Control System Design using MATLAB*. Prentice Hall, Upper Saddle River, NJ, USA, 1993.

[87] Shannan, J. E. and van der Ploeg, M. J. A vehicle handling model with active suspensions. *Journal of Mechanisms, Transmissions and Automation in Design*, 111:375–381, 1989.

[88] Sharp, R. S. and Crolla, D. A. Road vehicles suspension system design – a review. *Vehicle System Dynamics*, 16(3):167–192, 1987.

[89] Sharp, R. S. and Hassan, S. A. Relative performance capabilities of passive, active and semi-active car suspension systems. *Proc. IMechE, Journal of Transport Engineering*, 200(3):219–228, 1986.

[90] Sharp, R. S. and Hassan, S. A. On the performance capabilities of active automobile suspensions of limited bandwidth. *Vehicle System Dynamics*, 16(4):213–225, 1987.

[91] Sharp, R. S. and Hassan, S. A. Performance and design considerations for dissipative semi-active suspension systems for automobiles. *Proc. IMechE, Journal of Transport Engineering*, 201(2):149–153, 1987.

[92] Sharp, R. S. and Pan, D. On active roll control for automobiles. In *Proc. 12th IAVSD Symposium on the Dynamics of Vehicles on Roads and Tracks*, pages 566–583, Lyon, France, 1991.

[93] Sharp, R. S. and Pan, D. On the design of an active roll control system for a luxury car. *Proc. IMechE, Journal of Automobile Engineering*, 207(4):275–284, 1993.

[94] Skogestad, S. and Postlethwaite, I. *Multivariable Feedback Control – Analysis and Design*. John Wiley & Sons, Chichester, UK, 1996.

[95] Smith, M. C. Achievable dynamic response for automotive active suspension. *Vehicle System Dynamics*, 24(1):1–33, 1995.

[96] Srinathkumar, S. Eigenvalue/eigenvector assignment using output feedback. *IEEE Transactions on Automatic Control*, 23(1):79–81, 1978.

[97] Suresh, B. A. and Gilmore, B. J. Vehicle model complexity – how much is too much? In *Quality and Design Issues in Automotive Simultaneous Engineering*, number 940656 in SP-1035. SAE, Warrendale, PA, USA, 1994.

[98] Venhovens, P. J. Th. and Naab, K. Vehicle dynamics estimation using Kalman filters. In *Proc. 4th International Symposium on Advanced Vehicle Control*, pages 195–200, Nagoya, Japan, 1998.

[99] Vlk, F. Lateral dynamics of commercial vehicle combinations – a literature survey. *Vehicle System Dynamics*, 11(5):305–324, 1982.

[100] Vlk, F. Handling performance of truck-trailer vehicles: A state-of-the-art survey. *International Journal of Vehicle Design*, 6(3):323–361, 1985.

[101] Von Glasner, E.-Ch. Active safety of commercial vehicles. In *Proc. 2nd International Symposium on Advanced Vehicle Control*, pages 9–14, Tsukuba, Japan, 1994.

[102] Von Glasner, E.-Ch., Göhring, E., Povel, R., and Schützner, P. Analysis of intelligent suspension systems for commercial vehicles. *SAE Transactions*, 102(933008):896–904, 1993.

[103] Walker, G. W. *Constraints upon the Achievable Performance of Vehicle Suspension Systems*. Ph.D. thesis, University of Cambridge, Cambridge, UK, 1997.

[104] Walker, G. W. and Smith, M. C. Performance limitations and constraints for active and passive suspensions: A mechanical multi-port approach. *Vehicle System Dynamics*, 33(3):137–168, 2000.

[105] Williams, D. E. and Haddad, W. M. Nonlinear control of roll moment dustribution to influence vehicle yaw characteristics. *IEEE Transactions on Control Systems Technology*, 3(1):110–116, 1995.

[106] Winkler, C. B. Simplified analysis of the steady-state turning of complex vehicles. *Vehicle System Dynamics*, 29(3):141–180, 1998.

[107] Winkler, C. B., Blower, D., Ervin, R. D., and Chalasani, R. M. *Rollover of Heavy Commercial Vehicles*. SAE, Warrendale, PA, USA, 2000.

[108] Winkler, C. B., Bogard, S. E., Ervin, R. D., Horsman, A., Blower, D., Mink, C., and Karamihas, S. Evaluation of innovative converter dollies. Technical Report UMTRI-93-47, University of Michigan Transportation Research Institute, Ann Arbor, MI, USA, 1993.

[109] Winkler, C. B. and Ervin, R. D. On-board estimation of the rollover threshold of tractor semitrailers. In *Proc. 16th IAVSD Symposium on the Dynamics of Vehicles on Roads and Tracks*, pages 540–551, Pretoria, South Africa, 1999.

[110] Winkler, C. B. and Ervin, R. D. Rollover of heavy commercial vehicles. Technical Report UMTRI-99-19, University of Michigan Transportation Research Institute, Ann Arbor, MI, USA, 1999.

[111] Wonham, W. M. On pole assignment of multi-input controllable linear systems. *IEEE Transactions on Automatic Control*, 12(4):660–665, 1967.

[112] Woodrooffe, J. H. F. Truck size and weight practice in Canada – the engineering approach. *SAE Transactions*, 107(982821):624–637, 1998.

[113] Zhou, K., Doyle, J. C., and Glover, K. *Robust and Optimal Control*. Prentice Hall, Upper Saddle River, NJ, USA, 1996.